

Some pages of this thesis may have been removed for copyright restrictions.

If you have discovered material in Aston Research Explorer which is unlawful e.g. breaches copyright, (either yours or that of a third party) or any other law, including but not limited to those relating to patent, trademark, confidentiality, data protection, obscenity, defamation, libel, then please read our [Takedown policy](#) and contact the service immediately (openaccess@aston.ac.uk)

THE STEADY STATE PERFORMANCE
OF CONVERTER TYPE
REACTIVE POWER COMPENSATORS

JASON EDWARD HILL
Doctor of Philosophy

THE UNIVERSITY OF ASTON IN BIRMINGHAM

February 1995

This copy of the thesis has been supplied on condition that anyone who consults it is understood to recognise that its copyright rests with its author and that no quotation from the thesis and no information from it may be published without proper acknowledgement.

The University of Aston in Birmingham

The Steady State Performance of Converter Type Reactive Power Compensators

Jason Edward Hill

Doctor of Philosophy

1995

Summary

As a source or sink of reactive power, compensators can be made from a voltage sourced inverter circuit with the a.c. terminals of the inverter connected to the system through an inductive link and with a capacitor connected across the d.c. terminals.

Theoretical calculations on linearised models of the compensators have shown that the parameters characterising the performance are the reduced firing angle and the resonance ratio. The resonance ratio is the ratio of the natural frequency of oscillation of the energy storage components in the circuit to the system frequency. The reduced firing angle is the firing angle of the inverter divided by the damping coefficient, β , where β is half the R to X ratio of the link between the inverter and the system. The theoretical results have been verified by computer simulation and experiment.

There is a narrow range of values for the resonance ratio below which there is no appreciable improvement in performance, despite an increase in the cost of the energy storage components, and above which the performance of the equipment is poor with the current being dominated by harmonics.

The harmonic performance of the equipment is improved by using multiple inverters and phase shifting transformers to increase the pulse number. The optimum value of the resonance ratio increases with increasing pulse number indicating a reduction in the energy storage components needed at higher pulse numbers.

The reactive power output from the compensator varies linearly with the reduced firing angle while the losses vary as the square of it.

Key Words: ASVC, FACTS, GTO-SVC, STATCON

This thesis is dedicated to my girlfriend Mary.

Acknowledgements

I would like to thank my supervisor, Professor W. T. Norris, for his invaluable contributions to this work and for countless helpful discussions.

The practical stages of the project have been team efforts and the work outlined in the thesis could not have been accomplished without the efforts of many people to whom I am greatly indebted:

Mr. A. Ashbrook for designing and building the control circuit for the six pulse model;

Mr. R. T. Baker for his contributions in building the six pulse model;

Mr. M. P. Westrick for much of the preliminary work on the twenty-four pulse model;

Mr. S. M. Boardman and Mr. C. M. Chileshe for their work on the control scheme for the twenty-four pulse model;

the power engineering technical staff at Aston, Mr. L. Radford and Mr. B. Harrison, for assistance throughout the practical work.

In addition suggestions from Dr. D. R. Trainer, of GEC Stafford, when building the six pulse model were useful.

Advice offered from Mr. L. Babad concerning the design and building of this model and at other key times was also useful.

I am also grateful to Mr. D. A. James for discussions on his work on pulse width modulation.

I am appreciative of the time and assistance of Mr. A. P. Wilton with software and hardware to enable the computer simulations in the project to be performed satisfactorily.

I am also grateful to Dr. A. J. Power and Mr. M. L. Winfield of the National Grid Company for their contributions and advice on the direction of the project and to the National Grid Company for their sponsorship and financial contributions to the project.

Finally, I would like to thank the Engineering and Physical Sciences Research Council (EPSRC) for their financial support.

Contents

<u>Section</u>	<u>Title</u>	<u>Page</u>
Chapter 1	Introduction	
1-1	Definition of Reactive Power	21
1-2	The Role of Reactive Power Compensation	26
1-3	Motivation	30
1-4	Equipment used for Reactive Power Compensation	31
1-5	Ideal Characteristics	33
1-6	Devices	33
1-7	Nomenclature	34
1-8	Aims	34
Chapter 2	Performance of VSI and CSI Types of the Single Phase STATCON using Voltage and Current Sources	
2-1	Introduction	35
2-2	Circuit Description of the Voltage Sourced Inverter Type of STATCON	35
2-3	Performance of the Voltage Sourced Inverter Type of STATCON	36
2-4	System Current Harmonics from a Single Phase VSI Type of STATCON	40
2-5	Current Sourced Inverter Type of STATCON	43
2-6	Conclusions	46
Chapter 3	Performance of VSI and CSI Types of the Single Phase STATCON using Finite Energy Reservoirs	
3-1	Introduction	48
3-2	Voltage Sourced STATCON with Capacitor Energy Reservoir	48
3-3	Current Sourced STATCON with Inductor Energy Reservoir	54
3-4	Comparison Between the Two Types of STATCON	56
3-5	Conclusions	56

Chapter 4	The Single Phase Voltage Sourced STATCON	
4.1	Introduction	57
4.2	Method	57
4.3	Voltage Across the Capacitor	58
4.4	System Current	60
4.5	Characteristics of the Fundamental Component of the System Current	62
4.6	Total Harmonic Content	65
4.7	Characteristics of the Harmonics of the System Current	66
4.8	Choice of Circuit Parameters	69
4.9	Equivalent Circuit	70
4.10	Discussion on p_1 and q_1	72
4.11	Size of the Energy Storage Components	73
4.12	Operation at Reduced System Voltage	74
4.13	Conclusions	77
Chapter 5	The Three Phase Voltage Sourced STATCON	
5.1	Introduction	79
5.2	Power Circuit	79
5.3	Method	80
5.4	Nomenclature	81
5.5	Voltage Across the Capacitor	82
5.6	System Current	84
5.7	Characteristics of the Fundamental Component of the System Current	86
5.8	Total Harmonic Content	90
5.9	Characteristics of the Harmonics of the System Current	90
5.10	Choice of Circuit Parameters	92
5.11	Equivalent Circuit	93
5.12	Practical Arrangement	95
5.13	Control Scheme	95
5.14	Results	98
5.15	Experience of Commissioning	102
5.16	Size of the Energy Storage Components	102
5.17	Range of Reduced Firing Angle	103
5.18	Conclusions	106

Chapter 6	Twelve Pulse Voltage Sourced STATCONs	
6-1	Introduction	107
6-2	Methods of Harmonic Reduction	107
6-3	Multiple Pulse Configurations	112
6-4	Nomenclature	121
6-5	Voltage Across the Capacitor	122
6-6	System Current	125
6-7	Characteristics of the Fundamental Component of the System Current	128
6-8	Characteristics of the Harmonics of the System Current	133
6-9	Comparison of Series and Parallel Circuits	138
6-10	Comparison of the Currents from the Series and Parallel Circuits	139
6-11	Size of Energy Storage Components	140
6-12	Range of the Reduced Firing Angle	140
6-13	Conclusions	141
Chapter 7	Twenty-Four Pulse Voltage Sourced STATCONs	
7-1	Introduction	142
7-2	Transformer Arrangement	143
7-3	Nomenclature	148
7-4	Voltage Across the Capacitor	148
7-5	System Current	150
7-6	Characteristics of the Fundamental Component of the System Current	151
7-7	Characteristics of the Harmonics of the System Current	155
7-8	Comparison of Series and Parallel Circuits	159
7-9	Practical Arrangement	159
7-10	Results	160
7-11	Size of the Energy Storage Components	165
7-12	Range of the Reduced Firing Angle	166
7-13	Conclusions	166

Chapter 8	Conclusions and Proposals for Further Study	
8.1	Introduction	167
8.2	Method of Analysis	167
8.3	Calculation of Fourier Series	170
8.4	Definition of the Resonance Ratio	171
8.5	Significance of the Resonance Ratio	172
8.6	Optimisation of the Energy Storage Components	173
8.7	Practical Results	176
8.8	Summary of Important Formulae	177
8.9	Further Work	178
9	References	180
Appendix 1	Analysis of a Single Phase Voltage Sourced STATCON	184
Appendix 2	Expansion of Summation	191
Appendix 3	Analysis of a Three Phase Voltage Sourced STATCON	193
Appendix 4	Derivation of Equivalent Circuit for the Three Phase Voltage Sourced STATCON	205
Appendix 5	Analysis of a Twelve Pulse STATCON with Parallel Connected Transformer Primaries	209
Appendix 6	Analysis of a Twelve Pulse STATCON with Series Connected Transformer Primaries	222
Appendix 7	Analysis of a Twenty-Four Pulse STATCON with Parallel Connected Transformer Primaries	234
Appendix 8	Analysis of a Twenty-Four Pulse STATCON with Series Connected Transformer Primaries	249
Appendix 9	Details of the Experimental Work	263

Figures

<u>Number</u>	<u>Title</u>	<u>Page</u>
1-1	A Sinusoidal Voltage Source Feeding a Linear Load	21
1-2	General Phasor Diagram for a Lagging Current	22
1-3	Power Vector Diagram	24
1-4	Definition of Voltage and Current Vector Planes	25
1-5	Single Load Model of a Transmission Line	26
1-6	Phasor Diagram for the Single Load Model of a Transmission Line	26
1-7	A Transmission Line with Reactive Power Compensation	28
1-8	Symbol for a General Device Which Can be Turned On and Off	33
2-1	Single Phase Voltage Sourced STATCON with Battery	35
2-2	Equivalent Circuit of a Single Phase STATCON with Battery	36
2-3	Phasor Diagram for Reactive Power Generation in a Single Phase STATCON with Zero Firing Angle	37
2-4	Phasor Diagram for Reactive Power Absorption in a Single Phase STATCON with Zero Firing Angle	37
2-5	Phasor Diagram with a Firing Angle of Pi Rad for a Single Phase STATCON	38
2-6	Timing Diagram Showing a Positive Firing Angle	38
2-7	Phasor Diagrams for a General Firing Angle	39
2-8a	Simulation of the Steady State Performance of the VSI Type of Single Phase STATCON with the Inverter Output 20% Greater than the Supply Voltage	42
2-8b	Simulation of the Steady State Performance of the VSI Type of Single Phase STATCON with the Inverter Output 20% Smaller than the Supply Voltage	42
2-9	Single Phase Current Sourced STATCON with Constant Current Source	43
2-10a	Simulation of the Steady State Performance of the CSI Type of Single Phase STATCON Generating 1p.u. Reactive Power	45
2-10b	Simulation of the Steady State Performance of the CSI Type of Single Phase STATCON Absorbing 1p.u. Reactive Power	45
3-1	Equivalent Circuit of Single Phase STATCON with Capacitor	49
3-2	Phasor Diagram with a Positive Firing Angle	49
3-3a	Simulation of a Single Phase STATCON with Capacitor Energy Reservoir Generating Reactive Power	53

3.3b	Simulation of a Single Phase STATCON with Capacitor Energy Reservoir Absorbing Reactive Power	53
3.4a	Simulation of a Single Phase STATCON with Inductor Energy Reservoir Generating Reactive Power	55
3.4b	Simulation of a Single Phase STATCON with Inductor Energy Reservoir Absorbing Reactive Power	55
4.1	The Capacitor Voltage in a Single Phase STATCON for $k = 1, 1.5$ and 2	59
4.2	The Current in a Single Phase STATCON for $k = 1, 1.5$ and 2	61
4.3	Graphs of the Parameters Describing the Fundamental Component of the Current in a Single Phase STATCON	63
4.4	Graph of the Normalised Reactive Power Output from a Single Phase STATCON	64
4.5	Graph of the Normalised Losses in a Single Phase STATCON	64
4.6	Graph of the Normalised Total Harmonic Content as a Function of the Reduced Firing Angle in a Single Phase STATCON	66
4.7	Graphs of the Normalised Coefficient of the Harmonics in the Current for $n = 3, 5$ and 7 in a Single Phase STATCON	67
4.8	Graphs of the Parameters Describing the Coefficients of the Harmonics in the Current in a Single Phase STATCON	68
4.9	Equivalent Circuit for the Single Phase STATCON with a Capacitor Energy Reservoir	71
4.10	Phasor Diagrams for Zero Firing Angle in the Single Phase STATCON	73
4.11	Graph of the Maximum Reactive Power Output	75
4.12	Graph of the Losses when Generating Maximum Reactive Power	75
4.13	Graph of the Reactive Power Output with Maximum Losses of 5%	76
4.14	Graph of the Actual Losses when Limited at 5%	76
5.1	Circuit Diagram for the Three Phase STATCON with Capacitor Energy Reservoir	79
5.2	The Capacitor Voltage for a Three Phase STATCON for $k = 2, 4$ and 5	83
5.3	The Current in a Three Phase STATCON for $k = 2, 4$ and 5	85
5.4	Graphs of the Parameters Describing the Fundamental Component of the Current in a Three Phase STATCON	87
5.5	Graph of the Normalised Reactive Power Output from a Three Phase STATCON	89

5·6	Graph of the Normalised Losses in a Three Phase STATCON	89
5·7	Graph of the Normalised Total Harmonic Content as a Function of the Reduced Firing Angle in a Three Phase STATCON	90
5·8	Graphs of the Normalised Coefficient of the Harmonics in the Current for $n = 5$ and 7 in a Three Phase STATCON	91
5·9	Graphs of the Parameters Describing the Coefficients of the Harmonics in the Current in a Three Phase STATCON	92
5·10	Per Phase Circuit Model of a Three Phase STATCON	93
5·11	Per Phase Equivalent Circuit of a Three Phase STATCON	93
5·12	Graphs of the Voltage Source for the Equivalent Circuit of a Three Phase STATCON	94
5·13	Block Diagram of the Control Circuit for a 6–Pulse STATCON	96
5·14	Experimental, Theoretical and Simulation Results for Rated Reactive Power Generation from a Three Phase STATCON	99
5·15	Experimental, Theoretical and Simulation Results for Zero Reactive Power from a Three Phase STATCON	100
5·16	Experimental, Theoretical and Simulation Results for Rated Reactive Power Absorption from a Three Phase STATCON	101
5·17	Operating Region for Small Values of θ_{ob} for the Three Phase STATCON	103
5·18	Full Operating Region for Positive θ_0 for the Three Phase STATCON	104
5·19a	Graph of the Average Capacitor Voltage with a Small Value of the Resonance Ratio in a Three Phase STATCON	105
5·19b	Graph of the Average Capacitor Value with a Restricted Range of Firing Angle	105
6·1	Multi–Level Single Phase STATCON and Associated Wave Shape	110
6·2a	12–Pulse STATCON with Parallel Connected Transformer Primaries	113
6·2b	12–Pulse STATCON with Series Connected Transformer Primaries	113
6·3a	Single Transformer Parallel Connected 12–Pulse Transformer	115
6·3b	Single Transformer Series Connected 12–Pulse Transformer	115
6·4	12–Pulse Inverter Output Voltage	116
6·5a	Graph of the Currents in the Red Phases of the Secondaries in the Parallel Circuit	117
6·5b	Graph of the Current in the Red Phase of the Voltage Source in the Parallel Circuit	117

6.6	Graph of the Voltages Across Each of the Red Phase Primary Windings	119
6.7	Graph of the Voltages Across Each of the Red Phase Secondary Windings	119
6.8a	Graph of the Currents in the Red Phases of the Secondaries in the Series Circuit	120
6.8b	Graph of the Current in the Red Phase of the Voltage Source in the Series Circuit	120
6.9	Graph of the Inverter Output Voltage with the Leakage Reactance of the Transformers on the Primary Side	121
6.10a	The Capacitor Voltage for a Twelve Pulse Parallel STATCON for $k = 4, 7$ and 11	123
6.10b	The Capacitor Voltage for a Twelve Pulse Series STATCON for $k = 4, 7$ and 11	124
6.11a	The Current in a Twelve Pulse Parallel STATCON for $k = 4, 7$ and 11	126
6.11b	The Current in a Twelve Pulse Series STATCON for $k = 4, 7$ and 11	127
6.12a	Graphs of the Parameters Describing the Fundamental Component of the Current in a Twelve Pulse Parallel STATCON	129
6.12b	Graphs of the Parameters Describing the Fundamental Component of the Current in a Twelve Pulse Series STATCON	130
6.13	Graph of the Normalised Reactive Power Output from a Twelve Pulse Parallel STATCON	131
6.14	Graph of the Normalised Losses in a Twelve Pulse Parallel STATCON	131
6.15	Graph of the Normalised Reactive Power Output from a Twelve Pulse Series STATCON	132
6.16	Graph of the Normalised Losses in a Twelve Pulse Series STATCON	132
6.17	Graphs of the Normalised Coefficient of the Harmonics in the Current for $n = 11$ and 13 in a Twelve Pulse Parallel STATCON	134
6.18	Graphs of the Normalised Coefficient of the Harmonics in the Current for $n = 11$ and 13 in a Twelve Pulse Series STATCON	135
6.19	Graphs of the Parameters Describing the Coefficients of the Harmonics in the Current in a Twelve Pulse Parallel STATCON	136
6.20	Graphs of the Parameters Describing the Coefficients of the Harmonics in the Current in a Twelve Pulse Series STATCON	137
6.21a	The Current in the 12-Pulse Parallel Circuit for $k = 10$ and $\theta_{ob} = 1$	139

6-21b	The Current in the 12-Pulse Series Circuit for $k = 10$ and $\theta_{ob} = 1$	139
6-22	Operating Region for Small Values of the Firing Angle for the 12-Pulse STATCON	141
7-1a	Parallel Connected 24-Pulse Arrangement Using Star and Zigzag Transformers	143
7-1b	Series Connected 24-Pulse Arrangement Using Star and Zigzag Transformers	143
7-2	Parallel Connected 24-Pulse Arrangement Using Zigzag and Extended Delta Secondaries	144
7-3	Parallel Connected 24-Pulse Arrangement Using Star and Delta Primaries	145
7-4	Quasi 24-Pulse Transformer Arrangement	146
7-5	Simulation of Quasi Twenty-Four Pulse System Generating Reactive Power	147
7-6	The Capacitor Voltage for a Twenty-Four Pulse Series STATCON for $k = 10, 15$ and 22	149
7-7	The Current in a Twenty-Four Pulse Series STATCON for $k = 10, 15$ and 22	150
7-8a	Graphs of the Parameters Describing the Fundamental Component of the Current in a Twenty-Four Pulse Parallel STATCON	152
7-8b	Graphs of the Parameters Describing the Fundamental Component of the Current in a Twenty-Four Pulse Series STATCON	153
7-9	Graph of the Normalised Reactive Power Output from a Twenty-Four Pulse Series STATCON	154
7-10	Graph of the Normalised Losses in a Twenty-Four Pulse Series STATCON	154
7-11	Graphs of the Normalised Coefficient of the Harmonics in the Current for $n = 23$ and 25 in a Twenty-Four Pulse Series STATCON	156
7-12	Graphs of the Parameters Describing the Coefficients of the Harmonics in the Current in a Twenty-Four Pulse Parallel STATCON	157
7-13	Graphs of the Parameters Describing the Coefficients of the Harmonics in the Current in a Twenty-Four Pulse Series STATCON	158
7-14	Experimental, Theoretical and Simulation Results for Rated Reactive Power Generation from a Twenty-Four Pulse STATCON	162
7-15	Experimental, Theoretical and Simulation Results for Zero Reactive Power Output from a Twenty-Four Pulse STATCON	163
7-16	Experimental, Theoretical and Simulation Results for Rated Reactive Power Absorption from a Twenty-Four Pulse STATCON	164

7·17	Operating Region for Small Values of θ_{ob} for the 24–Pulse STATCON with Series Connected Transformer Primaries	166
A1·1	The Single Phase STATCON Circuit with Capacitor Energy Reservoir	184
A1·2	Single Phase Circuit with Devices 1 and 2 Turned On	185
A1·3	Single Phase Circuit with Devices 3 and 4 Turned On	186
A3·1	The Three Phase STATCON with Capacitor Energy Reservoir	193
A3·2	Three Phase Circuit with Devices 1, 5 and 6 Turned On	195
A3·3	Per Phase Circuit Model for the Three Phase STATCON	200
A3·4	Graphs of the Magnitude of the Normalised Harmonic Component of the Current as a Function of the Reduced Firing Angle	203
A4·1	Per Phase Equivalent Circuit	205
A5·1	The Twelve Pulse STATCON with Capacitor Energy Reservoir	209
A5·2	The Twelve Pulse STATCON During the Interval $-\pi/12 < \phi < \pi/12$	211
A5·3	Turns Ratios for the First Transformer	216
A6·1	Twelve Pulse Series Connected Transformer Arrangement	222
A7·1	Twenty–Four Pulse STATCON During the Interval $-\pi/8 < \phi < -\pi/24$	235
A7·2	Turns Ratios for the Advanced Phase–Shifting Transformers	241
A8·1	Twenty–Four Pulse Series Connected Transformer Arrangement	250
A9·1	Circuit Diagram for the 6–Pulse Practical Equipment	264
A9·2	Photograph of the 6–Pulse Practical Equipment	265
A9·3	Photograph of the 24–Pulse Practical Equipment	267

Tables

<u>Number</u>	<u>Title</u>	<u>Page</u>
2·1	Comparison of the Harmonics Generated by the Voltage Sourced and Current Sourced Single Phase STATCONs	47
5·1	On Devices in a Three Phase STATCON	80
6·1	On Devices in a Twelve Pulse STATCON	114
7·1	Actual and Nominal Phase Shifts	161
8·1	Values of κ	171
8·2	The Admittance of the Energy Reservoir at the Knee Point of the q_2 Against m Graphs	173
8·3	Optimised Values of the Energy Stores	176
A3·1	Current Relationships in the Three Phase Equipment	194
A5·1	Current Relationships in the Twelve Pulse Equipment	210
A7·1	Current Relationships in the Twenty-Four Pulse Equipment	234

Symbols

<u>Symbol</u>	<u>Definition</u>	<u>Page</u>
[A]:	column matrix of $A_1, A_2 \dots$ (A)	215
$A_1, A_2 \dots$:	integration constants (A)	58
a_n :	Fourier coefficient of the $\cos n\phi$ terms in I (A)	80
a_{nc} :	coefficient of the $\cos\theta_0$ contribution to a_n (A)	232
a_{ns} :	coefficient of the $\sin\theta_0$ contribution to a_n (A)	232
b_n :	Fourier coefficient of the $\sin n\phi$ terms in I (A)	80
b_{nc} :	coefficient of the $\cos\theta_0$ contribution to b_n (A)	232
b_{ns} :	coefficient of the $\sin\theta_0$ contribution to b_n (A)	232
C:	capacitance (F)	48
C_C :	cost of capacitance (£/VA)	174
C_L :	cost of inductance (£/VA)	174
C_T :	total cost of energy stores (£/VA)	174
cosna:	$f(n)$ used in 24-pulse algebra	255
cosnb:	$f(n)$ used in 24-pulse algebra	255
c_n :	t_n when $\theta_0 = 0$	66
d:	$f(\theta_0, \beta, k)$ used in 6-pulse algebra	197
d_n :	Fourier coefficient of $\cos n\phi$ terms of V_I (V)	80
d_{nc} :	coefficient of the $\cos\theta_0$ contribution to d_n (V)	200
d_{ns} :	coefficient of the $\sin\theta_0$ contribution to d_n (V)	200
e_n :	Fourier coefficient of $\sin n\phi$ terms of V_I (V)	80
e_{nc} :	coefficient of the $\cos\theta_0$ contribution to e_n (V)	200
e_{ns} :	coefficient of the $\sin\theta_0$ contribution to e_n (V)	200
[F]:	matrix of coefficients of [A] (Ω)	215
f:	$f(\theta_0, \beta, k)$ used in 6-pulse algebra	197
G:	$\frac{2(\beta^2+k^2)\cos(\theta_0+\gamma)}{[k - 2\beta e^{-\beta\pi}\sin k\pi - ke^{-2\beta\pi}]}$	187
h:	$\sqrt{(\beta^2+k^2-1)^2 + 4\beta^2}$	58
h_n :	$\sqrt{(\beta^2+k^2-n^2)^2 + 4\beta^2n^2}$	188
I:	current (A)	21
i:	any integer	40
I_{ab} :	current in blue phase of first transformer (A)	209
I_{ar} :	current in red phase of first transformer (A)	209
I_{ay} :	current in yellow phase of first transformer (A)	209
I_B :	current in blue phase (A)	25
I_{bb} :	current in blue phase of second transformer (A)	209
I_{br} :	current in red phase of second transformer (A)	209

I_{by} :	current in yellow phase of second transformer (A)	209
I_c :	capacitor current (A)	211
I_{cb} :	current in blue phase of third transformer (A)	234
I_{comp} :	current into a reactive power compensator (A)	28
I_{cr} :	current in red phase of third transformer (A)	234
I_{cy} :	current in yellow phase of third transformer (A)	234
I_{db} :	current in blue phase of fourth transformer (A)	234
I_{dc} :	constant current through the d.c. terminals of CSI (A)	43
I_{dr} :	current in red phase of fourth transformer (A)	234
I_{dy} :	current in yellow phase of fourth transformer (A)	234
I_H :	horizontal axis describing current plane (A)	25
I_L :	current through one inductor (A)	174
I_m :	peak of the fundamental component of I (A)	21
I_n :	component of the current of frequency $n\theta$ (A)	24
I_{nc} :	coefficient of I_n (A)	40
I_p :	component of I_1 in phase with V_S (A)	51
I_q :	component of I_1 leading V_S by $\pi/2$ radians (A)	51
I_R :	current in red phase (A)	25
I_{Rn} :	component of I_R of frequency $n\theta$ (A)	221
I_{rms} :	root mean square value of current (A)	65
I_V :	vertical axis describing current plane (A)	25
I_Y :	current in yellow phase (A)	25
J :	$\sum_{n=1}^{\infty} \frac{1}{h_n^2}$ for n odd	192
k :	resonance ratio	58
L :	inductance (H)	35
m :	$1/k$	62
N :	number of three phase converters	168
n :	harmonic number	24
$N_1, N_2 \dots$:	transformer turns ratios	216
P :	active power (W)	22
p :	instantaneous power (VA)	22
p_1 :	normalised value of I_p when $\theta_0 = 0$	62
P_{in} :	active power fed into the system (W)	50
P_{di} :	active power dissipated (W)	50
P_m :	the value of P when $Q = Q_m$ (W)	74
P_R :	active power at the receiving end of a transmission line (W)	27
P_S :	active power at the sending end of a transmission line (W)	27
Q :	reactive power (VA _r)	23

Q_m :	maximum value of Q (VAr)	74
Q_r :	reactive power at the receiving end of a transmission line (VAr)	27
Q_s :	reactive power at the sending end of a transmission line (VAr)	27
q_1 :	normalised value of I_q when $\theta_0 = 0$	62
q_2 :	dependence of the variation of I_q and I_p with θ_0	62
q_3 :	constant in derivation of I_p and I_q . $q_3 = 0$ for all circuits	201
R :	resistance (Ω)	36
R_T :	transmission line resistance (Ω)	26
S :	apparent power (VA)	23
sinna:	$f(n)$ used in 24-pulse algebra	255
sinnb:	$f(n)$ used in 24-pulse algebra	255
s_n :	dependence of the variation of t_n with θ_0	66
t :	time (s)	21
t_n :	normalised value of I_{nc}	66
[V]:	voltage column matrix (V)	215
V :	rms phase to phase system voltage (V)	174
V_+ :	potential of the positive terminal of the capacitor (V)	197
$V_{1\dots}$:	negatives of the constants in the six pulse equivalent circuit (V)	207
V_{ab} :	blue phase secondary voltage on first transformer (V)	210
V_{ad} :	additional source in three phase equivalent circuit (V)	93
V_{ar} :	red phase secondary voltage on first transformer (V)	117
V_{av} :	average voltage across the capacitor (V)	104
V_{ay} :	yellow phase secondary voltage on first transformer (V)	210
V_B :	blue phase to neutral voltage (V)	25
V_{bb} :	blue phase secondary voltage on second transformer (V)	210
V_{bbn} :	potential of V_{bb} relative to earth (V)	210
V_{br} :	red phase secondary voltage on second transformer (V)	117
V_{bmn} :	potential of V_{br} relative to earth (V)	210
V_{BX} :	potential in blue phase series transformer primary (V)	222
V_{BY} :	potential in blue phase series transformer primary (V)	249
V_{by} :	yellow phase secondary voltage on second transformer (V)	210
V_{byn} :	potential of V_{by} relative to earth (V)	210
V_{BZ} :	potential in blue phase series transformer primary (V)	249
V_c :	voltage across the capacitor (V)	58
V_{cb} :	blue phase secondary voltage on third transformer (V)	235
V_{cbn} :	potential of V_{cb} relative to earth (V)	235
V_{cr} :	red phase secondary voltage on third transformer (V)	235
V_{crn} :	potential of V_{cr} relative to earth (V)	235
V_{cy} :	yellow phase secondary voltage on third transformer (V)	235

V_{cyn} :	potential of V_{cy} relative to earth (V)	235
V_{db} :	blue phase secondary voltage on fourth transformer (V)	235
V_{dbn} :	potential of V_{db} relative to earth (V)	235
V_{dc} :	constant voltage across the d.c. terminals of VSI (V)	35
V_{dr} :	red phase secondary voltage on fourth transformer (V)	235
V_{dm} :	potential of V_{dr} relative to earth (V)	235
V_{dy} :	yellow phase secondary voltage on fourth transformer (V)	235
V_{dyn} :	potential of V_{dy} relative to earth (V)	235
V_{ec} :	voltage across the capacitor in the equivalent circuit (V)	70
V_H :	horizontal axis describing voltage plane (V)	25
V_I :	voltage at the a.c. terminals of the converter (V)	35
V_i :	magnitude of the fundamental component of V_I (V)	36
V_{IP} :	V_I as seen from the primary side of the transformers (V)	120
V_m :	peak of V_I on secondary of transformers (V) (peak of system voltage in single and three phase circuits)	21
V_N :	potential of neutral of second transformer (V)	209
V_n :	component of the voltage of frequency $n\theta$ (V)	25
$V_{n1\dots}$:	potentials of neutral points on transformers	249
V_R :	red phase to neutral voltage (V)	25
V_r :	rms voltage at the receiving end of a transmission line (V)	26
V_{RX} :	potential in red phase series transformer primary (V)	118
V_{RY} :	potential in red phase series transformer primary (V)	249
V_{RZ} :	potential in red phase series transformer primary (V)	249
V_S :	system voltage (V)	21
V_s :	rms voltage at the receiving end of a transmission line (V)	26
V_{SQ} :	square wave voltage source (V)	71
V_{sq} :	magnitude of V_{SQ} (V)	191
V_V :	vertical axis describing voltage plane (V)	25
V_Y :	yellow phase to neutral voltage (V)	25
V_{YX} :	potential in yellow phase series transformer primary (V)	222
V_{YY} :	potential in yellow phase series transformer primary (V)	249
V_{YZ} :	potential in yellow phase series transformer primary (V)	249
V_Z :	voltage across Z (V)	49
V_z :	magnitude of V_Z (V)	50
X_C :	reactance of C at the supply frequency (Ω)	58
X_E :	equivalent reactance of N sets of X_L (Ω)	177
X_L :	reactance of L at the system frequency (Ω)	36
X_T :	transmission line reactance at the system frequency (Ω)	26
Y_C :	susceptance of C at the system frequency (S)	69

Z:	impedance between V_I and V_S (Ω)	37
$Z(n)$:	$R + jnX_L - j\frac{XC}{n}$ (Ω)	191
Z_b :	base impedance (Ω)	175
β :	damping factor = $\frac{R}{2X_L}$	51
γ :	$\tan^{-1} \frac{\beta^2+k^2-1}{2\beta}$ (rad) (γ is in the range $-\pi/2 < \gamma < \pi/2$)	58
γ_n :	$\tan^{-1} \frac{\beta^2+k^2-n^2}{2\beta n}$ (rad) (γ_n is in the range $-\pi/2 < \gamma_n < \pi/2$)	188
δ :	phase angle along a transmission line (rad)	26
ε :	$\tan^{-1} \frac{R}{X_L}$ (rad)	37
η :	angle between I_1 and V_S (rad)	21
η_n :	angle between I_n and V_S (rad)	24
θ :	phase of V_S (rad)	21
θ_0 :	firing angle of converter (rad)	38
θ_{ob} :	reduced firing angle (rad) = $\frac{\theta_0}{\beta}$	51
κ :	constant giving the effective value of X_L as seen by C	171
μ :	phase of V_Z (rad)	49
ϕ :	phase of V_I (rad) = $\theta - \theta_0$	50
ψ_n :	angle between V_n and ϕ (rad)	223
ω :	angular frequency of the system (rad s ⁻¹)	21
ADC:	analogue to digital converter	96
CSI:	current sourced inverter	34
EPROM:	erasable programmable read only memory	96
GTO:	gate turn off (thyristor)	33
MCT:	metal oxide semiconductor controlled thyristor	33
MOSFET:	metal oxide semiconductor field effect transistor	95
NGC:	National Grid Company plc	31
PLL:	phase locked loop	96
PWM:	pulse width modulation	70
STATCON:	static converter	34
SVC:	static VAr compensator	31
THC:	total harmonic content	65
VSI:	voltage sourced inverter	34

Chapter 1

Introduction

As a preamble to presenting the work on the application of converter circuits to reactive power compensation, this chapter reviews the definitions of active and reactive power flows and the role of reactive power flow in the control of voltage on a transmission grid, starting with elementary considerations.

§1.1 Definition of Reactive Power

Given a sinusoidal supply voltage applied to a load the resulting current can either be of a single frequency or of multiple frequencies depending on whether the load is linear or non-linear.

Figure 1.1 shows a load with a sinusoidal system voltage of V_S resulting in a current of I . The direction of positive current flow is defined to be out of the positive terminal of the voltage source and into the load.

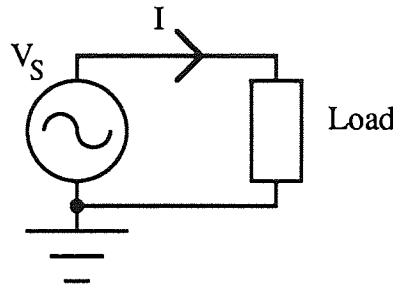


Figure 1.1. A Sinusoidal Voltage Source Feeding a Linear Load.

If the load is linear then, in the time domain, the voltage and current can be expressed as

$$V_S = V_m \sin \theta \quad (1.1)$$

and
$$I = I_m \sin(\theta - \eta) = I_m [\sin \theta \cos \eta - \cos \theta \sin \eta] \quad (1.2)$$

where

I_m is the peak of the current,

V_m is the peak of the supply voltage,

η , or often ϕ , is the angle between the current and the voltage,

$\theta = \omega t$,

ω is the angular frequency of the supply

and t is time.

The system voltage is the reference; η is the angle by which the current is ahead of, or behind, the system voltage. A positive value for η means that the current lags on the system voltage and a negative value means that the current leads the system voltage.

Figure 1.2 is a phasor diagram for a general supply voltage and current adopting the conventional (anti-clockwise) direction of rotation. In the figure the current is lagging on the system voltage.

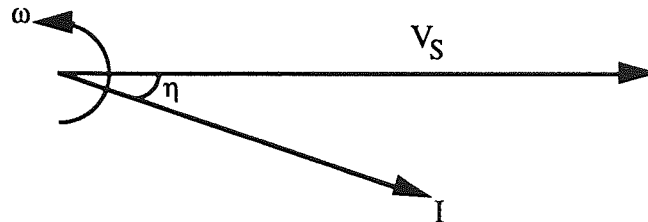


Figure 1.2. General Phasor Diagram for a Lagging Current.

The instantaneous power fed into the load, p , is the product of the voltage and the current:

$$p = V_m I_m \sin\theta \sin(\theta - \eta) \quad (1.3)$$

The units of p are Volt-Amperes, VA.

Expanding (1.3) and simplifying gives

$$p = \frac{V_m I_m}{2} [\cos\eta - \cos(2\theta - \eta)] \quad (1.4)$$

There are thus two components to the instantaneous power, the first of which is independent of the phase of the supply and the second of which is an oscillation at twice the supply frequency. The average of this second component is zero; it cannot do any useful work. It corresponds to an oscillatory energy exchange between the system and the load at twice the frequency of the supply.

The active power fed into the load, P , is the average, over a cycle, of the instantaneous power:

$$P = \frac{1}{2\pi} \int_0^{2\pi} p \, d\theta \quad (1.5)$$

The units of P are Watts, W.

From equation (1.4)

$$P = \frac{V_m I_m}{2} \cos\eta \quad (1.6)$$

The active power is the product of the rms value of the system voltage and the rms value of the component of current which is in phase with the system voltage.

The term $\cos\eta$ is generally referred to as the power factor.

The apparent power, S , is the value of the active power when $\eta = 0$:

$$S = \frac{V_m I_m}{2} \quad (1.7)$$

The units of apparent power are Volt–Amps, VA.

For a single frequency voltage and a linear load the reactive power flowing into the load, Q , is defined as the product of the rms value of the system voltage and the negative of the rms component of the current which is leading the system voltage by $\pi/2$ rads:

$$Q = \frac{V_m I_m}{2} \sin\eta \quad (1.8)$$

The units of Q are Volt–Amperes reactive, VAR.

The negative of the current component was used to satisfy convention: if the current is lagging on the system voltage then $\sin\eta$ is positive, reactive power is said to be absorbed by the load and Q is taken as positive. If the current leads the supply voltage then reactive power is generated in the load and Q is taken as negative.

This definition is useful because of the role of Q in system analysis. In particular, its use in the control of system voltage, section 1.2i, and in calculating the steady state power flows through a transmission grid, since reactive power is conserved.

The relationships between the three powers, apparent, active and reactive, are illustrated in the vector diagram of figure 1.3, again using a positive value for η .

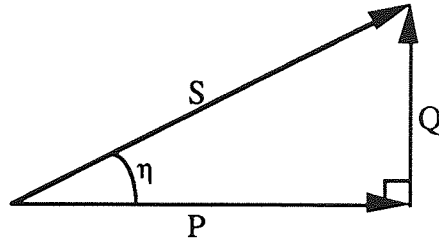


Figure 1.3. Power Vector Diagram.

These definitions are given in almost any basic text on electrical engineering (Hughes, 1987, Chpt. 7), (Weedy, 1987, Chpt. 2) etc.

In the case of a non-linear load then the current has harmonics and can be expressed as

$$I = \sum_{n=1}^{\infty} |I_n| \sin(n\theta - \eta_n) \quad (1.9)$$

where

I_n is the component of I of frequency $n\theta$,

and η_n is the angle between I_n and the supply voltage.

Following the same algebra outlined above gives

$$p = \frac{V_m I_m}{2} [\cos\eta - \cos(2\theta - \eta)] + \frac{V_m}{2} \sum_{n=2}^{\infty} |I_n| \{ \cos[(n-1)\theta + \eta_n] - \cos[(n+1)\theta - \eta_n] \} \quad (1.10)$$

where

I_m is the peak of the fundamental component of the current.

In this thesis the term reactive power has been used for the fundamental component of reactive power, as defined in equation (1.8), even when considering distorted current waveforms. The harmonics have been considered separately.

In considering three phase compensators, several definitions have been adopted for the reactive power. The method of Akagi, Kanazawa and Nabe (Akagi et al., 1984) and that of Schauder and Mehta (Schauder and Mehta, 1993) both involve defining two vector planes, one each for voltage and current, based on the three phase axes, V_R , V_Y and V_B in the voltage vector plane, and plotting the instantaneous voltage and current in these planes, as shown in figure 1.4. Each of the planes can then be defined using a

two axis system, V_H (coincident with V_R) and V_V in the voltage vector plane. The active power is defined as the vector sum of the products of the voltage and the component of the current along the same axis ($V_H I_H + V_V I_V$) and the reactive power as the vector sum of the products of the voltage and the component of the current along the axes in quadrature ($V_H I_V - V_V I_H$).

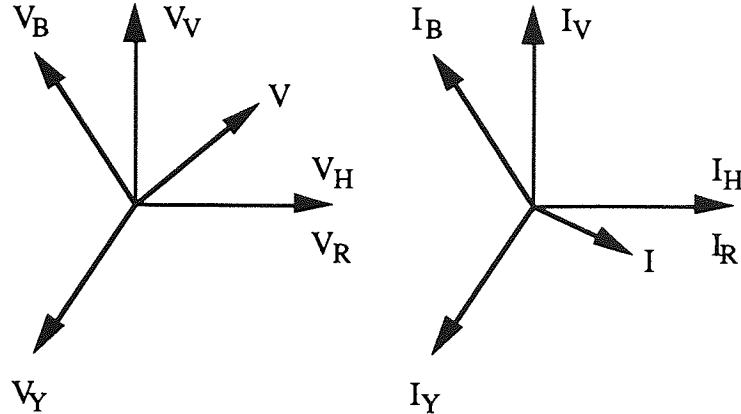


Figure 1-4. Definition of Voltage and Current Vector Planes.

Sometimes the reactive power is defined as the sum, over all frequencies, of the product of the voltage and the component of the current of the same frequency in quadrature (Shepherd & Zand, 1979, Section 9.1):

$$Q = \sum_{n=1}^{\infty} |V_n| |I_n| \sin \eta_n \quad (1.11)$$

where

V_n is the component of the voltage of frequency $n\theta$

Thus this definition depends upon the sum over all frequencies of the "reactive power" at each frequency. It is shown therein that this definition does not give the most suitable value of compensation components to minimise the difference between the apparent power and the average power so an alternative definition, based upon the product of the sum of the squares of the rms values of the components of the current in quadrature with the components of the voltage at a particular frequency and the sum of the squares of the rms voltage, is proposed (ibid., Section 9.3):

$$Q = \sqrt{\left(\sum_{n=1}^{\infty} V_n^2 \right) \left(\sum_{n=1}^{\infty} |I_n|^2 \sin^2 \eta_n \right)} \quad (1.12)$$

§1.2 The Role of Reactive Power Compensation

Having established what reactive power is, its use in electric power networks is now considered.

The control of the flow of reactive power has four main purposes:

- i) to improve the voltage regulation;
- ii) to achieve the maximum possible active power transfer;
- iii) to facilitate load balancing;
- iv) to reduce flicker.

i) Improvement in Voltage Regulation.

The voltage regulation can be defined as the deviation in the voltage from its nominal value. The voltage of the transmission network of England and Wales is specified to lie within $\pm 10\%$ of the nominal voltage, 400kV or 275kV (The Grid Code, 1994, Connection Condition 6.1.4).

In the simplest a.c. system a transmission line connects a generator to a load. The line is modelled by its inductance at the system frequency, X_T , and its resistance, R_T . The rms value of the voltage at the generator, i.e. the sending end, is denoted V_s and that at the receiving end V_r . The phase difference between the voltages at the sending and receiving ends is known as the transmission angle, δ .

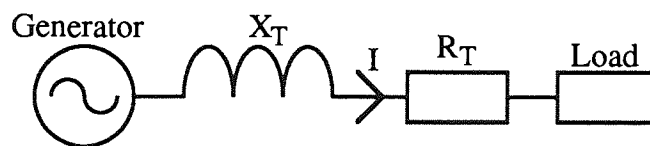


Figure 1.5. Single Load Model of a Transmission Line.

The phasor diagram for the system is shown in figure 1-6.

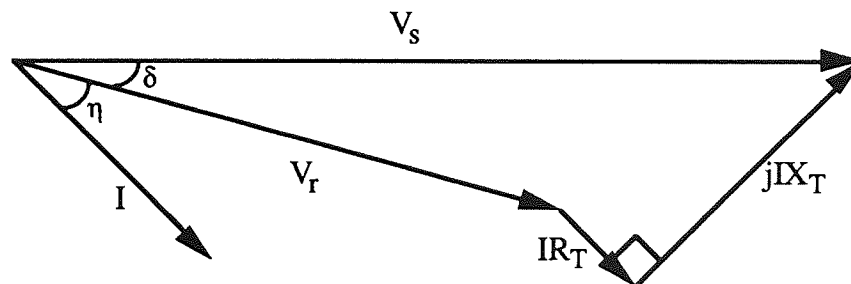


Figure 1.6. Phasor Diagram for the Single Load Model of a Transmission Line.

Applying Pythagoras' theorem to the phasor diagram gives

$$V_r^2 = [V_s - IR_T \cos(\delta + \eta) - IX_T \sin(\delta + \eta)]^2 + [IX_T \cos(\delta + \eta) - IR_T \sin(\delta + \eta)]^2 \quad (1.13)$$

The active and reactive powers received at the end of the line and injected into the load, from (1.6) and (1.8), are given by

$$P_r = V_r I \cos \eta \quad (1.14)$$

$$Q_r = V_r I \sin \eta \quad (1.14a)$$

The active and reactive power sent into the line and the load are given by

$$P_s = V_s I \cos(\delta + \eta) \quad (1.15)$$

$$Q_s = V_s I \sin(\delta + \eta) \quad (1.15a)$$

Substituting (1.15) and (1.15a) in (1.13) gives

$$V_r^2 = \left(V_s - \frac{R_T P_s}{V_s} - \frac{X_T Q_s}{V_s} \right)^2 + \left(\frac{X_T P_s}{V_s} - \frac{R_T Q_s}{V_s} \right)^2 \quad (1.16)$$

In general the resistance of a transmission line is very much less than the reactance and so the terms involving R_T in (1.16) can be neglected (Weedy, 1987, table 3.2a) so $P_s = P_r = P$. In addition, for lines other than very long ones, i.e. less than several hundred km, under all power transfer conditions,

$$V_s^2 - X_T Q_s \gg X_T P_s \quad (1.17)$$

Thus equation (1.14) can be written

$$V_r \approx V_s - \frac{X_T Q_s}{V_s} \quad (1.18)$$

The voltage difference along the line is mainly a function of the reactive power transmitted; when the load is absorbing reactive power the voltage at the receiving end of the line falls, but it rises when the load is generating reactive power.

The reactive power generated or absorbed by the system, and therefore the voltage at the receiving end of the load, can thus be altered by adding (capacitive or inductive) circuits in parallel with the load. Figure 1.7 shows the transmission line of figure 1.5 with a reactive power compensator drawing a current, I_{comp} , from the line. This current is defined to be positive flowing out of the positive terminal of the voltage source, i.e. the compensator is regarded as a load on the system and the current is defined in the same way as for a general load, figure 1.1.

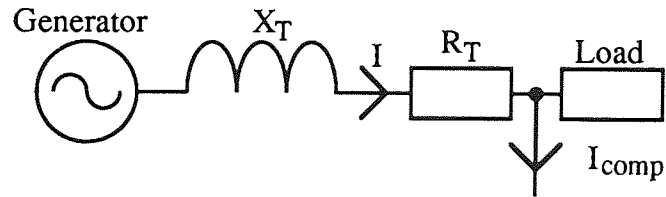


Figure 1.7. A Transmission Line with Reactive Power Compensation.

If the current, I_{comp} , is made to lead on the voltage at the receiving end of the line then reactive power is generated at the load end of the line and the voltage rises; if I_{comp} lags on V_r then V_r will be reduced. If the compensator current is exactly in quadrature with the receiving end voltage then there is no exchange of active power between the compensator and the load.

As generators or very large loads are added or removed the voltage at a point on the transmission network will be altered. Control of the reactive power flow along the line can therefore be used to prevent the voltage at a point on the system falling outside of the permitted range.

From figure (1.6) the angle between the sending end and receiving end voltages can be calculated from

$$\sin\delta = \frac{X_T P_s - R_T Q_s}{V_r V_s} \quad (1.19)$$

Again neglecting the term in R_T gives

$$P \approx \frac{V_r V_s}{X_T} \sin\delta \quad (1.20)$$

The active power transmitted depends upon the phase difference along the line and on the (nearly constant) voltages at the sending and receiving ends of the line.

These formulae relating the active and reactive power flows to the magnitudes of the voltages and the transmission angle through the parameters of the line can be found in standard texts on power systems (Weedy, 1987, section 2.7).

ii) Increase in Active Power Flow

The control of reactive power flow, and therefore of voltage, can be used to achieve the maximum active power that can be transmitted along a line without loss of stability.

As an example of this, consider a lossless transmission line with a purely resistive load, i.e. as in figure 1.5 but with $R_T = 0$. In figure 1.6 then, $\eta = 0$ and $V_r = V_s \cos\delta$.

Substituting for V_r in equation (1.20) gives

$$P = \frac{V_s^2}{X_T} \sin\delta \cos\delta \quad (1.21)$$

$$= \frac{V_s^2}{2X_T} \sin 2\delta \quad (1.21a)$$

For maximum power transmission δ is $\pi/4$ radians. δ is restricted to be in the range $0 \leq \delta \leq \pi/4$ to prevent voltage collapse. In practice, the range of δ will be less than this to allow for transients. Of course, the power flow may be limited by the current carrying capability of the line.

If a reactive power compensator is introduced at the receiving end of the line, as in figure 1.7, then the voltage at the receiving end can be increased. As an example, assume that the compensator acts to sustain the voltage at the receiving end of the line so that $V_r = V_s$.

The active power transmitted is thus, from equation (1.20),

$$P = \frac{V_s^2}{X_T} \sin\delta \quad (1.22)$$

Comparing equations (1.21a) and (1.22) it is apparent that the maximum active power transmitted has been increased by a factor of 2, and now occurs at an angle of $\pi/2$.

iii) Load Balancing.

This is ensuring that the currents drawn by all of the phases of the system are of the same magnitude and have the same phase relationship as the applied voltage (Miller, 1982, section 1.9). In a multiple phase transmission system unbalance can cause, amongst other effects, saturation of transformer cores and excessive neutral currents (ibid., section 1.2). The permissible phase unbalance on the transmission grid of England and Wales is 1% negative sequence components (The Grid Code, 1994, Connection Condition 6.1.5b). Converter types of compensator have been used for this role (Liang et al., 1991).

iv) Flicker Reduction.

Flicker is the visible fluctuations in the luminosity of electric lighting due to the switching of large loads. Of particular concern are arc furnaces connected to the transmission grid at points of low short circuit capacity. The compensator is then usually sited adjacent, i.e. at the same electrical node, to this equipment and uses fast acting control to reduce these voltage variations (Miller, 1982, Chpt. 9).

§1.3 Motivation

This research is prudent at this time because the voltage and current ratings of gate turn off thyristors are continuing to increase and are now at the levels where they could be of use in the transmission of electricity (McMurray, 1987). The technical feasibility of using force-commutated converter circuits for reactive power control has been known for at least 25 years (Heumann, 1966) but it is only recently that self-commutating devices with sufficient power ratings have become available and led to the possibility of producing equipment of adequate rating.

Conventional thyristors have been used in some cases (Sumi et al., 1981), (Walker, 1986), (Epstein et al., 1986) but the commutation circuits were widely viewed as being too complex (Gyugyi et al., 1990). The largest of these equipments was 20MVA whereas a practical equipment would be around 100MVA.

In addition the solution to a problem in the transmission of electricity is not a purely technical matter. Systems cannot be extended as grid system operators feel it necessary: there are concerns about the environment, rights of way etc. Thus there is a need to use existing lines more effectively.

Also, in England and Wales, following the decomposition and subsequent privatisation of the Central Electricity Generating Board, generation and transmission have been separated. Transmission is now the responsibility of the National Grid

Company (NGC). This means that the generators can site a power station based solely on their costs, including NGC's connection charge, and NGC has to compensate for any reactive power demands that the siting of the power station in that particular place produces. Thus the need for reactive power compensation has increased over recent years and is expected to increase still further (Bradley, 1993).

§1.4 Equipment used for Reactive Power Compensation

The role of reactive power in a transmission network is now understood and so it is instructive to consider the equipment that has been used to do this in the past and the relative advantages and disadvantages of the various types of equipment so that the relative merits of the converter circuits, the performance of which is to be discussed in this thesis, can be assessed.

Reactive power compensators may be classified as either static or rotating. The rotating equipment is the synchronous condenser. Static equipments in use at the present time, apart from the converter circuits to be discussed, are mechanically switched capacitors (MSC) and inductors, or reactors (MSR), saturated reactors (SR), thyristor switched capacitors (TSC) and thyristor controlled reactors (TCR). Compensators are often made by combining a number of the above equipments. In particular most static VAR compensators (SVCs) are made up of thyristor switched capacitors and thyristor controlled reactors. A review of the static VAR compensators in use worldwide was carried out in 1986 (Erinmez, 1986).

i) Synchronous Condenser

This is a synchronous machine connected to the mains. It is able to generate or absorb reactive power depending on the excitation applied to the field windings (Hindmarsh, 1977, Section 8.6).

The disadvantages of this type of machine are the same as those of all electrical machines:

- 1) They have high ohmic losses in the stator and rotor windings.
- 2) They are large and relatively expensive.
- 3) They have high maintenance costs.

The main advantage of this particular equipment in reactive power compensation is that it can raise its output under highly reduced voltage conditions by an increase in the applied excitation. It does not produce any significant harmonics.

ii) Static VAr Compensator

The use of thyristor technology has enabled the on load connection of capacitors and point on wave switching of inductors to generate or absorb reactive power (Mohan et al., 1989, section 16.3). Point on wave switching is not used for the capacitor elements of the SVC because of the inrush currents into the capacitors. Instead, if in bringing the capacitors into the circuit, the reactive power generated is excessive then the inductors are also brought into circuit and point on wave switching of the inductors allows the excess generation to be trimmed off.

The advantages of this type of equipment are:

- 1) It has no moving parts, so wear is small.
- 2) It has low losses, compared with the synchronous condenser.

The disadvantages of this type of equipment are:

- 1) Under reduced voltage conditions, if the equipment is already operating at full reactive power generation, then the output will decrease instead of increasing to support the voltage.
- 2) The equipment generates significant harmonics.

iii) Saturated Reactors

These compensators are used to reduce flicker, because of their ability to sustain a constant voltage, independently of the current that is drawn. This is clearly an advantage in flicker reduction but makes them unsuitable for transmission networks because the voltage is constant at the supply voltage.

In addition to these equipments there are a number of other equipments such as the "power doubling VAr generator" and the "ac/ac frequency changer" (Gyugyi, 1981). These have not found application on transmission networks, probably because of the large number of devices required and the harmonics that are generated.

All of these equipments are connected in shunt with the power system. Series compensation of transmission lines is also used. This consists of adding capacitors into the transmission line to reduce the reactance of the line. This enables higher maximum power flows, although shunt inductive compensation is often necessary to limit the voltage (Miller, 1982, Section 2.5), (Weedy, 1987, section 5.4).

§1.5 Ideal Characteristics

Before considering the performance of the converter circuits it is worth considering the steady state properties of an ideal compensator as a reference equipment. An ideal compensator would

- a) be able to generate or absorb a given amount of reactive power under any voltage conditions.
- b) be of low initial cost.
- c) have low losses.
- d) be small. This would mean that the site costs would be low.
- e) be portable so that as generating stations, or large loads, were commissioned or closed down the compensation equipment could be relocated at the most appropriate place in the new system.
- f) not generate any harmonics.

§1.6 Devices

The terms thyristor, gate turn off thyristor, GTO thyristor, GTO and switch have been used interchangeably in this thesis for any device, or parallel and/or series connected string of devices, with self-commutation capability or with suitable forced commutation circuits.

In addition to the GTO thyristor other devices may become available in the near future. Of particular interest is the MOS Controlled Thyristor (MCT) which, it is hoped, will be simpler to turn on and off, will have a lower gate current, lower losses than GTOs that are available at present, and will be able to switch at higher frequencies (Le Du et al., 1992)

Although the term thyristor has been used in this thesis the work is valid for any switch. The symbol used for this general device is shown in figure 1.8.

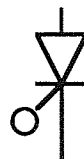


Figure 1.8. Symbol for a General Device which can be Turned On and Off.

§1.7 Nomenclature

There are several different names used in the literature for the type of reactive power compensator to be studied in this thesis. These include

Advanced static VAR compensator (ASVC)
STATCON (from static converter)
Static VAR Generator (SVG)
Advanced Static VAR Generator (ASVG)
Self- and Line-Commutated Converter Compensators (SCC and LCC)
Voltage and Current Sourced Inverter Compensator (VSI and CSI)
Gate turn-off (GTO) based converters
GTO static VAR Compensator (GTO-SVC)
Converter Compensator (CONCOM)
Shunt Converter Compensator (ShuntCom)

The term STATCON has been used in the most recent literature and is used in this thesis.

§1.8 Aims

The purpose of this thesis is to establish the steady state performance of some of the converter circuits which can be used for reactive power compensation and to discuss the factors which influence the economics of choosing that most applicable to the high power transmission environment.

Of particular interest are:

- 1) the choice of a suitable control parameter to vary the reactive power,
- 2) the losses as a function of the reactive power output,
- 3) the harmonics generated by the equipment,
- 4) the size of the energy storage components in the equipment.

I have used an exact analysis method to be confident of the range of validity of the findings and to understand the source of the features of the characteristics.

Experimental work on low power models has been used to validate the theoretical findings and assumptions. Simulation studies have also been used to verify the theoretical results and have provided useful guidance in the work; where appropriate the simulation results are included.

Performance of VSI and CSI Types of the Single Phase STATCON using Voltage and Current Sources

§2.1 Introduction

In this chapter the operation of the two types of single phase static converters (STATCONs) using voltage and current sources is detailed. The sources are taken to be ideal and of variable amplitude. Knowledge is assumed about the basic operation of inverter circuits. There are a large number of available texts on this topic (Lander, 1987, Chpt. 5), (Williams, 1992, Chpt. 14) etc.

§2.2 Circuit Description of the Voltage Sourced Inverter Type of STATCON

The circuit consists of a voltage sourced inverter (VSI) with the a.c. terminals connected to the system through some inductance which will have resistance. The inductance, L , may be introduced deliberately or may be the leakage reactance of a transformer or a combination of the two. The d.c. side has a constant voltage source, i.e. a battery, connected across it. The circuit for a single phase equipment is given as figure 2.1.

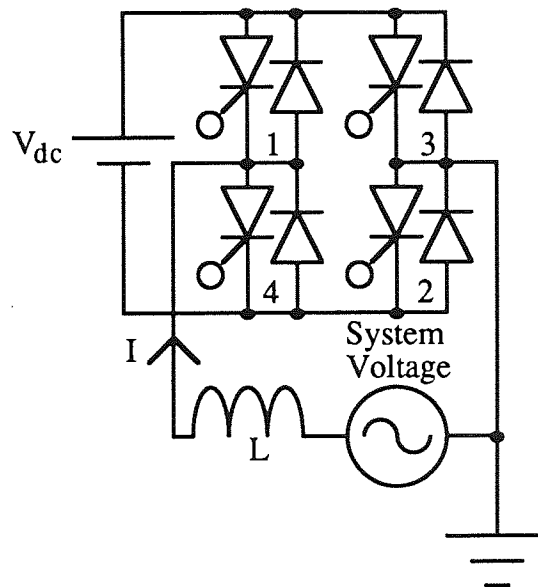


Figure 2.1. Single Phase Voltage Sourced STATCON with Battery.

As in a conventional single phase inverter the devices are switched in pairs with diagonally opposite devices being turned on together; 1 and 2 then 3 and 4. One pair of devices is turned on for 180° and is then turned off for 180° ; there is always one pair of devices turned on and one pair turned off. The voltage produced, with a constant voltage source, at the a.c. terminals of the inverter, V_I , is a square wave with the same

fundamental frequency as the system. The equivalent circuit is shown in figure 2-2. The resistance in the circuit is that associated with the inductance plus twice that in one of the devices, as discussed in Appendix 1. The resistance of a device when turned off has been taken as infinite. The on state voltage drop in the devices has been neglected therefore the impedance between the two voltage sources is linear. The reactance of the inductance at the supply frequency is X_L .

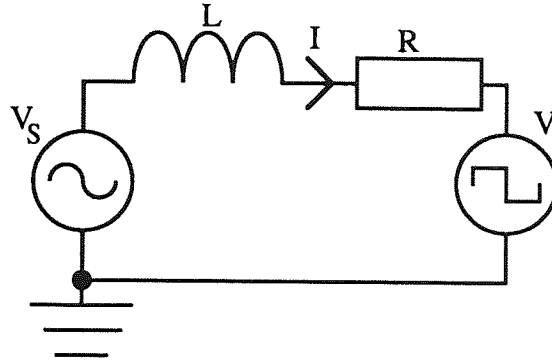


Figure 2-2. Equivalent Circuit of a Single Phase STATCON with Battery.

§2-3 Performance of the Voltage Sourced Inverter Type of STATCON

The performance of the circuit depends upon the firing angle of the inverter. The discussion is therefore separated into three parts: with the inverter operated so that the fundamental component of the voltage at the inverter output terminals is in phase with the system voltage, with the two voltages in anti-phase, and with a general phase angle between the two voltages.

a) Zero Firing Angle

The voltage at the a.c. terminals of the inverter is in opposition to the system voltage; the net voltage across the inductance and resistance is the difference between the system voltage and the inverter output voltage.

If the magnitude of the fundamental frequency component of the voltage at the a.c. terminals of the inverter, V_i , where, from Fourier series, $V_i = 4V_{dc}/\pi$, is larger than the magnitude of the system voltage, V_m , then the fundamental frequency component of the net voltage across the impedance, $V_S - V_I$, will be in the opposite sense to the system voltage. The current through an inductor lags the voltage across it so the current in the circuit will lag the net voltage across the impedance but lead the system voltage.

If the system voltage is defined as $V_m \sin \theta$ and the fundamental component of the inverter voltage as $V_i \sin \theta$ then the fundamental component of the current generated, I_1 , is given by

$$I_1 = -\frac{V_m - V_i}{Z} \cos(\theta + \epsilon) \quad (2.1)$$

where

$$Z = \sqrt{R^2 + X_L^2}$$

and $\epsilon = \tan^{-1} \frac{R}{X_L}$ (ϵ is a small positive angle)

The current will lead the system voltage by an angle of slightly greater than 90° , as shown in the phasor diagram of figure 2.3; the negative of the current will lag the inverter output voltage by an angle of slightly less than 90° .

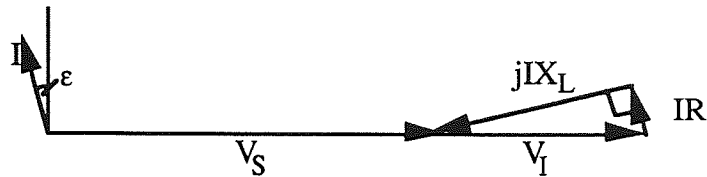


Figure 2.3. Phasor Diagram for Reactive Power Generation in a Single Phase STATCON with Zero Firing Angle.

The current leading the system voltage by an angle greater than 90° means that the direction of active power flow is from the inverter output terminals into the system.

If V_S and V_I are again in phase but V_i is less than V_m then the net fundamental voltage across the impedance will be of the same phase as the system voltage. The current will lag the system voltage as shown in the phasor diagram of figure 2.4. The current is described by equation 2.1.

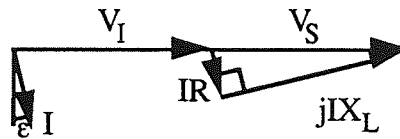


Figure 2.4. Phasor Diagram for Reactive Power Absorption in a Single Phase STATCON with Zero Firing Angle.

The current in figure 2.4 lags the system voltage by an angle of less than 90° ; the direction of active power flow is from the supply to the inverter output terminals.

b) 180° Firing Angle

If the voltage at the a.c. terminals of the inverter is in anti-phase with the system voltage then the net voltage across the inverter is always of the same phase as the system voltage and so the equipment can only absorb reactive power, as shown in the phasor diagram of figure 2-5. The fundamental component of the current is given by

$$I_1 = -\frac{V_m + V_i}{Z} \cos(\theta + \epsilon) \quad (2.2)$$

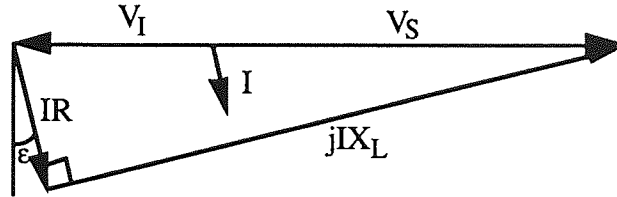


Figure 2-5. Phasor Diagram with a Firing Angle of Pi Rad for a Single Phase STATCON.

c) General Firing Angle.

If the devices are fired so that the a.c. voltage at the inverter terminals is neither in phase nor in anti-phase with the system voltage then the fundamental component of the voltage at the a.c. terminals of the inverter is $V_i \sin(\theta - \theta_0)$ where θ_0 is the firing angle of the inverter. A positive value for θ_0 means that the fundamental component of the inverter output voltage lags the supply voltage and a negative value means that it leads the supply voltage. Figure 2-6 shows a timing diagram for a small positive value of θ_0 .

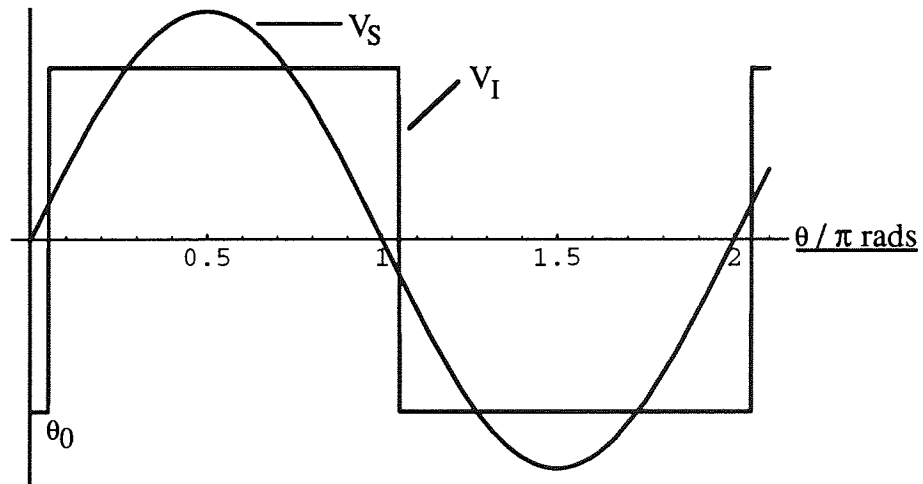


Figure 2-6. Timing Diagram Showing a Positive Firing Angle.

The fundamental component of the current is given by

$$I_1 = -\frac{V_m - V_i \cos \theta_0}{Z} \cos(\theta + \epsilon) + \frac{V_i \sin \theta_0}{Z} \sin(\theta + \epsilon) \quad (2.3)$$

Equations (2.1) and (2.4) are particular cases of equation (2.5), evaluated for $\theta_0 = 0$ and π respectively.

If the inverter were operated with a firing angle which was neither zero nor π then there would be an additional current flow, almost in phase with the system voltage, resulting in increased losses in the system. Phasor diagrams for both positive and negative θ_0 with $V_i > V_m$ and $V_i < V_m$ are given as figure 2.7.

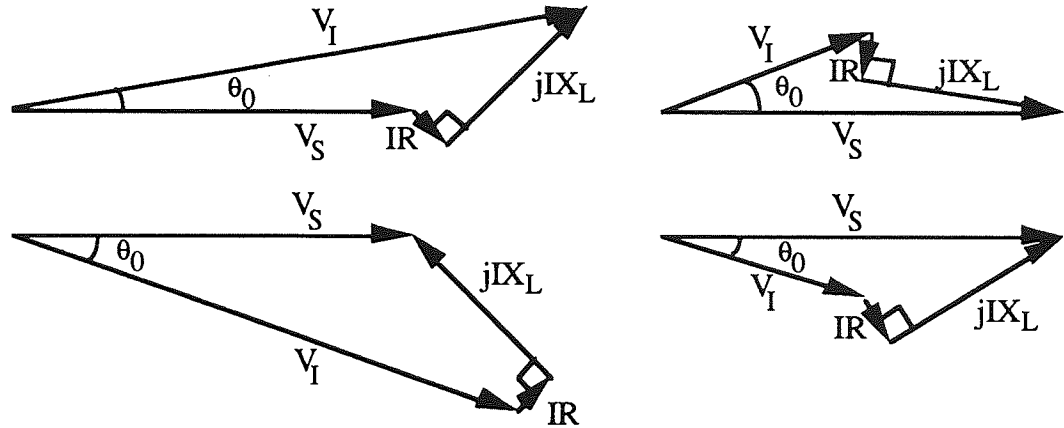


Figure 2.7. Phasor Diagrams for a General Firing Angle.

Thus for minimum losses the inverter is operated with the output voltage either in phase or in anti-phase with the system voltage.

If the system voltage is defined to be 1 per unit (p.u.) and the equipment to have a rating of 1p.u. then, in the case of operating with the voltages in phase, the inductance, to give 1p.u. current, will be small. In the case of operating with the voltages 180° out of phase the inductance must be at least 1p.u. to limit the current to the rated value. Fixed capacitors must also be added so that the compensator can generate and absorb reactive power. To minimise the size of the equipment the firing angle must therefore be zero.

§2.4 System Current Harmonics from a Single Phase VSI Type of STATCON

The supply voltage and impedance generate a current of fundamental frequency which lags the system voltage by almost 90° . The square wave generates a triangular current which leads the system voltage by almost 90° . The net current is the triangular current plus the negative cosine current. Only the odd harmonics will be produced because the square wave voltage and the system voltage are both half wave anti-symmetric functions and therefore the current is also half wave anti-symmetric, see Appendix 1.

The fundamental component of the current with zero firing angle was given in equation (2.1):

$$I_1 = -\frac{V_m - V_i}{Z} \cos(\theta + \epsilon)$$

The coefficient of the fundamental component of the current, I_{1c} , with this firing angle, is defined as

$$I_{1c} = \frac{V_i - V_m}{Z} \approx \frac{V_i - V_m}{X_L} \quad (2.4)$$

Thus I_{1c} is positive if the compensator is generating reactive power and negative when absorbing reactive power. For rated reactive power at the rated system voltage the peak of the current is $\sqrt{2}$ p.u. so I_{1c} is in the range $-\sqrt{2} \leq I_{1c} \text{ p.u.} \leq \sqrt{2}$.

The harmonics in a square wave decrease as $1/n$ so the magnitude of the harmonics, for $n = 4i \pm 1$, with $i = 1, 2, \dots$, are given by

$$|I_n| = \frac{V_i}{n(nX_L + R)} \approx \frac{V_i}{n^2 X_L} \quad (2.5)$$

The approximate value of $|I_n|$ is therefore given by

$$|I_n| \approx \frac{|V_m + I_{1c} X_L|}{n^2 X_L} \quad (2.6)$$

Thus to minimise the magnitude of the harmonics X_L should be large.

Figures 2-8a and 2-8b show digital computer simulations of the steady state performance of the circuit with the output voltage in phase with the system voltage. The inductance was taken as 0.2p.u. and the rms value of V_S as 1p.u. The first figure shows the fundamental of the square wave 1.2 times the system voltage and the second shows the fundamental of the square wave 0.8 times the system voltage. The graphs show generation and absorption of 1p.u. reactive power respectively. This value of inductance is a typical value for the leakage reactance of a large power transformer (Weedy, 1987, Table A.2.4). The X/R ratio of the inductance was taken as 50 and the on state resistance of the devices was taken as 0.001p.u. The volt drop in the devices was taken as zero. The simulations were performed using the Saber[†] suite of commercial simulation software.

The dashed line is the system voltage and the solid line is the current out of the positive terminal of the system voltage. This convention is used in all of the simulation results in the thesis.

In the case of rated reactive power generation the current can be regarded as a triangular current of 6p.u. less a cosine current of 5p.u. When absorbing rated reactive power the triangular component to the current is 4p.u. The peaks in the current waveform are directed away from the x-axis when the equipment is generating reactive power but are directed towards the x-axis when absorbing reactive power. The peaks are more prominent in figure 2-8a.

[†] Saber is a trademark of Anology, Inc.

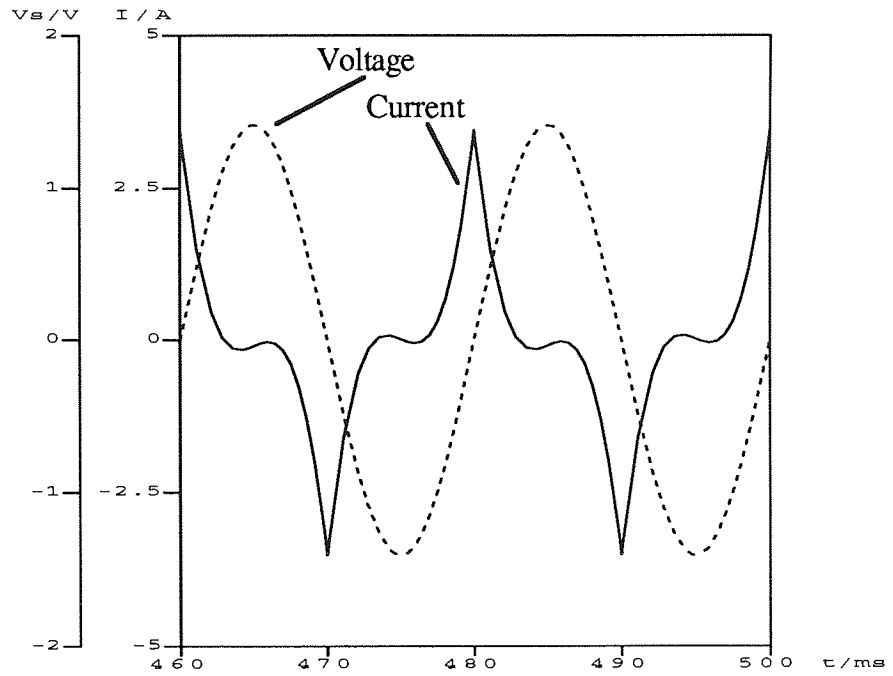


Figure 2-8a. Simulation of the Steady State Performance of the VSI Type of Single Phase STATCON with the Inverter Output 20% Greater than the Supply Voltage.

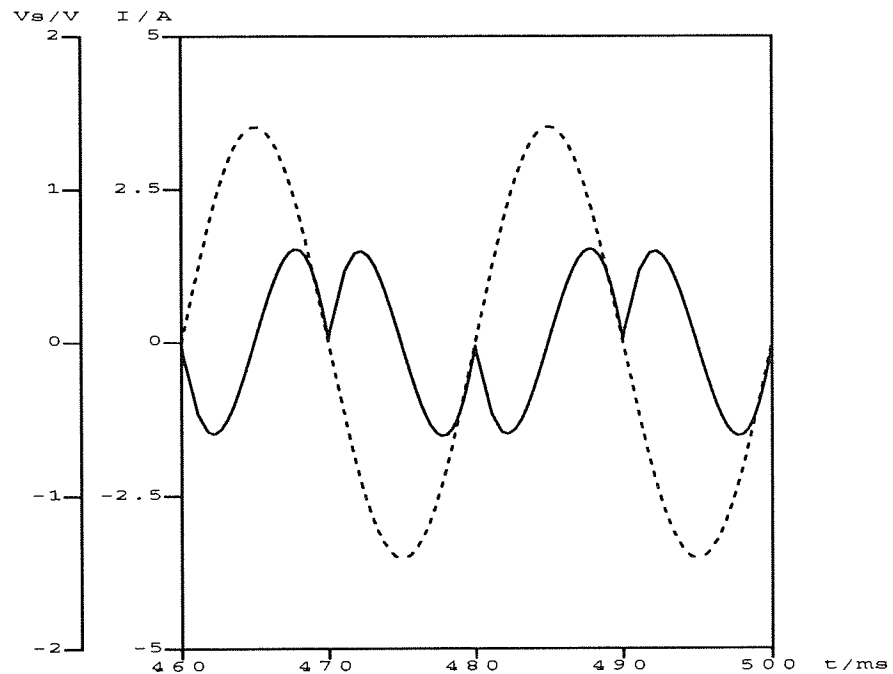


Figure 2-8b. Simulation of the Steady State Performance of the VSI Type of Single Phase STATCON with the Inverter Output 20% Smaller than the Supply Voltage.

§2.5 Current Sourced Inverter Type of STATCON

The circuit is given as figure 2.9. It differs from the voltage sourced circuit in that it does not have anti-parallel (reactive) diodes. This is because, in this circuit, the current always travels through the device that is turned on. In the voltage sourced inverter, when a particular device is turned on, if the current is not in phase with the inverter output voltage, i.e. the load is partly reactive, then at some stage during the half-cycle the direction of the current reverses hence anti-parallel diodes are necessary. The controllable devices are assumed to be of the symmetric type, i.e. they can withstand being reverse biased (Mohan et al., 1989, Chpt. 24).

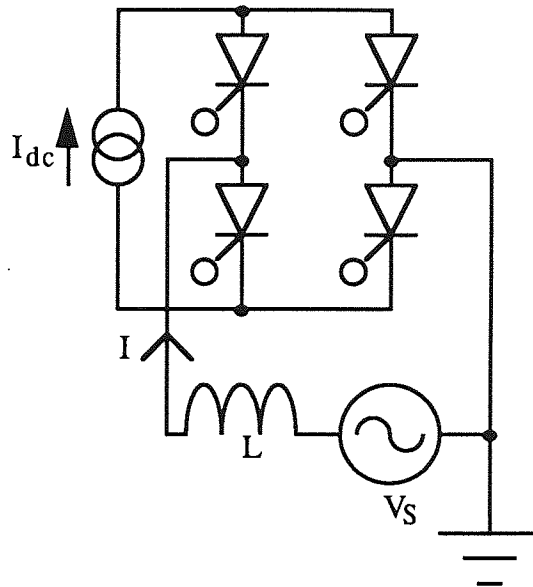


Figure 2.9. Single Phase Current Sourced STATCON with Constant Current Source.

The diagonally opposite pairs of thyristors are again fired together and again one pair is turned on for 180° and is then turned off for 180° ; a square wave current is generated at the a.c. terminals of the inverter.

To generate reactive power with minimum losses the fundamental component of the current, I_1 , must lead the system voltage by $\pi/2$ rads so thyristors 3 and 4 are turned on quarter of a cycle before the system voltage rises through zero. To produce a current which is lagging on the supply voltage by $\pi/2$ rads thyristors 3 and 4 are turned on quarter of a cycle after the system voltage rises through zero. The reactive power is varied between -1 p.u. and $+1$ p.u., at the rated system voltage, by varying the value of the d.c. current source in the range $0 < I_{dc} \text{ (p.u.)} < \pi/(2\sqrt{2})$.

Again only odd harmonics are generated in the system current, they decrease with increasing harmonic number as $1/n$. For $n = 4i \pm 1$, the magnitude of a harmonic in the system current of order n is given by

$$|I_n| = \frac{|I_1|}{n} \quad (2.7)$$

Figures 2.10a and b show simulated results of 1p.u. reactive power generation and absorption respectively, using the same parameter values that were used to produce figure 2.8. Again the solid line is the system current and the dotted line is the system voltage.

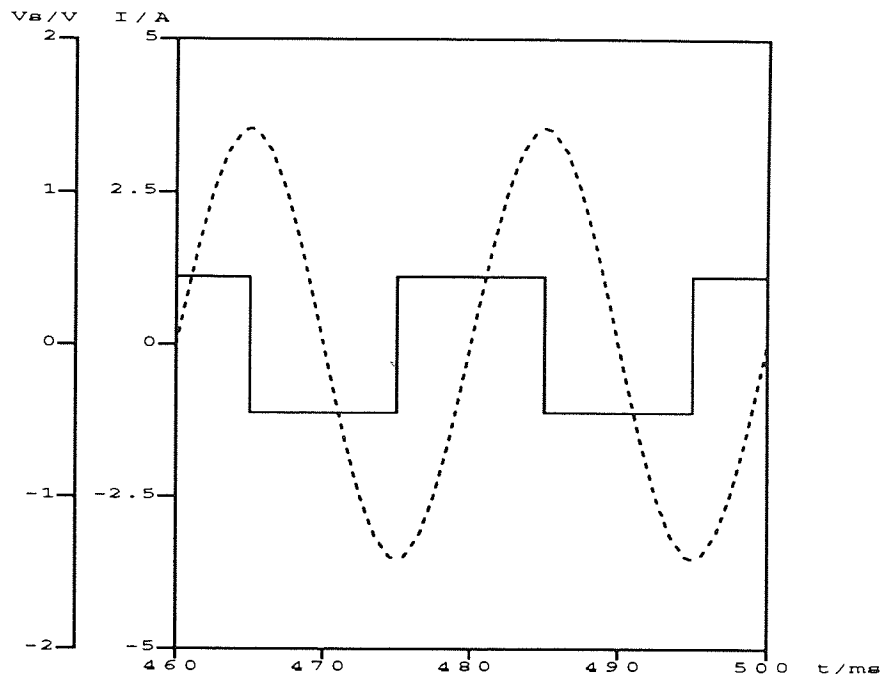


Figure 2-10a. Simulation of the Steady State Performance of the CSI Type of Single Phase STATCON Generating 1p.u. Reactive Power.

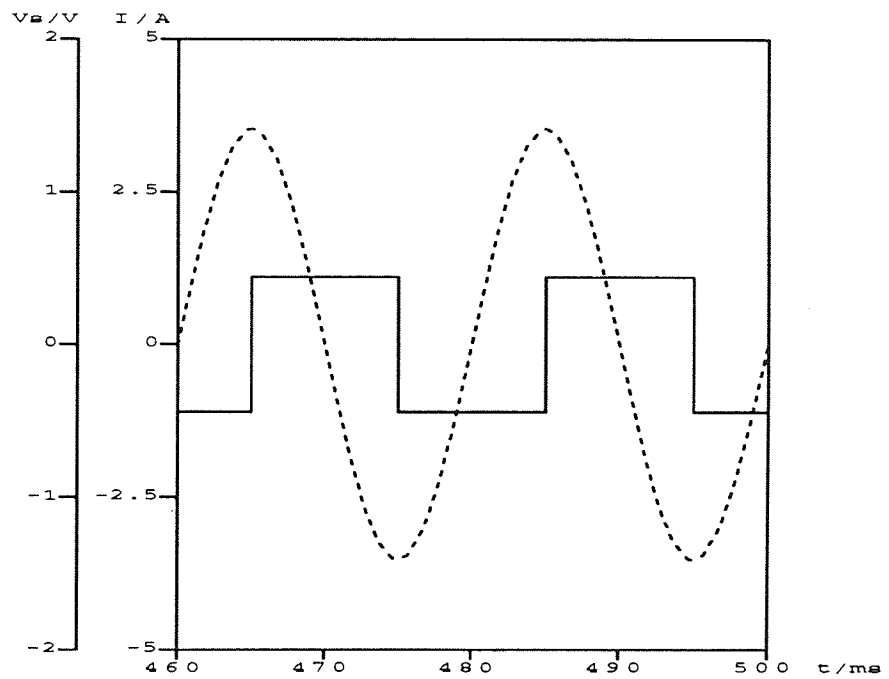


Figure 2-10b. Simulation of the Steady State Performance of the CSI Type of Single Phase STATCON Absorbing 1p.u. Reactive Power.

§2.6 Conclusions

The performance of the single phase STATCON with ideal voltage and current sources of variable magnitude has been discussed. Both circuits have been shown to be capable of generating and absorbing reactive power. A change in the polarity of the reactive power output of the equipment does not necessitate a change in the polarity of the current or voltage source but does necessitate a change in the firing pattern of the current sourced inverter.

Consideration of losses and equipment size has led to the following choice of firing angles:

- 1) If a voltage sourced inverter is used then the first pair of thyristors, i.e. devices 1 and 2 of figure 2.1, are fired at 0° , i.e. the square wave voltage at the a.c. terminals of the inverter is in phase with the supply voltage.
- 2) If a current sourced inverter is used then the first pair of thyristors are fired at 90° , for reactive power generation, and at 270° for reactive power absorption.

In the voltage sourced equipment the approximate magnitude of the harmonics decreases with increasing n as $1/n^2$. A larger value of X_L means less pronounced harmonics for a given reactive power output but means that the voltage source has to be capable of generating a larger voltage to be able to generate the rated reactive power.

In the current sourced equipment the magnitude of the harmonics decreases with increasing n as $1/n$. The value of X_L does not effect the amount of harmonics.

Table 2.1 compares the rms per unit values of the first few harmonics between the voltage sourced and current sourced equipments at rated reactive power generation and absorption. The value of X_L was taken to be 0.2 p.u. and R was assumed to be negligible.

Table 2.1. Comparison of the Per Unit Harmonics Generated by the Voltage Sourced and Current Sourced Single Phase STATCONs.

n	<u>Rated Generation</u>		<u>Rated Absorption</u>	
	VSI	CSI	VSI	CSI
3	0.667	0.333	0.444	0.333
5	0.240	0.250	0.160	0.250
7	0.122	0.143	0.082	0.143

These ideal sources are obviously simplifications. In practice these would have to be produced from the a.c. system fed through a transformer, step up in the case of the voltage sourced equipment and step down in the case of the current sourced, into a controlled rectifier. Energy storage components would then be needed to limit the ripple in the voltage or current from the output of the rectifier.

Performance of VSI and CSI Types of the Single Phase STATCON using Finite Energy Reservoirs

§3.1 Introduction

In this chapter the ideal sources of voltage and current used in the work presented as chapter 2 are replaced by a capacitor and an inductor respectively. Simulations are given for large values of capacitance and inductance and comparisons between the two equipments are made. Since these components store energy they are referred to as energy reservoirs (Gyugyi, 1981).

This chapter is intended to show the performance of the two types of equipment, in a general sense, and to illustrate the differences between the equipments so that a full analysis can be carried out on the circuit most suitable for reactive power compensation on a high voltage transmission network.

§3.2 Voltage Sourced STATCON with Capacitor Energy Reservoir

In the voltage sourced circuit with a constant voltage source the source can be considered as a battery. The direction of active power flow was shown to reverse as the value of the battery voltage was varied. There must therefore be a battery voltage for which there is no net charge flow through the battery. The current through the battery is the system current when thyristors 3 and 4 are turned on and is the negative of the system current when thyristors 1 and 2 are turned on. The current through the battery is therefore half wave symmetric so the battery must not experience any net charging or discharging over half a cycle. For this particular value of battery voltage then the battery does not need to provide any energy; it stores energy during one part of the cycle and returns it to the circuit during another, ergo it can be replaced by a capacitor, C. The capacitor has to be large enough that, during the period when charge is flowing out of it, it is not fully depleted; the capacitor must be sufficiently large so that the voltage across it is always greater than zero otherwise, for sensible values of inductance, the current flow will be excessive.

The capacitor cannot be charged in the opposite direction because, at zero voltage, the diodes which are usually reverse biased, because they are anti-parallel to the devices which are turned off, become available for conduction. The current does not therefore flow through the capacitor but circulates through the bridge using these newly available diodes.

For a large capacitor at zero firing angle there will be a certain current flow which will produce no net charging or discharging of the capacitor over a half cycle and will therefore be sustainable; this will be the steady state. If the capacitor were very large then the current flow would be identical to that using a battery of the same voltage, whereas with a smaller value of capacitance there will be some ripple in the voltage across the capacitor which will affect the current wave shape. The equivalent circuit, analogous to that of figure 2-2, is given as figure 3-1.

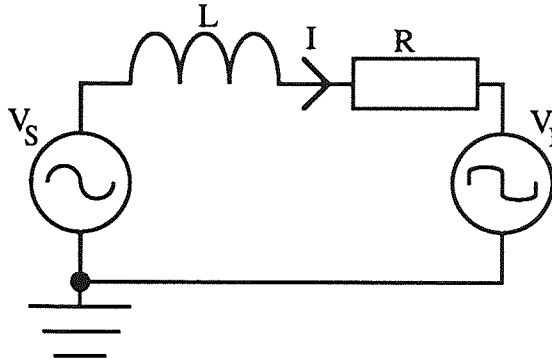


Figure 3-1. Equivalent Circuit of a Single Phase STATCON with Capacitor.

The value of the voltage across the capacitor can be controlled by altering the firing angle of the inverter. The equipment will again reach a steady state in which there is no net flow of charge either into or out of the capacitor. This can be understood in a simplified way by considering the losses in the equipment. This explanation neglects the effects of the harmonics in the system current and assumes that the capacitor is not discharged.

If the inverter voltage is moved, relative to the system voltage, by a small angle θ_0 then there is a change in the active power that flows from the system into the compensator, as discussed in section 2-3. The losses dissipated in the resistance must therefore change so that, in the steady state, there is again no net flow of charge through the capacitor. Figure 3-2 shows a phasor diagram with a positive value for θ_0 .

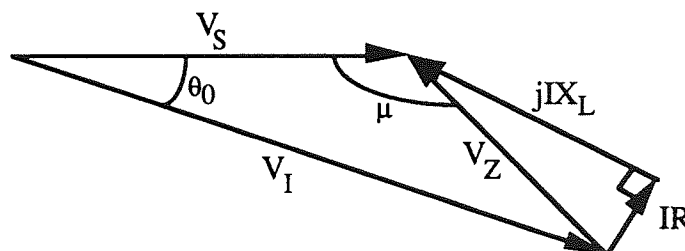


Figure 3-2. Phasor Diagram with a Positive Firing Angle.

For conciseness the definition of the phase angle of the inverter output is introduced:

$$\phi = \theta - \theta_0 \quad (3.1)$$

The voltage across the impedance of $Z (= R + jX_L)$, V_Z , is given by

$$V_Z = V_S - V_I \quad (3.2)$$

From figure 3.2

$$V_Z = V_Z \sin(\theta + \mu) \quad (3.3)$$

where

V_Z is the magnitude of the voltage across Z .

The system current, I , is given by

$$I = -\frac{V_Z}{Z} \cos(\theta + \mu + \epsilon) \quad (3.4)$$

The angle μ can be calculated by equating the active power fed into the system with the power dissipated in the resistance.

The active power fed into the system, P_{in} , is the rms component of the current which is in phase with the rms supply voltage:

$$P_{in} = \frac{V_m V_Z}{2 Z} \sin(\mu + \epsilon) \quad (3.5)$$

The active power dissipated in the system, P_{di} , is the rms component of the current squared and multiplied by the resistance:

$$P_{di} = \frac{V_Z^2 R}{2 Z^2} = \frac{V_Z^2}{2 Z} \sin \epsilon \quad (3.6)$$

In the steady state the active power dissipated is equal to the active power fed into the system so equating (3.5) and (3.6) gives

$$V_m \sin(\mu + \epsilon) = V_Z \sin \epsilon \quad (3.7)$$

Applying the sine rule to figure 3.2 gives

$$\frac{V_Z}{\sin \theta_0} = \frac{V_m}{\sin(\theta_0 + \mu)} \quad (3.8)$$

Comparing equation (3.7) and (3.8) gives

$$\frac{\sin \epsilon}{\sin(\mu + \epsilon)} = \frac{\sin(\mu + \theta_0)}{\sin \theta_0} \quad (3.9)$$

Simplifying gives

$$\tan\mu = -\tan(\theta_0+\epsilon) \quad (3.10)$$

$$\mu = -(\theta_0+\epsilon) \text{ or } \pi - (\theta_0+\epsilon) \text{ or } \dots$$

From figure 3.2, μ must be in the range $0 < \mu < \pi$ so

$$\mu = \pi - (\theta_0+\epsilon) \quad (3.11)$$

Substituting for μ in (3.8) gives

$$V_z = \frac{V_m \sin\theta_0}{\sin\epsilon} \quad (3.12)$$

Substituting for V_z from (3.12) and μ from (3.11) gives

$$I = \frac{V_m \sin\theta_0}{Z \sin\epsilon} \cos(\theta - \theta_0) \quad (3.13)$$

The variation of the component of current in phase with the system voltage, I_p , and that in quadrature, I_q , can be written out explicitly, using $\sin\epsilon = R/Z$:

$$I_q = \frac{V_m \sin 2\theta_0}{Z \sin\epsilon} = \frac{V_m \sin 2\theta_0}{2X_L \beta} \approx \frac{V_m}{2X_L} \theta_{ob} \quad (3.14)$$

$$I_p = \frac{V_m \sin^2\theta_0}{Z \sin\epsilon} = \beta \frac{V_m \sin^2\theta_0}{2X_L \beta^2} \approx \beta \frac{V_m}{2X_L} \theta_{ob}^2 \quad (3.15)$$

where

$$\beta \text{ is the damping factor} = \frac{R}{2X_L} \quad (3.16)$$

$$\text{and } \theta_{ob} \text{ is the reduced firing angle} = \frac{\theta_0}{\beta} \quad (3.17)$$

The approximation in the above equations is that θ_0 is small.

From equations (3.14) and (3.15) the reactive and active powers can be written as

$$Q = -\frac{V_m^2 \sin 2\theta_0}{4X_L \beta} \approx -\frac{V_m^2}{4X_L} \theta_{ob} \quad (3.18)$$

$$P = \frac{V_m^2 \sin^2\theta_0}{4X_L \beta} \approx \beta \frac{V_m^2}{4X_L} \theta_{ob}^2 \quad (3.19)$$

Thus as θ_0 is increased the reactive power generated by the equipment increases and if θ_0 is decreased the reactive power absorbed is increased (Edwards et al., 1988), (Sumi et al., 1981), (Trainer & Tennakoon, 1990).

In practice the variable d.c. voltage source referred to in chapter 2 would be made from a controlled rectifier bridge and suitable d.c. link components. Using a capacitor has the advantage that only one converter is required. The size and cost of the equipment are less and the losses are reduced.

Figures 3-3a and b show simulations of this circuit using the same parameter values as those used to produce figure 2-8 with a capacitor of admittance 5p.u. The firing angles used were 0.05 and -0.05 ms. These values have not been optimised in any way but illustrate the performance. A large value for the capacitor was chosen to prevent it being discharged.

The general shape of these graphs is similar to those from the circuit using a constant voltage source, figure 2-8. The value of β is 0.015 and the values of θ_{ob} are + and $-\pi/3$ radians. The currents in the graphs are larger than + or -1 p.u. indicating that the system is very sensitive to the firing angle at low values of β .

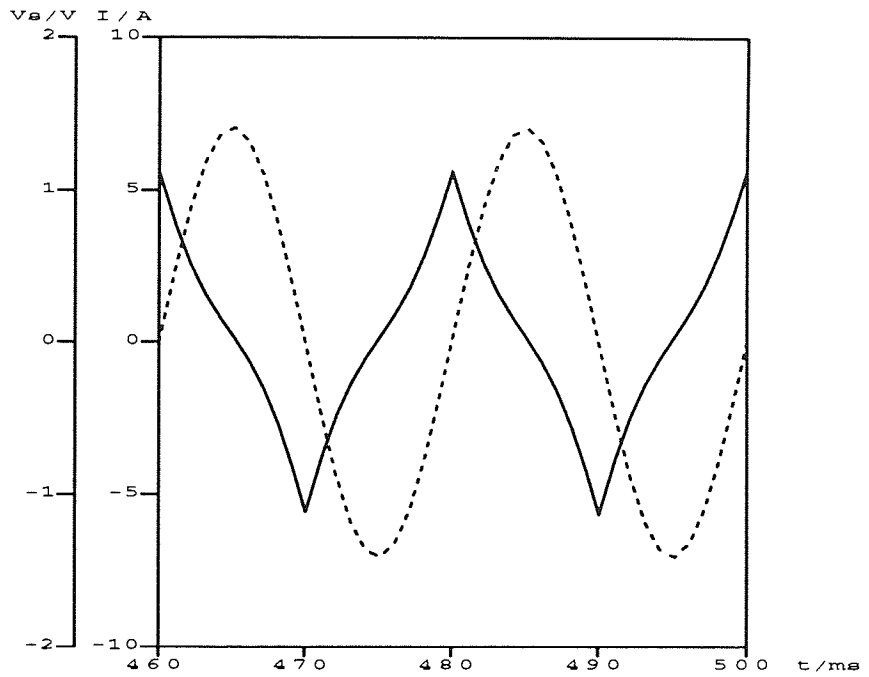


Figure 3-3a. Simulation of a Single Phase STATCON with Capacitor Energy Reservoir Generating Reactive Power.

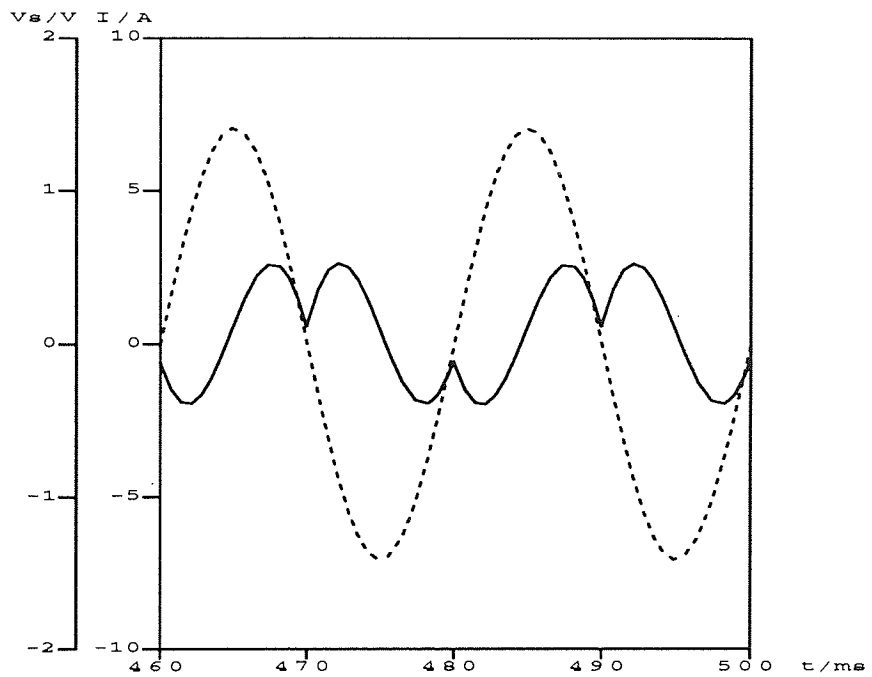


Figure 3-3b. Simulation of a Single Phase STATCON with Capacitor Energy Reservoir Absorbing Reactive Power.

§3.3 Current Sourced STATCON with Inductor Energy Reservoir

Again in the CSI type of STATCON the firing of the inverter is altered by a small amount to vary the energy stored in the reservoir (Alexandrovitz et al., 1984), (Walker, 1986) and the steady state is reached when the active power fed into the system is equal to that dissipated in the resistance. If the thyristors are fired to produce a leading current then to increase the current the firing angle is increased from 270° by a small amount and if a lagging current is being produced then to increase the current the firing angle is reduced from 90° leading. Thus the current leads or lags the system voltage by less than 90° and active power flows into the system and increases the current.

Figures 3.4a and b show simulations of the system current and voltage using the same parameters as those used to produce figure 3.3 but with an inductor of 2p.u. with an X to R ratio of 25 as the energy reservoir. The firing angles used were 16 and 4ms.

Despite a large value for the energy reservoir inductance there is substantial ripple in the current. The troughs and swells in the current show some asymmetry because of the losses in the energy reservoir. Comparing the firing angles for the voltage sourced and current sourced circuits, the voltage sourced STATCON is more sensitive to the firing angle.

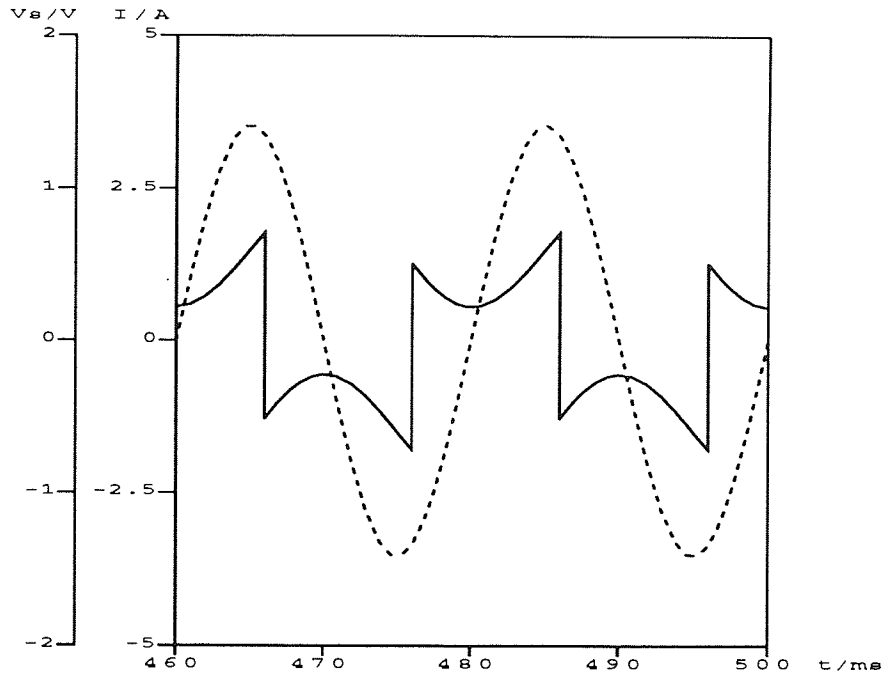


Figure 3-4a. Simulation of a Single Phase STATCON with Inductor Energy Reservoir Generating Reactive Power.

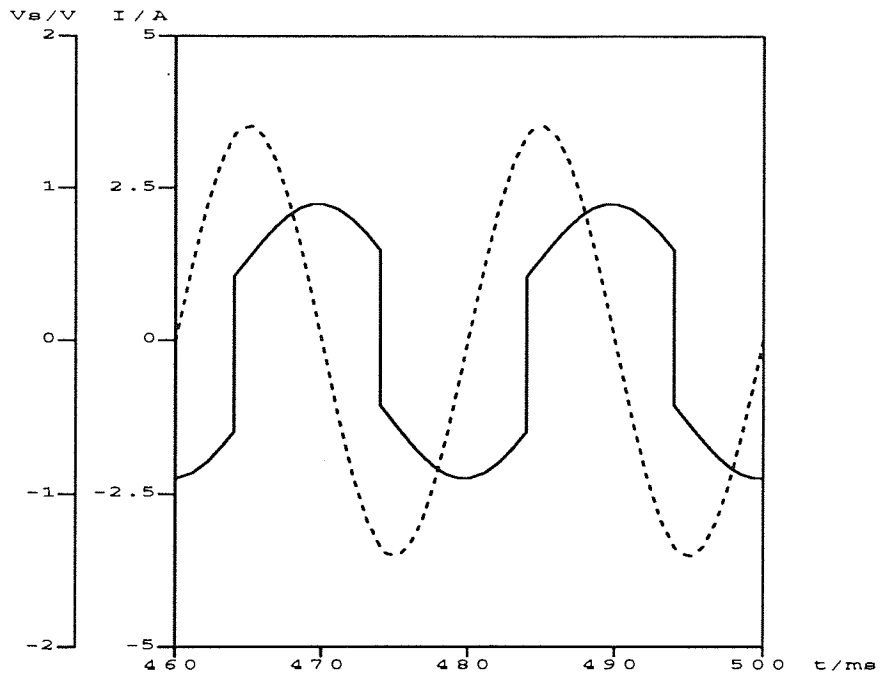


Figure 3-4b. Simulation of a Single Phase STATCON with Inductor Energy Reservoir Absorbing Reactive Power.

§3.4 Comparison Between the Two Types of STATCON

It is necessary to consider the circuit most suitable to the high power transmission environment.

In the circuits as drawn in figures 2.1 and 2.9 the VSI requires anti-parallel diodes while the CSI does not. This then would seem to be an obvious advantage in using the current sourced inverter. This is true if symmetric devices, such as MOSFETs, are used. If anti-symmetric devices, such as GTO thyristors, are used then diodes have to be included in series with the device to prevent damage under reverse biased conditions. This means that the losses are greater in the CSI case, when using anti-symmetric devices, because the current circulates continually through four devices. In the VSI case the current only passes through two devices at any one time. In addition when an inductor is being used as the energy reservoir the resistance will be greater than when a capacitor is being used, giving greater losses for the same reactive power output.

The current sourced equipment generates a square wave current and the voltage sourced equipment generates a square wave voltage. The supply to both circuits in the high voltage environment will have some inductance because of the leakage reactance of the connecting transformer. This means that the stepped current will generate large spikes of voltage. These need to be suppressed by adding capacitors.

The voltage sourced circuit is therefore better suited to high power applications. The largest models reported in the literature have used voltage sourced converters (Sumi et al., 1981), (Mori et al. 1993).

§3.5 Conclusions

This chapter has shown that the ideal sources used in chapter 2 can be replaced by energy storage components and the reactive power output varied by varying the firing angle of the thyristors by a small amount about the operating points used with the ideal sources. The advantages over the equipment with rectified sources providing the d.c voltage or current are lower losses and reduced size and cost.

The voltage sourced converter with a capacitor as the energy reservoir has been shown to be the most suitable for use in the high power transmission environment.

The Single Phase Voltage Sourced STATCON

§4.1 Introduction

Having established that the voltage sourced inverter, using a capacitor as the energy reservoir, is the most suitable circuit for reactive power compensation in high power applications, this chapter presents the results from a mathematical analysis investigating the steady state performance of this circuit. Relationships of particular interest are the variation of reactive power, losses, and harmonics as functions of the system voltage, the sizes of the energy stores, the resistance and the firing angle.

§4.2 Method

The analysis is given as appendix 1. A controllable device and associated anti-parallel diode were modelled as a small linear resistance when turned on and an infinite resistance when turned off. The turn on and turn off times were taken to be zero. For simplicity the on state resistance in the controllable devices and the diodes was assumed to be the same and the volt drops were neglected. Between switching instants the circuit therefore consists of a capacitor (the energy reservoir), an inductor (the supply inductance), resistance (from the inductor and the devices) and the supply voltage. Thus a second order differential equation describing the R L C circuit between switching instants can be generated and solved.

There are two unknown constants in the general solution to this equation. These are determined from the boundary conditions. The switching of the devices acts to reverse the voltage at the a.c. terminals of the inverter at each switching instant; the voltage across the capacitor must repeat every half cycle and the system current must be the negative of its value half a cycle earlier, i.e. the capacitor voltage must be half wave symmetric and the system current must be half wave anti-symmetric. The solution of the differential equation has what is conventionally known as a steady state component, i.e. the particular integral, and a transient component, i.e. the complementary function. In this work however altering the circuit topology every half cycle means that the transient solution does not die away; it is stimulated every half cycle and is therefore part of the full steady state solution.

§4.3 Voltage Across the Capacitor

The voltage across the capacitor, V_C , from appendix 1, during $0 \leq \phi \leq \pi$, is given by

$$V_C = -\frac{V_m}{h} (\beta^2 + k^2) \cos(\phi + \theta_0 + \gamma) - X_L e^{-\beta\phi} [(\beta A_1 - k A_2) \sin\phi + (k A_1 + \beta A_2) \cos\phi] \quad (4.1)$$

where

k is the resonance ratio; the ratio of the damped natural frequency of the circuit to the supply frequency: $k = \sqrt{\frac{X_C}{X_L} - \beta^2}$

$$\gamma = \tan^{-1} \frac{\beta^2 + k^2 - 1}{2\beta}$$

$$h = \sqrt{(\beta^2 + k^2 - 1)^2 + 4\beta^2}$$

A_1 and A_2 are the two constants from the solution to the second order differential equation describing the circuit between switching intervals. Expressions for these are given in appendix 1.

X_C is the reactance of the capacitor at the system frequency.

Figure 4.1 shows examples of the ratio of the voltage across the capacitor, V_C , to the peak of the supply voltage, V_m , for three different values of the resonance ratio, k , and for three different values of the reduced firing angle, θ_{ob} .

The figures show that the voltage across the capacitor has an amount of ripple superimposed on the d.c. value. The amount of ripple increases with a higher value for the resonance ratio, i.e. for a lower value of capacitance with a fixed value of inductance. The frequency of the ripple is twice the system frequency.

In the third figure the voltage on the capacitor dips below zero for $\theta_{ob} = \pm 1$. The analysis of appendix 1 was performed assuming continuous current through the capacitor. The diodes in the circuit prevent the voltage across the capacitor from reversing; the minimum voltage across the capacitor is zero, as discussed in chapter 3. These graphs of the voltage across the capacitor illustrate the increase in ripple at higher values of the resonance ratio but the actual voltage across the capacitor would not fall below zero. This is not a serious omission because the equipment would not be operated in this manner; the current flow, for sensible values of inductance, would be excessive.

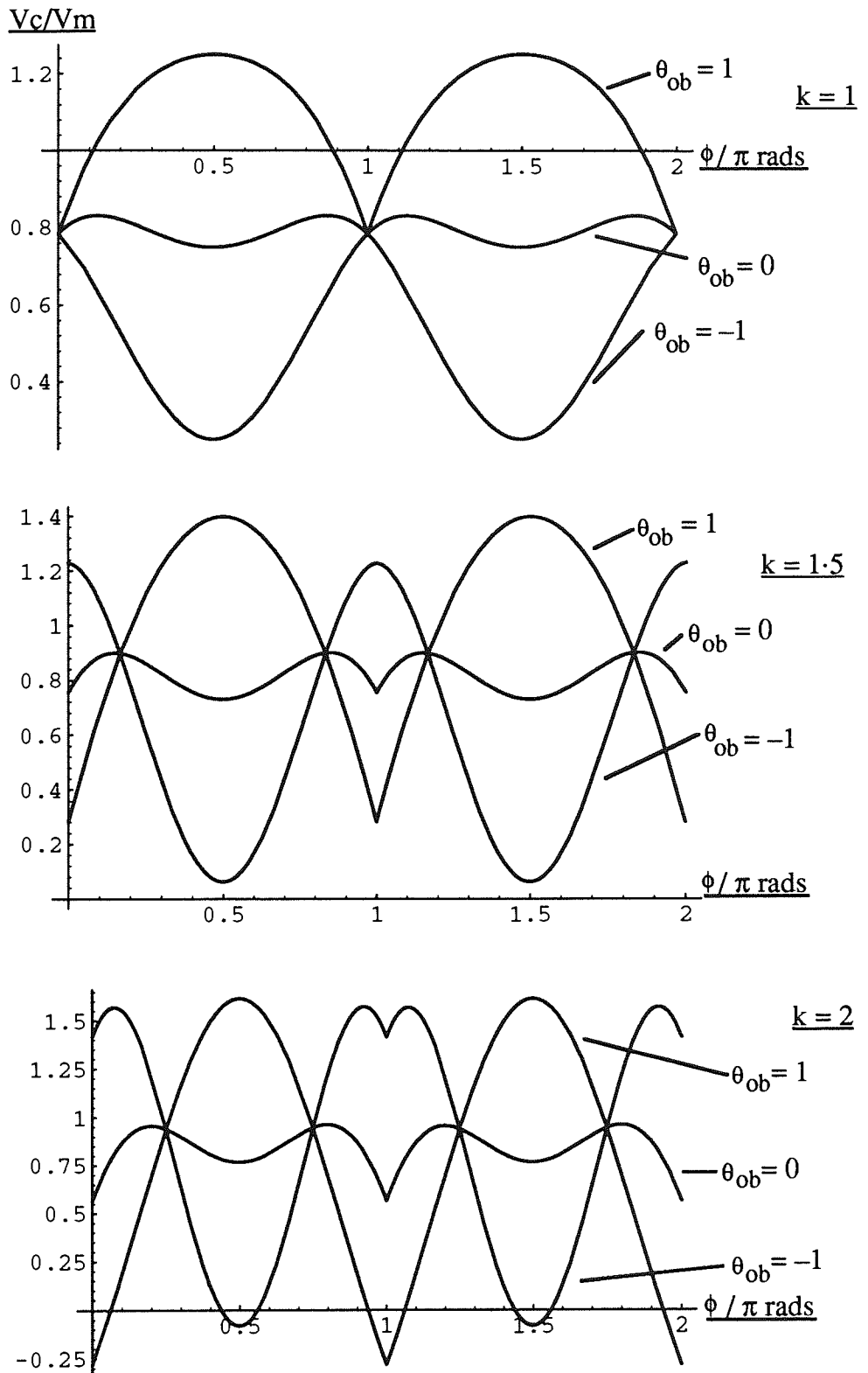


Figure 4.1. The Capacitor Voltage in a Single Phase STATCON for $k = 1, 1.5$ and 2 .

The capacitor voltage shows swells when generating reactive power and troughs when absorbing. When the equipment is generating substantial reactive power, ($\theta_{ob} = 1$) the capacitor voltage has only one maximum during each switching era, with these values of the resonance ratio, at $\phi = \pi/2$ radians, and has a minimum at each of the switching epochs. When the equipment is absorbing substantial reactive power ($\theta_{ob} = -1$) and the resonance ratio is low, the capacitor voltage has only one minimum, again at $\phi = \pi/2$, and has a maximum at each of the switching epochs. At high values of the resonance ratio, or when the output from the equipment is small, there are multiple oscillations in the voltage across the capacitor with no definite instant for the maxima or minima.

§4.4 System Current

Appendix 1 also gives the system current, for $0 \leq \phi \leq \pi$:

$$I = \frac{V_m}{hX_L} \sin(\phi + \theta_0 + \gamma) + A_1 e^{-\beta\phi} \sin k\phi + A_2 e^{-\beta\phi} \cos k\phi \quad (4.2)$$

Figure 4.2 illustrates the system current for the same values of reduced firing angle and resonance ratio used in figure 4.1. Again the graphs have been produced assuming continuous current flow through the capacitor and so the curves of figure 4.1 that are unrealistic will have unrealistic counterparts in figure 4.2.

The graphs show that as the resonance ratio is increased the harmonic content of the waveforms increases. In addition, the value of the fundamental component decreases as the resonance ratio increases.

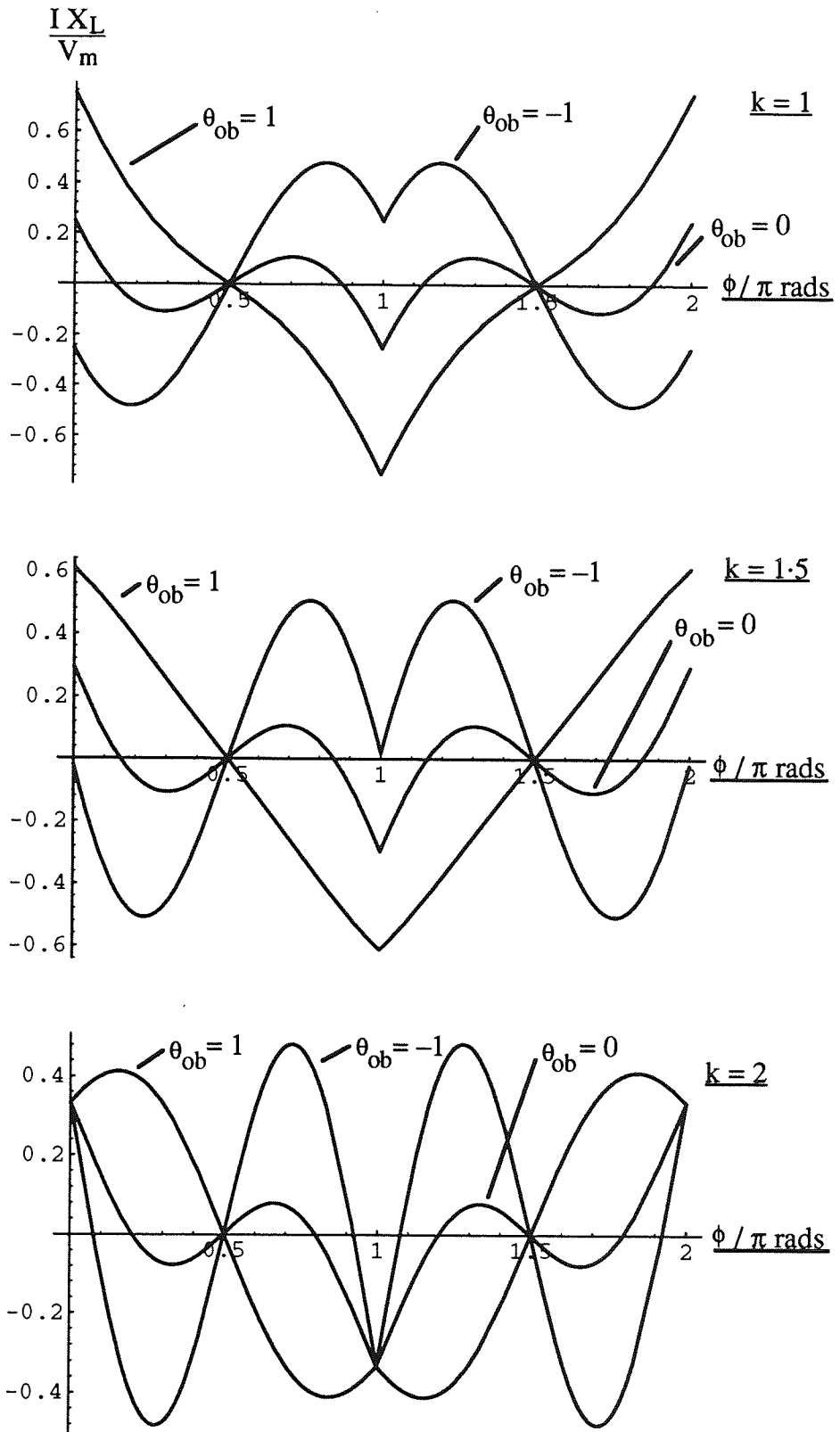


Figure 4-2. The Current in a Single Phase STATCON for $k = 1, 1.5$ and 2 .

§4.5 Characteristics of the Fundamental Component of the System Current

Appendix 1 gives the Fourier series for the system current. It is shown that the form of the fundamental frequency component of the current in (leading) quadrature with the system voltage, I_q , and that in phase, I_p , can be expressed in terms of the firing angle, θ_0 , the damping factor, β , and the factors p_1 , q_1 and q_2 where these factors are functions of k and β only; they are independent of θ_0 .

From appendix 1:

$$I_q = \frac{V_m}{X_L} \left(q_1 + q_2 \frac{\sin 2\theta_0}{2\beta} \right) \approx \frac{V_m}{X_L} [q_1 + q_2 \theta_{ob}] \quad (4.3)$$

$$I_p = \frac{\beta V_m}{X_L} \left(p_1 + q_2 \frac{\sin^2 \theta_0}{\beta^2} \right) \approx \frac{\beta V_m}{X_L} [p_1 + q_2 \theta_{ob}^2] \quad (4.4)$$

Figure 4.3 shows graphs of p_1 , q_1 and q_2 as a function of m , where $m = 1/k$, for three different values of β , 0.1, 0.01 and 0.001 with the curves superimposed. The graphs illustrate that these parameters exhibit no significant dependence on β over this range. m has been used for the horizontal axis, rather than k , because using m gives the plateau region of the curves as m tends to a large value so it is clear where the x-axis can be truncated. In addition, because m is a function of the reactance of the inductors and the admittance of the capacitor it is related to the size of the equipment. Thus it is desirable that m should be as small as possible.

The forms of these equations, (4.3) and (4.4), recur in the higher pulse number circuits.

The range of m is determined essentially from the q_2 graph. It is required that q_2 is as large as possible for minimum losses so m should be large, but this means large energy storage components. m would therefore be chosen to be in the range $0.5 \leq m \leq 0.8$.

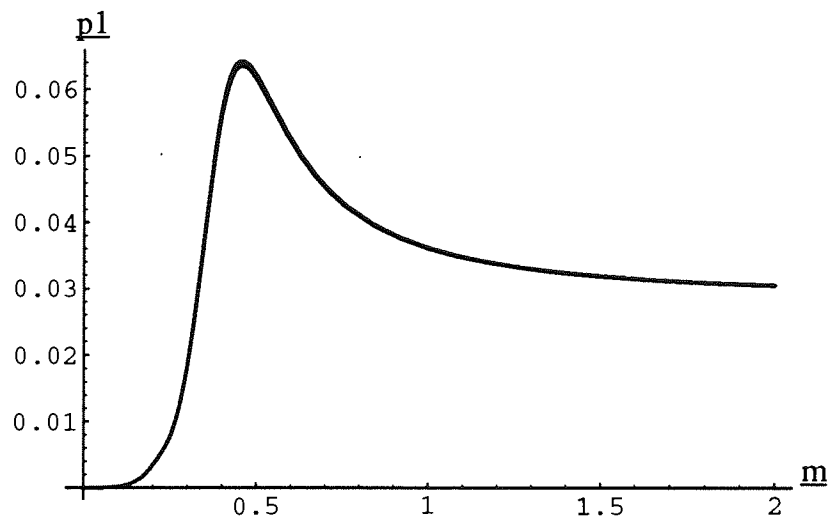
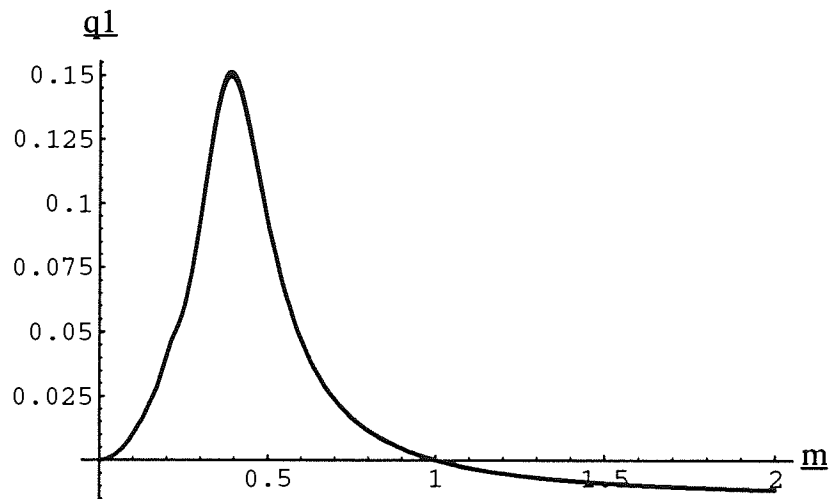
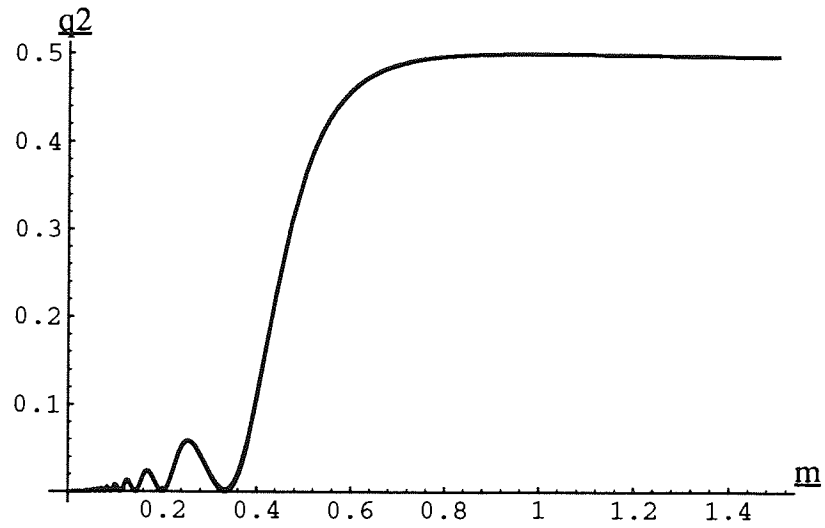


Figure 4-3. Graphs of the Parameters Describing the Fundamental Component of the Current in a Single Phase STATCON.

Figure 4.4 shows how the normalised reactive power output varies with the reduced firing angle for different values of the resonance ratio. Figure 4.5 shows how the normalised losses vary.

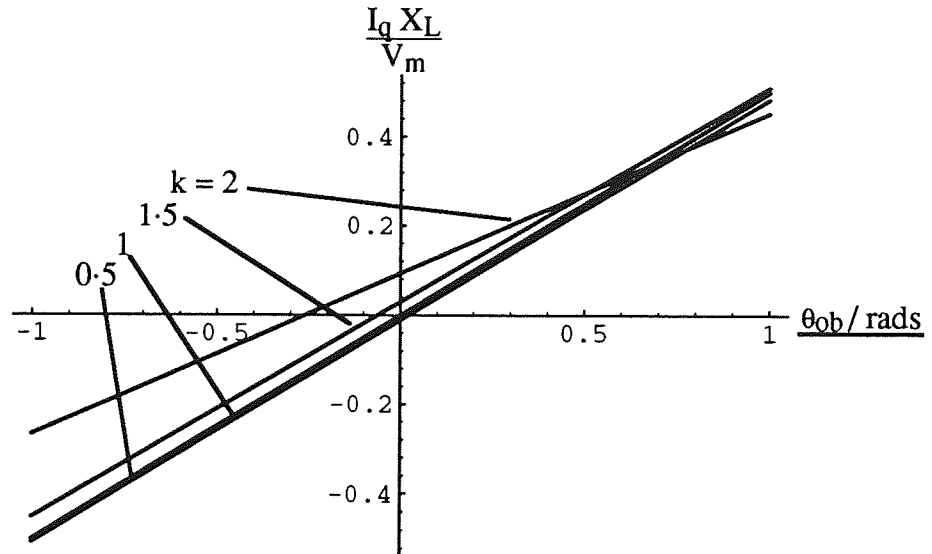


Figure 4.4. Graph of the Normalised Reactive Power Output from a Single Phase STATCON.

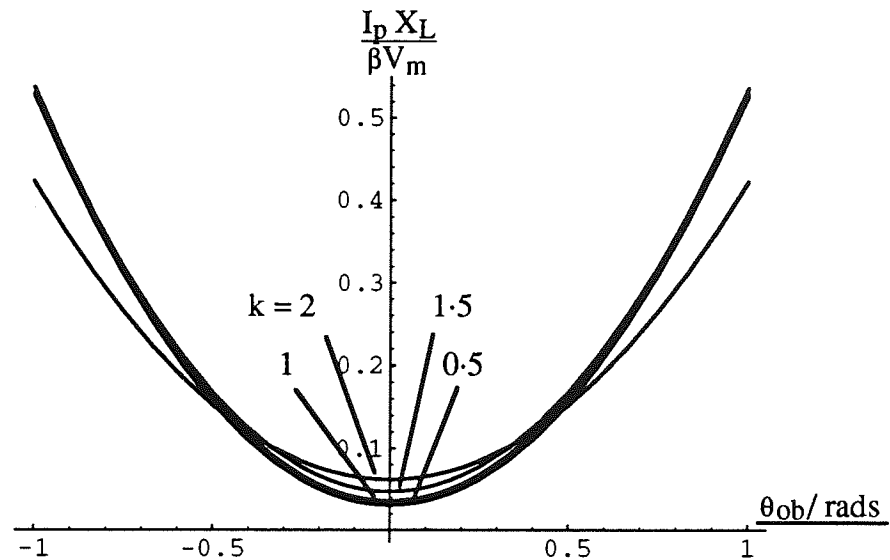


Figure 4.5. Graph of the Normalised Losses in a Single Phase STATCON.

§4.6 Total Harmonic Content

In the steady state the input active power must be equal to the power dissipated in the resistance. The total harmonic content can therefore be calculated by comparing the input active power to the losses from the fundamental component of the current.

The input active power, P_{in} , is given by

$$P_{in} = \frac{V_m I_p}{2} \quad (4.5)$$

The total harmonic content, THC, is defined as the sum of the rms value of all of the harmonics hence

$$I_{rms}^2 = \frac{I_p^2}{2} + \frac{I_q^2}{2} + THC^2 \quad (4.6)$$

The power dissipated in the resistance, P_{di} , is given by

$$P_{di} = I_{rms}^2 R \quad (4.7)$$

Substituting for R in terms of β from (3.16) and for I_{rms}^2 from (4.6) gives

$$P_{di} = \beta X_L (I_p^2 + I_q^2 + 2THC^2) \quad (4.8)$$

Equating the input active power with that dissipated:

$$V_m I_p = 2\beta X_L (I_p^2 + I_q^2 + 2THC^2) \quad (4.9)$$

Simplifying (4.9) and substituting the expressions for I_p and I_q , from (4.3) and (4.4), gives

$$THC = \frac{V_m}{\sqrt{2}X_L} \sqrt{\frac{1}{2} \left(p_1 + q_2 \frac{\sin^2\theta_0}{\beta^2} \right) - \left(q_1 + q_2 \frac{\sin 2\theta_0}{2\beta} \right)^2 - \beta^2 \left(p_1 + q_2 \frac{\sin^2\theta_0}{\beta^2} \right)^2} \quad (4.10)$$

Figure 4.6 shows a graph of the normalised total harmonic content as a function of the reduced firing angle for different values of the resonance ratio.

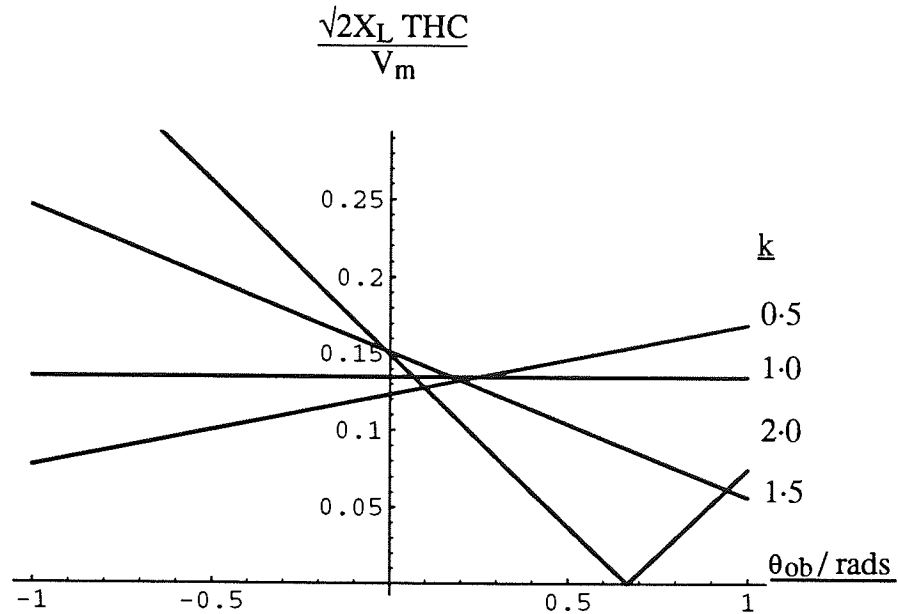


Figure 4.6. Graph of the Normalised Total Harmonic Content as a Function of the Reduced Firing Angle in a Single Phase STATCON.

The graph shows that there is no real optimum value of k in terms of the harmonics that are produced; if k is chosen so as to give relatively good harmonic performance when the equipment is generating reactive power then the harmonic performance is relatively poor when absorbing reactive power and vice versa. When $k = 1$ the total harmonic content is not dependent on the firing angle, i.e. the total harmonic content of the current is independent of the magnitude of the fundamental component.

§4.7 Characteristics of the Harmonics of the System Current

The Fourier analysis given in appendix 1 also shows the form of the coefficient of the harmonic of frequency $n\theta$, I_{nc} . Figure 4.7 shows graphs of the normalised coefficients of the harmonics for $n = 3, 5$ and 7 for different values of k .

$$I_{nc} = \frac{V_m}{X_L} t_n = \frac{V_m}{X_L} \left(c_n \cos\theta_0 - s_n \frac{\sin\theta_0}{\beta} \right) \approx \frac{V_m}{X_L} [c_n - s_n \theta_{ob}] \quad (4.11)$$

The curves for the different values of n show the same general shape but decrease in size with increasing n . These graphs mirror the shape of the THC graph, figure 4.6, and again there is no variation in a particular harmonic with the fundamental component at $k = 1$.

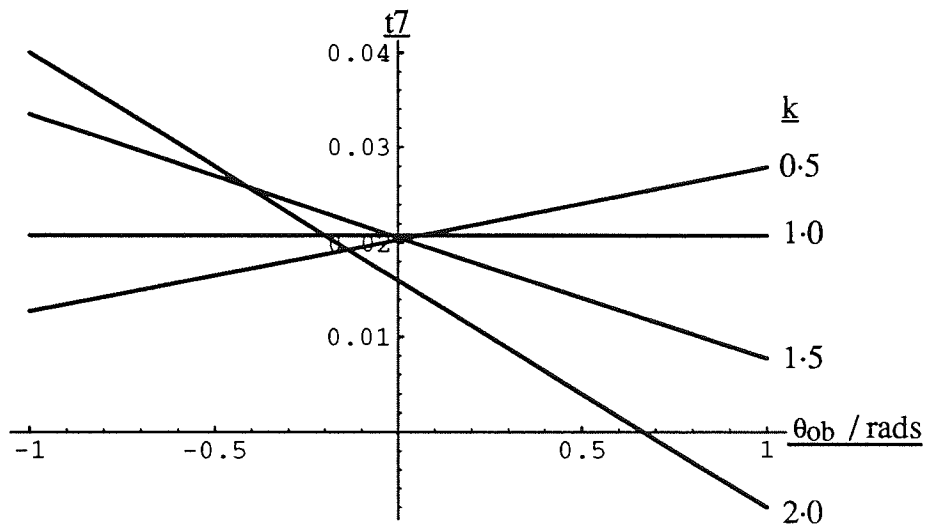
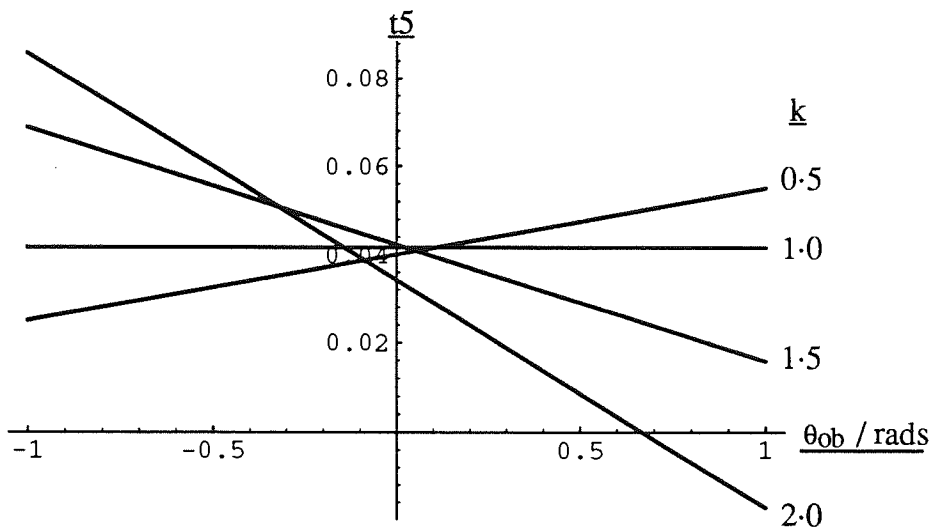
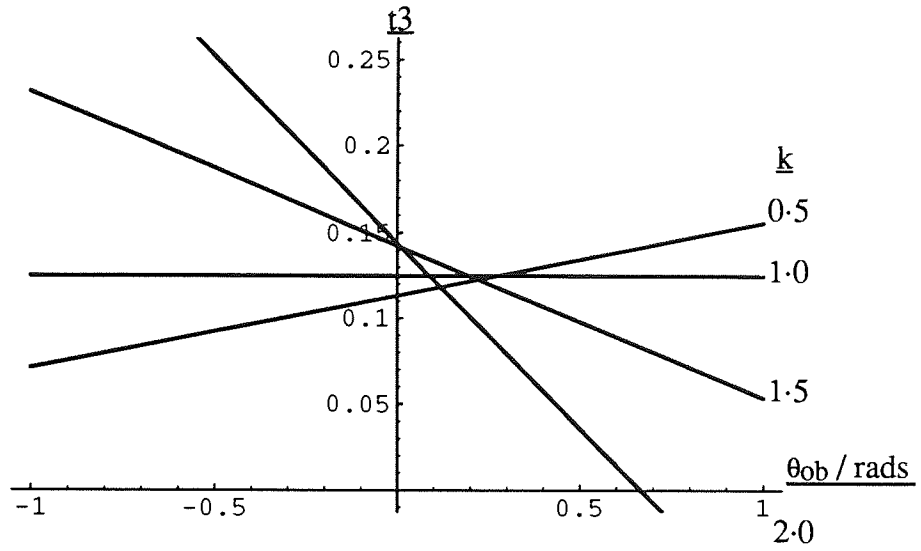


Figure 4.7. Graphs of the Normalised Coefficient of the Harmonics in the Current for $n = 3, 5$ and 7 in a Single Phase STATCON.

Figure 4-8 shows graphs of c_n and s_n , again for $n = 3, 5$ and 7 , as functions of the reciprocal of the resonance ratio, m . These graphs were also plotted for $\beta = 0.1, 0.01$ and 0.001 . These parameters, like those describing the fundamental frequency component, exhibit no significant dependence on the damping factor.

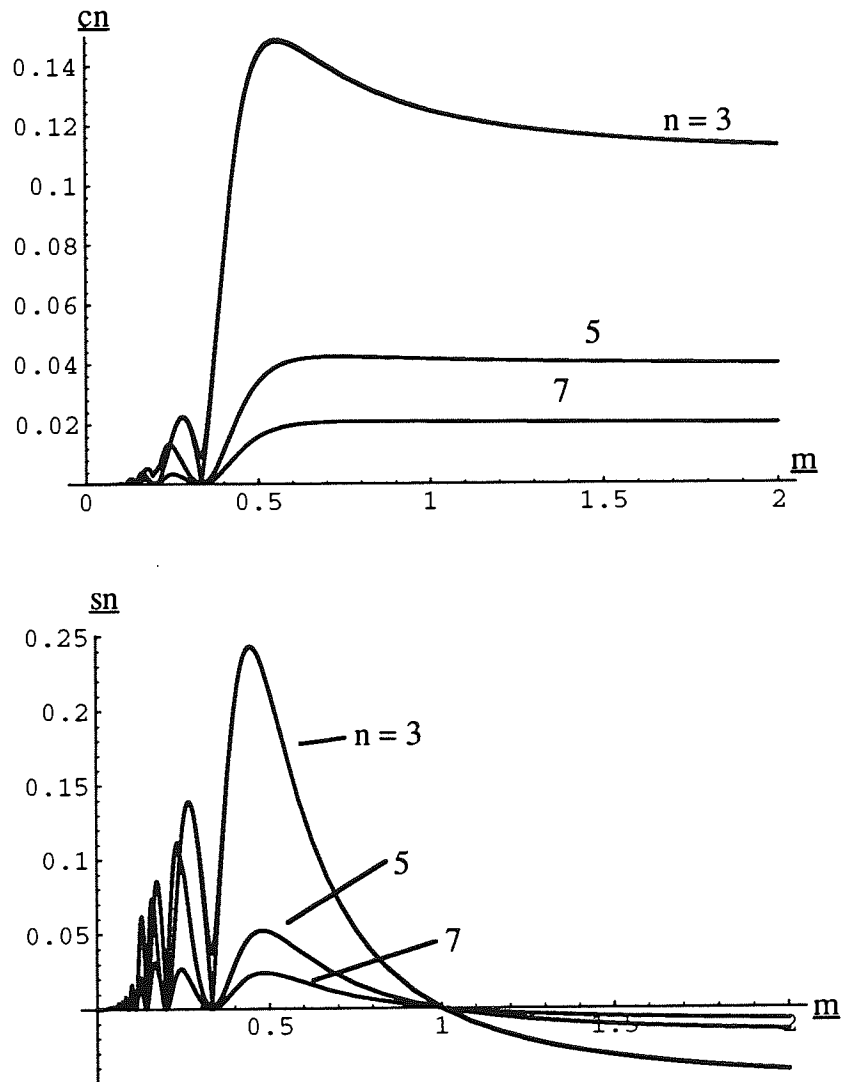


Figure 4-8. Graphs of the Parameters Describing the Coefficients of the Harmonics in the Current in a Single Phase STATCON.

The graph of s_n passes through zero at about $k = m = 1$ for all values of n so there can be no change in the magnitude of the current harmonic with a variation in the firing angle, as shown in figure 4-7.

§4.8 Choice of Circuit Parameters

Figures 4.3 to 4.8 illustrate the following features

- 1) The control parameter of interest is the reduced firing angle, θ_{ob} ; apart from this parameter the equipment shows no dependence on the firing angle and very little variation with the damping coefficient, as shown in equations (4.3), (4.4) and (4.11).
- 2) q_2 is very much larger than q_1 and p_1 ; the reactive power and losses, when operating at significant reactive power output, are described almost entirely by q_2 .
- 3) q_2 appears to be constant value $m (= 1/k) > 0.8$, as shown in figure 4.3.

At substantial output the ratio of the losses to the output is given by

$$\frac{P}{Q} \approx \frac{\beta q_2 \theta_{ob}^2}{q_2 \theta_{ob}} = \beta \theta_{ob} = \theta_0 \quad (4.12)$$

For this ratio to be as small as possible at rated reactive power then, for a circuit of fixed β , V_m and X_L , q_2 should be as large as possible and from figure 4.3 this means that m should be greater than 0.8.

The reciprocal of the resonance ratio, m , is a measure of the size and cost of the energy stores, assuming β is small,

$$m \approx \sqrt{X_L Y_C} \quad (4.13)$$

where

Y_C is the admittance of the capacitance.

For the cost, and size, of the energy stores to be as small as possible the value of m should be low. Clearly there is a compromise to be struck on the exact value of m . A sensible choice would be in the range $0.5 \leq m \leq 0.8$.

If the equipment were connected to a high voltage system then there would be a step down transformer. The leakage reactance of this is generally in the range of 0.1 to 0.2 p.u. (Weedy, 1987, table A.2.4). The size of the transformers will not be greatly affected by the value of the leakage reactance so if reduction in size is important then this value of leakage reactance should be as large as possible to minimise the size of the capacitor, for a given value of the resonance ratio.

The value of V_m chosen depends upon the voltage rating of the devices and that of the capacitor. For fixed values of β , q_2 and X_L , V_m should be as large as possible. However as the voltage rating is increased the number of devices connected in series would have to be increased and the resistance associated with each string of devices would increase. The value of V_m therefore depends upon the cost of the capacitor and

devices per unit voltage and the value of the resistance at different voltages. This question of the choice of the voltage rating of the equipment has not been addressed.

For minimum losses it is desirable for X_L to be as small as possible, assuming that the other parameters are constant.

These considerations on V_m and X_L have assumed that the firing angle of the equipment can be controlled to any degree of accuracy. Using a very large value of V_m and very small values of X_L and β then the range of θ_0 to vary the reactive power between ± 1 p.u. would be small. In this case then the control system would have to be very accurate. The precision of firing the devices may put a limit on the values of these parameters.

The choice of X_L may also effect the value of β . If the resistance of the devices was negligible in comparison to that of the transformer then as X_L was varied, the X to R ratio of the transformer would stay constant, as would β . If the resistance of the devices dominated however, as X_L was varied, the resistance would be constant and β would vary. In addition the volt drop in the devices and the switching losses may be non-trivial so the effective resistance will be non-linear and β will also depend upon the current. The effective value of the resistance in a three phase system using PWM to reduce the harmonics, in which the losses would be very much larger than when using 180° firing, has been shown to be non-linear (Pedersen & Rasmussen, 1994).

Clearly the exact value of each of the parameters is a complicated matter depending upon the losses, the harmonics, the controllability and the cost of the components. An example optimisation based on the cost of the energy storage components and the cost of the losses has been performed (Norris and Hill, 1993).

§4.9 Equivalent Circuit

In appendix 1 the circuit was solved by producing the second order differential equation which describes the R L C circuit between switching intervals and using the conditions that the voltage across the capacitor must repeat every half cycle and the current must reverse every half cycle to evaluate the unknowns in the general solution.

An alternative approach is to say that the second order differential equation has a forcing function due to the system voltage. Thus the particular integral solution corresponds to the conventional steady state response of an R L C circuit to the system voltage. The complementary function solution corresponds to the solution of the homogeneous form of the equation. The original equation was formed by

differentiating the voltage across each of the components in the circuit. The voltage applied to the R L C circuit, to give the particular integral, must therefore be a constant, over the interval that the equation is defined, i.e. between switching instants. An equivalent circuit, to describe the performance of the circuit between switching instants, can therefore be produced which consists of an R L C circuit with a constant voltage source and the system voltage. The values of the passive components are the same as those in the actual circuit. The voltage at the inverter terminals in the actual circuit reverses every half cycle so, in the equivalent circuit, the voltage across the capacitor and constant (between switching intervals) voltage source must also reverse. The voltage across the capacitor must be continuous and therefore the voltage across the capacitor in the equivalent circuit, V_{ec} , must be zero at the switching instants. This means that the voltage source which produces the constant voltage over a half cycle produces a square wave, V_{SQ} , over the whole cycle with the voltage steps occurring at the switching instants. The equivalent circuit is given as figure 4.9.

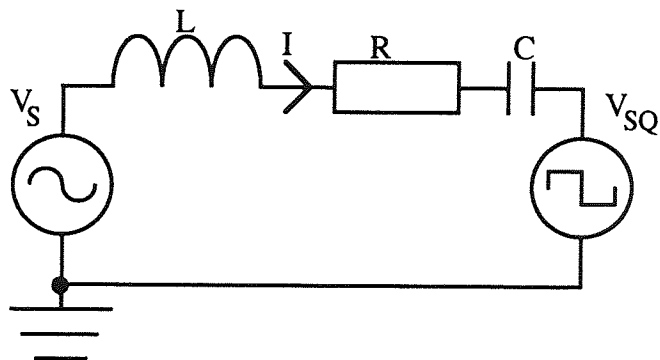


Figure 4.9. Equivalent Circuit for the Single Phase STATCON with a Capacitor Energy Reservoir.

The current through the capacitor in the equivalent circuit is the system current. The current through the capacitor in the actual circuit is a switched version of the system current. The voltage across the capacitor in the equivalent circuit will therefore not be the same as that in the actual circuit.

The amplitude of V_{SQ} can be calculated from one of three facts:

- 1) The voltage across the capacitor being zero at the switching instants, as discussed above.
- 2) The input active power must equal that dissipated in the resistance in the circuit.
- 3) Because the voltage across the capacitor and the system current are continuous then the step in voltage of V_{SQ} at the switching instants must be equal to the step in voltage across the inductance at the switching instants. Thus the derivative of the current can be calculated and then the step in voltage across the inductor, which is twice the value of the amplitude of the square wave, can be calculated.

The amplitude of V_{SQ} is derived in appendix 2 using the first of these methods: the other two are given elsewhere (Hill & Norris, 1994). The expression for the current derived using this equivalent circuit agrees with the Fourier series from the analysis of the full circuit, appendix 1.

§4.10 Discussion on p_1 and q_1

Figures 4.4 and 4.5 show the effect of altering the reduced firing angle on the reactive power output and the losses. In general terms delaying the firing angle with respect to the supply voltage raises the d.c. voltage across the capacitor and increases the reactive power generated and advancing the firing angle lowers the d.c. voltage across the capacitor and increases the reactive power absorbed by the equipment. The approximate analysis of chapter 3 predicts this but does not indicate the p_1 and q_1 terms in equations (4.3) and (4.4).

At a firing angle of zero the reactive power generated or absorbed by the equipment is directly proportional to q_1 . For a large value of capacitance, $m > 1$, the equipment absorbs reactive power and, because of the resistance in the circuit, absorbs some active power; the current lags the system voltage by an angle slightly less than 90° . For a small value of capacitance the current leads the system voltage by slightly less than 90° .

The equivalent circuit of figure 4.9 is helpful in considering the phasor diagrams showing p_1 and q_1 . The voltage at the a.c. terminals of the inverter, V_I , is the sum of the voltage across the capacitor, V_{ec} , and that of the square wave voltage source, V_{SQ} .

Because the voltage out of the inverter is not sinusoidal there will always be current flow, even when the fundamental component of the inverter output voltage is equal to the system voltage. There must therefore be some losses in the equipment at all firing angles; p_1 must be finite.

Because of the losses in the system the fundamental component of the current, I_1 , will not be exactly in quadrature with the system voltage which, when the firing angle is zero, is of the same phase as the fundamental frequency component of the square wave voltage, V_{SQ} . The fundamental component of the voltage across the capacitor in the equivalent circuit, V_{ec} , will not therefore be of exactly the same phase as the fundamental component of V_{SQ} . In the actual circuit the fundamental frequency component of the ripple on the voltage at the a.c. terminals of the converter must be slightly out of phase with the system voltage; at a firing angle of zero the fundamental component of the inverter output voltage is not in phase with the system voltage.

Figure 4-10 shows phasor diagrams for zero firing angle for both large and small values of k .

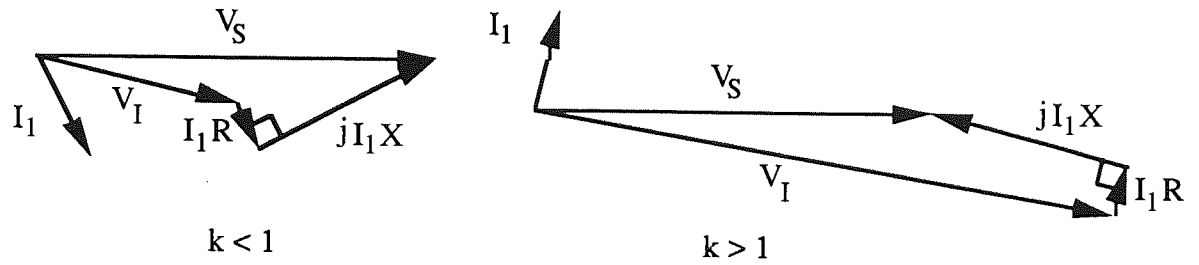


Figure 4-10. Phasor Diagrams for Zero Firing Angle in the Single Phase STATCON.

In figure 4-10 the differences between the fundamental component of the voltage at the a.c. terminals of the converter, V_I , and the system voltage, V_S , have been greatly exaggerated; the magnitudes of these voltages are almost identical and the phase difference between them is very small.

§4-11 Size of the Energy Storage Components

One of the expected advantages of the use of converters as reactive power compensators is an overall reduction in the size of the equipment, coming about through a reduction in the size of the energy storage components (Edwards et al., 1988), (Gyugyi et al., 1990). In order to produce a simple comparison between the amount of energy storage components in a STATCON and those in a conventional SVC, i.e. a thyristor switched capacitor and a thyristor controlled reactor, the size of the harmonic filters in both equipments are neglected.

As a point of comparison it was assumed that the inverter was connected to the system through a transformer of leakage reactance 0.2p.u. The value of m chosen was the knee point of the graph of q_2 against m , from figure 4-3; $m = 0.6$ so $k = 5/3$. Thus from the definition of k , assuming β is small, the admittance of the capacitor is 1.8p.u. These values are not necessarily optimum but are probably similar to the values that an optimisation would produce.

A conventional single phase static VAR compensator would consist of a 1p.u. capacitor and a 1p.u. inductor. Thus in the single phase equipment there is no obvious reduction in the size of the energy storage components.

§4.12 Operation at Reduced System Voltage

Another of the purported advantages of the STATCON over a conventional SVC is the ability to generate reactive power at reduced system voltage (Edwards et al., 1988).

In a conventional SVC, if the equipment is generating rated reactive power and there is a reduction in the system voltage, then the reactive power will fall. As discussed in chapter 1, when there is reduced system voltage is exactly when the maximum rated reactive power generation is required.

From equations (4.3) and (4.4) the reactive and active powers are

$$Q = -\frac{V_m^2}{2X_L} \left(q_1 + q_2 \frac{\sin 2\theta_0}{2\beta} \right) \quad (4.14)$$

$$P = \frac{\beta V_m^2}{2X_L} \left(p_1 + q_2 \frac{\sin^2 \theta_0}{\beta^2} \right) \quad (4.15)$$

If the system voltage is reduced then the firing angle in (4.14) can be increased to maintain the reactive power output, although at the expense of increased losses. Assuming that the capacitor is never discharged, the maximum value of the reactive power, Q_m , occurs when the firing angle is $\pi/4$, at which point the active power is defined as P_m . Neglecting p_1 and q_1 and approximating q_2 to 0.5 gives

$$Q_m \approx -\frac{V_m^2}{8\beta X_L} \quad (4.16)$$

$$P_m \approx \frac{V_m^2}{8\beta X_L} \quad (4.17)$$

Thus, assuming the leakage reactance of the transformer is 0.2 p.u. and that β is 0.01, rated reactive power can be generated as long as the system voltage is greater than 0.13. To generate this reactive power at this voltage then the active power is also 1 p.u. This is much larger than that which would be permissible for any significant length of time but does illustrate the potential usefulness of the equipment to provide reactive power at low system voltages.

Figure 4.11 shows a plot of the maximum possible reactive power generation, Q_m , as a function of the system voltage, with the output limited at 1 p.u. Figure 4.12 shows a plot of the losses at this reactive power output. Since V_m is the peak value, $V_m = \sqrt{2}$ p.u. is the nominal voltage.

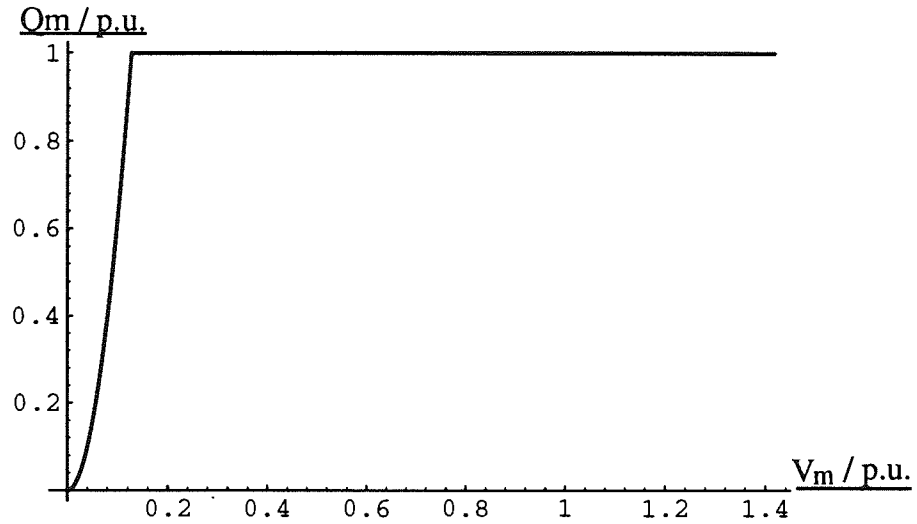


Figure 4-11. Graph of the Maximum Reactive Power Output.

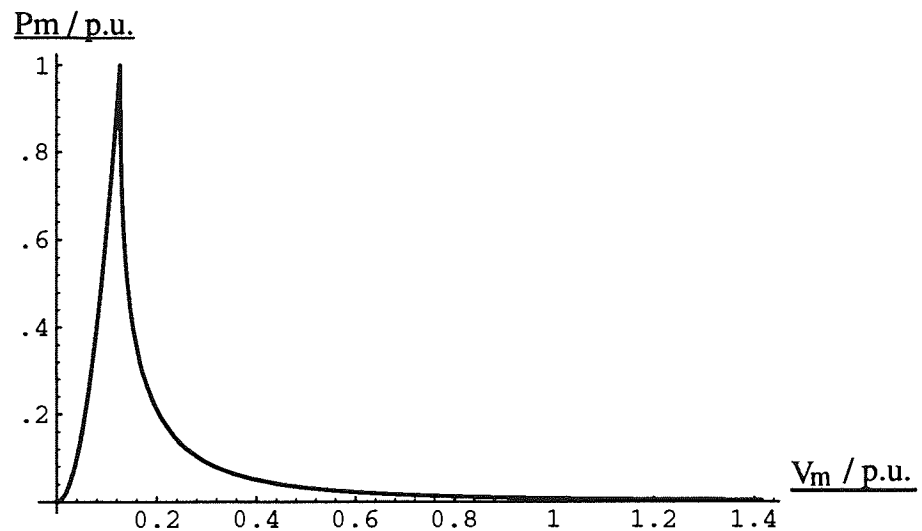


Figure 4-12. Graph of the Losses when Generating Maximum Reactive Power.

A more realistic method of assessing the steady state performance of the equipment under reduced voltage conditions is to stipulate the maximum permissible losses, which is a function of the firing angle, for a given system voltage and then plot the reactive power output for this firing angle. If the maximum losses are taken to be 5%, with β and X_L as above, then the reactive power output is as shown in figure 4-13, with the output limited at 1p.u., and the actual losses are as given in figure 4-14.

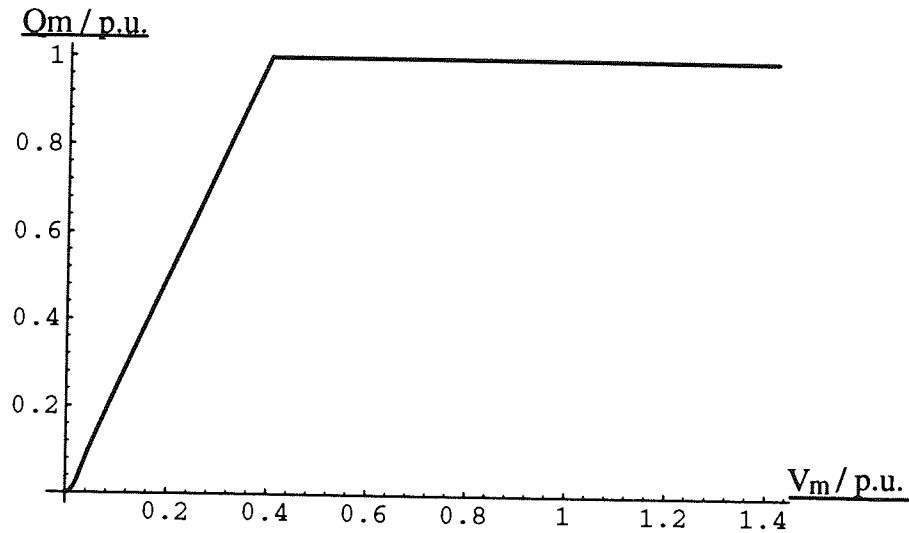


Figure 4-13. Graph of the Reactive Power Output with Maximum Losses of 5%.

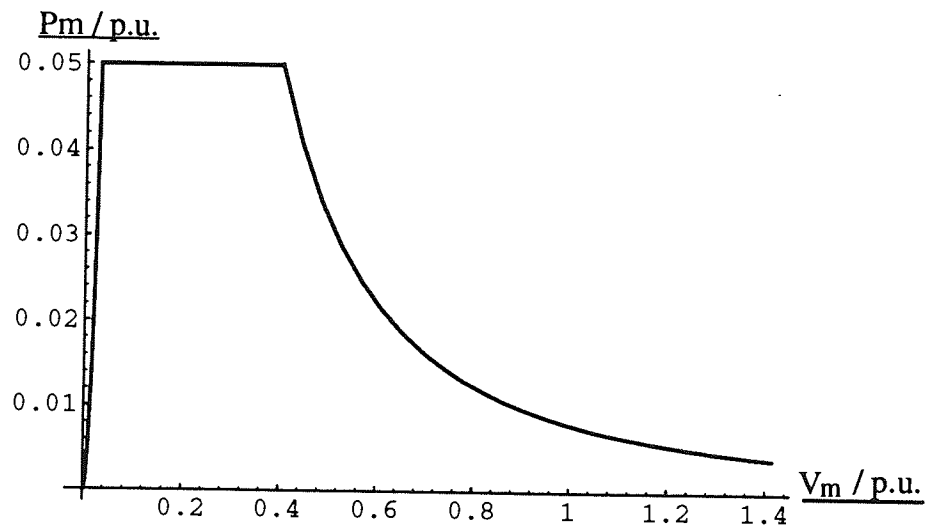


Figure 4-14. Graph of the Actual Losses when Limited at 5%.

All of this work has assumed that the formulae derived in appendix 1 are valid, i.e. that the current through the reservoir is continuous. It was shown, in figure 4-1, that an increase in the firing angle causes the ripple on the voltage across the capacitor to increase. If the value of the resonance ratio is too high then, when using an increased firing angle, the voltage across the capacitor might fall to zero during some part of the half cycle, even if it would not under normal conditions. This would, at the very least, reduce the effectiveness of the equipment. For a given value of the resonance ratio then this would restrict the possible range for the firing angle and would therefore increase the necessary supply voltage to be able to generate 1p.u. reactive power for a given amount of losses.

§4-13 Conclusions

Expressions have been derived for the fundamental frequency components of the system current in phase, I_p , and in quadrature, I_q , with the system voltage and for the coefficient of the harmonics, I_{nc} . These can be approximated to

$$\begin{aligned}I_q &\approx \frac{V_m}{X_L} [q_1 + q_2 \theta_{ob}] \\I_p &\approx \frac{\beta V_m}{X_L} [p_1 + q_2 \theta_{ob}^2] \\I_{nc} &\approx \frac{V_m}{X_L} [c_n - s_n \theta_{ob}]\end{aligned}$$

The reactive power, Q , and the active power, P , are therefore given by

$$\begin{aligned}Q &\approx -\frac{V_m^2}{2X_L} [q_1 + q_2 \theta_{ob}] \\P &\approx \frac{\beta V_m^2}{2X_L} [p_1 + q_2 \theta_{ob}^2]\end{aligned}$$

If the resonance ratio is chosen to be on the plateau region of the q_2 against m graph then q_2 can be approximated to 0.5 and q_1 and p_1 can be approximated to 0:

$$\begin{aligned}Q &\approx -\frac{V_m^2}{4X_L} \theta_{ob} \\P &\approx \frac{\beta V_m^2}{4X_L} \theta_{ob}^2\end{aligned}$$

The reactive power output and the coefficient of the harmonics can be seen to vary approximately linearly with the reduced firing angle while the losses vary quadratically. The importance of the reduced firing angle as a control parameter has been drawn out and it has been shown that the equipment has very little further dependence on either the firing angle or the damping coefficient.

The effect of the choice of the resonance ratio on the system has been illustrated. In particular, as the size of the capacitor is reduced the amount of ripple across it increases, causing extra stresses on the capacitor and devices. The presence of harmonics has been shown to be impressive for all values of the resonance ratio. For a small capacitor the system current is dominated by harmonics and the performance of the equipment is poor. Above a certain size of capacitor there is an increase in size and cost of the equipment without any significant improvement in performance. A suitable range for the resonance ratio has been shown to be $1.1 < k < 2$.

An equivalent circuit has been produced consisting of a square wave voltage source in series with a capacitor of the same value as the energy reservoir. This has been used to explain the presence of the q_1 and p_1 terms in the expressions for the fundamental component of the current.

The sizes of the energy storage components has been discussed and the equipment has been shown to offer no vast improvements on conventional SVCs.

The performance of the equipment at reduced voltage has been shown to be superior to that of a conventional SVC.

The Three Phase Voltage Sourced STATCON

§5.1 Introduction

In chapter 4 the results of the analysis on the steady state performance of the single phase equipment were presented. In this chapter the corresponding results for the three phase equipment are given and discussed.

Results from a 1kVAr model are included together with a description of the practical arrangement and control scheme. Some unexpected aspects of the performance of the machine which came to light during the commissioning stage are discussed.

§5.2 Power Circuit

The circuit diagram is shown in figure 5.1. The devices are numbered in the order that they are turned on. As in the single phase case knowledge of the operation of the inverter circuit is assumed.

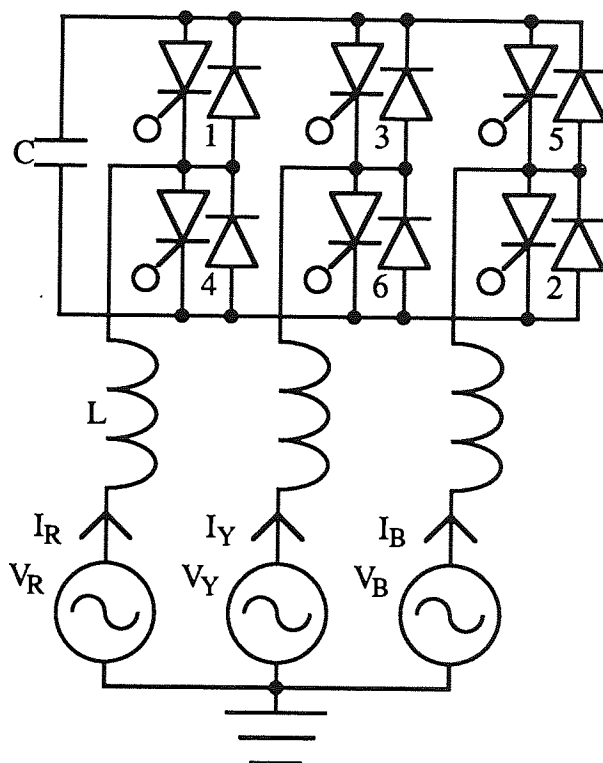


Figure 5.1. Circuit Diagram for the Three Phase STATCON with Capacitor Energy Reservoir.

The devices which are turned on, as a function of time, are given in table 5.1.

Table 5-1. On Devices in a Three Phase STATCON.

<u>Era</u>	<u>On Devices</u>		
$0 < \phi < \pi/3$	5	6	1
$\pi/3 < \phi < 2\pi/3$	6	1	2
$2\pi/3 < \phi < \pi$	1	2	3
$\pi < \phi < 4\pi/3$	2	3	4
$4\pi/3 < \phi < 5\pi/3$	3	4	5
$5\pi/3 < \phi < 2\pi$	4	5	6

§5-3 Method

Appendix 3 gives the derivation of the expressions for the current and the Fourier series. The method used was similar to that used in the single phase case; differential equations describing the currents in each of the phases during one era were produced and solved. The current in one phase during one era is the current in another phase during a different era and so from the general expressions for the currents in the three phases during one era, general expressions for the current in one phase during the first half cycle were produced. The three unknown coefficients, from the solutions to the differential equations, were then determined by ensuring that the current in the chosen phase was continuous at each of the changes of circuit topology, and that the voltage across the capacitor repeated with a period of one sixth of that of the supply. The current during the whole cycle was then determined from the fact that it must be half wave anti-symmetric.

Finding the Fourier series of the current can be simplified by finding the Fourier series of the voltage at the a.c. terminals of the inverter, d_n and e_n , and then calculating that of the current, a_n and b_n , from this, rather than directly, because the voltage at the a.c. terminals depends on only two of the constants from the solutions to the differential equations, rather than all three. Further, because the variation of the current with θ_0 is always as either $\cos\theta_0$ or $\sin\theta_0$, the a_n and b_n contributions to the Fourier series can be evaluated in terms of the parameters A_1 and A_2 and then computed at either $\theta_0 = 0$ or $\theta_0 = \pi/2$. This avoids trying to separate the θ_0 dependence in the A_1 and A_2 terms and significantly reduces the amount of algebra that has to be performed. This means that explicit expressions for the parameters p_1 , q_1 , q_2 , s_n and c_n have not been determined but these parameters have been plotted to show how they vary with k , θ_0 and β .

Using these techniques to simplify finding the Fourier series means that the s_n and c_n terms are defined in terms of $\sqrt{a_n^2 + b_n^2}$, i.e. the sign of the terms is not found explicitly. The sign was determined by comparing the situation with a very low value of the resonance ratio, i.e. a very large capacitor, to the results that would be obtained in

the circuit if a battery had been used as the energy reservoir. In the battery case the circuit would be operated with zero firing angle and the impedance between the system voltage and the stepped voltage produced at the a.c. terminals of the inverter would be the resistance and inductance, Z . In this case it can be shown that each of the harmonic coefficients must be positive so c_n must be positive for all n at small k . The value of c_n is therefore defined over the whole range of m provided that c_n does not reach zero. If it does then the sign of the square root sign has to be reversed so that c_n varies as a smooth function and is not reflected at $c_n = 0$.

For s_n the fact that as the firing angle is increased the d.c. voltage across the capacitor is raised means that, for very low values of k , the coefficient of a particular harmonic must also increase. s_n must therefore be negative at low values of k and again must vary smoothly.

§5.4 Nomenclature

The relationships describing the resonance ratio and the resistance in the circuit are different from those in the single phase case, as discussed in appendix 3.

R is the resistance in each phase of the circuit. It is the resistance in the inductance plus that of one device. In the single phase circuit the resistance includes the resistance of two devices.

The resonance ratio, k , is again the ratio of the damped natural frequency oscillations of the circuit to the system frequency. Because there are always two inductors connected to one terminal of the capacitor and one to the other terminal, the total inductance is equivalent to two parallel connected inductors in series with a third. The total inductance is therefore $3L/2$ hence

$$k = \sqrt{\frac{2X_C}{3X_L} - \beta^2} \quad (5.1)$$

§5.5 Voltage Across the Capacitor

The voltage across the capacitor, during the interval $0 \leq \phi \leq \pi/3$, is given by

$$V_c = \frac{3V_m}{2h} (\beta^2 + k^2) \cos(\theta_0 + \phi + \gamma - 2\pi/3) + \frac{3X_L e^{-\beta\phi}}{2} [(\beta A_1 - k A_2) \sin k\phi + (k A_1 + \beta A_2) \cos k\phi] \quad (5.2)$$

Figure 5.2 shows graphs of the voltage across the capacitor using three different values of the reduced firing angle for three different values of the resonance ratio. As in the single phase case graphs in which the capacitor voltage falls below zero are included to show the effect of increasing the resonance ratio but the equipment would not perform like this and would not be operated in this region.

As in the single phase circuit, the ripple on the capacitor voltage increases as the resonance ratio increases. The ripple frequency is six times the system frequency. Again the voltage shows swells when the equipment is generating reactive power and troughs when absorbing reactive power. In this case, for all of the values of k considered, the voltage across the capacitor has only a single maximum or minimum during each switching interval.

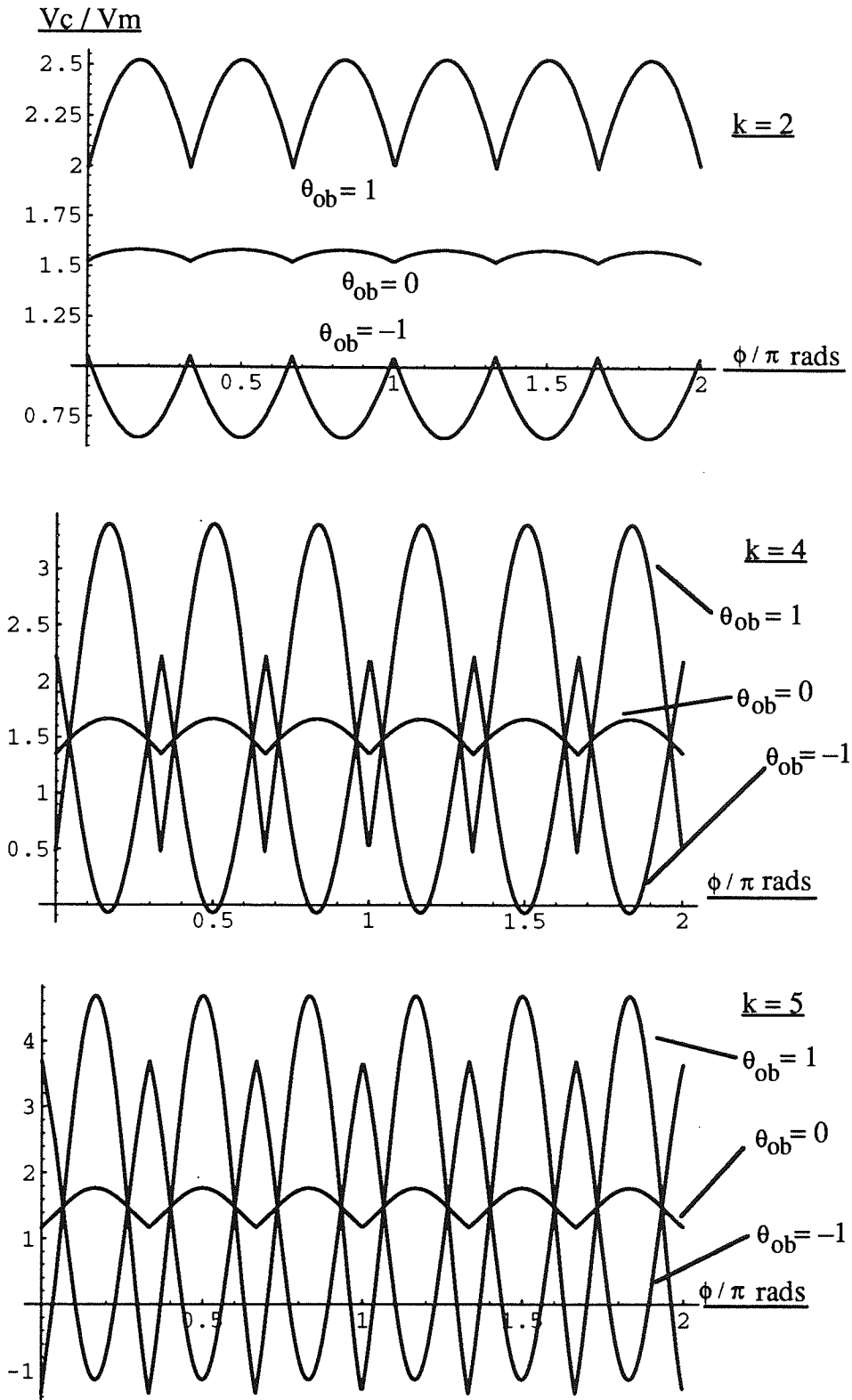


Figure 5-2. The Capacitor Voltage for a Three Phase STATCON for $k = 2, 4$ and 5 .

§5.6 System Current

The system current is described by different expressions during the first three eras, each of one sixth of a cycle duration. The current in the second half cycle is the negative of its value during the first half cycle. The expressions are

$$I = \frac{V_m}{hX_L} \sin(\theta_0 + \phi + \gamma) - \frac{\sqrt{3}V_m (\beta^2 + k^2)}{2hX_L (1 + 4\beta^2)} [\cos(\theta_0 + \phi + \gamma - 2\pi/3) - 2\beta \sin(\theta_0 + \phi + \gamma - 2\pi/3)] \\ - \frac{A_1}{2} e^{-\beta\phi} \sin k\phi - \frac{A_2}{2} e^{-\beta\phi} \cos k\phi + A_3 e^{-2\beta\phi} \\ \text{for } 0 \leq \phi \leq \pi/3 \quad (5.3)$$

$$I = \frac{V_m}{hX_L} \sin(\theta_0 + \phi + \gamma) - A_1 e^{-\beta(\phi - \pi/3)} \sin[k(\phi - \pi/3)] - A_2 e^{-\beta(\phi - \pi/3)} \cos[k(\phi - \pi/3)] \\ \text{for } \pi/3 \leq \phi \leq 2\pi/3 \quad (5.3a)$$

$$I = \frac{V_m}{hX_L} \sin(\theta_0 + \phi + \gamma) + \frac{\sqrt{3}V_m (\beta^2 + k^2)}{2hX_L (1 + 4\beta^2)} [\cos(\theta_0 + \phi + \gamma - 4\pi/3) - 2\beta \sin(\theta_0 + \phi + \gamma - 4\pi/3)] \\ - \frac{A_1}{2} e^{-\beta(\phi - 2\pi/3)} \sin[k(\phi - 2\pi/3)] - \frac{A_2}{2} e^{-\beta(\phi - 2\pi/3)} \cos[k(\phi - 2\pi/3)] - A_3 e^{-2\beta(\phi - 2\pi/3)} \\ \text{for } 2\pi/3 \leq \phi \leq \pi \quad (5.3b)$$

$$I(\phi) = -I(\phi - \pi) \quad \text{for } \pi \leq \phi \quad (5.3c)$$

Figure 5.3 shows graphs of the system current for the same parameter values as those used to produce the capacitor voltages of figure 5.2.

The graphs again show that as the resonance ratio is increased the distortion in the current waveform is increased. The six intervals per cycle are noticeable with cusps in the current waveform appearing at the switching epochs because the step in the voltage at the a.c. terminals of the inverter gives a sudden change in the gradient of the current.

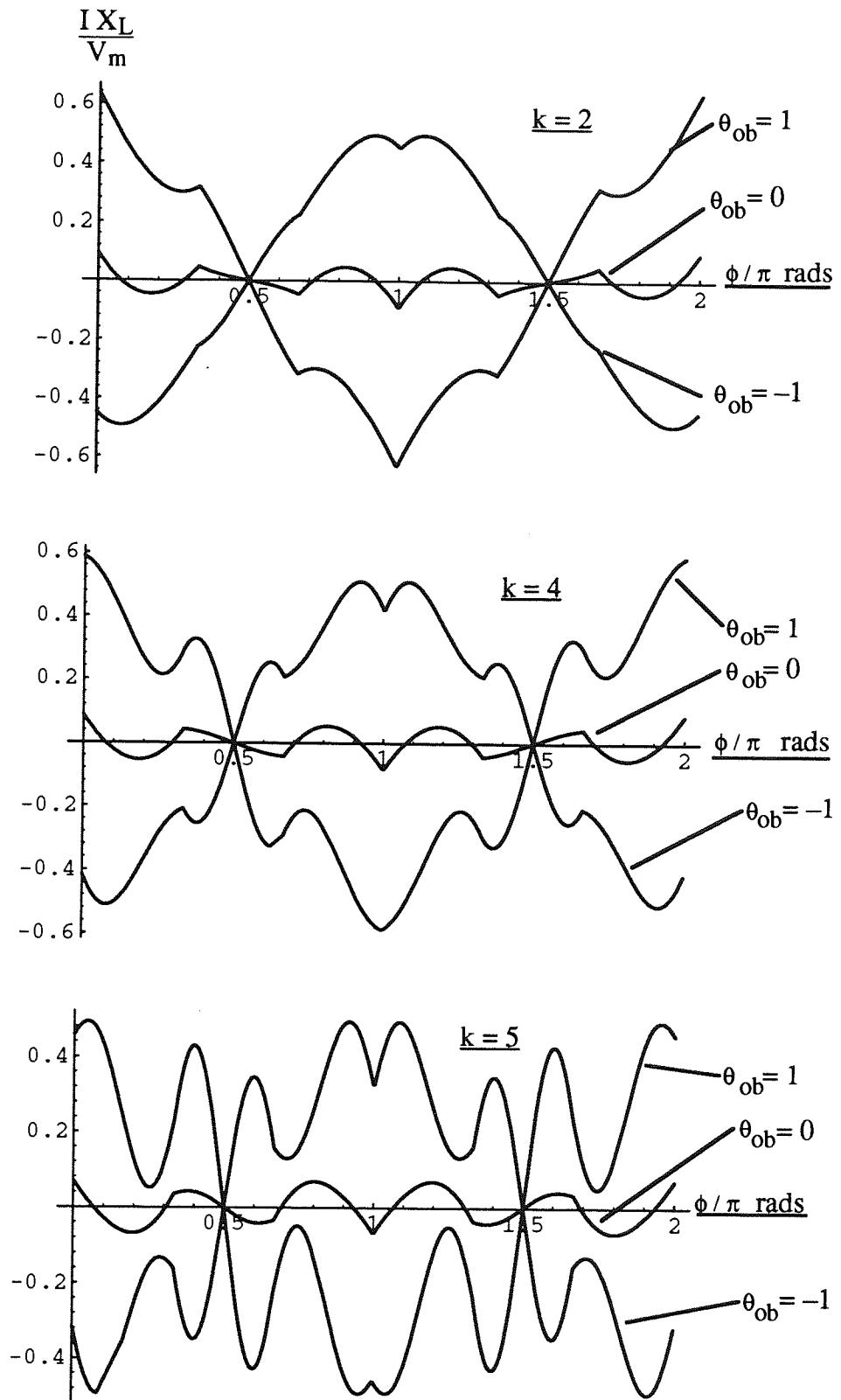


Figure 5.3. The Current in a Three Phase STATCON for $k = 2, 4$ and 5 .

§5.7 Characteristics of the Fundamental Component of the System Current

The Fourier analysis of appendix 3 shows that the form of the fundamental component of the current is the same as that in the single phase circuit:

$$I_q = \frac{V_m}{X_L} \left(q_1 + q_2 \frac{\sin 2\theta_0}{2\beta} \right) \approx \frac{V_m}{X_L} [q_1 + q_2 \theta_{ob}] \quad (5.4)$$

$$I_p = \frac{\beta V_m}{X_L} \left(p_1 + q_2 \frac{\sin^2 \theta_0}{\beta^2} \right) \approx \frac{\beta V_m}{X_L} [p_1 + q_2 \theta_{ob}^2] \quad (5.5)$$

Figure 5.4 shows the parameters p_1 , q_1 and q_2 as a function of m , for $\beta = 0.001$, 0.01 and 0.1 . Again there is very little dependence on β .

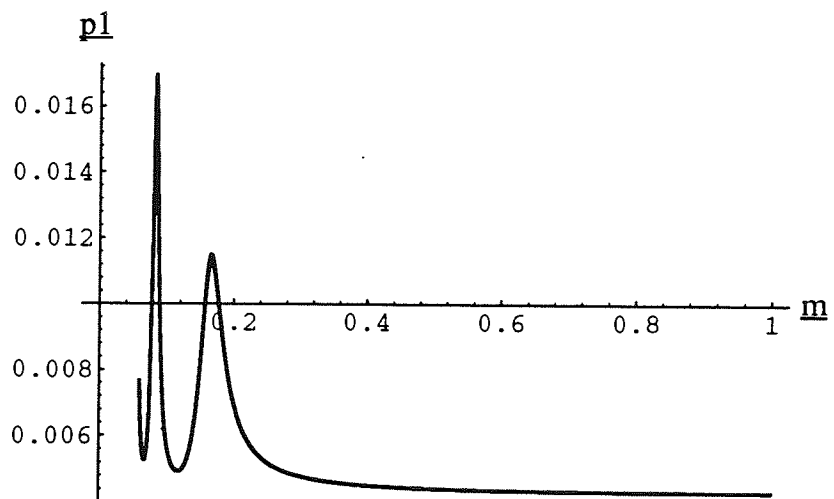
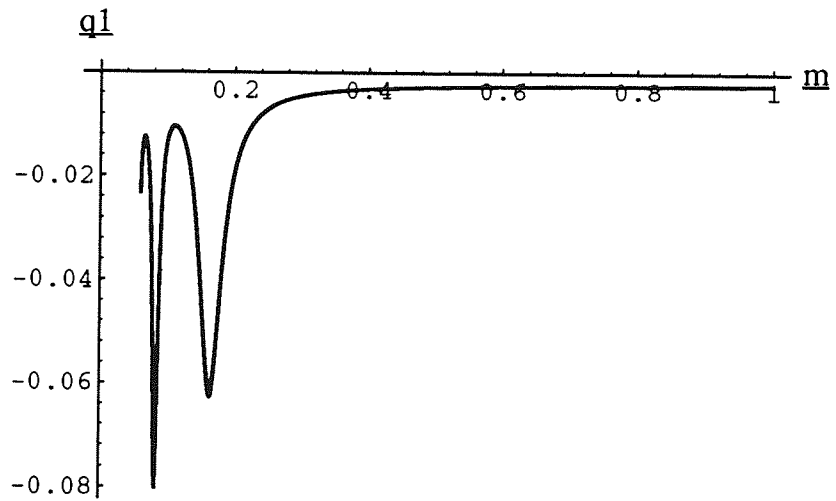
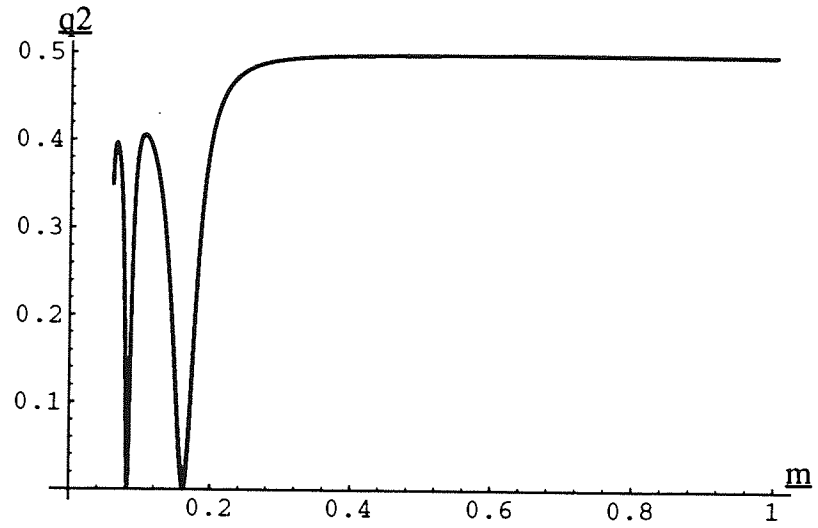


Figure 5-4. Graphs of the Parameters Describing the Fundamental Component of the Current in a Three Phase STATCON.

Comparing figure 5-4 to the equivalent figure for the single phase equipment, figure 4-3, the following points are apparent:

- 1) The figures all tend to a limit as m increases.
- 2) The value of the plateau region of the q_2 graph has the same value.
- 3) q_2 is again very much bigger than p_1 and q_1 .

Contrasting the two figures:

- 1) The plateau region on the q_2 graph starts at a lower value of m .
- 2) The q_1 graph is always negative

Figure 5-5 shows how the normalised reactive power output varies and figure 5-6 shows how the normalised losses vary with the reduced firing angle for three different values of the resonance ratio.

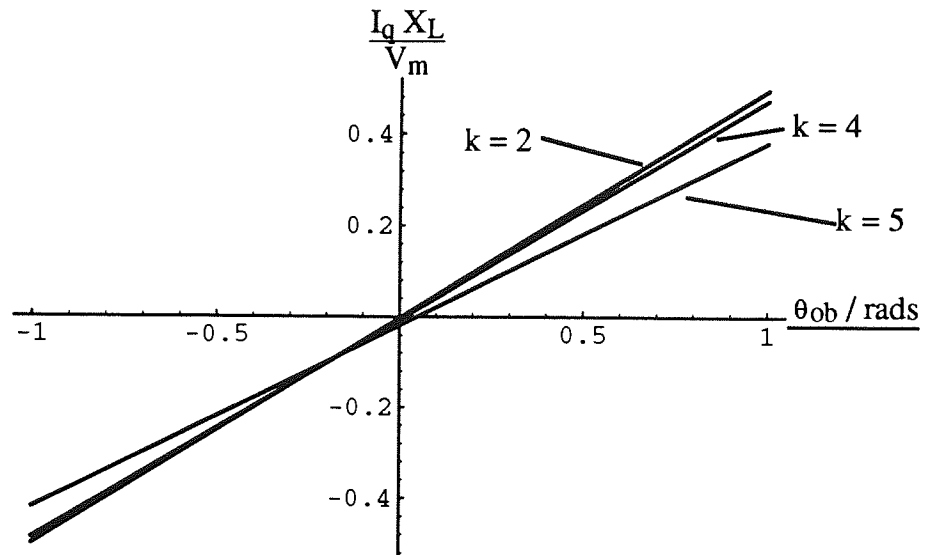


Figure 5.5. Graph of the Normalised Reactive Power Output from a Three Phase STATCON.

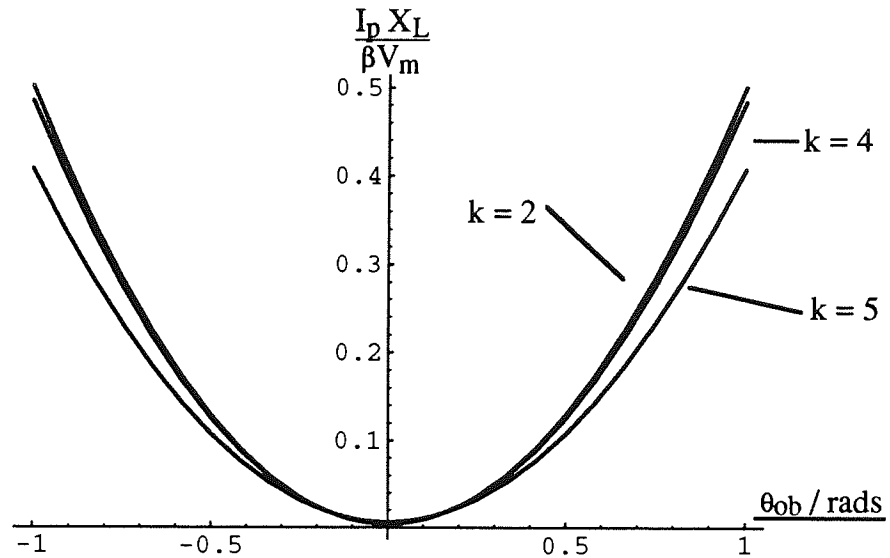


Figure 5.6. Graph of the Normalised Losses in a Three Phase STATCON.

§5.8 Total Harmonic Content

As in the single phase equipment the parameters describing the fundamental frequency component of the current can be used to compute the total harmonic content, equation (4.12). Figure 5.7 shows the normalised total harmonic content as a function of the reduced firing angle for several values of the resonance ratio.

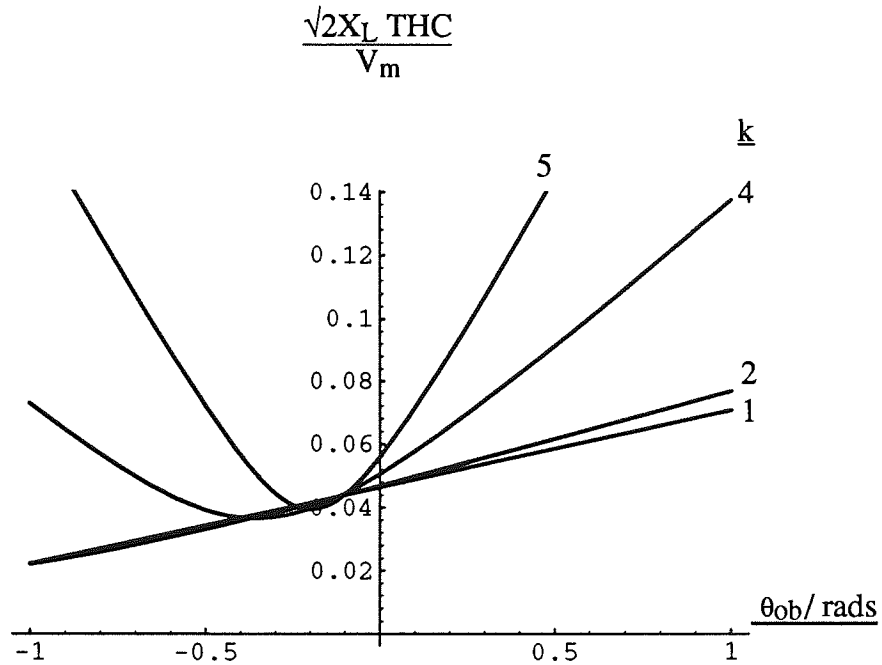


Figure 5.7. Graphs of the Normalised Total Harmonic Content as a Function of the Reduced Firing Angle in a Three Phase STATCON.

The values of THC are lower than those from the single phase circuit, as would be expected from comparing figures 5.3 and 4.2.

§5.9 Characteristics of the Harmonics of the System Current

The Fourier analysis given in appendix 3 also shows that the variation of the coefficients of the harmonics is approximately of the same form as that in the single phase. In the three phase equipment harmonics are generated for $n = 6i \pm 1$, for $i = 1, 2, \dots$

$$I_{nc} = \frac{V_m}{X_L} t_n \approx \frac{V_m}{X_L} [c_n - s_n \theta_{ob}] \quad (5.6)$$

Figure 5.8 shows graphs of t_n for $n = 5$ and 7 as a function of the reduced firing angle and figure 5.9 shows c_n and s_n for $\beta = 0.1, 0.01$ and 0.001 . Again there is very little difference between these functions for the different values of β .

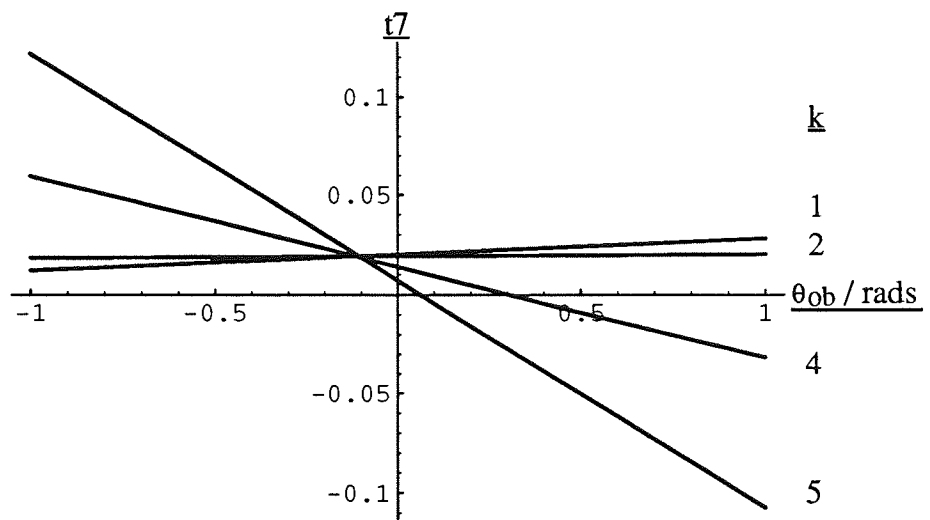
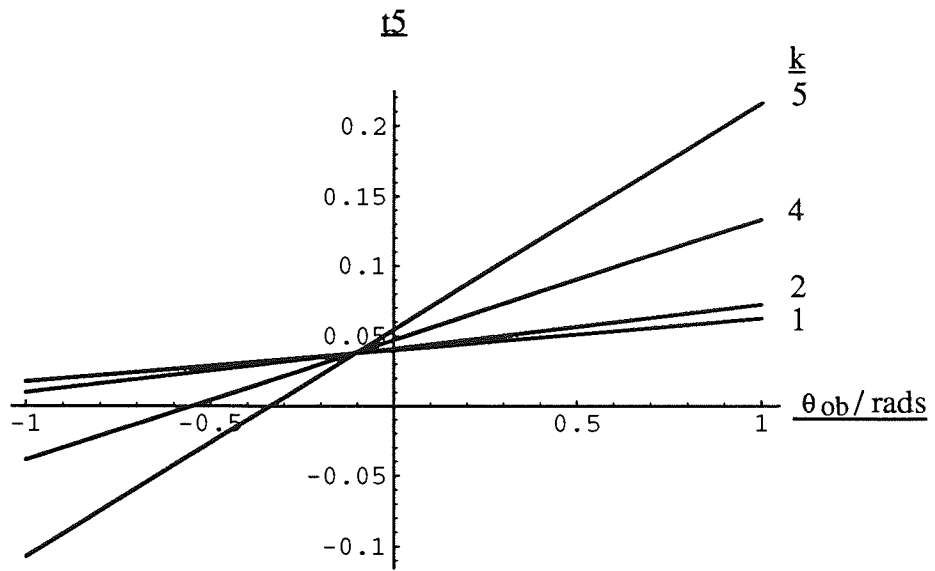


Figure 5.8. Graphs of the Normalised Coefficient of the Harmonics in the Current for $n = 5$ and 7 in a Three Phase STATCON.

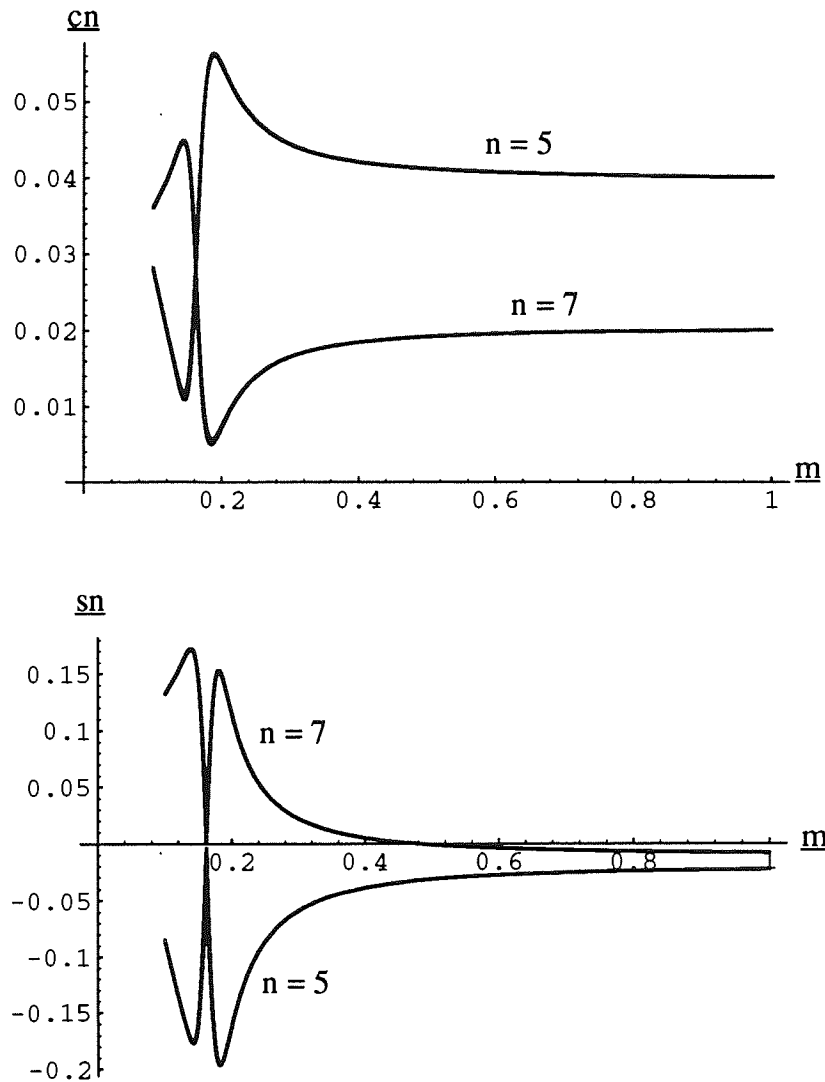


Figure 5.9. Graphs of the Parameters Describing the Coefficients of the Harmonics in the Current in a Three Phase STATCON.

§5.10 Choice of Circuit Parameters

The plateau region of the q_2 graph, figure 5.4, begins at a lower value of m than in the single phase equipment and therefore the equipment can be operated with the same value of q_2 for a smaller capacitor, assuming a fixed value for the inductances. A suitable range for k is $2 < k < 5$.

§5.11 Equivalent Circuit

Following on from the equivalent circuit developed for the single phase equipment, it is desirable to derive an equivalent circuit for the three phase equipment.

The per phase circuit model is given as figure 5.10.

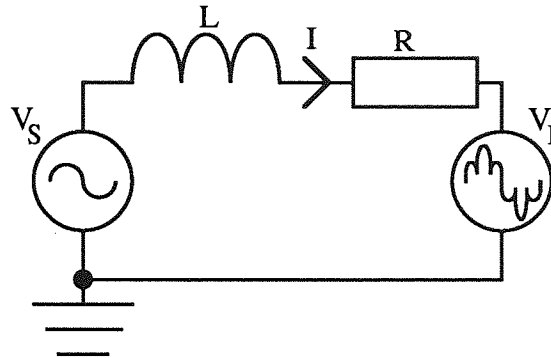


Figure 5.10. Per Phase Circuit Model of a Three Phase STATCON.

The model used for the equivalent circuit was a capacitor in series with a voltage source, as in the single phase case. From the definition of the resonance ratio, the capacitance is three halves that of the energy reservoir. The voltage at the a.c. terminals of the inverter, V_I , was calculated, from equation (5.2), and then the expressions for the current, from (5.3) to (5.3c), were used to calculate the voltage across the capacitor in the equivalent circuit, V_{ec} . The additional voltage source, V_{ad} , is the difference between V_I and V_{ec} . The derivation is presented as appendix 3.

The equivalent circuit is given as figure 5.11.

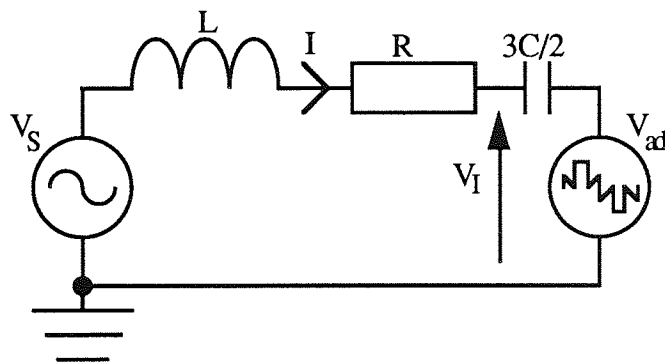


Figure 5.11. Per Phase Equivalent Circuit of a Three Phase STATCON.

Figure 5.12 shows the voltage source behind the capacitor, V_{ad} , for $k = 2, 4$ and 5 for three different values of θ_{ob} .

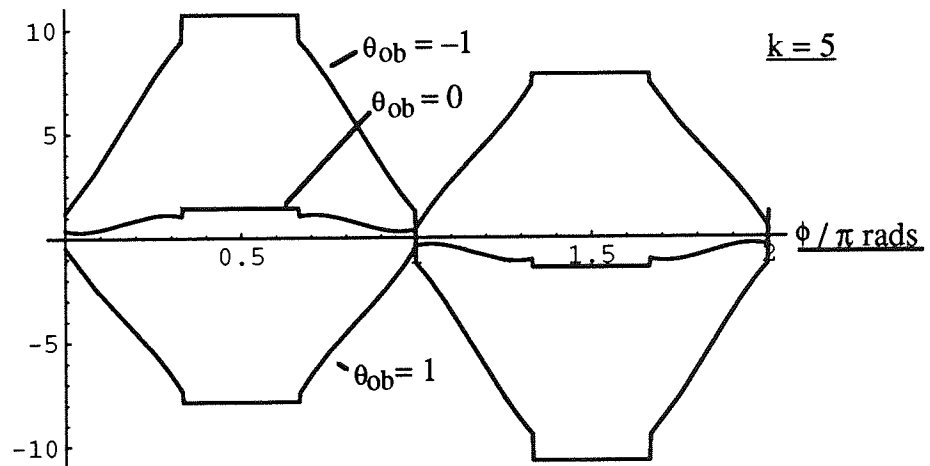
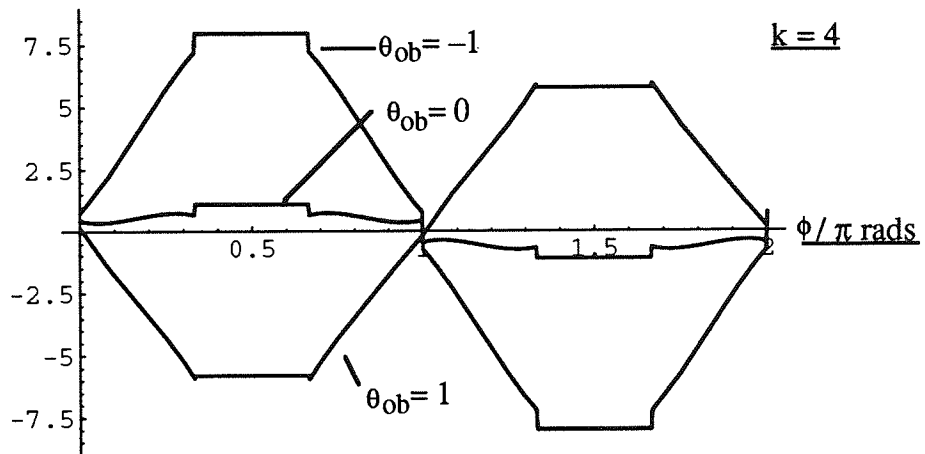
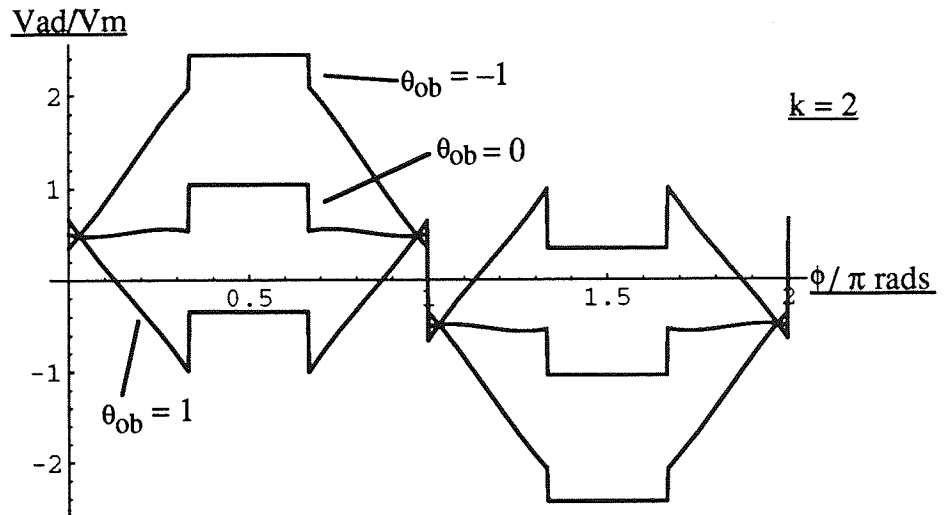


Figure 5-12. Graphs of the Voltage Source for the Equivalent Circuit of a Three Phase STATCON for $k = 2, 4$ and 5 .

The additional voltage source, V_{ad} , shows steps at the switching epochs. The amplitude of V_{ad} increases with increasing k , at least over the range investigated. During the interval $\pi/3 < \phi < 2\pi/3$, the voltage is a constant because, as in the single phase equipment, the equation describing the current in the equivalent circuit is the same as that in the actual circuit.

§5.12 Practical Arrangement

The rating of the model was chosen to be 1kVAr. The supply voltage used was 240V rms phase to phase; $V_m = 196V$. The leakage reactance of a high power transformer is between 10 and 20% of its rating, so the value of the inductors was chosen to be 40mH which is about 20% of the rating. The higher end of the range of values was chosen so that in the event of a fault the build up of current in the system would be slower, giving the fuses more time to operate before any damage to the equipment occurred. The resistance of the inductors was measured and found to be 1.5Ω . This gives a value for β of about 0.06. The exact value cannot be calculated because the (effective) resistance of the devices is not known, although it can be calculated from the results.

The value of capacitance was chosen to be $20\mu F$ based on figure 5.4. This corresponds to a value for the resonance ratio of about 2.9. Again the exact value of the resonance ratio cannot be calculated because β is not known exactly.

MOSFETs were chosen as the controllable devices because of their ease of turn on and turn off and availability at this low power level.

Further details of the practical arrangement are given in appendix 9.

§5.13 Control Scheme

The specification of the model was that it should demonstrate the steady state performance of a three phase STATCON (Ashbrook & Hill, 1993a), (Ashbrook & Hill, 1993b). It was not designed to perform under abnormal system conditions or to measure any aspect of the transient performance of such a machine.

The reactive power output was adjusted by controlling the firing angle of the inverter. The control circuit thus has to perform two tasks:

- 1) To detect when each of the MOSFETs should be turned on or off, relative to the first device being turned on.
- 2) To detect when the first MOSFET should be turned on, relative to the supply voltage.

A block diagram of the control scheme is shown in figure 5-13.

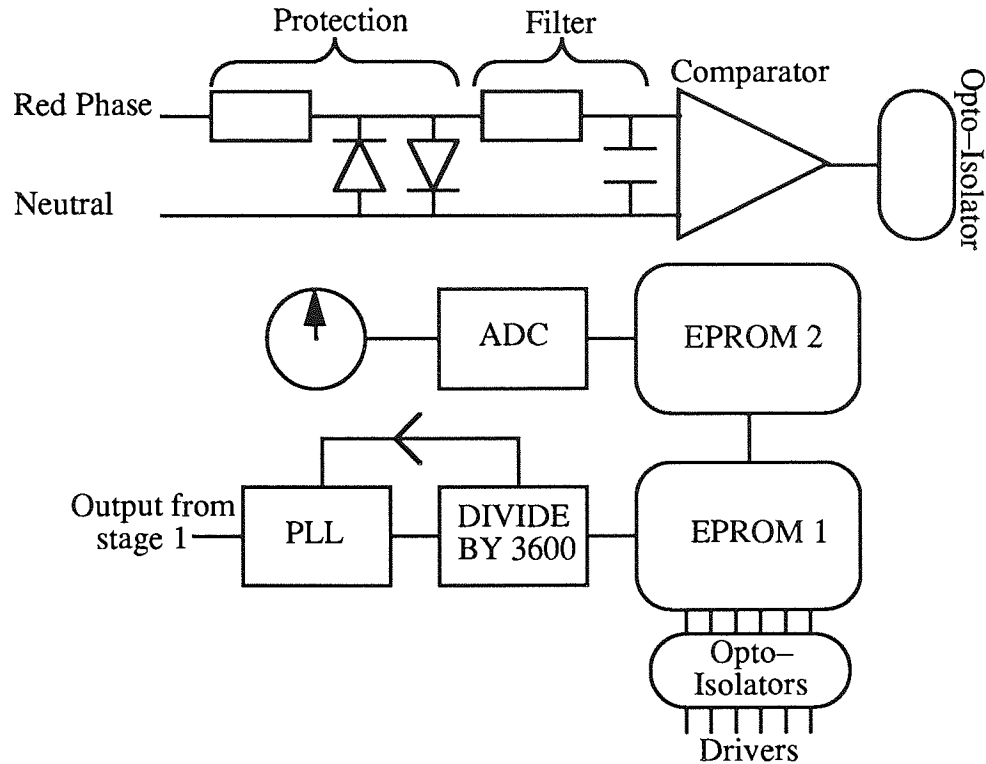


Figure 5-13. Block Diagram of the Control Circuit for a 6-Pulse STATCON.

The phase of the mains was detected by measuring the red phase to neutral voltage; the other two phases were assumed to be ideally related. The protection circuit limits the voltage across the devices in stage 1 to $\pm 0.7V$. A filter was included to remove any high frequency noise from the mains. The cut-off frequency of the filter was 15kHz and so the phase shift affected on a 50Hz signal is very small. The filtered signal was then fed into a comparator, producing a square wave with a fundamental frequency equal to that of the mains. The output from this comparator was then fed into an opto-isolator. This reduces the rise and fall times of the square wave and provides noise immunity for the digital circuitry.

In drawing up specifications for the model it was decided that the reactive power should appear to vary continuously with the position of the potentiometer so, to use a digital control scheme, it was realised that the firing angle of the inverter would have to be controlled very accurately. From computer simulations it was deduced that the range of firing angles would be $< \pm 6^\circ$, allowing for the uncertainty about the effective resistance of the devices. In order to make the reactive power appear to vary continuously then the steps in the firing angle were chosen to be 0.1° which corresponds to a step in the reactive power output of slightly less than 20VAr.

With this degree of accuracy in the firing angle the normal frequency variations of the mains, $\pm 0.5\text{Hz}$ (The Grid Code, 1994, Connection Condition 6.1.2), are too much. A phase locked loop, PLL, was therefore included in the circuit to compensate for frequency fluctuations. The output from the phase locked loop was fed into a divide by 3600 sub-circuit; the output from this was a square wave with a fundamental frequency 3600 times greater than the mains, i.e. at the nominal mains frequency the output of the divide sub-circuit is 180kHz.

EPROM 1 consists of 3600 words of six bits each, one bit relating to each MOSFET. This EPROM is clocked by the high frequency signal from the output of the divide sub-circuit and delivers a series of ones or zeroes to the MOSFET driver chips. Stage 2 of figure 5-13 then performs task 1 of the requirements of the control circuit.

The position of the potentiometer was read, and converted into a digital number, once in every cycle. The output from the ADC was then fed into EPROM 2. This consists of 128 words, i.e. $\pm 6.4^\circ$ in steps of 0.1° , relating the output of the ADC to the point of EPROM 1 at which the pointer in that EPROM should be when the system voltage rises through zero.

The phase shift produced between the mains voltage and the fundamental frequency component out of the opto-isolator of stage 1, because of the filter, can thus be seen to cause a slight shift in the position of the potentiometer to produce a specified reactive power. Since this is manually adjusted this is not serious. The EPROMs could have been written to compensate for this effect but, since it is small, they were not.

Example: Consider that the system is to generate 0.5p.u. reactive power assuming that to generate 1p.u. reactive power the firing angle is 6° and that the reactive power varies linearly with the firing angle.

The potentiometer is manually adjusted, with a voltage range of 0 – 5V. When the system voltage rises through zero the ADC is clocked. It measures the voltage at the potentiometer as 3.75V and converts this into a digital number. This digital number is fed into EPROM 2 and the pointer jumps to the address with this number. The word in this address corresponds to a firing angle of 3° . Thus the actual data of this word is the binary form of 30. This is then fed into EPROM 1 and the pointer in that EPROM jumps to address 30 and runs through the addresses in synchronism with the mains. This continues until the start of the cycle after the potentiometer is next adjusted.

§5-14 Results

Figure 5-14a shows experimental results for 1p.u. reactive power generation. Figure 5-14b shows the theoretical results and figure 5-14c shows simulations results. Figure 5-15 shows the same for zero fundamental current and figure 5-16 shows the results for 1p.u. reactive power absorption.

The values of firing angle used for the theoretical results were calculated from the q_1 and q_2 graphs using $k = 2.9$ and $\beta = 0.06$. For rated reactive power generation $\theta_0 = 1.52^\circ$, for zero fundamental output $\theta_0 = 0.028^\circ$ and for rated reactive power absorption $\theta_0 = -1.47^\circ$.

Some differences between the theoretical and practical results are apparent. In particular there is some asymmetry in the current waveforms in the practical results which is not present in the theoretical results. This is due to the different characteristics in the diodes and controlled devices when they are conducting (Trainer & Tennakoon, 1990).

The simulations were performed including modelling of the characteristics of the devices from the data sheets: the MOSFET volt drop was taken as 4V and its on state resistance as 0.8Ω while the diode volt drop was taken as 1.4V and its dynamic resistance as 0.02Ω . The firing angles used were 3.0° for rated reactive power generation, 0.05° for zero fundamental output and -2.9° for rated absorption. These values of firing angle were used because, with these device characteristics, they give the correct magnitude of current. The actual firing angles in the practical equipment would be larger because the losses in the equipment would be greater than in the simulations due to neglecting the snubber losses and inaccurate modelling of the switching losses in the simulations.

An alternative method of simulation was to apply a fairly crude model of the MOSFET and diode, with a small value for the dynamic resistance of the devices, and then to adjust the volt drops of the devices until the correct amount of asymmetry in the waveform was observed, at the correct firing angle. Thus this very crude model adjusts the device characteristics to include the other losses in the circuit. At rated current the parameters for this model were a volt drop of 20V for the MOSFET and an on state resistance of $1m\Omega$ and for the diode a volt drop of 0.7V and a dynamic resistance of $1m\Omega$. This model gives less accurate simulations of the results at low current because, unlike with the more realistic device model, the total voltage across the devices does not reduce significantly at low current.

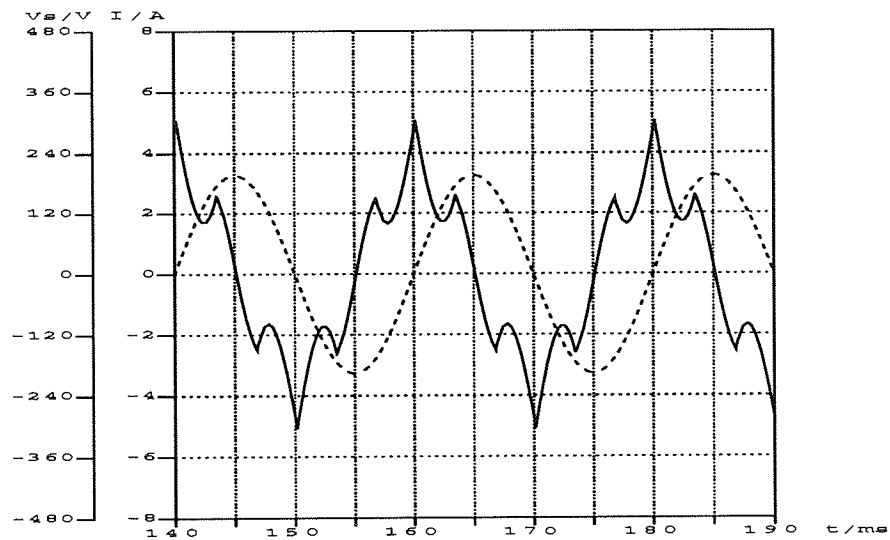
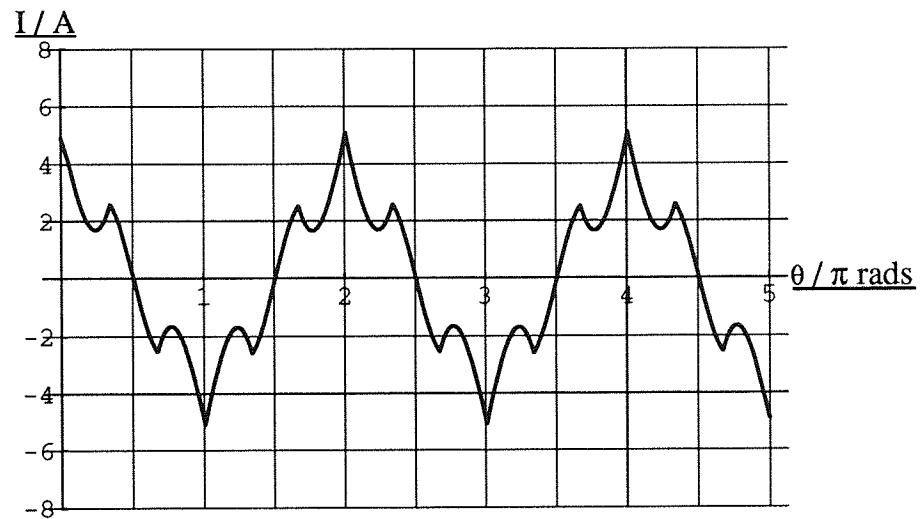
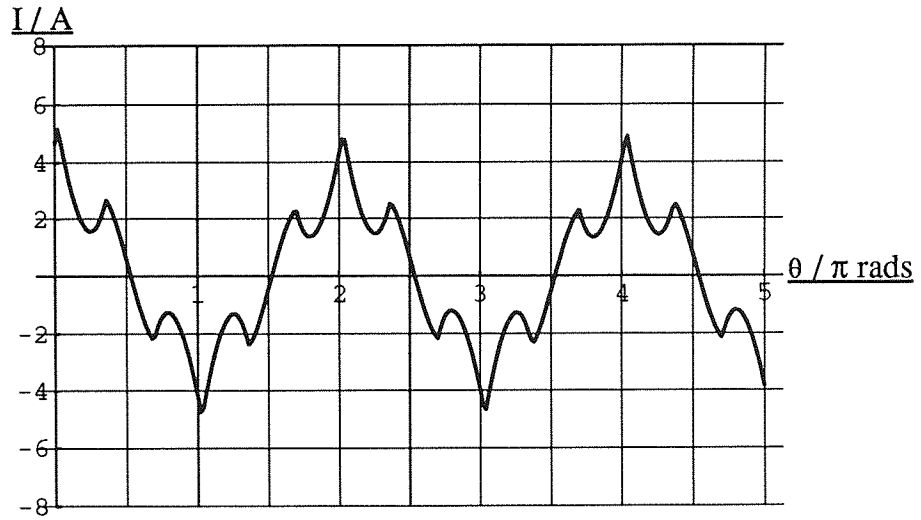


Figure 5.14. Experimental, Theoretical and Simulation Results for Rated Reactive Power Generation from a Three Phase STATCON.

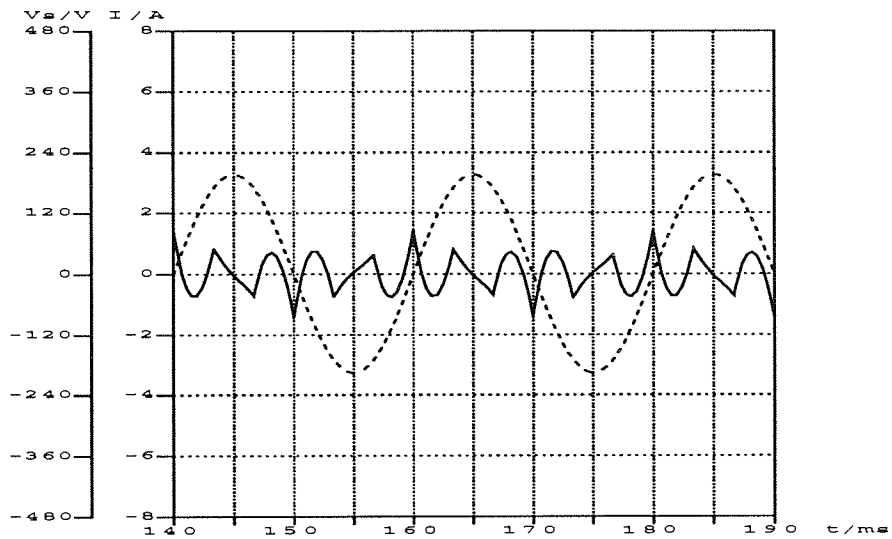
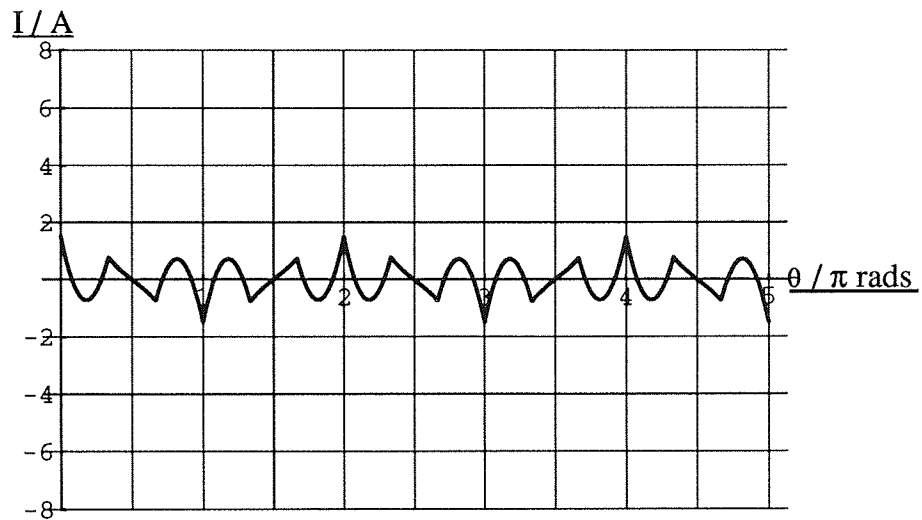
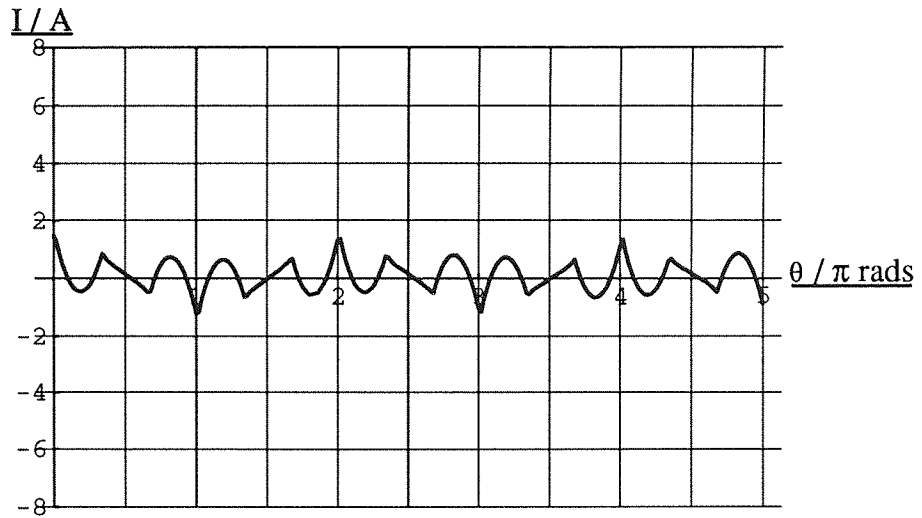


Figure 5.15. Experimental, Theoretical and Simulation Results for Zero Reactive Power from a Three Phase STATCON.

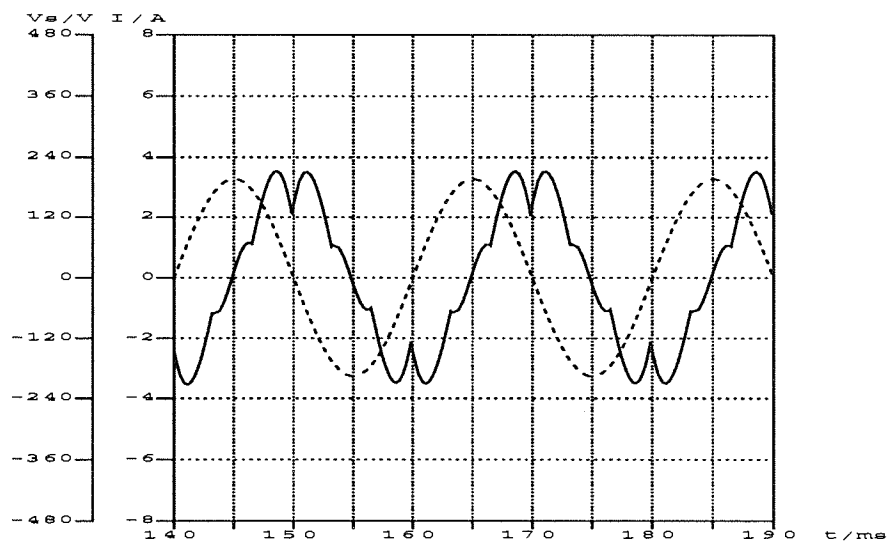
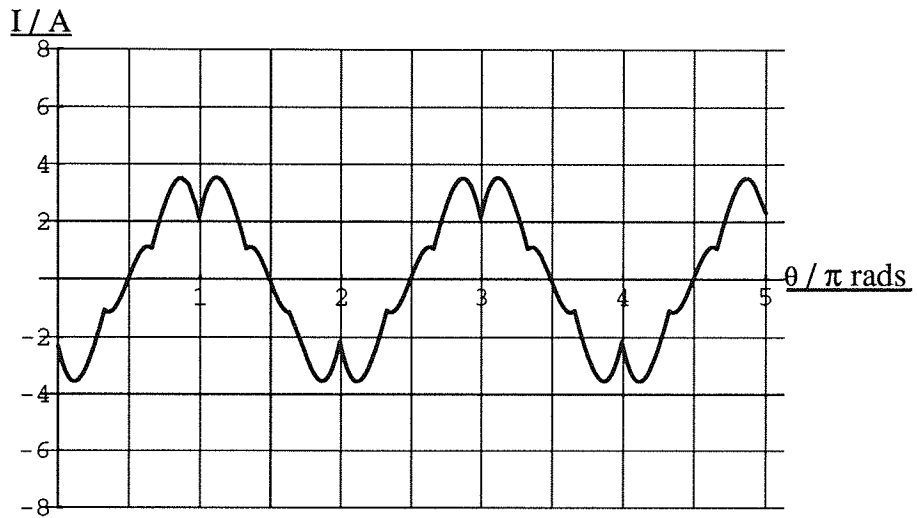
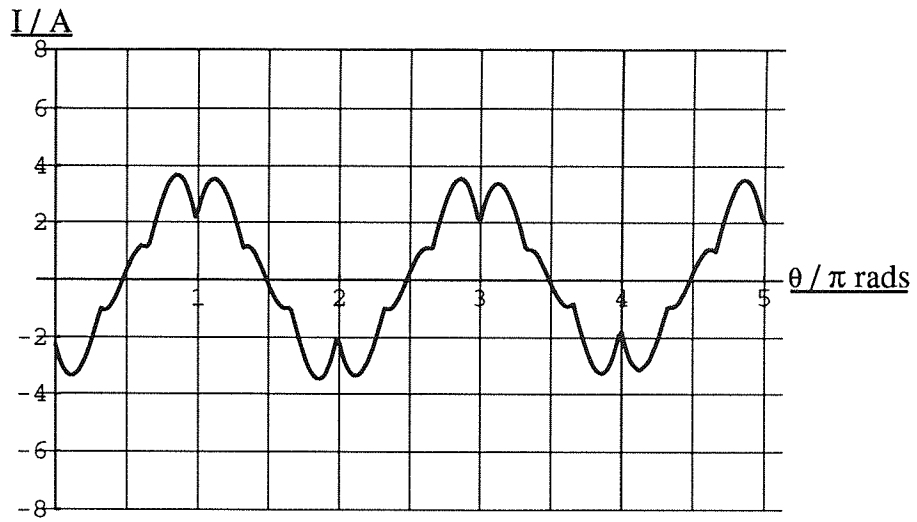


Figure 5-16. Experimental, Theoretical and Simulation Results for Rated Reactive Power Absorption from a Three Phase STATCON.

Effective values for the resistance of the circuit can be found by substituting the values for the firing angles in the formula for the reactive power:

$$Q = -\frac{3V_m^2}{2X_L} \left(q_1 + q_2 \frac{\sin 2\theta_0}{2\beta} \right) \quad (5.7)$$

Using the value of k given above gives $q_1 = -0.0037$ and $q_2 = 0.495$. Substituting these values, and the ones for V_m and X_L , in (5.7) and substituting for β in terms of R gives

$$Q = -4586 \left(-0.0037 + 6.223 \frac{\sin 2\theta_0}{R} \right) \quad (5.8)$$

In the practical equipment at rated current the firing angle is approximately 5° so the effective R is approximately 5Ω , significantly larger than the 2.3Ω from the resistance of the inductors plus the on state resistance of the MOSFETs.

§5.15 Experience of Commissioning

The equipment has proved to be very sensitive to the continual normal fluctuations in the mains voltage. Deflections of the needle of the VAR meter as large as 50VAR have been detected. This may not be an accurate reflection of how big the actual swings in the reactive power are because the meter may be under or indeed over-damped and may be affected by the presence of harmonics. It is probable that the high voltage of the transmission network would be less prone to constant fluctuations than the low voltage in the laboratory where this work was carried out but this problem still needs addressing. It is expected that the solution lies in the use of closed loop control.

The equipment has also been noted to hum violently with large positive readings for both the active and reactive power readings. After a short time normal operation of the equipment resumes. It is believed that these are due to fluctuations in the supply to the equipment. Improvements might be sought in the control scheme or in filtering.

§5.16 Size of the Energy Storage Components

As with the single phase equipment the relative sizes of the energy stores is of interest. In this case the knee point of the q_2 graph occurs at $m = 0.24$. Assuming reactances of 0.2p.u. for the inductors then the admittance of the capacitor, assuming β is small, is 0.2p.u. This compares favourably with the components in a conventional SVC in which there would have to be three inductors of 1p.u. each and three capacitors of 1p.u. each, although the capacitor in the STATCON would have to be rated for a higher voltage than those in the conventional SVC. Again these figures have not been optimised but illustrate the potential savings in the energy storage components.

§5.17 Range of Reduced Firing Angle

As in the single phase equipment, if the firing angle is too large then the capacitor can be discharged and the effectiveness of the compensator is reduced. It has been shown that the normalised current depends upon k and θ_{ob} only, for small θ_0 and β . Thus the normalised voltage across the capacitor can only depend upon these parameters. At very high values of the resonance ratio the voltage across the capacitor can have multiple (local) maxima or minima in it. It is therefore difficult to determine when the voltage is at a minimum and so whether this minimum is above zero. Numerical methods could have been used to solve the transcendental equation for the first solution on each side of zero of θ_{ob} , as a function of k , when V_c is set to zero but this would have been complicated.

The region of m of interest is on, or near, the plateau region of the q_2 versus m graph. For these values of m there is only a single swell or trough in the capacitor voltage during each era, as shown in figure 5.2, so the minimum capacitor voltage when the equipment is generating reactive power is at $\phi = 0$ and when absorbing reactive power is at $\phi = \pi/6$. Figure 5.17 shows a graph of the range of θ_{ob} for which the capacitor is not discharged as a function of m for $0.2 < m < 0.5$.

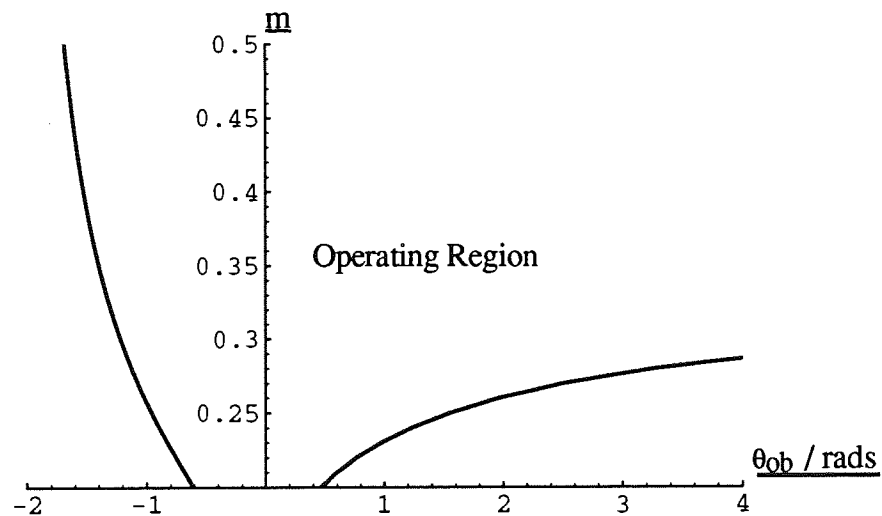


Figure 5.17. Operating Region for Small Values of θ_{ob} for the Three Phase STATCON.

From figure 5-17 it appears as though the minimum value of θ_{ob} tends to a limit at high values of m but that there is no restriction on the maximum value of θ_{ob} . However, θ_0 must be in the range $-\pi < \theta_0 \leq \pi$. Figure 5-18 shows a graph of the range for θ_0 as a function of m for a much large range of θ_0 for $\beta = 0.01$. It can be seen that the firing angle does indeed approach a limit near $\theta_0 = \pi$.

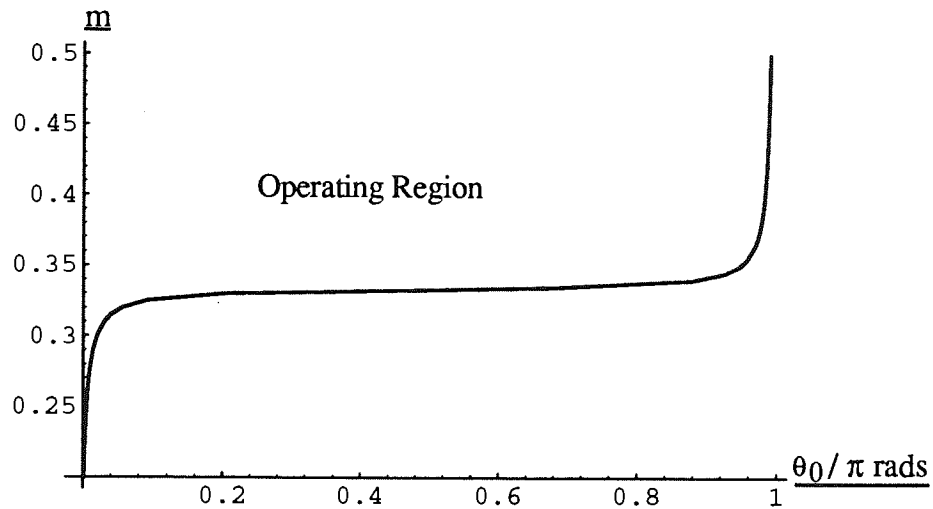


Figure 5-18. Full Operating Region for Positive θ_0 for the Three Phase STATCON.

This asymmetry in the permissible range of θ_0 can be best understood by considering the voltage across the capacitor at very high m . As the value of m increases the ripple on the capacitor is reduced, in the limit of very high m then the voltage across the capacitor tends to a constant value, i.e. its average, V_{av} . Figure 5-19a shows a plot of the average value of the voltage across the capacitor for $m = 100$ and $\beta = 0.01$; the average voltage across the capacitor is positive for a much greater range of positive values of θ_0 than for negative ones. Figure 5-19b shows the same plot over a much smaller range of θ_{ob} .

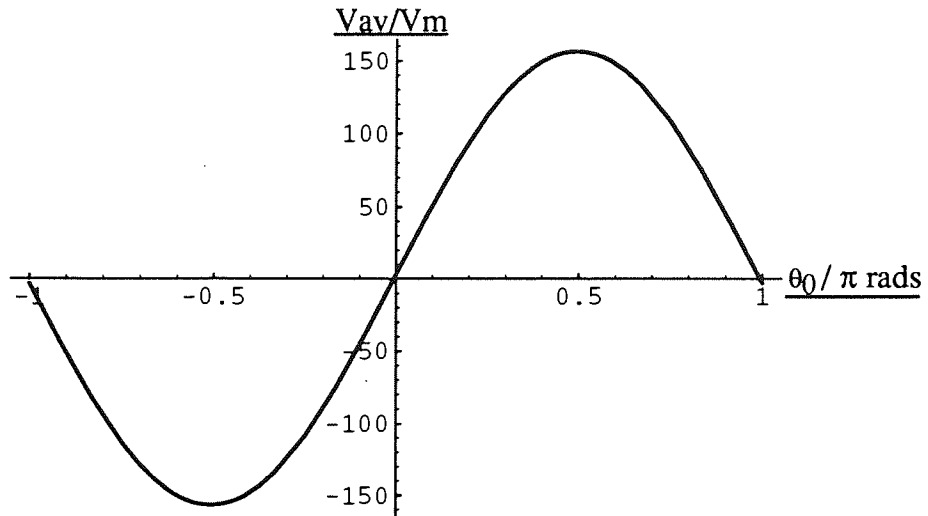


Figure 5-19a. Graph of the Average Capacitor Voltage with a Small Value of the Resonance Ratio in a Three Phase STATCON.

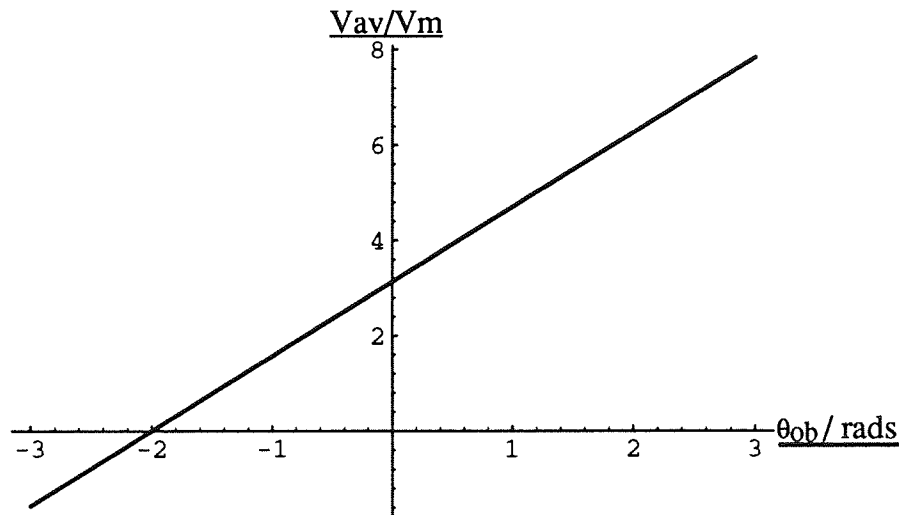


Figure 5-19b. Graph of the Average Capacitor Voltage with a Restricted Range of Firing Angle.

As the value of m is decreased the ripple in the capacitor voltage will increase and there will be regions in the $\theta_{ob} - m$ plane for which, although the average voltage across the capacitor is greater than zero, the instantaneous voltage across the capacitor will fall below zero so the range of θ_{ob} will reduce.

If it is intended to use the equipment under conditions of very low system voltage then this may effect the choice of m , i.e. m would be chosen such that the equipment could be operated with a large range of values for θ_0 .

§5.18 Conclusions

This chapter has highlighted similarities and differences between the single phase and three phase equipments. The reduced firing angle defines the behaviour of the equipment with respect to the firing angle and damping, and the value of the resonance ratio plays a very small part in the wave shape of the current provided that it is chosen to be below 5.

The magnitudes and form of the harmonics, as a function of the resonance ratio and reduced firing angle, have been quantified.

A per phase equivalent circuit has been developed. The impedance elements in this circuit consist of the inductance and resistance from the actual circuit and a capacitor which is 1.5 times the value of the capacitor in the actual circuit. Expressions for the voltage source have been given and examples plotted.

The experimental results show good agreement with the theoretical results; slight differences are due to the approximations in modelling the devices. The firing angle to obtain rated current in the practical equipment is larger than the theoretical value. This is due to ignoring the volt drop in the devices in the theoretical work.

The range of θ_{ob} for different values of m has been calculated. It has been shown that if a value of m is chosen on the plateau region of the q_2 against m graph then the available range of θ_{ob} is greater than $-1 \leq \theta_{ob} \leq 1$.

The energy storage components required have been shown to be much lower than those in a conventional SVC.

Twelve Pulse Voltage Sourced STATCONs

§6.1 Introduction

Chapters 4 and 5 have shown the results for the single and three phase circuits respectively. Harmonics are present for $n = 4i \pm 1$ in the single phase case and $6i \pm 1$ in the three phase case, for $i = 1, 2, \dots$. The three phase equipment is referred to as six pulse because the voltage across the a.c. terminals of the converter is stepped with the steps having a duration of one-sixth of the supply period.

The maximum permissible voltage harmonics that can be introduced onto the transmission grid of England and Wales from a conventional static VAR compensator are specified by the National Grid Company (High Speed Response Variable Static Var Compensators, 1992, Section 4.2) and it is likely that those from a STATCON will be similar, if not identical. There are no limits stipulated for the magnitude of a particular current harmonic that may be injected into the system because this will depend upon the impedance of the system, at the point of connection, to that frequency. However, although the waveform from the three phase equipment is superior to that from the single phase equipment, it is still highly distorted, far more so than that likely to be permissible; some method of harmonic reduction technique must be applied to the equipment.

In this chapter possible methods of reducing the harmonics are discussed and analyses carried out on two circuits using multiple secondary phases.

§6.2 Methods of Harmonic Reduction

There are four possible ways of reducing the harmonics from the STATCON:

- 1) The first is by adding filters to the circuit.
- 2) The second is to use pulse width modulation (PWM) to eliminate the low frequency harmonics generated and, if necessary, add filters to reduce the higher frequency ones. Filters for reducing high frequency harmonics are smaller and cheaper than those for low frequency harmonics.
- 3) The third is to use a number of capacitors connected in series across the d.c. terminals of the inverter and to use a set of switches to step up and down this stack so that the voltage waveform at the a.c. terminals of the inverter has a higher pulse number.
- 4) The fourth is to use a number of inverters to neutralise the lower harmonics generated, and again to use filters if there are significant amounts of higher harmonics.

a) Filtering

Filtering is widely used in low power electronic circuits for the elimination of unwanted frequencies. Passive filtering is a simple technique that does not require any complex circuitry.

The disadvantages of this technique are the large cost and physical size of the harmonic filters. Indeed one of the principle attributes of the STATCON is the reduced overall size of the equipment, compared to a conventional SVC, through the reduced size of the energy storage components, as illustrated in section 5-17. An advantage of this technique is that the filters will reduce all harmonics above the cut-off frequency, including any which are generated as a result of non-ideal operation, i.e. through imperfect switches, supply voltage, transformer etc. The increased cost and size of the filters makes this option unattractive.

b) Pulse Width Modulation

The use of pulse width modulation (PWM) to reduce the amount of harmonics in inverter output waveforms is well documented (Lander, 1987, Chpt. 5), (Mohan et al., 1989, Chpt. 6). The stepped waveform produced at the a.c. terminals of a three phase inverter can be stepped at a higher rate to reduce the harmonics present and the reactive power output can still be controlled by adjusting the phase angle between the system voltage and the inverter output voltage (James and Hill, 1994, section 4). This method of harmonic reduction eliminates the low frequency harmonics but increases the amount of harmonics at higher frequencies (ibid., section 4).

PWM (or SHEM – selective harmonic elimination modulation) has been used in laboratory models of STATCONs of both the current sourced (Van Wyk et al., 1986), (Moran et al., 1989a) and voltage sourced (Moran et al., 1989b), (Liang et al., 1991) types.

The disadvantage of this method is that there is an increase in the switching losses in the circuit. This makes this method of harmonic elimination unsuited to the high power transmission environment (Mori et al., 1993).

As discussed in section 1-6, work is being undertaken by semiconductor device manufacturing companies on developing the MCT. When this becomes available at high power levels this option may become economically viable.

c) Multiple Level Converters

In this method a stack of capacitors replaces the single one used as the energy reservoir. As an example of this, figure 6-1 shows a single phase two level STATCON. This connection of devices seems to be the simplest but connections using fewer devices are possible. Controllable devices have been shown on both sides of the lower pairs of devices to prevent short-circuiting the capacitors.

One possible wave shape that could be produced at the a.c. terminals is also shown in figure 6-1, together with the device combinations which can be used to give each voltage. The ripple on the voltage across the capacitors has been neglected. This waveform is clearly superior to the square wave that would be produced from the single phase equipment using only one capacitor. All of these switching configurations may not be reasonable as some of them may cause the capacitors to be discharged.

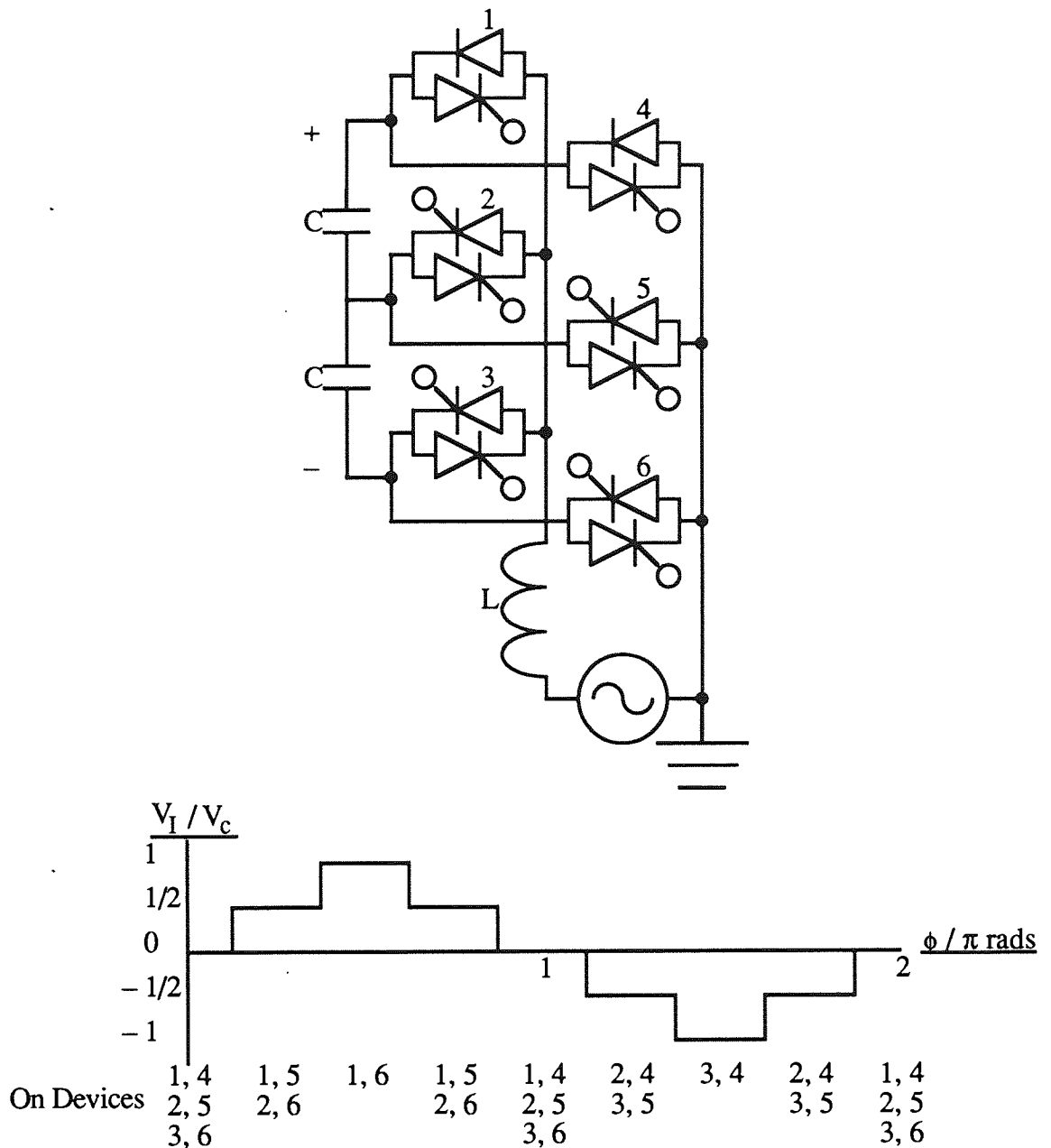


Figure 6-1. Multi-Level Single Phase STATCON and Associated Wave Shape.

The most obvious disadvantage of this method is that there is an increase in the number of devices in the circuit, although this may not be as bad as the figure suggests.

The characteristics of the different devices need not be the same. In the first half cycle devices 1 and 6 have high voltage but low current requirements. In the next half cycle devices 3 and 4 have the same requirements. During the regions where V_I is zero the devices conducting must be able to withstand a high current but at low voltage. Thus devices 1, 3, 4 and 6 could be chosen to be able to withstand the full voltage but less than the rated current and devices 2 and 5 chosen to withstand the full current but only a fraction of the rated voltage. The switching pattern would be chosen to take

these factors into account. This might enable the equipment to avoid, or reduce, series and/or parallel connection of the devices.

The number of times a switch is turned on and off in a cycle depends upon the switching pattern used but will be less than when using PWM.

The size of the capacitors is not known. The total capacitance may have to be larger than when using only a single capacitor.

d) Multiple Phase Converters

In this option the harmonics are eliminated by combining the outputs from a number of six pulse converters through phase shifting transformers. The disadvantages of this method are that the phase shifting transformer is complicated, large and expensive. This method will not neutralise any harmonics introduced into the system by non-ideal conditions.

The increased number of converters obviously means that there will be an increase in the number of turn ons and turn offs in a cycle. This does not necessarily increase the switching losses in the equipment because each of the switches is carrying only a fraction of the current that it would be carry if only a single circuit were used.

Because the capacitor is switched between the incoming phases more frequently, it is expected that the use of multiple inverter topologies will facilitate a reduction in the size of the energy reservoir.

This technique is also referred to as multiple pulse number.

The largest STATCON built to date (80MVA) has used this technique (Mori et al., 1993) as have all of the reported prototype models applied to actual power systems, (Sumi et al., 1981), (Edwards et al. 1988) as opposed to laboratory scale models. For this reason, it was decided to consider this method of harmonic reduction in the rest of the work presented in this thesis. The other methods are worthy of consideration, and indeed after further work one of the other methods suggested may prove to be the most economic. Areas of particular interest in the other methods are discussed in section 8.8.

§6.3 Multiple Pulse Configurations

These large equipments referred to above have used eight converters, i.e. a forty-eight pulse system, six converters and two converters respectively. The technique described for two converters uses only star and delta transformers, while that for higher pulse numbers requires zigzag transformers.

There are two transformer configurations which can be used with parallel connected converters for many (>12) pulse systems (Sumi et al., 1981). For a 12 pulse system these circuits are shown in figures 6.2a and b; the primaries of the transformers can be arranged in either series or parallel. The phase shift between the two inverters is half of the duration of each of the pulses at the a.c. terminals, i.e. 30° .

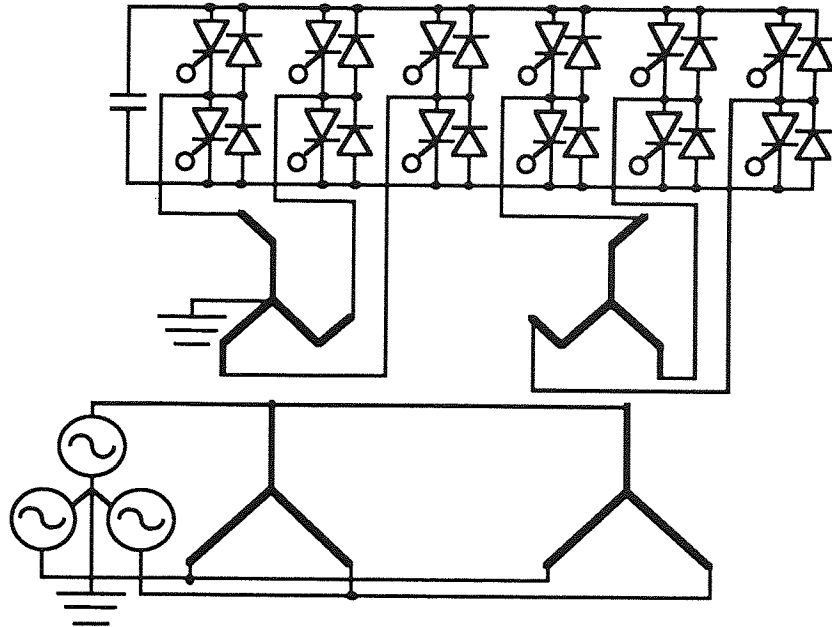


Figure 6-2a. 12-Pulse STATCON with Parallel Connected Transformer Primaries.

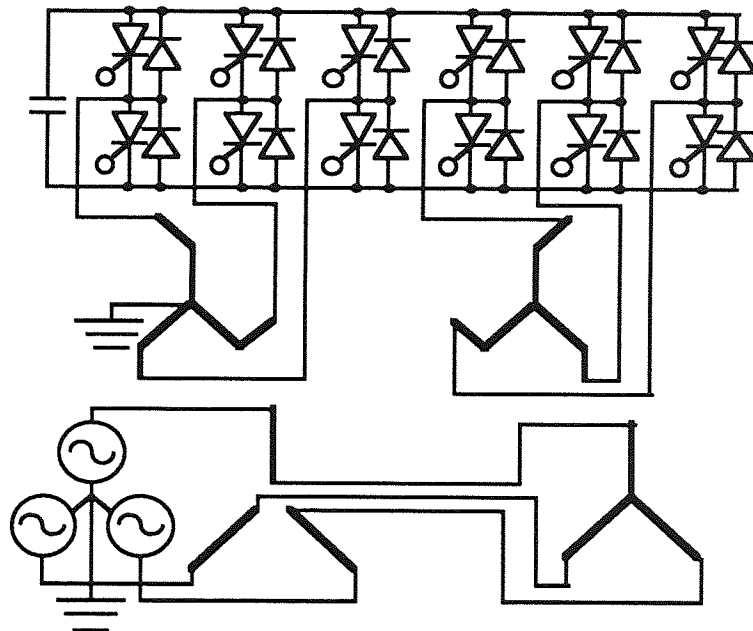


Figure 6-2b. 12-Pulse STATCON with Series Connected Transformer Primaries.

The transformer arrangement is made up of two phase-shifting transformers with conventional star windings for the primaries and zigzag windings for the secondaries. In the case of the series connected primaries, one of the transformers is of the open star type. Only one of the star points on the secondary side of the transformers is earthed, as discussed in appendix 5.

The voltage on one phase of the secondary of the transformers is the vector sum, according to the turns ratios, of the voltage from two different phases on the primary side, appendix 5.

The switches in each of the converters are fired in the same order as those in the six pulse equipment and the firings between the two inverters are displaced by 30° , as in table 6.1. The instant when the red phase voltage of the supply rises through zero is taken as $\phi = 0$. Inverter 1 is the inverter connected to the transformer with the output leading on the supply voltage, i.e. the left hand inverter as drawn in figure 6.2.

Table 6.1. On Devices in a Twelve Pulse STATCON.

<u>Era</u>	<u>On Devices in Inverter 1</u>	<u>On Devices in Inverter 2</u>
$-\pi/12 < \phi < \pi/12$	5 6 1	4 5 6
$\pi/12 < \phi < \pi/4$	5 6 1	5 6 1
$\pi/4 < \phi < 5\pi/12$	6 1 2	5 6 1
$5\pi/12 < \phi < 7\pi/12$	6 1 2	6 1 2
$7\pi/12 < \phi < 3\pi/4$	1 2 3	6 1 2
$3\pi/4 < \phi < 11\pi/12$	1 2 3	1 2 3
$11\pi/12 < \phi < 13\pi/12$	2 3 4	1 2 3
$13\pi/12 < \phi < 5\pi/4$	2 3 4	2 3 4
$5\pi/4 < \phi < 17\pi/12$	3 4 5	2 3 4
$17\pi/12 < \phi < 19\pi/12$	3 4 5	3 4 5
$19\pi/12 < \phi < 7\pi/4$	4 5 6	3 4 5
$7\pi/4 < \phi < 23\pi/12$	4 5 6	4 5 6

Because the phase shift between the two secondaries is 30° , this can be produced by using only star and delta transformers, i.e. using one transformer of 0° and the other of 30° . The current produced on the secondary sides of the transformers is identical with that produced from the connection discussed above. The current on the primary side is not identical but is similar, in particular the same harmonics are present. The transformer with 0° phase shift is obviously not necessary and so only a single transformer needs to be used.

The parallel and series form of these transformer configurations are shown in figures 6.3a and b.

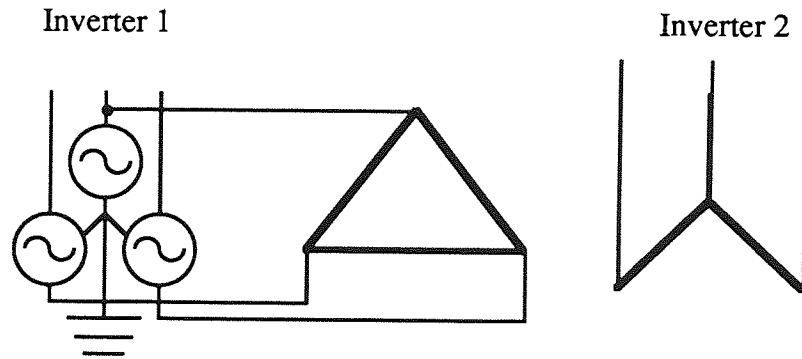


Figure 6-3a. Single Transformer Parallel Connected 12-Pulse Arrangement.

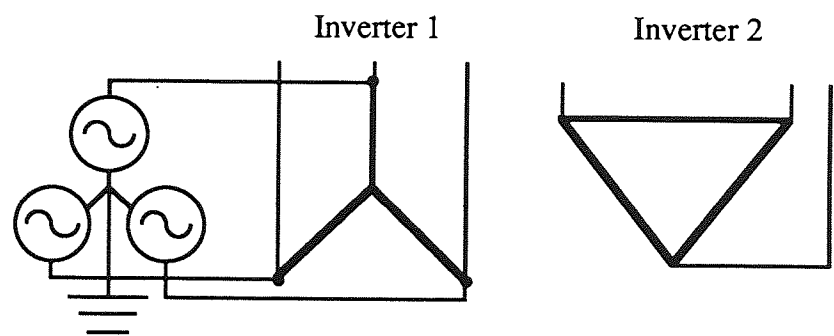


Figure 6-3b. Single Transformer Series Connected 12-Pulse Arrangement.

The transformer arrangements used in figure 6-3 avoid using zigzag transformers. However the output from these, as with the other twelve pulse circuits discussed, has harmonics for $n = 12i \pm 1$, where $i = 1, 2, \dots$. Filters can be included to eliminate these (Edwards et al., 1988) but, as discussed in section 6-2a, the use of filters is undesirable because of their size and cost. The equipment described in this reference is 1MVA and it is recognised there that for equipments of larger rating it may be advantageous to use a higher pulse number to reduce the harmonics further. For a pulse number of greater than twelve it is necessary to use transformer phase-shifts different from 30° so this technique cannot be directly extended. These circuits are not then analysed further but the series and parallel ones, as shown in figure 6-2, are, as a precursor to circuits of higher pulse number.

Referring to figures 6-2a and b the transformer with the secondary leading the supply voltage shall be referred to as transformer 1 and that lagging the supply voltage as transformer 2.

a) Parallel Connection

The voltage at the a.c. terminals, V_I , for the red phase of transformer 1 is given as figure 6-4 using $k = 4$ and $\theta_{ob} = 1$. It is similar to that in the six pulse equipment but has higher frequency ripple and is phase shifted by 15° . The current that is produced on the secondary side of the transformer is therefore similar to the current that is produced in the six pulse equipment.

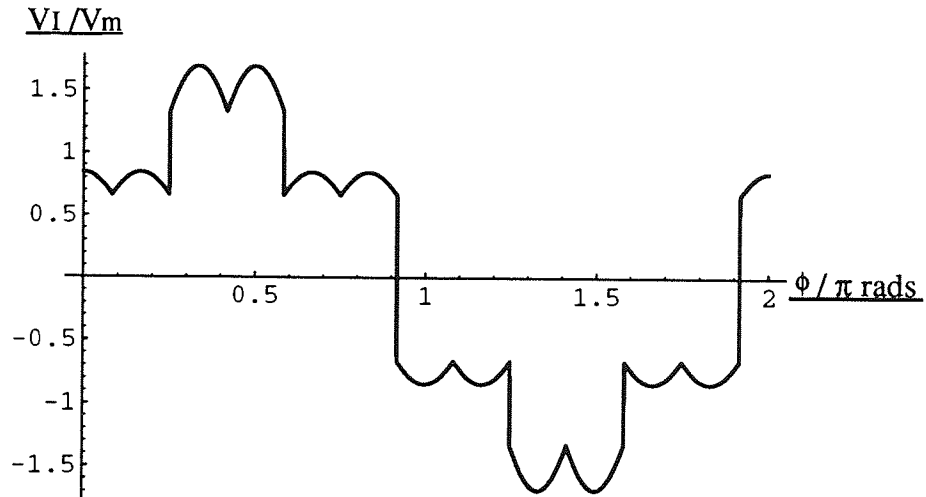


Figure 6.4. 12-Pulse Inverter Output Voltage.

The current in one phase of the primary side is made up from summing, through the appropriate turns ratios, the currents from all of the phases on the secondary side to which that phase of the primary is coupled. Figure 6-5a shows examples of normalised leading currents, using $\theta_{ob} = 1$, in the two red phases on the secondary side with a small value of the resonance ratio, $k = 0.01$. Figure 6-5b shows the resultant normalised current in the red phase of the primary side.

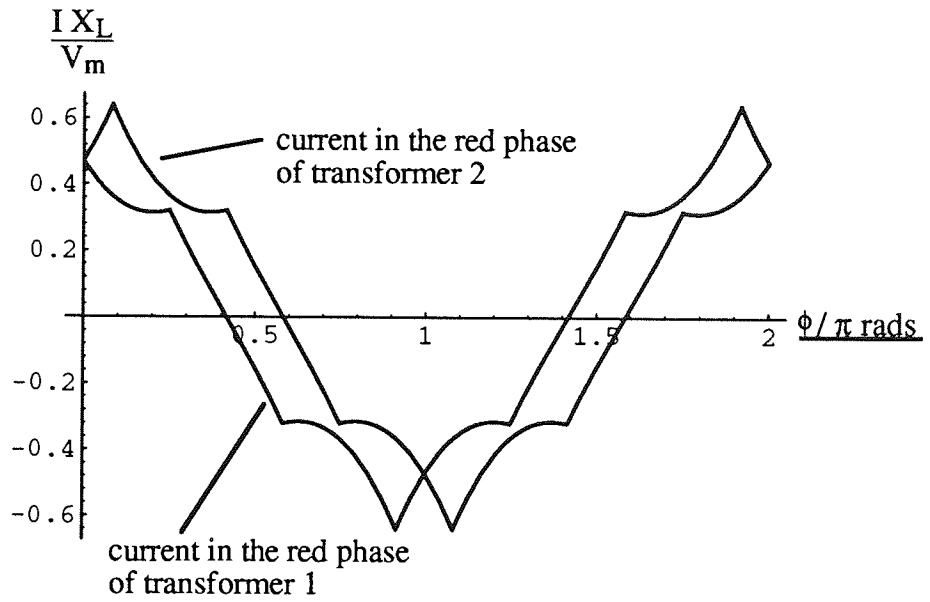


Figure 6-5a. Graph of the Currents in the Red Phases of the Secondaries in the Parallel Circuit.

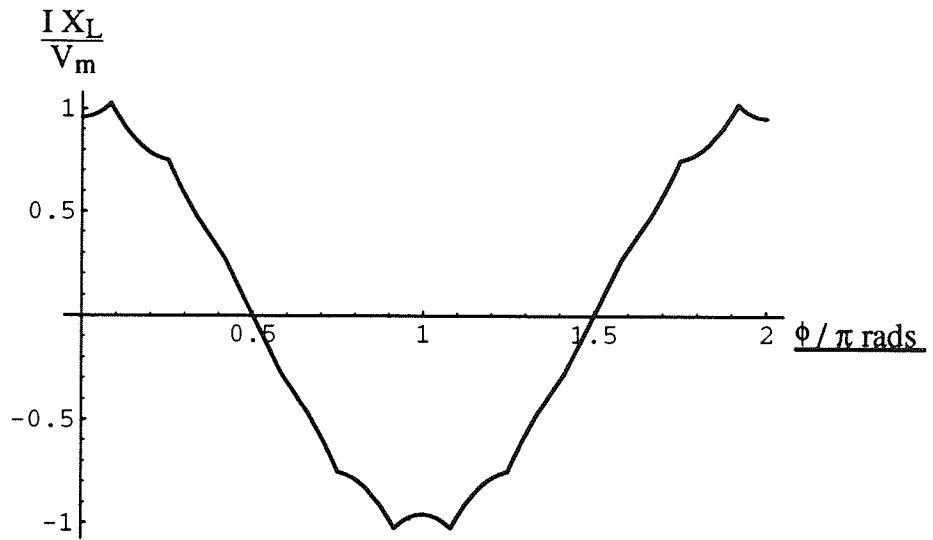


Figure 6-5b. Graph of the Current in the Red Phase of the Voltage Source in the Parallel Circuit.

b) Series Connection

For low values of the resonance ratio the system current wave shape and the voltage at the a.c. terminals of the inverter appear very similar to those from the parallel circuit. The voltage across each of the primaries of the transformers depends upon the system current. Figure 6-6 shows the voltage across each of the red phases of the two primaries and figure 6-7 shows the voltage across each of the red phases of the two secondaries. V_{RX} is the voltage at the midpoint of the two primary windings in the red phase and V_R is the red phase to neutral voltage. The solid line of figure 6-6 is the voltage across the first primary, $V_R - V_{RX}$, and the dashed line is the voltage across the second primary. V_{ar} and V_{br} are the red phase voltages on the secondaries of the first and second transformers respectively. The solid line of figure 6-7 is V_{ar} and V_{br} is the dashed line.

Both graphs have been produced using $\theta_{ob} = 1$ and $k = 0.01$. Figure 6-8a shows the resulting currents in each of the secondaries and figure 6-8b shows the current on the primary side of the transformer. The wave shape for the graph of the system current appears very similar to that in the parallel case. At much higher values of the resonance ratio differences between the two system current wave shapes are discernible.

V_R and $V_R - V_{RX} / V_m$

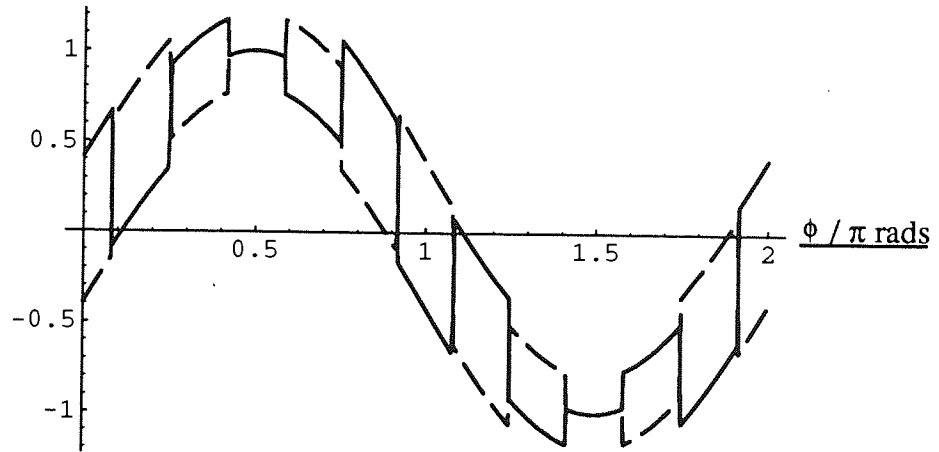


Figure 6.6. Graph of the Voltages Across Each of the Red Phase Primary Windings.

V_{ar} and V_{br} / V_m

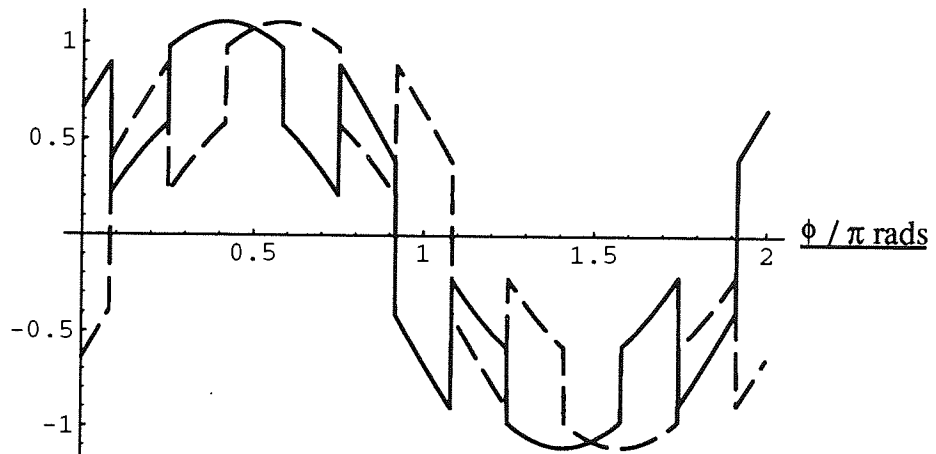


Figure 6.7. Graph of the Voltages Across Each of the Red Phase Secondary Windings.

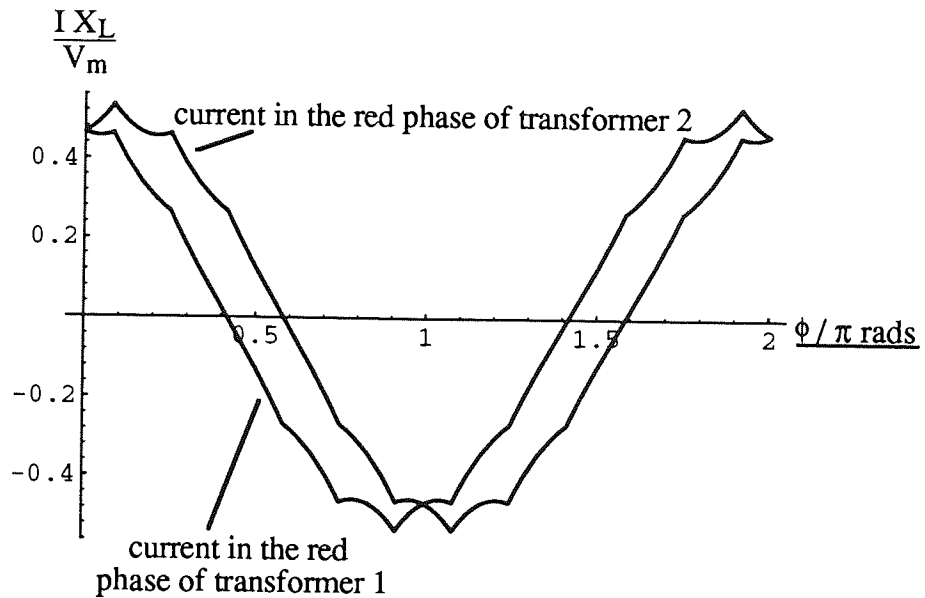


Figure 6-8a. Graph of the Currents in the Red Phases of the Secondaries in the Series Circuit.

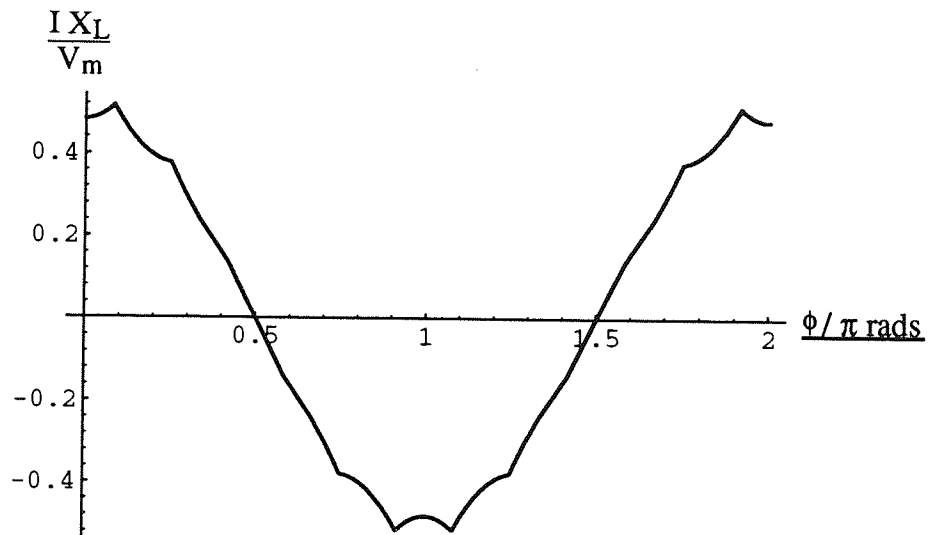


Figure 6-8b. Graph of the Current in the Red Phase of the Voltage Source in the Series Circuit.

The analyses of the parallel and series connected circuits are presented as appendices 5 and 6 respectively.

This discussion has modelled the transformers with a leakage reactance on the secondary side. They can, of course, be modelled with it on the primary side. Figure 6-9 shows a graph of the 12-pulse inverter output voltage as seen from the primary side in the red phase, V_{IP} , of the transformers using $k = 4$ and $\theta_{ob} = 1$ in the primary connected case. This is similar to the wave shape that would be produced at the a.c. terminals of the inverter from a multi-level equipment.

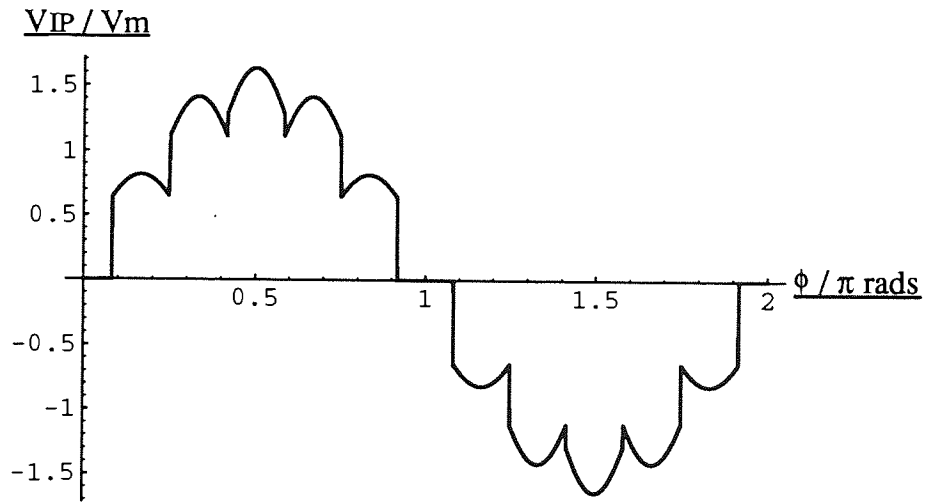


Figure 6.9. Graph of the Inverter Output Voltage with the Leakage Reactance of the Transformers on the Primary Side.

§6.4 Nomenclature

Most of the terms are as defined in the single and three phase cases. The resistance is as in the three phase circuit. There are five constants included in the general solutions to the differential equations in the parallel case but only three in the series case. These are denoted A_1 to A_5 in the parallel case and A_1 to A_3 in the series case.

The resonance ratio is defined slightly differently in the two cases:

$$\text{Parallel circuit} \quad k = \sqrt{\frac{4}{3} \frac{X_C}{X_L} - \beta^2} \quad (6.1)$$

$$\text{Series circuit} \quad k = \sqrt{\frac{2+\sqrt{3}}{3} \frac{X_C}{X_L} - \beta^2} \quad (6.1a)$$

V_m is also defined slightly differently in the two cases: it is the peak of the applied voltage in the parallel connected case and is half of the peak of the applied voltage in the series connected case. Thus in both cases it is the peak of the fundamental component of the voltage on the transformer secondaries. Defining the amplitude of the applied voltage in this way means that the amplitude of the fundamental component of the current in the parallel circuit is twice that in the series circuit, for the same reactive power output.

§6.5 Voltage Across the Capacitor

The voltage across the capacitor, during $-\pi/12 \leq \phi \leq \pi/12$, for the parallel circuit is shown in appendix 5:

$$V_c = \frac{3V_m}{2h} (\beta^2 + k^2) \cos\pi/12 \sin(\phi + \theta_0 + \gamma) + \frac{3X_L e^{-\beta\phi}}{4} [(\beta A_1 - k A_2) \sin\phi + (k A_1 + \beta A_2) \cos\phi] \quad (6.2)$$

and for the series circuit, from appendix 6:

$$V_c = \frac{6V_m}{(2 + \sqrt{3})h} (\beta^2 + k^2) \cos\pi/12 \sin(\phi + \theta_0 + \gamma) + \frac{3X_L e^{-\beta\phi}}{2 + \sqrt{3}} [(\beta A_1 - k A_2) \sin\phi + (k A_1 + \beta A_2) \cos\phi] \quad (6.2a)$$

Figure 6.10a shows graphs of the voltage across the capacitor in the parallel circuit for three different values of the reduced firing angle for three different values of the resonance ratio and figure 6.10b shows the same for the series connected case. Again the graphs illustrate the increase in ripple on the capacitor with increasing resonance ratio and the ones in which the voltage falls below zero should not be interpreted literally.

The graphs are very similar but with slightly less ripple in the series connected case. The ripple frequency is twelve times that of the system frequency. For these values of k there is only a single maximum or minimum in the voltage during each switching era.

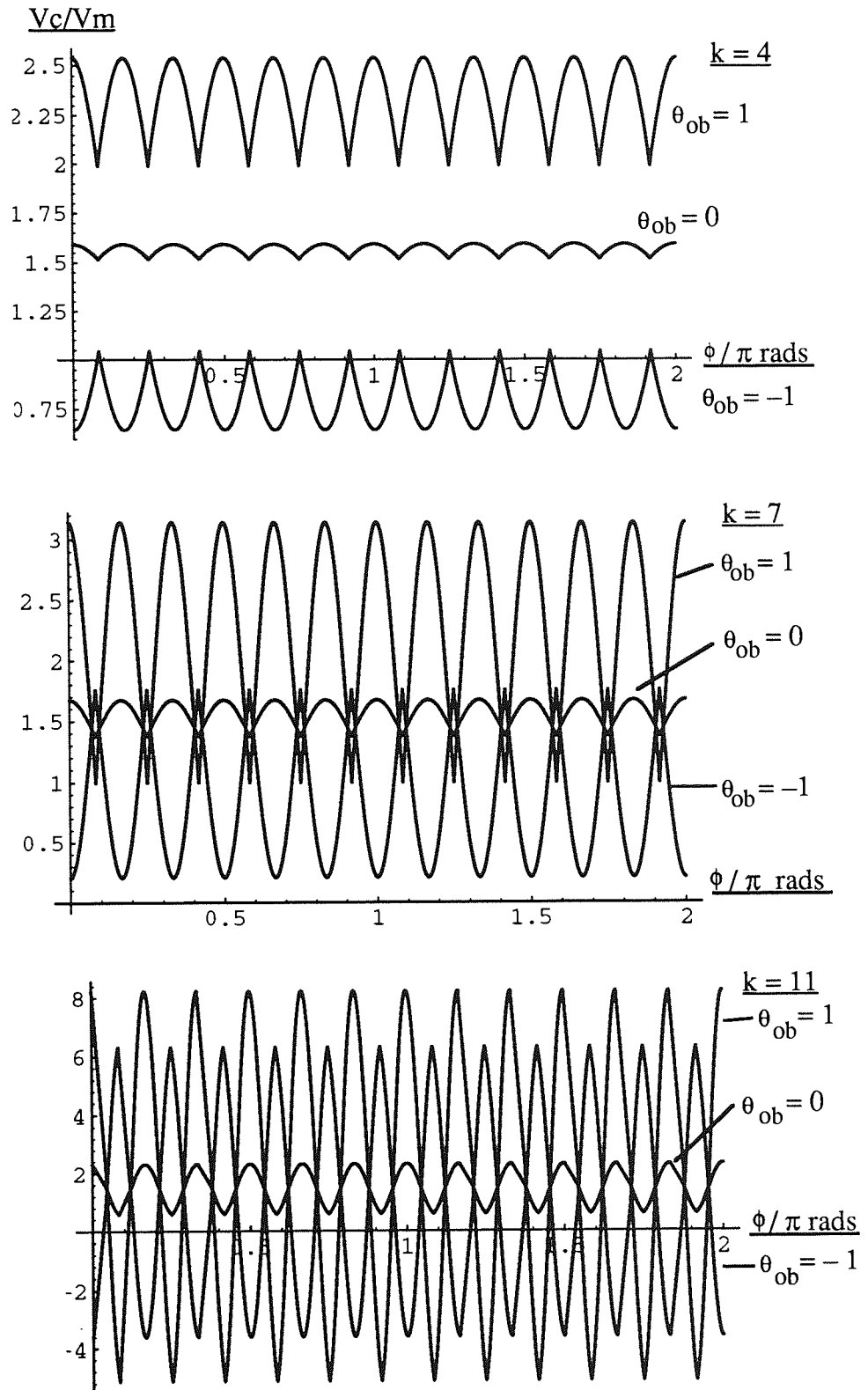


Figure 6-10a. The Capacitor Voltage for a Twelve Pulse Parallel STATCON for $k = 4, 7$ and 11 .

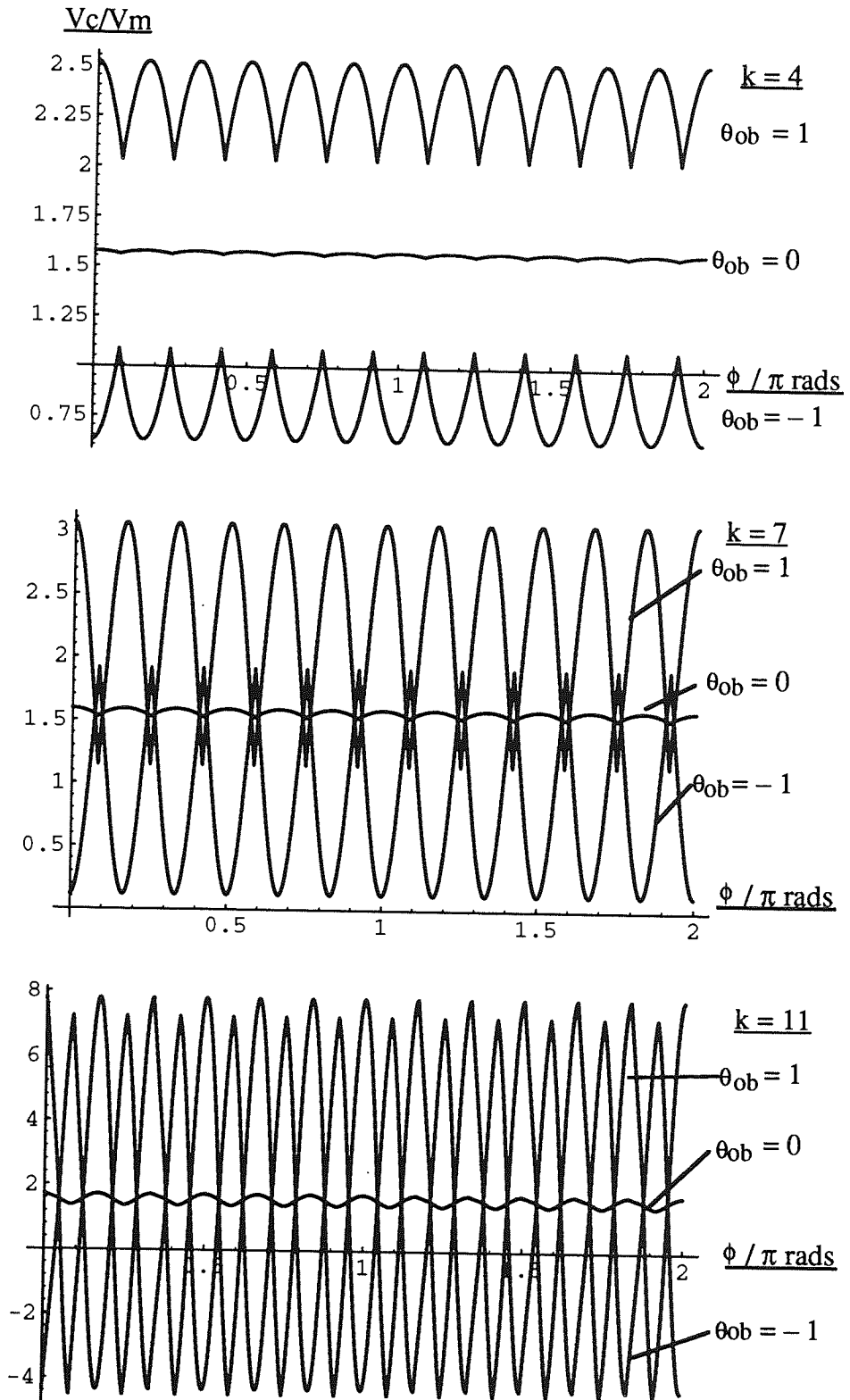


Figure 6-10b. The Capacitor Voltage for a Twelve Pulse Series STATCON for $k = 4, 7$ and 11 .

§6-6 System Current

Figure 6-11a shows the current on the primary side of the transformers for the circuit with the transformer primaries connected in parallel and figure 6-11b shows the same for the series connected circuit.

The wave shapes are similar in the two cases but are of different amplitude. As in the six pulse circuit, cusps in the waveforms are noticeable at the switching epochs.

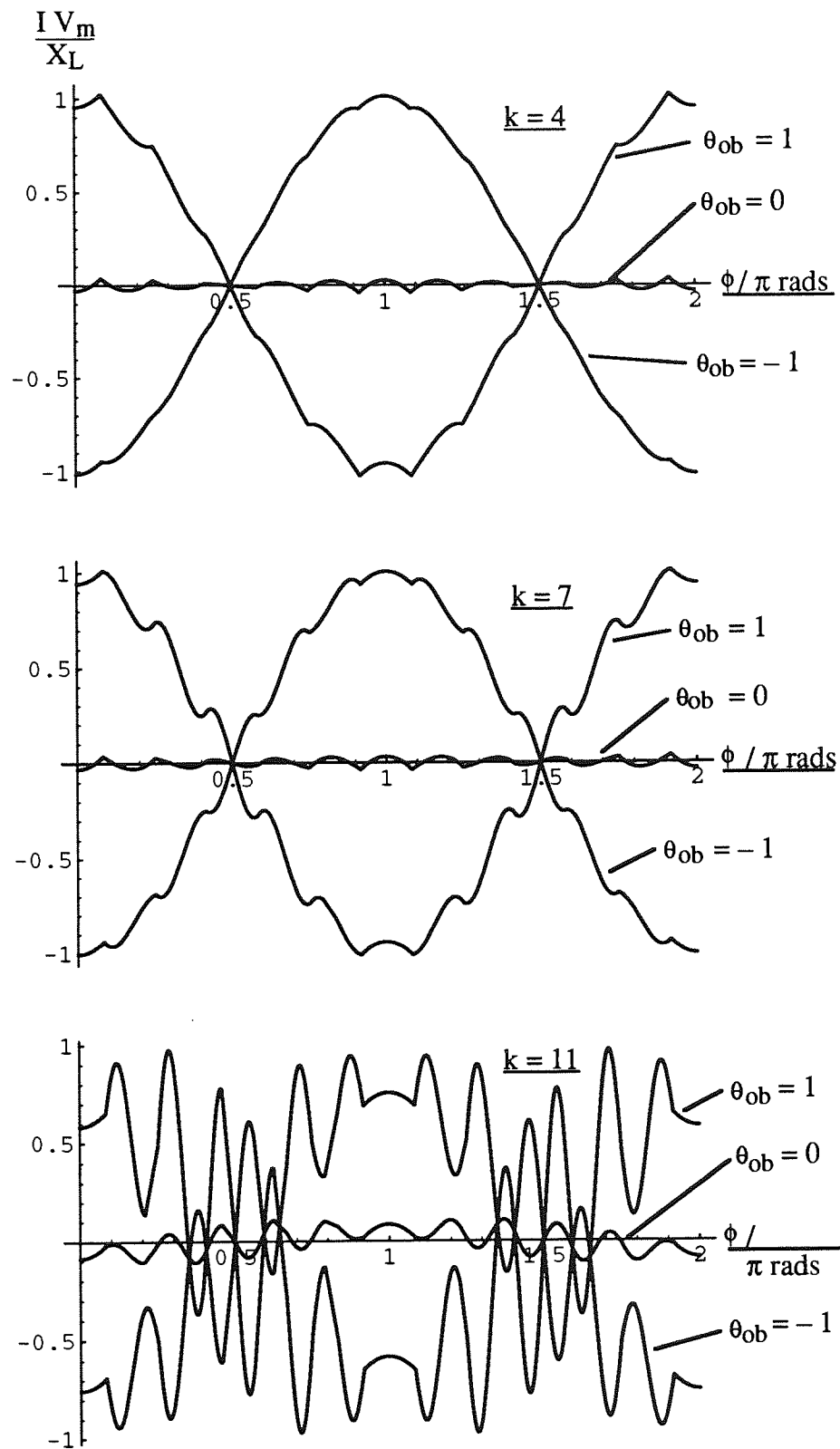


Fig. 6-11a. The Current in a Twelve Pulse Parallel STATCON for $k = 4, 7$ and 11 .

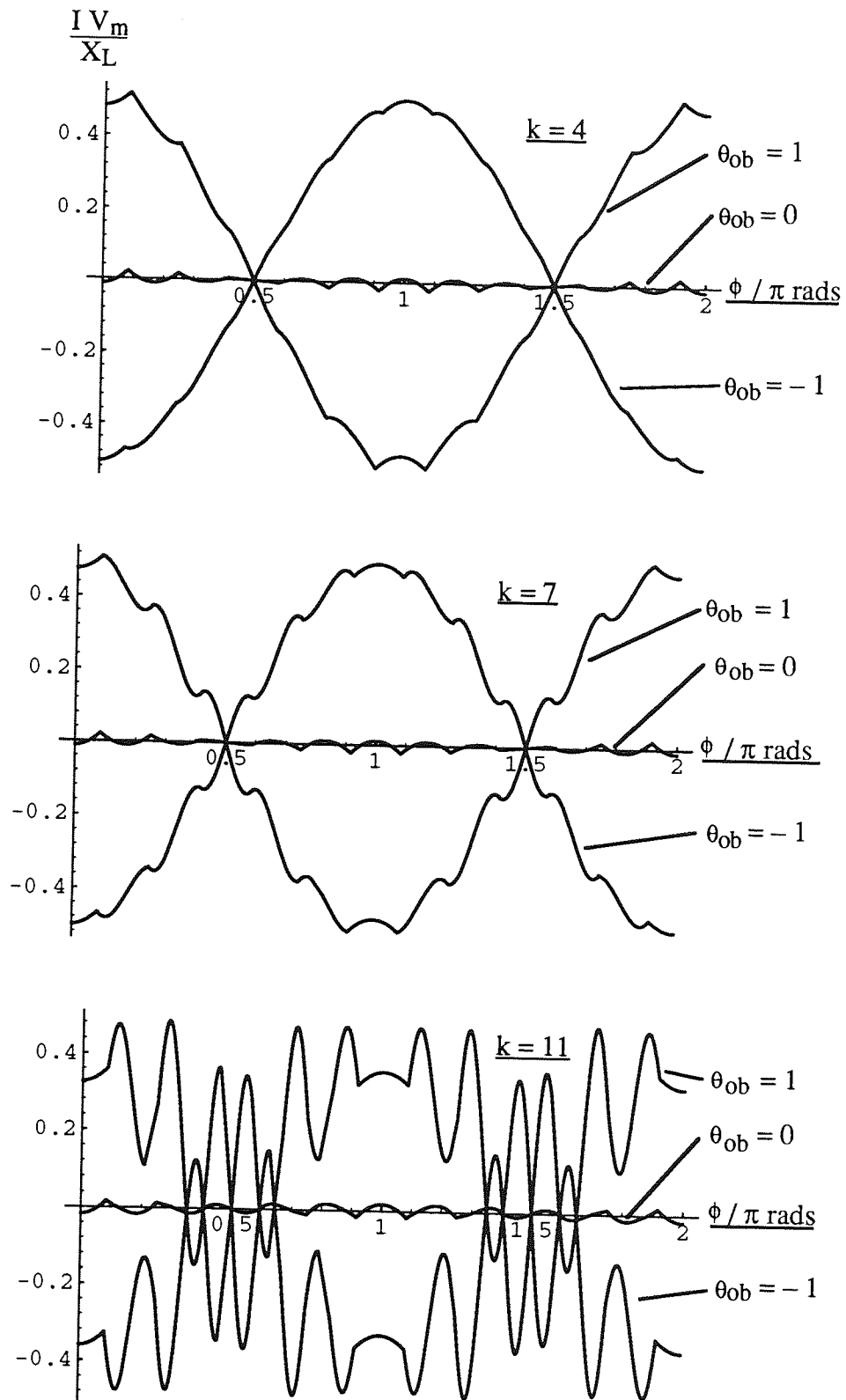


Fig. 6-11b. The Current in a Twelve Pulse Series STATCON for $k = 4, 7$ and 11 .

§6.7 Characteristics of the Fundamental Component of the System Current

The Fourier analyses given in appendices 5 and 6 show that the form of the fundamental component of the current in the parallel connected case is

$$I_q = \frac{2V_m}{X_L} \left[q_1 + q_2 \frac{\sin 2\theta_0}{2\beta} \right] \approx \frac{2V_m}{X_L} [q_1 + q_2 \theta_{ob}] \quad (6.3)$$

$$I_p = \frac{2\beta V_m}{X_L} \left[p_1 + q_2 \frac{\sin^2 \theta_0}{\beta^2} \right] \approx \frac{2\beta V_m}{X_L} [p_1 + q_2 \theta_{ob}^2] \quad (6.4)$$

and in the series connected case:

$$I_q = \frac{V_m}{X_L} \left[q_1 + q_2 \frac{\sin 2\theta_0}{2\beta} \right] \approx \frac{V_m}{X_L} [q_1 + q_2 \theta_{ob}] \quad (6.5)$$

$$I_p = \frac{\beta V_m}{X_L} \left[p_1 + q_2 \frac{\sin^2 \theta_0}{\beta^2} \right] \approx \frac{\beta V_m}{X_L} [p_1 + q_2 \theta_{ob}^2] \quad (6.6)$$

Figure 6.12a shows the parameters for the parallel connected case using $\beta = 0.1$, 0.01 and 0.001 and figure 6.12b shows the same for the series connected case.

The q_2 graphs for the series and parallel cases appear to be very similar. As in the single phase and three phase cases the choice of m will be about the knee point on this graph, $5 < k < 10$. The p_1 and q_1 graphs in the series case have the same form as those in the parallel case but are of lower amplitude. This means that the losses are lower in the series connected case.

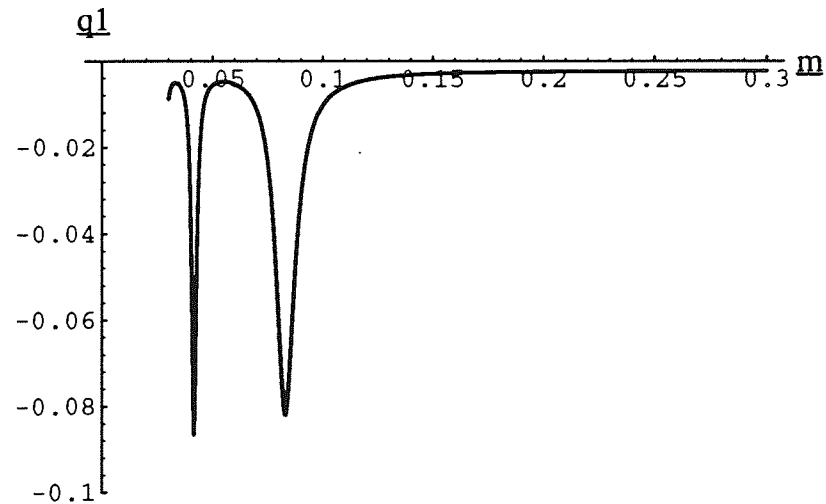
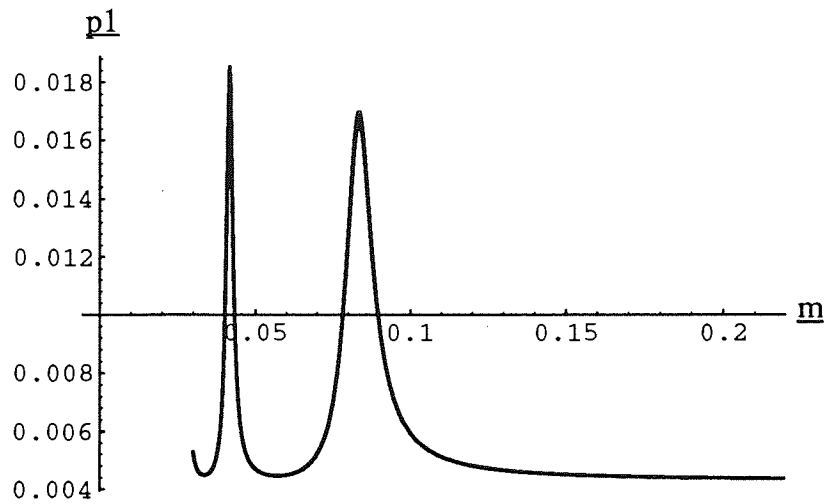
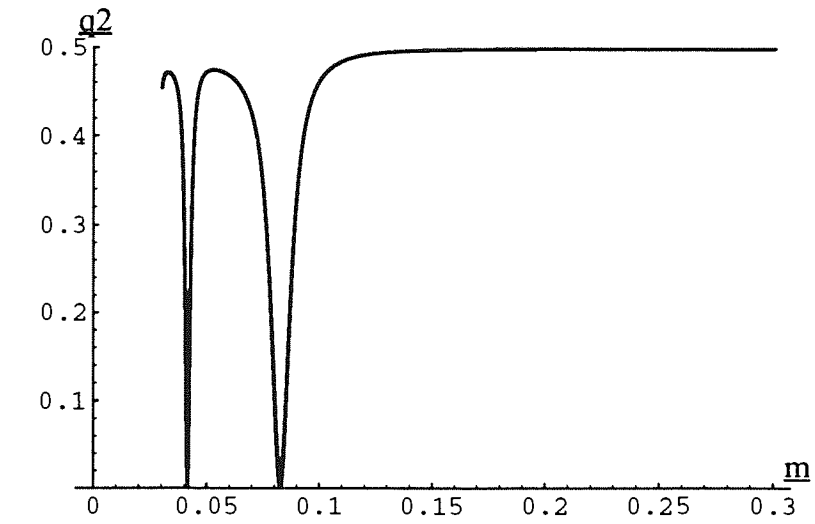


Figure 6-12a. Graphs of the Parameters Describing the Fundamental Component of the Current in a Twelve Pulse Parallel STATCON.

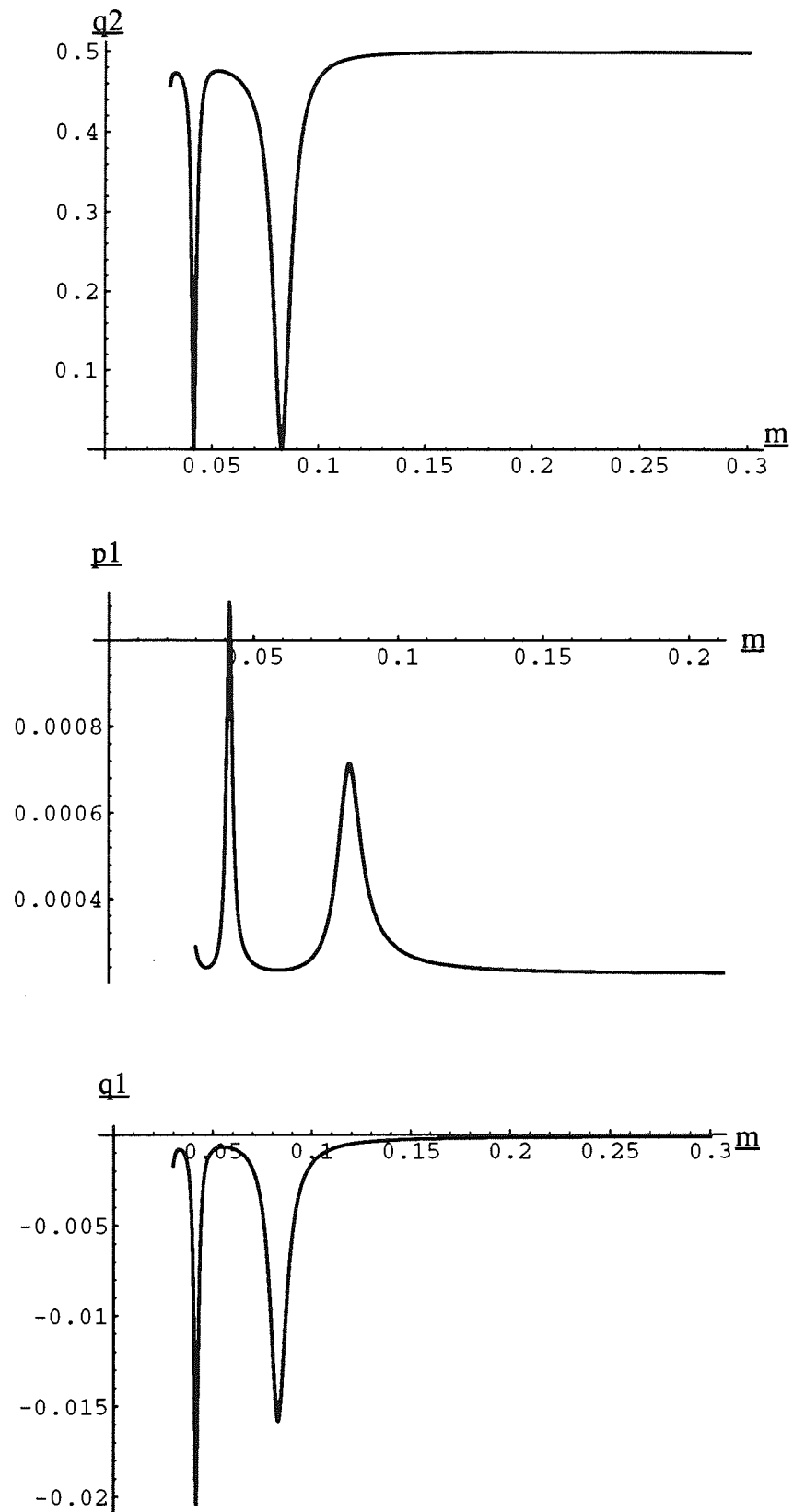


Figure 6-12b. Graphs of the Parameters Describing the Fundamental Component of the Current in a Twelve Pulse Series STATCON.

Figure 6-13 shows how the normalised reactive power varies and figure 6-14 shows how the normalised losses vary with the reduced firing angle in the parallel case. Figure 6-15 and 6-16 show the same for the series case.

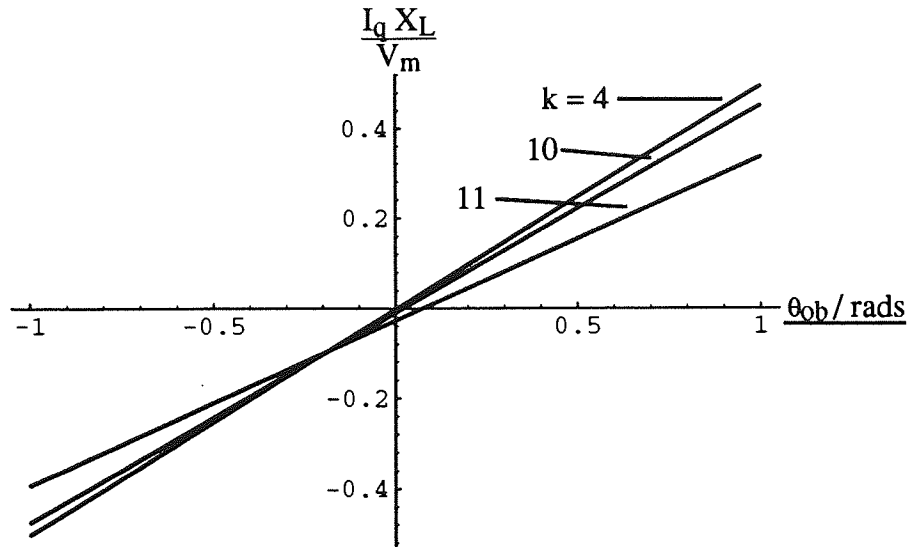


Figure 6-13. Graph of the Normalised Reactive Power Output from a Twelve Pulse Parallel STATCON.

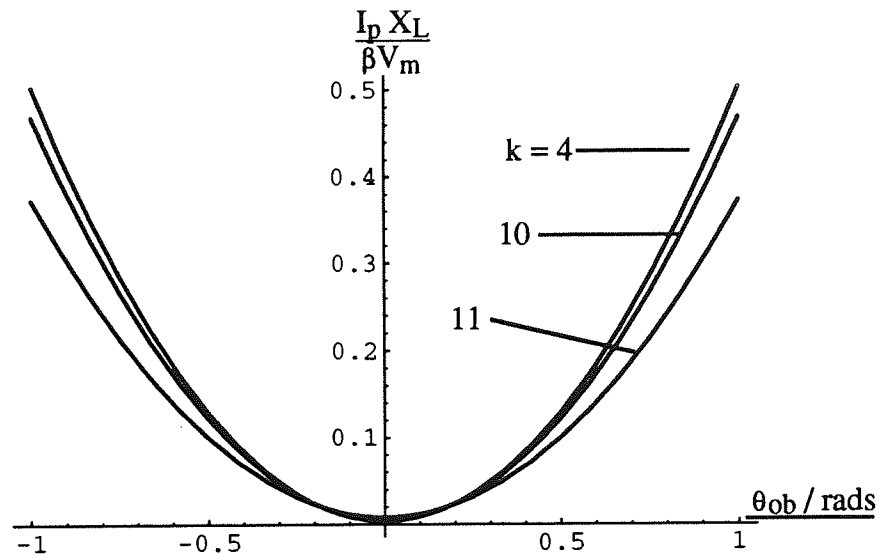


Figure 6-14. Graph of the Normalised Losses in a Twelve Pulse Parallel STATCON.

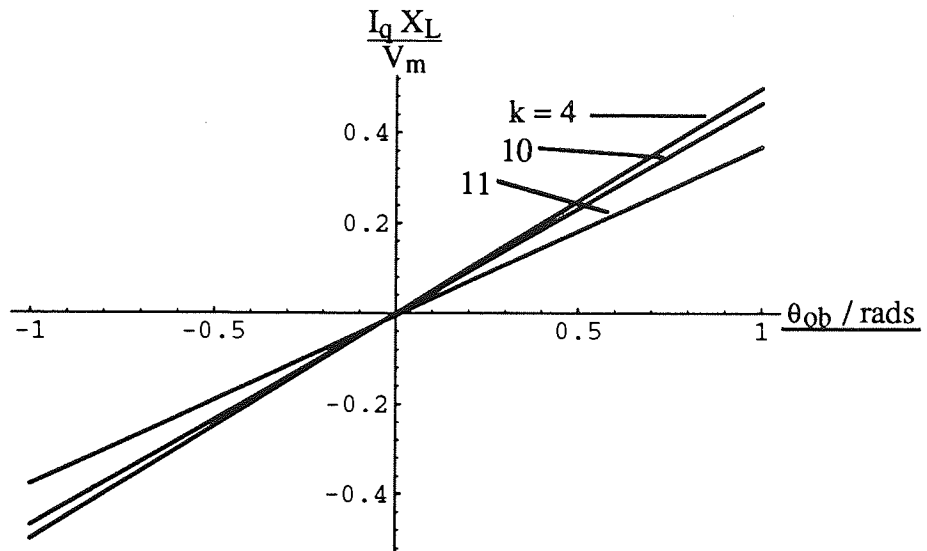


Figure 6-15. Graph of the Normalised Reactive Power Output from a Twelve Pulse Series STATCON.

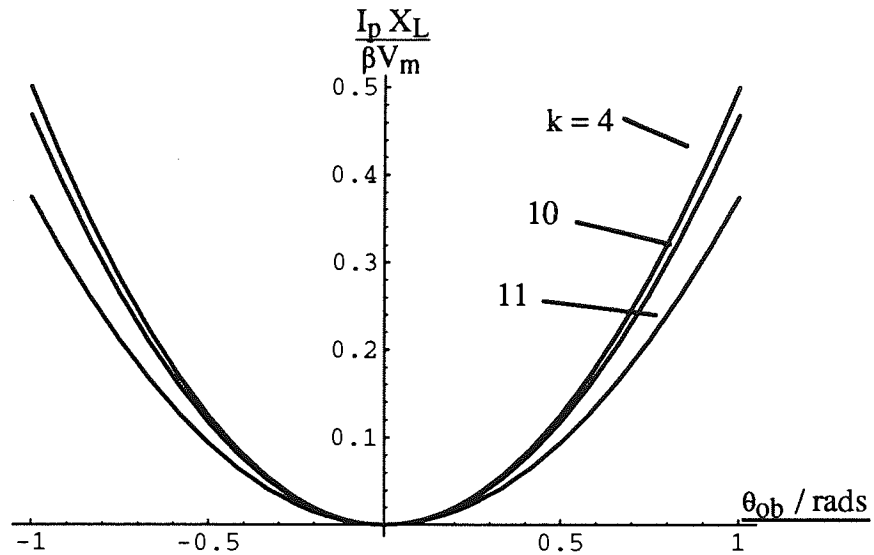


Figure 6-16. Graph of the Normalised Losses in a Twelve Pulse Series STATCON.

§6·8 Characteristics of the Harmonics of the System Current

The form of the harmonics, in both the series and parallel cases, is similar to that in the single and three phase cases.

In the parallel case:

$$I_{nc} = \frac{2V_m}{X_L} t_n \approx \frac{2V_m}{X_L} [c_n - s_n \theta_{ob}] \quad (6·7)$$

and in the series case:

$$I_{nc} = \frac{V_m}{X_L} t_n \approx \frac{V_m}{X_L} [c_n - s_n \theta_{ob}] \quad (6·8)$$

Figure 6·17 shows t_n for $n = 11$ and 13 as a function of the reduced firing angle for various values of the resonance ratio in the parallel case and figure 6·18 shows the same for the series case. Figures 6·19 and 6·20 show the graphs of c_n and s_n for the parallel and series cases respectively.

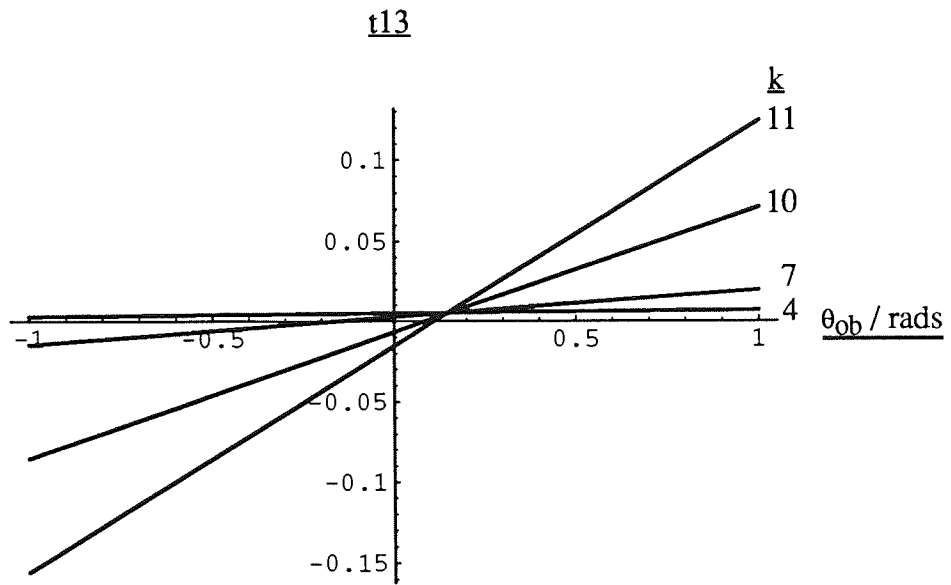
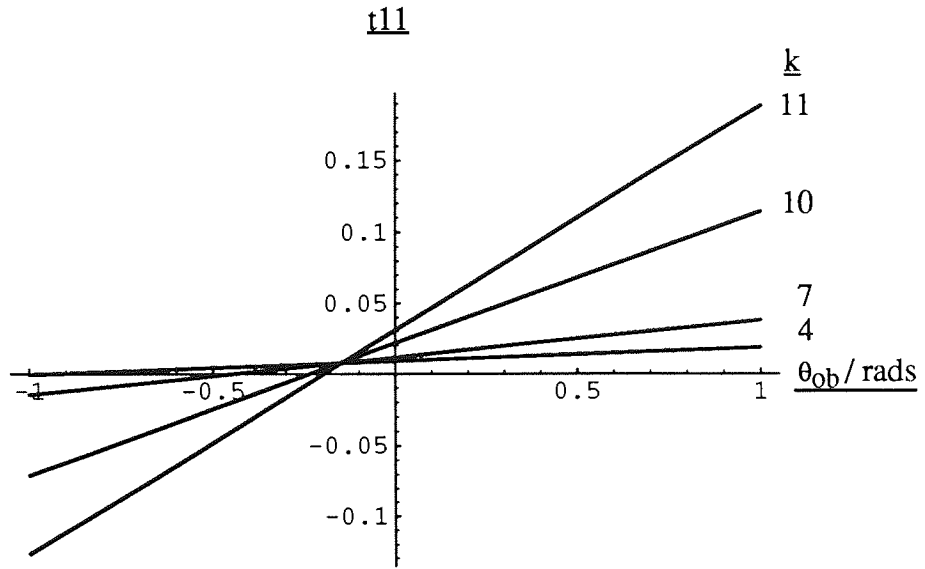


Figure 6.17. Graphs of the Normalised Coefficient of the Harmonics in the Current for $n = 11$ and 13 in a Twelve Pulse Parallel STATCON.

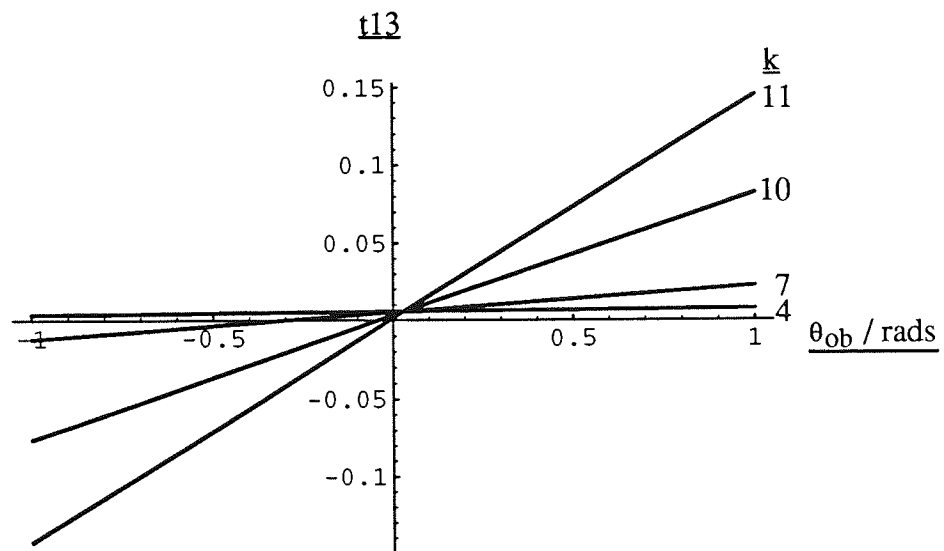
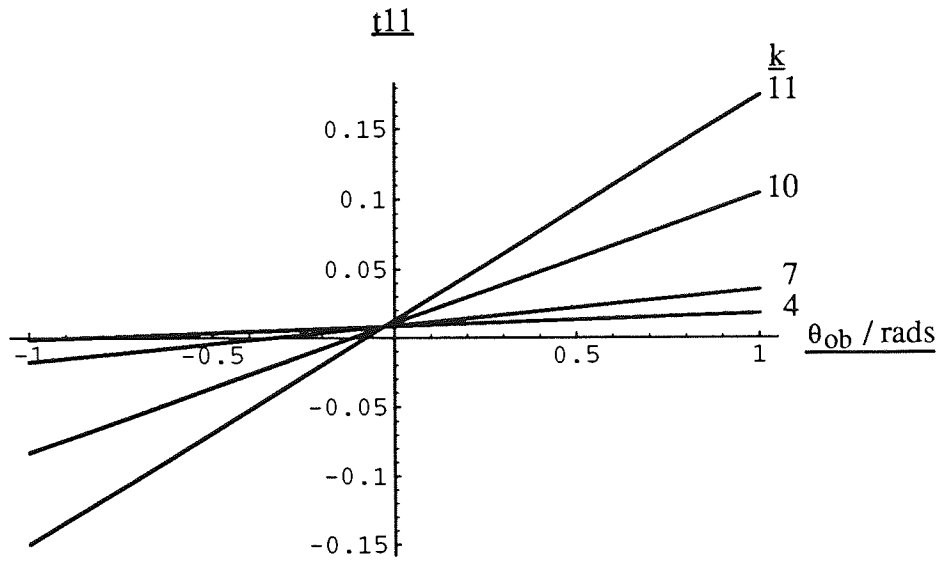


Figure 6.18. Graphs of the Normalised Coefficient of the Harmonics in the Current for $n = 11$ and 13 in a Twelve Pulse Series STATCON.

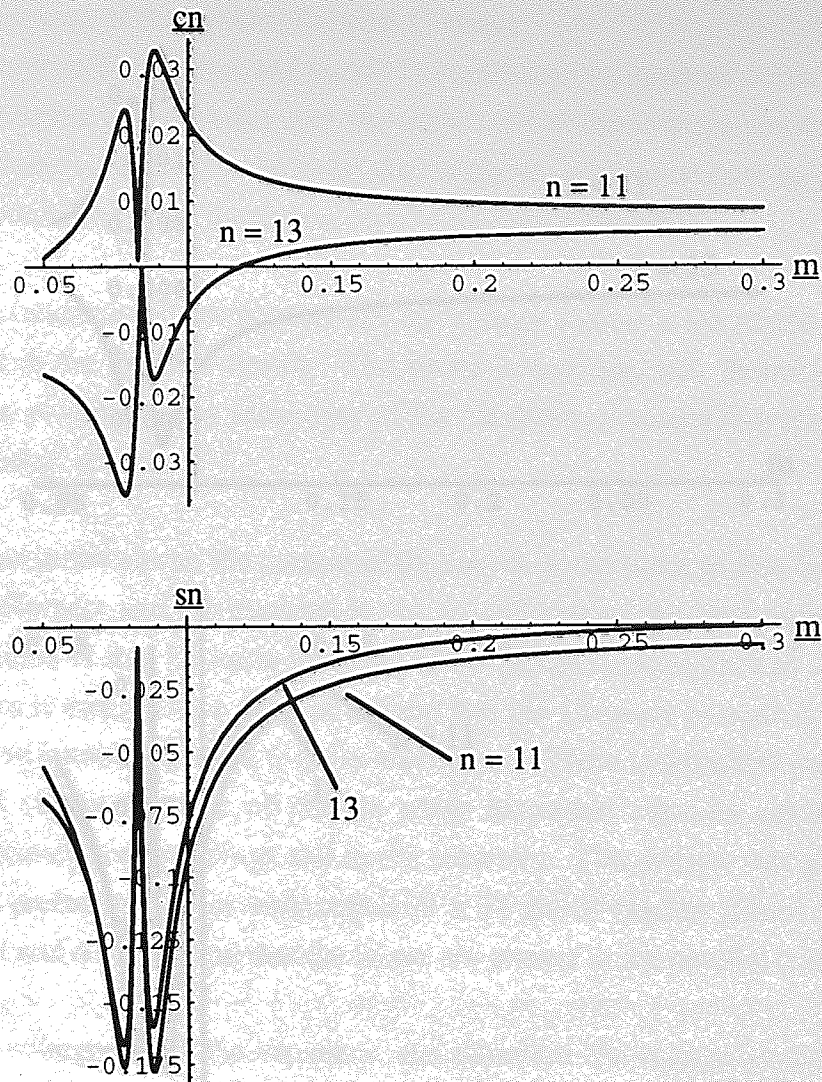


Figure 6-19. Graphs of the Parameters Describing the Coefficients of the Harmonics in the Current in a Twelve Pulse Parallel STATCON.

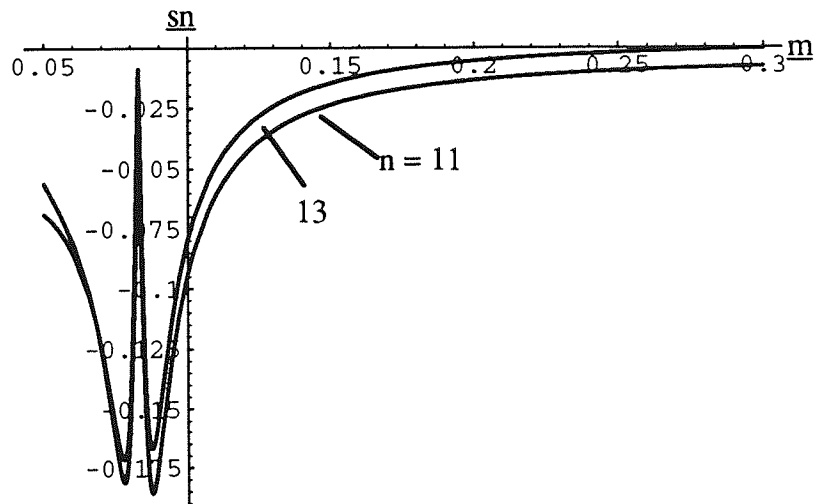
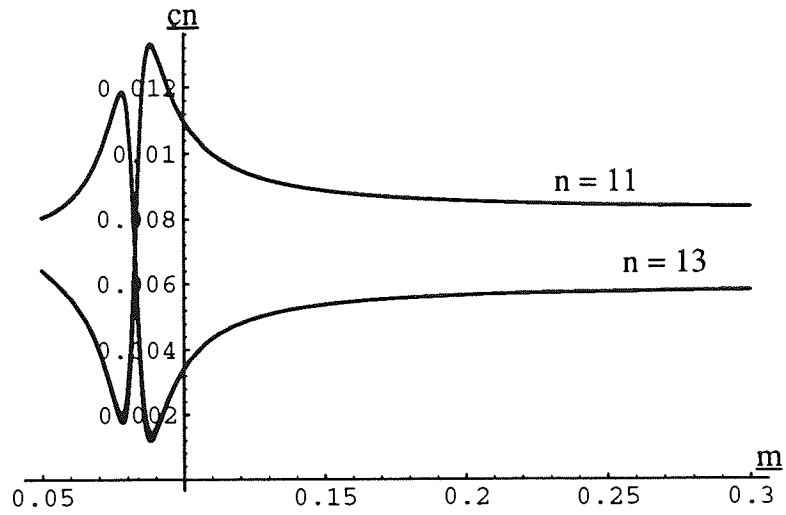


Figure 6-20. Graphs of the Parameters Describing the Coefficients of the Harmonics in the Current in a Twelve Pulse Series STATCON.

§6.9 Comparison of Series and Parallel Circuits

To compare the series and parallel circuits the two systems are assumed to have the same reactive power rating and the amplitude of the voltage source in the series connected case is assumed to be twice that in the parallel connected case. This means that there would be higher insulation costs in the series circuit.

The fundamental current through the voltage source in the series circuit will be half of that in the parallel circuit. The series connection will therefore have lower losses in the winding of the secondary of the transformer connecting the equipment to the transmission system.

In the series circuit the current in the source is the same as that in the primaries of the transformers and the currents in the secondaries of the transformers are phase shifted versions of this 12-pulse current. In the parallel circuit each of the currents in the primaries is essentially a 6-pulse current and the 12-pulse current in this source is made up from combining these 6-pulse waveforms. There is therefore greater losses in the parallel circuit because of the six pulse harmonic currents circulating in the secondary transformer windings and in the inverters. This reason was given as being decisive in preferring series connection in a 36 pulse system (Sumi et al., 1981). Figures 6.14 and 6.16 confirm that the losses are greater in the parallel connected case.

The voltage across the capacitor, and therefore the voltage across the devices, may be slightly greater in the parallel connected circuit because of the increased harmonics on the secondary side of the transformers, but this effect is likely to be small.

In the parallel circuit the higher harmonic content of the current in the inverters means that the thyristors would have to extinguish a higher instantaneous current when operating at maximum VAr generation. The peak turn off current is the limiting factor in the rating of GTO thyristors and so this may be detrimental to the rating of the equipment (Larsen et al., 1992).

In the series connected circuit the minimum size of the capacitor that can be used is slightly less than that in the parallel case.

At high power the series connection of the transformer primary windings is probably preferable, giving rise to lower losses and a lower rating for the devices and capacitor and a lower capacitance value. These advantages probably outweigh the disadvantage of the increased cost of the insulation. At low voltage parallel connection is more suitable because of the larger current flow in the voltage source.

§6.10 Comparison of the Currents from the Series and Parallel Circuits

In section 6.7 it was shown that the maximum value of k of interest was $k = 10$. In section 6.3 it was stated that the currents are of similar shape, albeit of different magnitude. Figure 6.21a shows the current from the parallel circuit for $k = 10$, using $\theta_{ob} = 1$, and 6.21b shows the same from the series case. The wave shapes appear very similar.

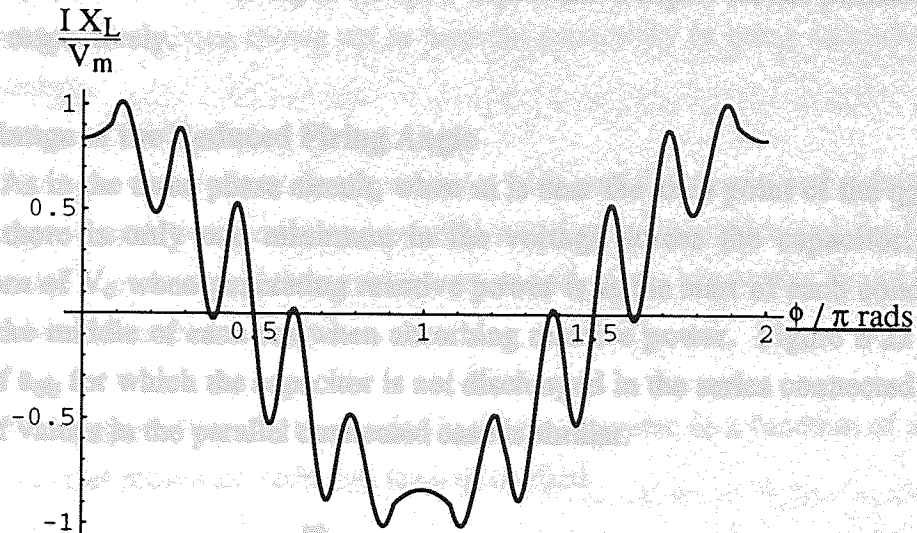


Figure 6.21a. The Current in the 12-Pulse Parallel Circuit for $k = 10$ and $\theta_{ob} = 1$.

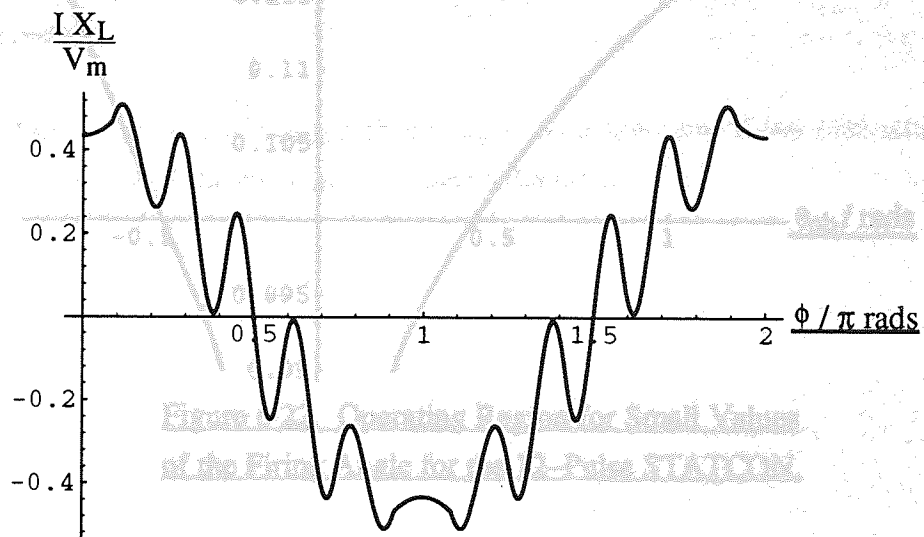


Figure 6.21b. The Current in the 12-Pulse Series Circuit for $k = 10$ and $\theta_{ob} = 1$.

§6-11 Size of the Energy Storage Components

The q_2 graphs appear to be identical and therefore for both the series and parallel connected circuits the knee point of the graph is at $m = 0.11$. In the twelve pulse circuit, because there are two converters, each transformer is rated at 0.5p.u. and thus taking X_L as 20% of the rating of the transformer, as in the single phase and six pulse circuits, then X_L is 0.1p.u. of the rating of the equipment. Assuming β is small then the admittances of the capacitor are 0.16p.u. and 0.15p.u. for the parallel and series circuits respectively.

§6-12 Range of the Reduced Firing Angle

As in the three phase circuit, when m is near the knee point of the q_2 against m graph, there is only one minimum in the voltage across the capacitor, V_c . The minimum of V_c when generating reactive power is at the start of each conduction era and in the middle of each era when absorbing reactive power. Figure 6-22 shows the range of θ_{ob} for which the capacitor is not discharged in the series connected case. The range of values in the parallel connected case is similar.

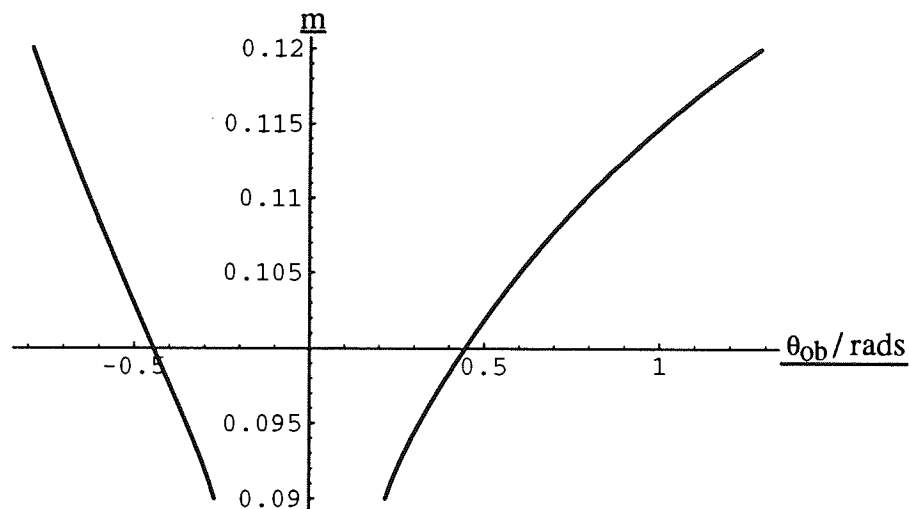


Figure 6-22. Operating Region for Small Values of the Firing Angle for the 12-Pulse STATCON.

§6.13 Conclusions

Four different methods of harmonic reduction have been discussed and it has been argued that at the present time, and for the foreseeable future, multiple phase inverters may offer the best prospect of harmonic reduction with low losses and without introducing large energy storage components.

Possible twelve pulse circuits have been discussed and single transformer configurations have been shown not to have the possibility of being extended to higher pulse numbers.

Multiple transformer configurations with parallel connected converters have been analysed with both series and parallel transformer primaries and the form of the fundamental component of the system current and of the harmonics found to be as in the single and three phase cases.

The magnitude of the harmonics in the two circuits, as a function of the reduced firing angle and resonance ratio, has been quantified.

A comparison between the two circuits has been undertaken and the series circuit has been shown to be the most suitable for the high power transmission environment.

The range of the reduced firing angle, as a function of the resonance ratio, to prevent discharge of the capacitor has been calculated.

Twenty-Four Pulse Voltage Sourced STATCONs

§7.1 Introduction

In chapter 6 the results of combining two inverter circuits to produce a twelve pulse system were discussed. In this chapter combining four inverters in a twenty-four pulse system is considered. Consideration is given to the transformer arrangement and the use of star, delta, extended delta and zigzag windings, with both series and parallel connection of the transformer primaries.

A simulation of a quasi twenty-four pulse system which requires only conventional transformers, but still requires multiple transformers, with series connected primaries is included, together with a discussion of the advantages and disadvantages of such a system.

Practical results from a twenty-four pulse system using zigzag secondaries and star and delta connected primaries are included and the performance compared with the theoretical results. Possible causes for the discrepancies are discussed and simulation has been used to verify which of these possible causes is the principle one.

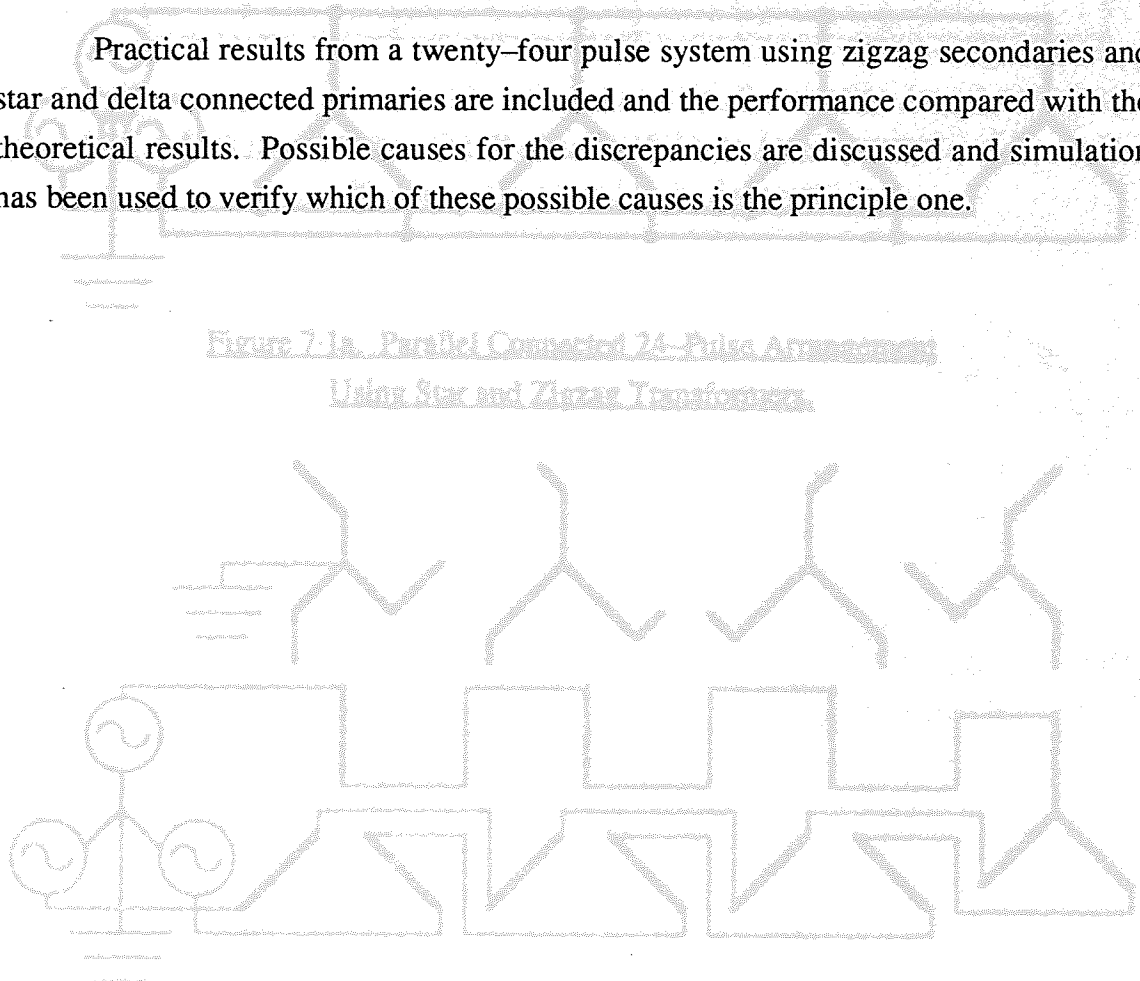


Figure 7.1a. Parallel Connected 24-Pulse Arrangement
Using Star and Zigzag Transformers.

Figure 7.1b. Series Connected 24-Pulse Arrangement
Using Star and Zigzag Transformers.

§7.2 Transformer Arrangement

A number of different transformer arrangements are possible. Figure 7.1a shows the parallel connected case using star connected primaries and zigzag secondaries. Figure 7.1b shows the series connected case using the same transformers. As in the twelve pulse case the phase shifts are symmetrically disposed about zero. In this case the phase shift between each transformer is 15° . The phase shifts relative to the supply voltage are therefore -22.5° , -7.5° , 7.5° and 22.5° .

As in the twelve pulse equipment the transformer secondaries are arranged in parallel with only one of the star points earthed.

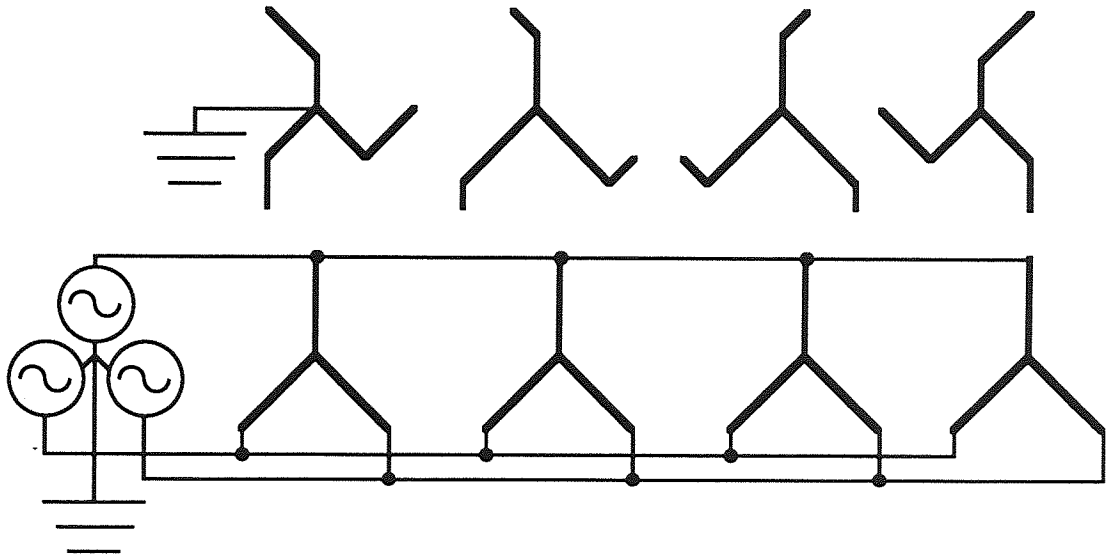


Figure 7.1a. Parallel Connected 24-Pulse Arrangement
Using Star and Zigzag Transformers.

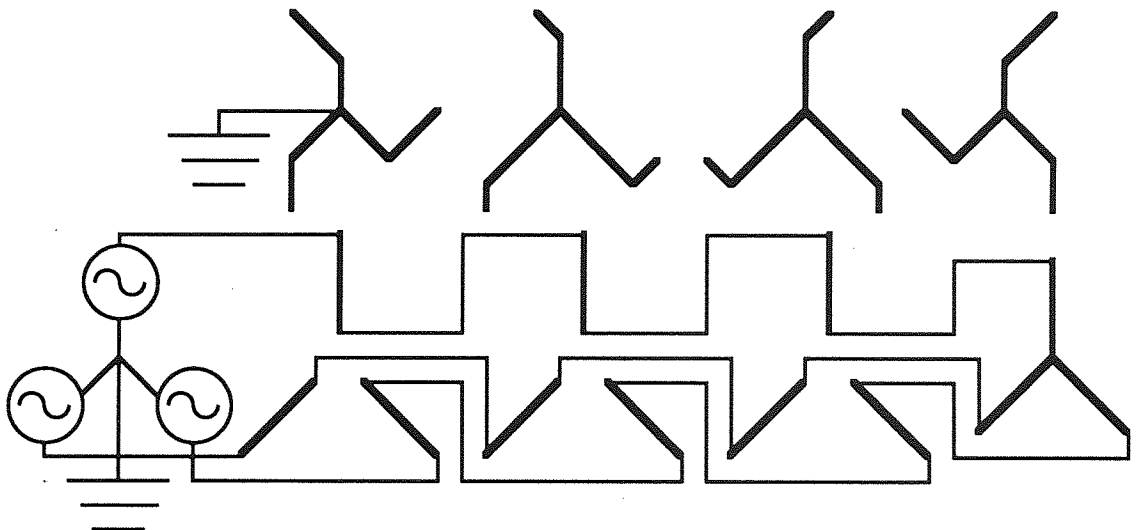


Figure 7.1b. Series Connected 24-Pulse Arrangement
Using Star and Zigzag Transformers.

Equivalent transformer configurations can also be produced using delta and extended delta transformers. Figure 7.2 shows how extended delta transformers can be used on the secondary side, in the parallel connected case, in place of two zigzag windings, to achieve the + and - 22.5° phase shifts. The use of extended delta transformers may reduce the overall size of the equipment.

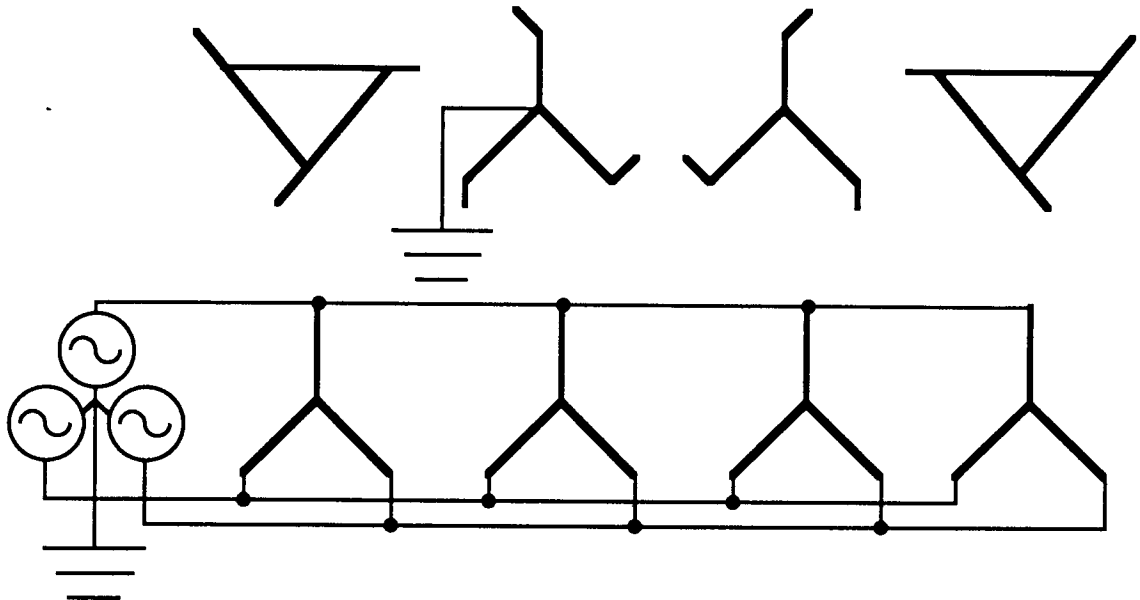


Figure 7.2. Parallel Connected 24-Pulse Arrangement
Using Zigzag and Extended Delta Secondaries.

Figure 7.3 shows how two delta and two star connected transformers can be used as primaries with four zigzag transformers on the secondaries. In this case the four zigzag windings are all made up of turns ratios so as to produce phase shifts of + or -7.5° . The $+22.5^\circ$ phase shift is made by combining a delta primary winding with a phase shift of $+30^\circ$, relative to the supply, with a zigzag secondary winding of -7.5° . The -22.5° phase shift uses a $+7.5^\circ$ zigzag secondary and a delta primary winding connected in the opposite sense to that with the $+30^\circ$ phase shift. Again this configuration may be preferred if the overall size is reduced.

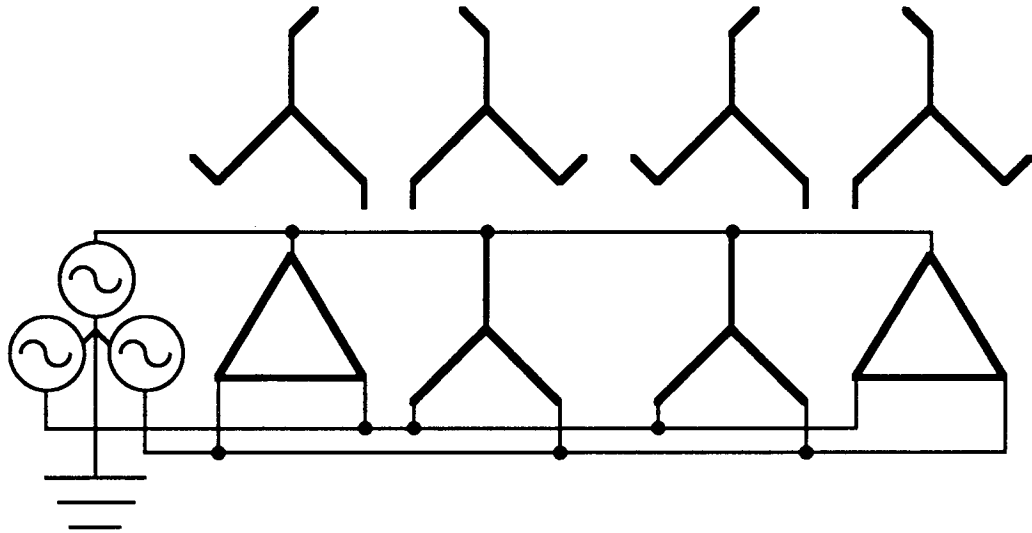


Figure 7.3. Parallel Connected 24-Pulse Arrangement Using Star and Delta Primaries.

Under ideal circumstances the configurations given in figures 7.2 and 7.3 would produce the same current in the voltage source as that from the configuration using only star and zigzag windings, figure 7.1a. Under non-ideal conditions different harmonics could be generated. In particular, an amount of third harmonic could be generated in the secondaries of the transformers and so the use of two delta transformers, as in figure 7.3, would prevent the third harmonics from these transformers being produced in the source. As discussed in chapter 6, if a further transformer is used between the transmission system and the multiple transformers this could be wound as star – delta, with the star connected winding on the high voltage side, so that no third harmonic would be fed into the transmission system anyway.

A quasi multi-pulse configuration, which uses only star and delta transformers with series connected primaries, has also been suggested (Gyugyi et al., 1990). The transformer configuration for a quasi 24-pulse circuit is shown in figure 7.4. Each pair of transformers, i.e. one star and one delta secondary, can be considered as one module. The two inverters in each module are fired 30° apart. The phase shift between the modules is 15° . The inverters in the first module are fired at 7.5° after the system voltage and at 22.5° ahead of the system voltage, assuming $\theta_0 = 0$, and those in the second module are both fired ahead of the system voltage, by angles of 7.5° and 37.5° .

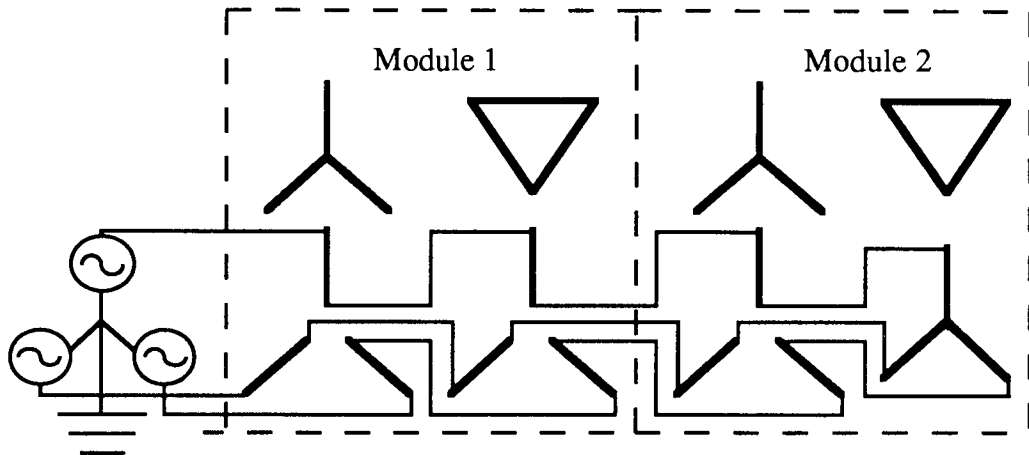


Figure 7.4. Quasi 24-Pulse Transformer Arrangement.

Figure 7.5 shows a simulation of a quasi 24-pulse system generating reactive power using a small value for the resonance ratio. The value of k chosen was 5, based on the definition of k used in the full 24-pulse series connected circuit, see §7.3. The value of θ_{ob} used was 1. The peak of the supply voltage was taken as 4, i.e. $V_m = 1$, and X_L was also taken as 1. The waveform is a significant improvement on that produced in the 12-pulse case using a low value of k , figure 6.8b.

This transformer arrangement is attractive because it does not need any phase shifting transformers, other than the conventional star – delta ones. Unfortunately, it produces a current with a greater harmonic content than that from the full multi-pulse arrangement: in the case of the 24-pulse circuit there are harmonics for $24i \pm 1$, for $i = 1, 2, \dots$ whereas in the case of the quasi 24-pulse circuit harmonics exist for $12i \pm 1$ (Gyugyi et al., 1990). This was confirmed using the Fourier transform routine in the simulation package. The magnitudes of these additional harmonics are reduced in comparison to those produced in the twelve pulse circuit.

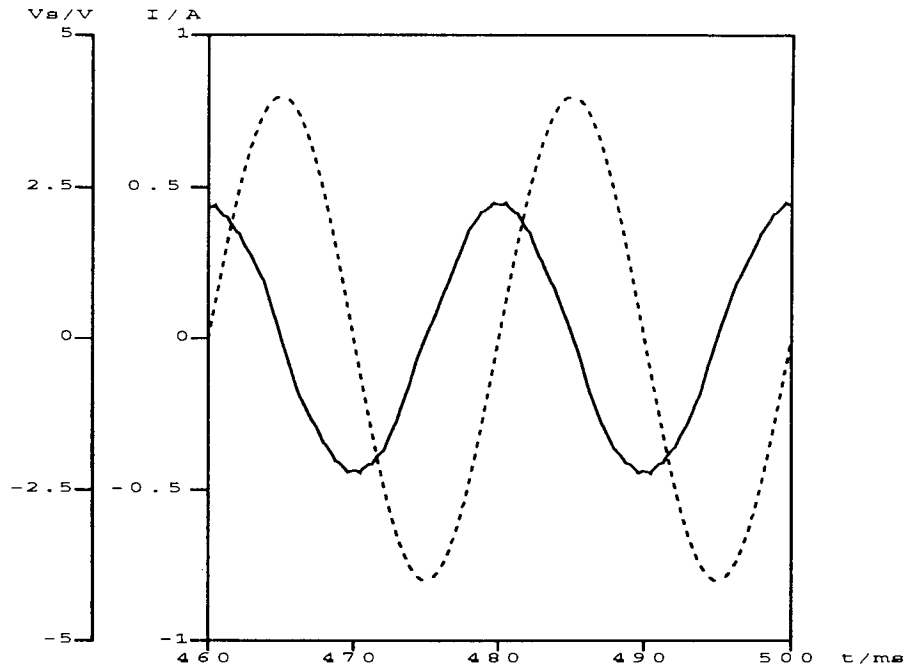


Figure 7.5. Simulation of Quasi Twenty-Four Pulse Equipment Generating Reactive Power Output.

Filters could be introduced to eliminate the small amounts of these 11th and 13th harmonics, in addition to any that might be used for the higher frequencies.

The circuit still requires multiple transformer configurations, albeit that they are not unconventional phase-shifting ones, so most of the disadvantages of using multiple transformer arrangements, as discussed in section 6.2d, still apply. The disadvantages of using filters are discussed in chapter 6.2a. The advantages in being able to use "off the shelf" transformers is probably not worth the disadvantages of having to include extra filters. There are no reported cases of this system being built practically as either a small scale model or a full scale equipment. This circuit will not therefore be analysed further; only the parallel and series connected full 24-pulse systems shall be considered.

§7·3 Nomenclature

The definitions of the resonance ratios are again different in the series and parallel connected circuits:

$$\text{parallel circuit} \quad k = \sqrt{\frac{8}{3} \frac{X_C}{X_L} - \beta^2} \quad (7.1)$$

$$\text{series circuit} \quad k = \sqrt{\frac{(\sqrt{2}+1)(\sqrt{3}+1)(\sqrt{3}+\sqrt{2})}{6\sqrt{2}} \frac{X_C}{X_L} - \beta^2} \quad (7.1a)$$

V_m is again defined as the peak of the fundamental frequency component of the voltage that is applied to the secondaries of the transformers and so is the peak of the system voltage in the parallel case but one quarter of that in the series connected case.

§7·4 Voltage Across the Capacitor

As in the twelve pulse case the voltage across the capacitor is very similar in the series and parallel connected cases so graphs have only been produced for the series connected circuit. The formula for the parallel case is given in appendix 7 and that for the series case in appendix 8.

The ripple frequency of the capacitor voltage is twenty-four times the system frequency. Again for these values of k there is only one maximum or minimum.

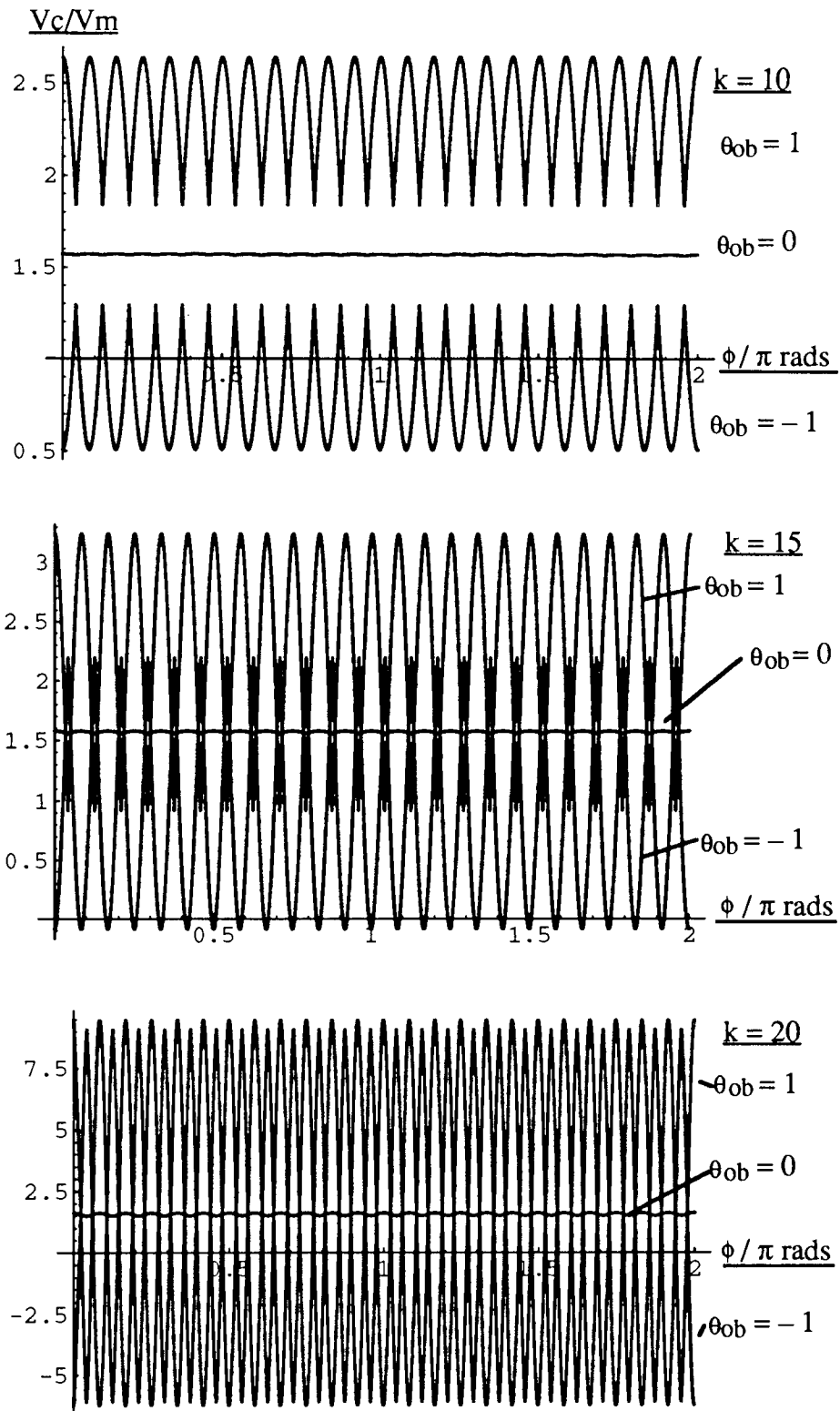


Figure 7.6. The Capacitor Voltage for a Twenty-Four Pulse Series STATCON for $k = 10, 15$ and 20 .

§7.5 System Current

Figure 7.7 shows graphs of the system current in the series case. Again the wave shapes in the parallel equipment would be similar.

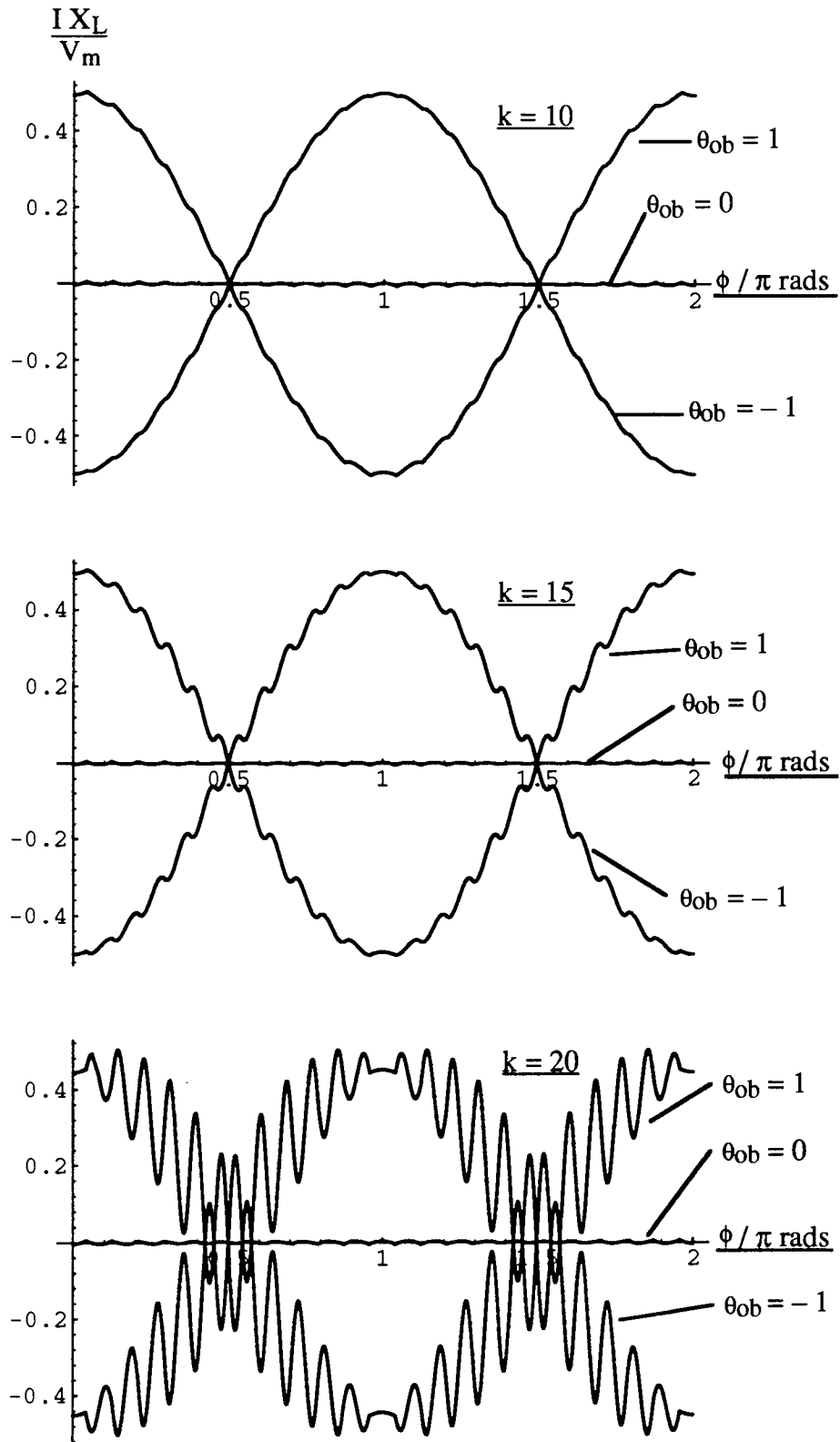


Figure 7.7. The Current in a Twenty-Four Pulse Series STATCON for $k = 10, 15$ and 20 .

§7.6 Characteristics of the Fundamental Component of the System Current

As in all of the other circuits considered the reactive power varies linearly with the reduced firing angle and the losses vary quadratically. In the parallel connected case:

$$I_q = \frac{4V_m}{X_L} \left(q_1 + q_2 \frac{\sin 2\theta_0}{2\beta} \right) \quad (7.2)$$

$$I_p = \frac{4\beta V_m}{X_L} \left(p_1 + q_2 \frac{\sin^2 \theta_0}{\beta^2} \right) \quad (7.3)$$

and in the series connected case:

$$I_q = \frac{V_m}{X_L} \left(q_1 + q_2 \frac{\sin 2\theta_0}{2\beta} \right) \quad (7.4)$$

$$I_p = \frac{\beta V_m}{X_L} \left(p_1 + q_2 \frac{\sin^2 \theta_0}{\beta^2} \right) \quad (7.5)$$

where, as in the twelve pulse equipment, the parameters p_1 , q_1 and q_2 are defined differently in the two cases. Figure 7.8a shows these parameters for the parallel connected case and figure 7.8b shows them for the series connected case.

As in the twelve pulse circuit the q_2 graphs appear identical while the plateau regions of the p_1 and q_1 graphs are appreciably smaller in the series connected case. The parameters have been plotted for $\beta = 0.001, 0.01$ and 0.1 in the series connected case and the curves superimposed; none of the parameters exhibit any significant dependence on β over the range of interest.

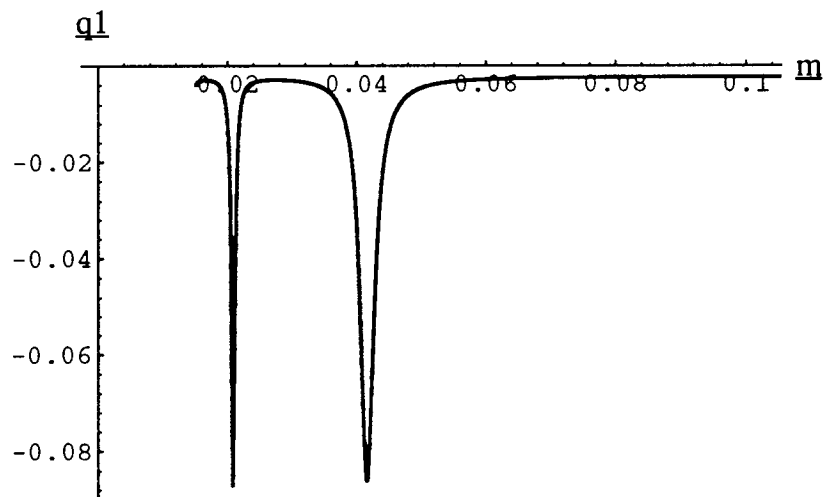
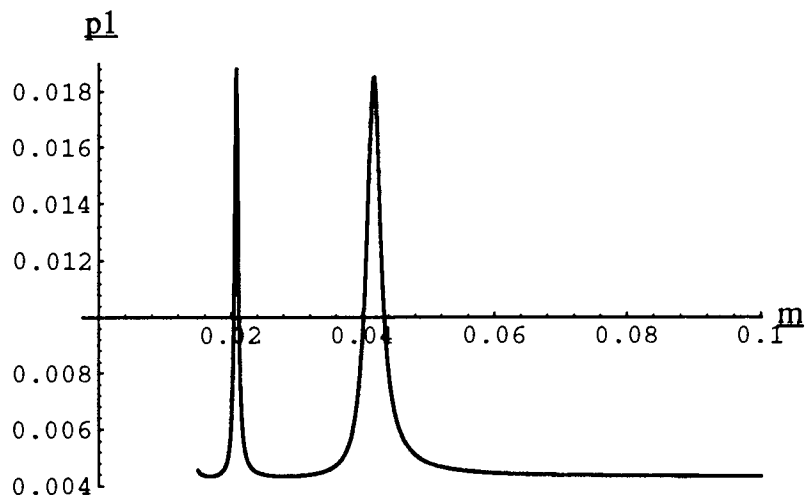
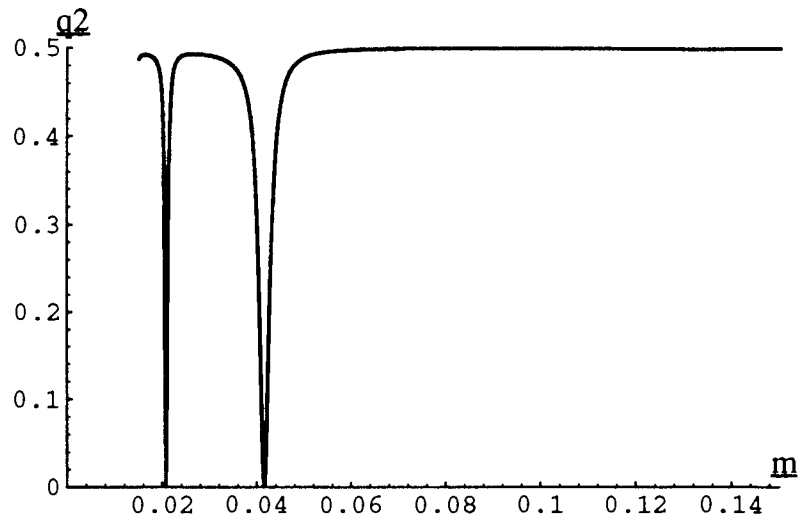


Figure 7-8a. Graphs of the Parameters Describing the Fundamental Component of the Current in a Twenty-Four Pulse Parallel STATCON.

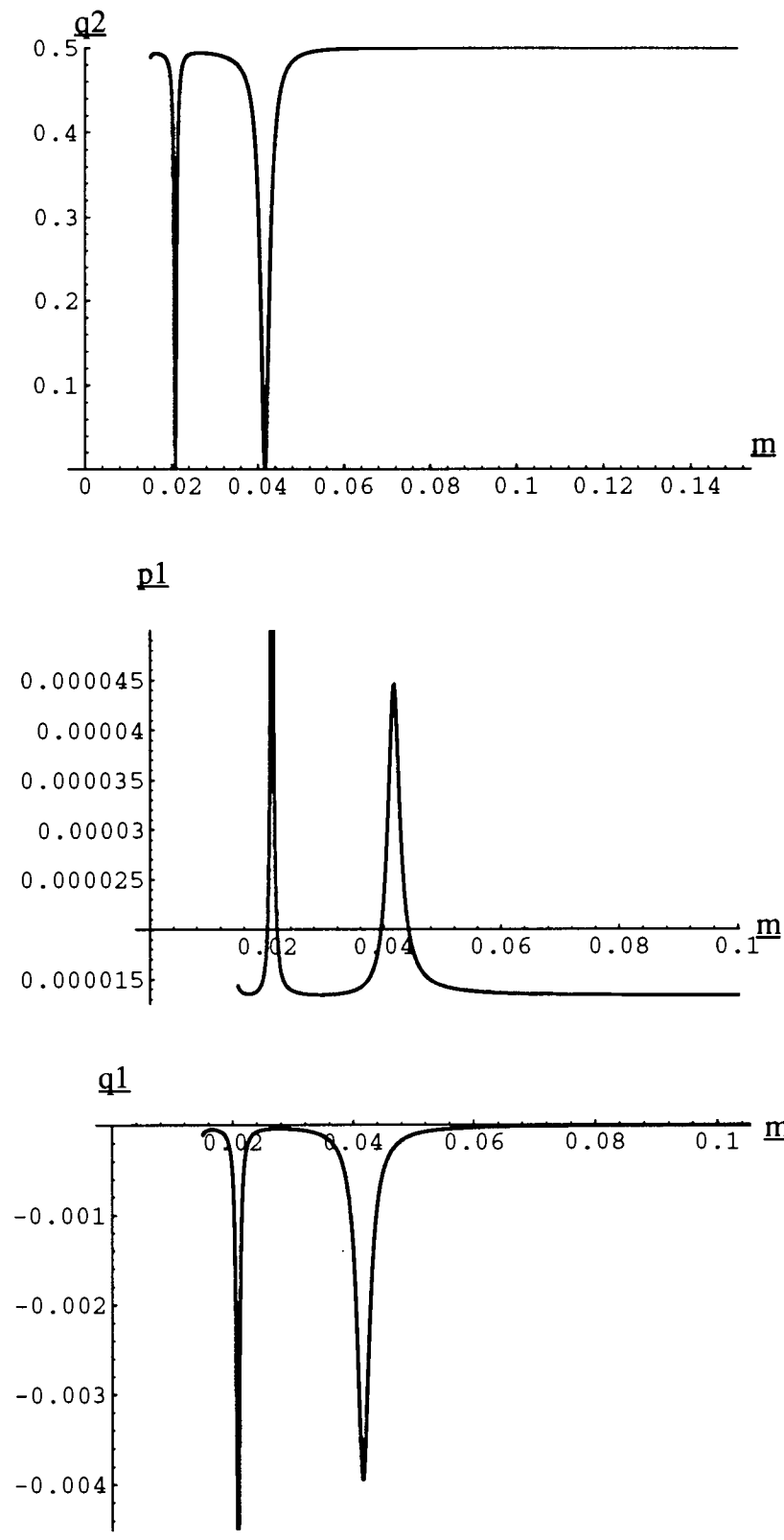


Figure 7-8b. Graphs of the Parameters Describing the Fundamental Component of the Current in a Twenty-Four Pulse Series STATCON.

Figure 7.9 shows the variation in reactive power with the reduced firing angle in the series connected case and figure 7.10 shows the variation of the losses. As in the twelve pulse equipment the figures would be similar for the parallel connected case.

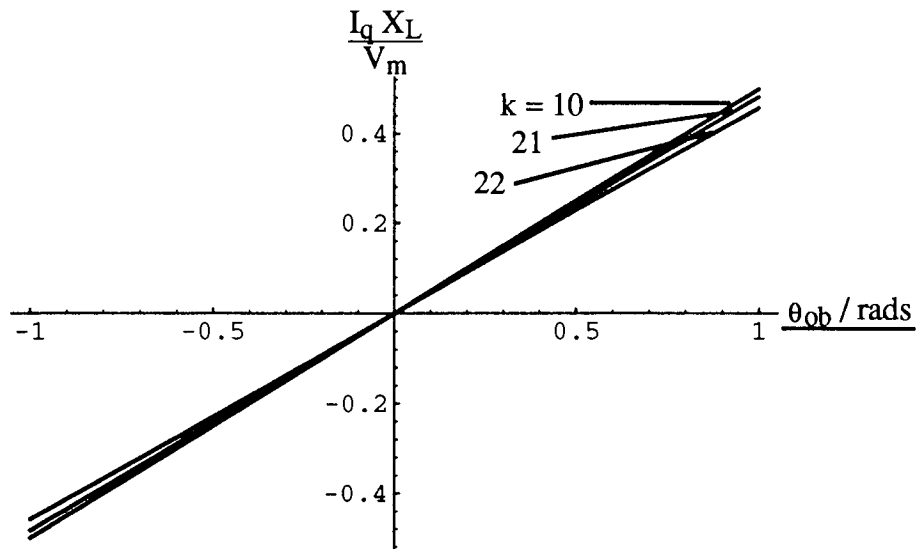


Figure 7.9. Graph of the Normalised Reactive Power Output from a Twenty-Four Pulse Series STATCON.

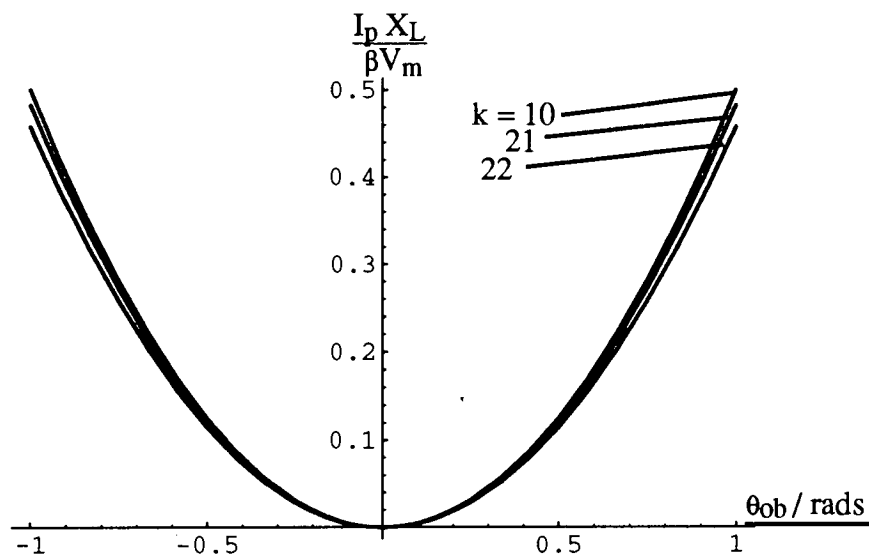


Figure 7.10. Graph of the Normalised Losses in a Twenty-Four Pulse Series STATCON.

§7·7 Characteristics of the Harmonics of the System Current

As in all of the other cases investigated the harmonics vary nearly linearly with the reduced firing angle. In the parallel case:

$$I_n = \frac{4V_m}{X_L} t_n \approx \frac{4V_m}{X_L} [c_n - s_n \theta_{ob}] \quad (7.6)$$

and in the series case:

$$I_n = \frac{V_m}{X_L} t_n \approx \frac{V_m}{X_L} [c_n - s_n \theta_{ob}] \quad (7.7)$$

where, as in the twelve pulse case, c_n and s_n are defined differently in the two cases.

Figures 7·11 show graphs of t_n for $n = 23$ and 25 as a function of the reduced firing angle for various values of the resonance ratio in the series connected case, the equivalent figures in the parallel connected case would be similar.

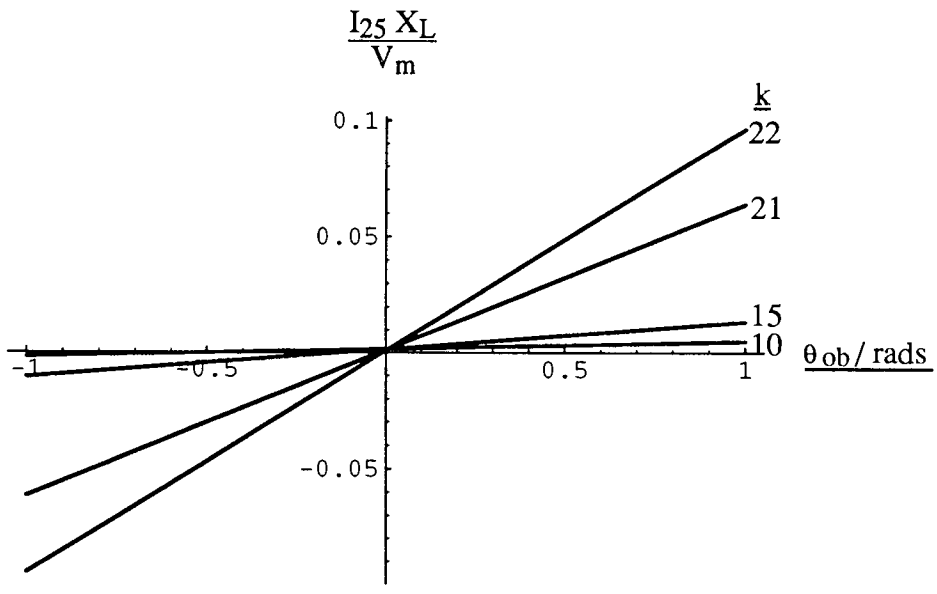
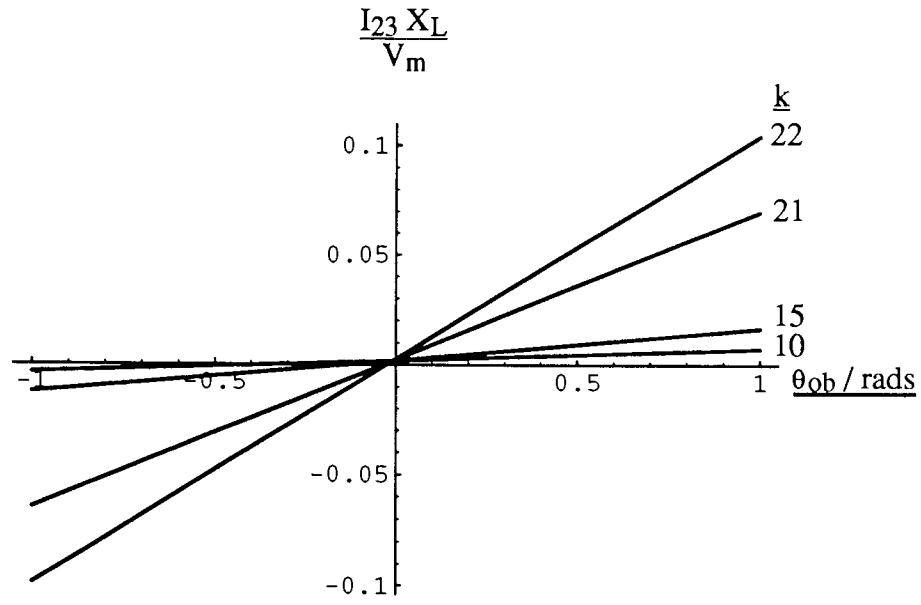


Figure 7.11. Graphs of the Normalised Coefficient of the Harmonics in the Current for $n = 23$ and 25 in a Twenty-Four Pulse Series STATCON.

Figure 7.12 shows graphs of s_n and c_n in the parallel case and figure 7.13 shows them in the series case for $\beta = 0.001, 0.01$ and 0.1 .

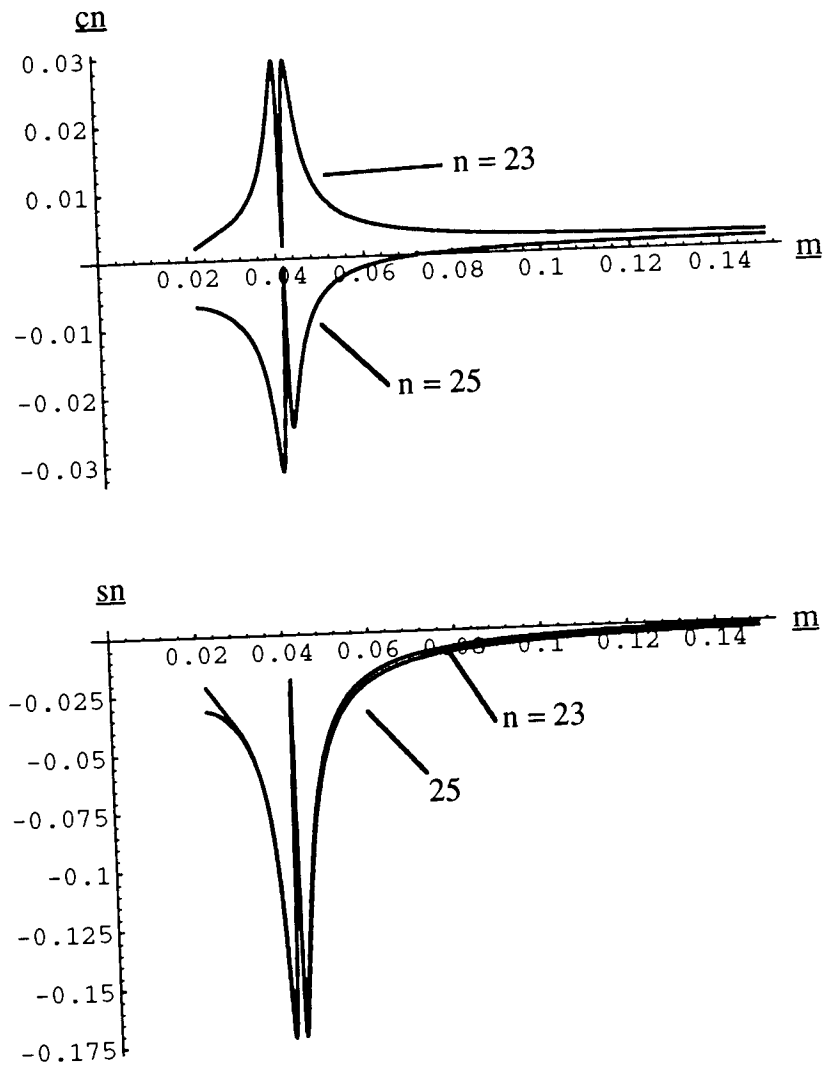


Figure 7.12. Graphs of the Parameters Describing the Coefficients of the Harmonics in the Current in a Twenty-Four Pulse Parallel STATCON.

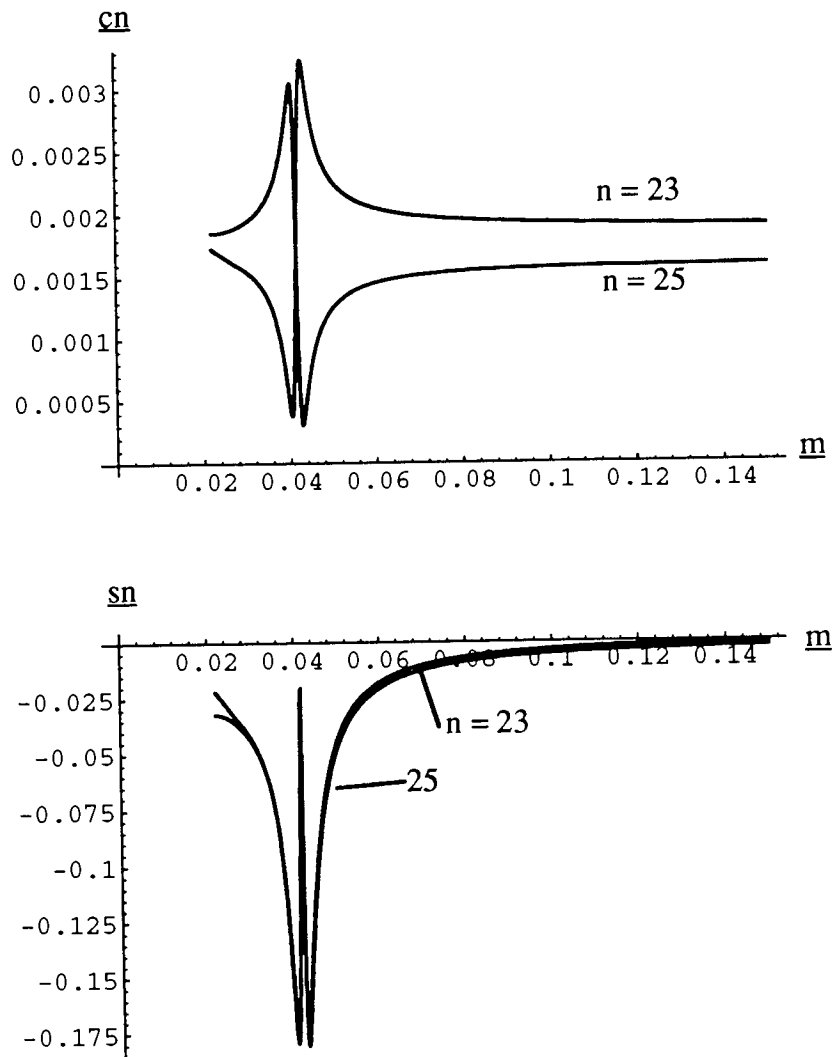


Figure 7-13. Graphs of the Parameters Describing the Coefficients of the Harmonics in the Current in a Twenty-Four Pulse Series STATCON.

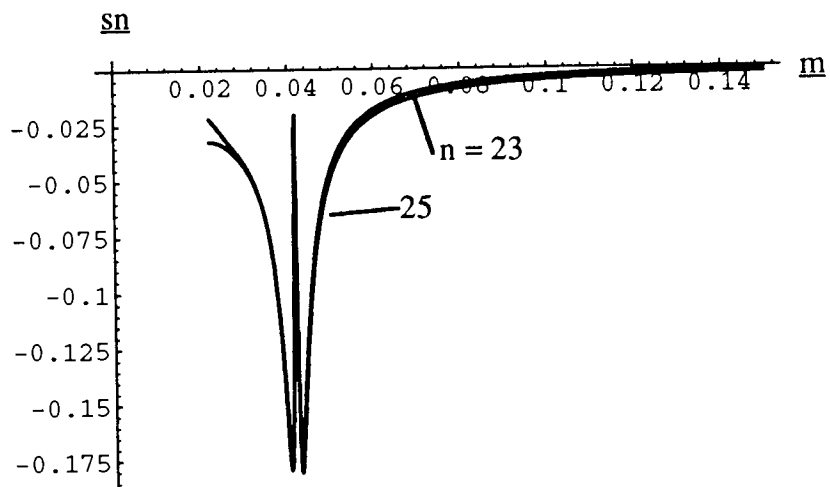
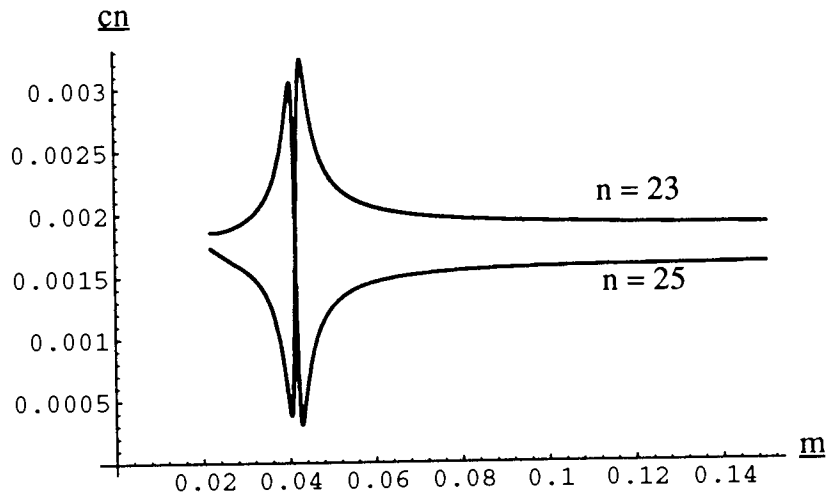


Figure 7.13. Graphs of the Parameters Describing the Coefficients of the Harmonics in the Current in a Twenty-Four Pulse Series STATCON.

§7·8 Comparison of Series and Parallel Circuits

The arguments advanced in the twelve pulse case also apply in this case. In particular it is again true that the resonance ratios are defined differently in the two cases and the graphs of q_2 appear to be identical. Thus the value of the capacitor, for the same values of k and X_L , can be smaller in the series connected case than in the parallel case. The losses will again be smaller in the series connected case.

The current in the parallel connected case is sixteen times bigger than that produced in the series connected case for the same system voltage. The parallel connected case was therefore chosen for a laboratory model.

§7·9 Practical Arrangement

Following on from the six pulse 1kVAr model the rating of the twenty-four pulse model was chosen to be 4kVAr at 240V rms phase to phase so the same MOSFET and diode devices could be used.

The practical arrangement is discussed in detail in appendix 9.

The leakage reactances of the transformers were modelled on a high power transformer and were therefore chosen to be 15% of the rating of each of the transformers, i.e. 15% on a 1kVA rating, $\approx 27.5\text{mH}$.

From this value of the leakage reactance and figure 7·8 the value of the capacitance can be computed. The capacitance was chosen to be $10\mu\text{F}$. This corresponds to a value for the resonance ratio of about 14.

The control system used was similar to that used for the six pulse equipment but with an increase in the size of EPROM 1 to accommodate all twenty-four devices.

The transformer arrangement used was that given in figure 7·3.

§7.10 Results

Figure 7.14a shows experimental results for rated reactive power generation. Figure 7.14b shows the theoretical results and figure 7.14c the simulation results. Figure 7.15 shows the same for zero reactive power output and figure 7.16 shows them for rated reactive power absorption.

For the theoretical results the value of β used was the same as that in the six pulse case, $\beta = 0.06$, and the value of k was 14. The firing angles used were based on the values of q_1 and q_2 with these values of β and k . For rated reactive power generation $\theta_0 = 1.05^\circ$, for zero fundamental reactive power $\theta_0 = 0.017^\circ$ and for rated absorption $\theta_0 = -1.02^\circ$.

In comparison with the theoretical results the experimental ones are somewhat disappointing. The harmonic neutralisation is not as good as had been expected.

Possible causes for these differences include:

- 1) Non-ideal characteristics of the devices.
- 2) Non-ideal mains voltage.
- 3) Unbalance between the leakage reactances in the transformers.
- 4) Unbalance in the resistances in each phase.
- 5) Departures from the nominal phase shifts in the transformers.

The first two of these factors can be discounted because they also effect the six pulse equipment and although the practical results from the six pulse model were not identical with the theoretical ones the differences were slight; much less noticeable than with the twenty-four pulse model.

Of the latter three factors the last one seems to be the most likely cause of the deficiencies since the system is so sensitive to the firing angle. The actual phase shifts on the transformers were measured to see if there was indeed any departure from the nominal phase shifts. The phase shifts are tabulated in table 7.1 where the uncertainty associated with each result corresponds to the reading error on the oscilloscope. The nominal phase shift refers to the phase shift between the mains voltage and the transformer voltage of the same phase, it is thus the same for each phase of the transformer.

Table 7.1. Actual and Nominal Phase Shifts

<u>Transformer and Phase</u>	<u>Nominal Phase Shift</u>	<u>Measured Phase Shift</u> <u>($\pm 0.5^\circ$)</u>
1 red	Leading by 22.5°	Leading by 21°
1 yellow		Leading by 26°
1 blue		Leading by 18°
2 red	Leading by 7.5°	Leading by 7°
2 yellow		Leading by 6°
2 blue		Leading by 7°
3 red	Lagging by 7.5°	Lagging by 10°
3 yellow		Lagging by 10°
3 blue		Lagging by 8°
4 red	Lagging by 22.5°	Lagging by 24°
4 yellow		Lagging by 26°
4 blue		Lagging by 25°

In order to verify that these departures from the nominal phase shifts are indeed the cause of the discrepancies between the experimental and the theoretical results the computer simulations were carried out using the actual phase shifts. The devices were modelled as in the simulations of the six pulse model, section 5.14. The firing angles used were 4.5° , 1.6° and -1.3° . These values of the firing angle were found by adjusting their values until the current magnitude was the same as that from the experimental model.

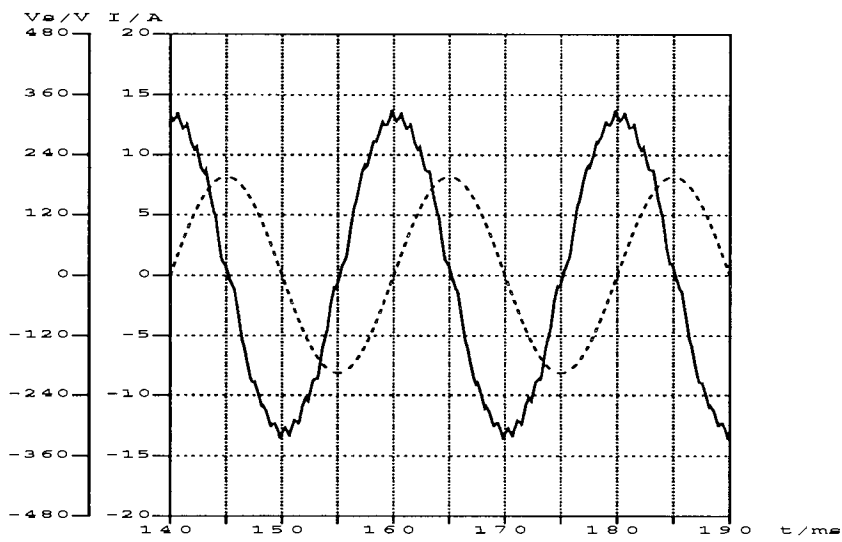
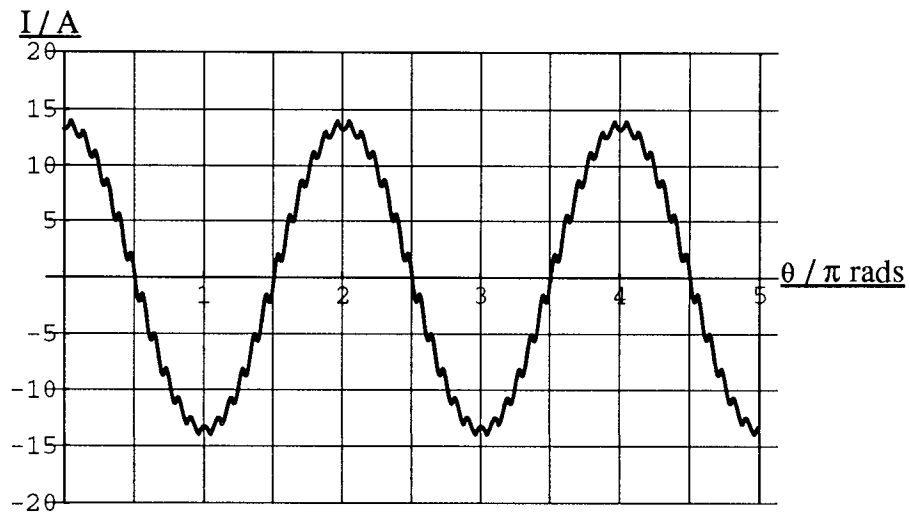
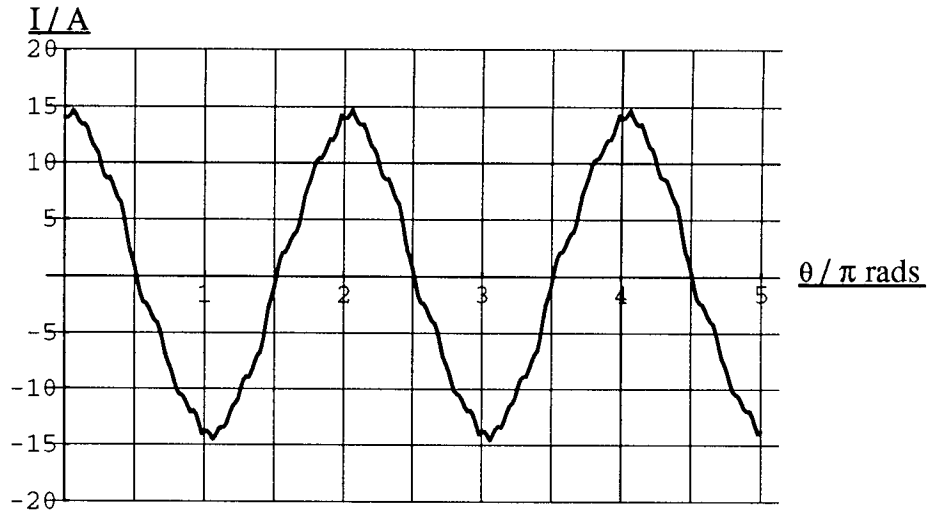


Figure 7.14. Experimental, Theoretical and Simulation Results for Rated Reactive Power Generation from a Twenty-Four Pulse STATCON.

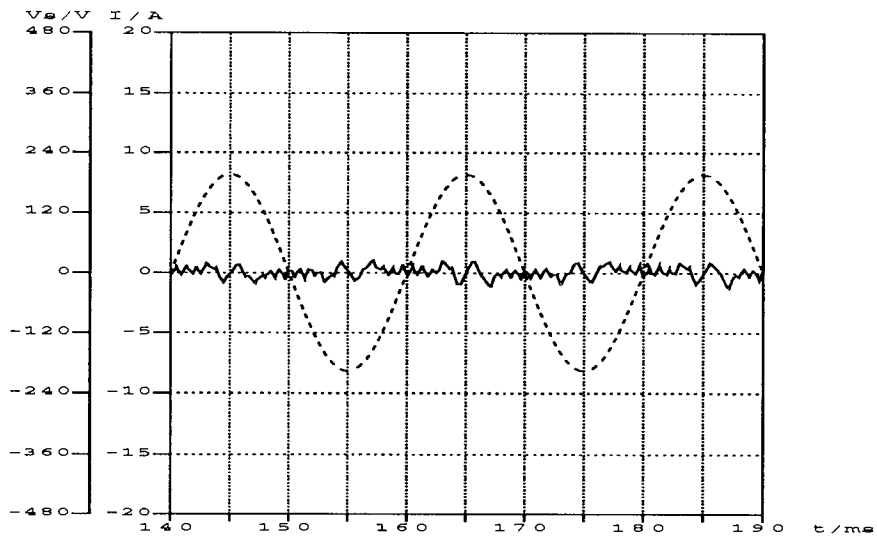
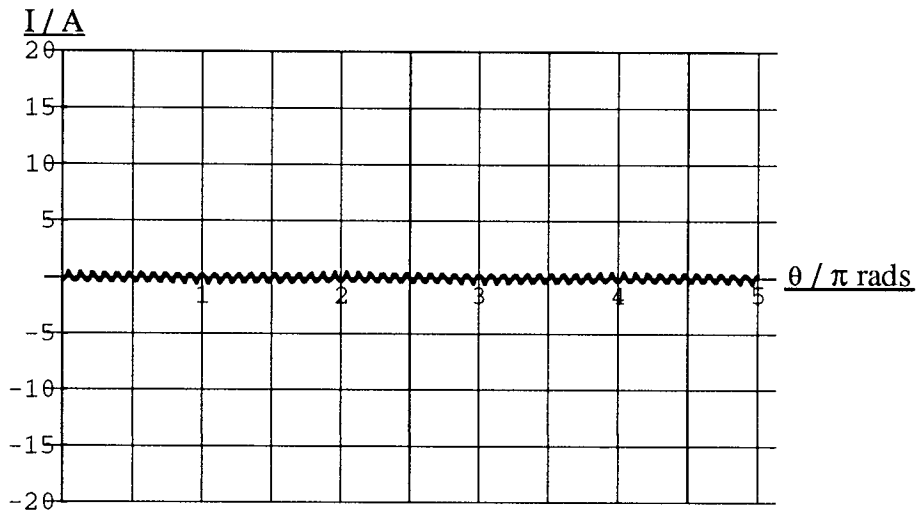
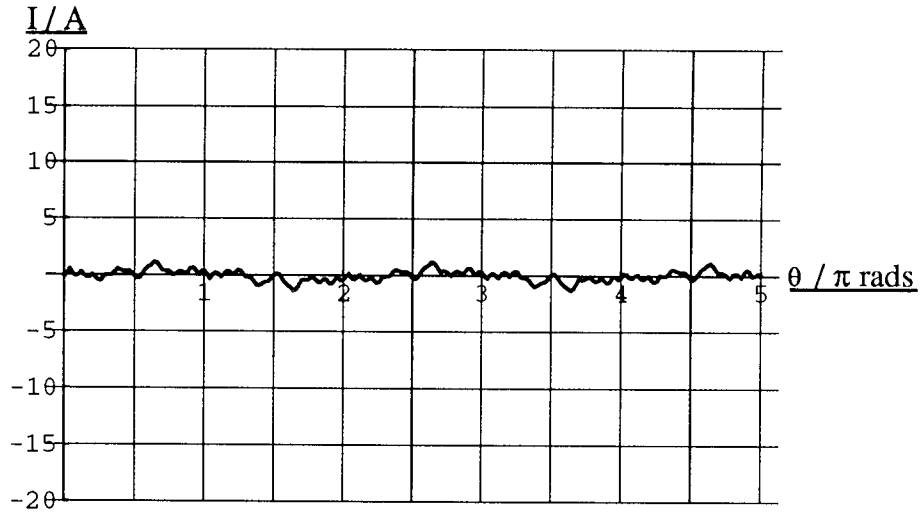


Figure 7-15. Experimental, Theoretical and Simulation Results for Zero Reactive Power Output from a Twenty-Four Pulse STATCON.

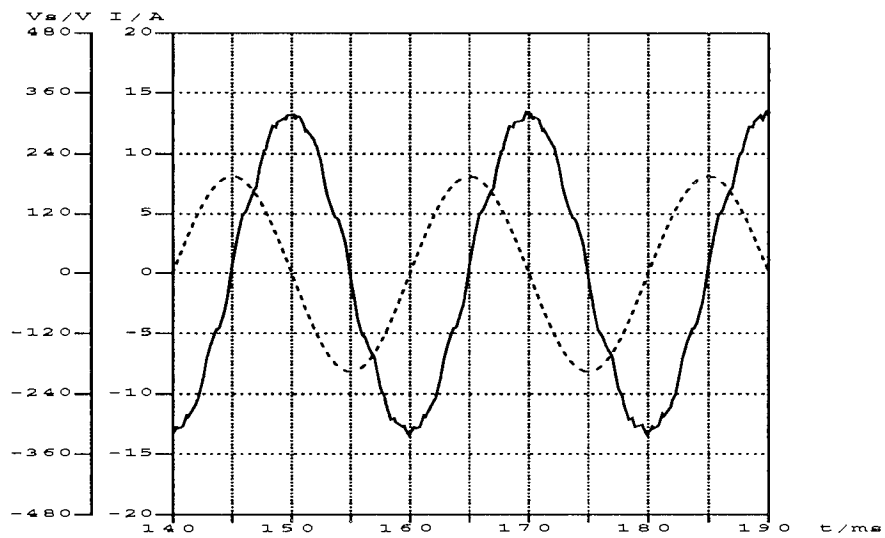
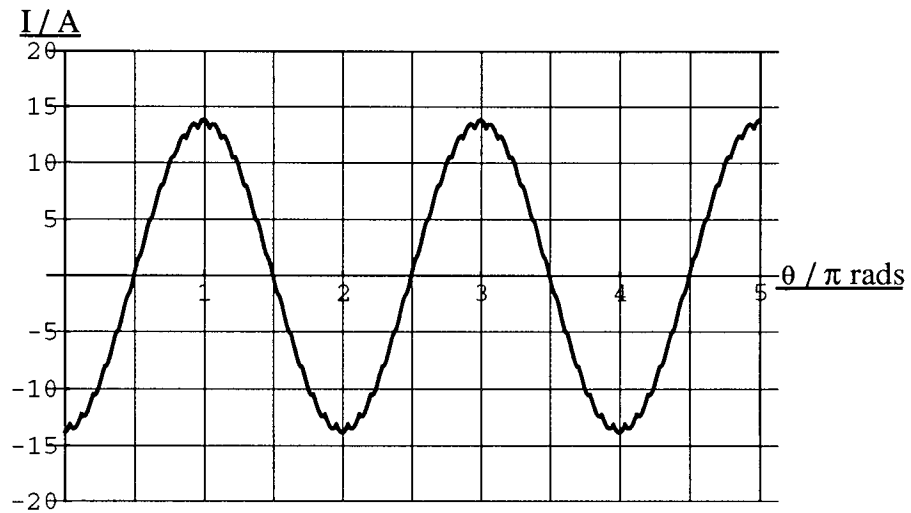
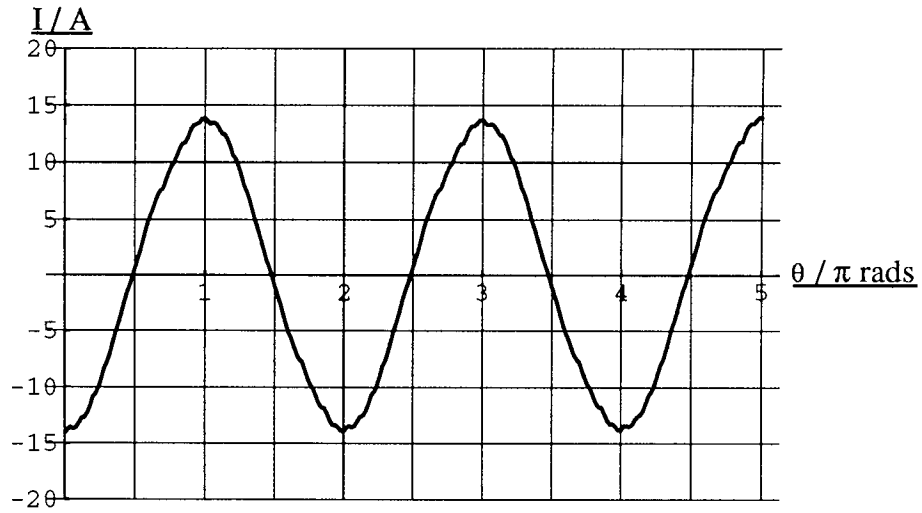


Figure 7.16. Experimental, Theoretical and Simulation Results for Rated Reactive Power Absorption from a Twenty-Four Pulse STATCON.

The wave shapes of the simulations are much closer to the experimental results than the theoretical results. Using the Fourier transform routine within the simulation package the harmonics present in these current waveforms can be calculated. The anticipated 23rd and 25th harmonics, at 1.15kHz and 1.25kHz, are noticeable but there are larger components for the 3rd, 5th, 7th, 9th and 11th harmonics.

The improved matching between the simulated waveforms and the actual ones shows that precise phase shifts are necessary to produce good harmonic neutralisation; the introduction of negative phase sequence currents on the secondary sides of the transformers significantly effects the harmonic cancellation.

The effects of negative phase sequence can be amplified at certain values of the resonance ratio; if the practical deficiencies in the circuit introduce a particular harmonic and the circuit is resonant at that harmonic, i.e. k is equal to the harmonic number, then the wave-shape becomes highly distorted (Trainer et al., 1994). If k is chosen near to the knee point of the q_2 against m graph then for this to occur the harmonics produced must be close to the 23rd and 25th predicted. This is not the case for this model.

A possible method of improving the performance of the model may lie in altering the firing angle of the MOSFETs. This is an area worthy of further study.

The other factors mentioned above will also contribute to the production of non-ideal harmonics in the system current. The use of air-gapped transformers may help to reduce the effects of these other factors by improved balancing of the leakage reactances of the transformers (Sumi et al., 1993).

§7.11 Size of the Energy Storage Components

As in the earlier work, as a point of comparison the knee point of the q_2 graph is chosen as a reference point, β is assumed to be negligible, and the inductances are assumed to be 20%. The knee point, from figure 7.8, is at $m = 0.048$. Taking X_L as 0.05p.u. gives the admittance of the capacitor as 0.12p.u. in the parallel case and 0.11p.u. in the series case.

§7.12 Range of the Reduced Firing Angle

As in the six and twelve pulse circuits, over the range of interest of the resonance ratio, the voltage across the capacitor has only one maximum or minimum during each interval. Thus the minimum voltage across the capacitor when it is generating reactive power is at the start of the interval and the minimum when it is absorbing reactive power is at the midpoint of the interval. Figure 7.17 shows the range of the reduced firing angle with m close to the edge of the plateau region for the series connected case. The graph for the parallel connected case is similar.

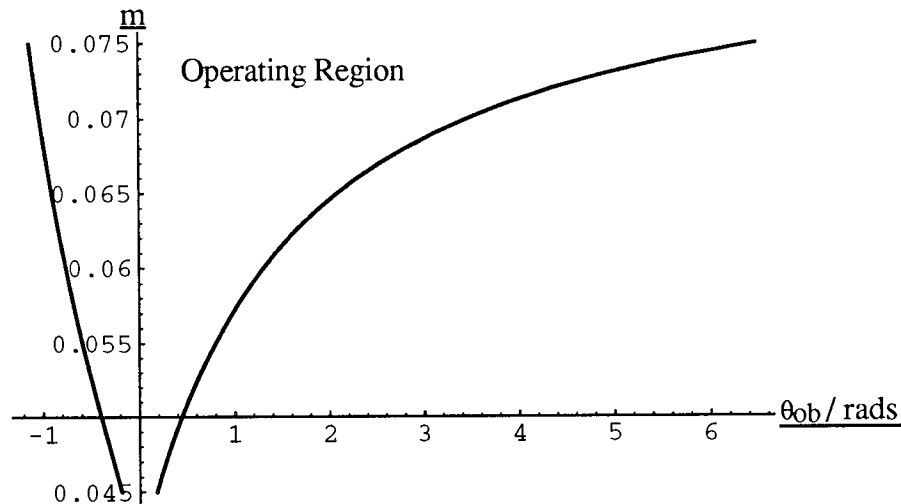


Figure 7.17. Operating Region for Small Values of θ_{ob} for the 24-Pulse STATCON with Series Connected Transformer Primaries.

§7.13 Conclusions

The various possible transformer configurations to produce 24-pulse and quasi 24-pulse STATCONs have been discussed. It has been argued that the use of additional filters makes the quasi 24-pulse system unattractive. Analyses have been carried out for both the series and parallel connection of a full 24-pulse system showing the form of the fundamental as a function of the reduced firing angle and the resonance ratio and quantifying the harmonics.

Experimental results for a full 24-pulse system with parallel connected primaries have been presented together with theoretical results. Simulation has been used to show that the main cause of the discrepancies between the two sets of results are a result of departures in the phase shifts of the transformers from the nominal values.

The range of θ_{ob} over the range of m of interest has been quantified.

Chapter 8

Conclusions and Proposals for Further Study

§8.1 Introduction

This chapter draws out the general conclusions from work which has been spread over more than one chapter and indicates potentially fruitful areas of further research.

§8.2 Method of Analysis

Much of the work presented has been the results from the mathematical analyses performed on the various circuits using a capacitor as the energy reservoir. From these a general method has been established which could be used to analyse a STATCON of any pulse number.

a) Common Tasks

Whether the transformer primaries were connected in series or parallel the following tasks were performed:

- 1) The relationships between the currents on the secondary side and those on the primary side were defined, as were those between the two sets of voltages.
- 2) The phase relationships between the current in one phase on the secondary side of the transformers, during the whole cycle, and the currents in all of the phases on the secondary side during one interval were established.
- 3) The effective circuit configuration during one interval was established.
- 4) Using the fact that because there are no triple- n harmonics generated in the equipment the sum of the voltages and the sum of the currents out of each transformer secondary must be zero, the potential of the neutral points of the transformer secondaries during the chosen interval were established, in terms of the voltage across the capacitor.
- 5) Differential equations describing the current in each phase of the circuit were then produced, in terms of the phase to neutral voltages on the secondary sides of the transformers, the voltage of the positive terminal of the capacitor and the voltage across the capacitor.

b) Parallel Connected Transformer Primaries

In the equipment with the transformer primaries arranged in parallel the following steps were taken

- 1) The voltages on each of the secondaries of the transformers, relative to their respective neutral points, were defined.
- 2) The second order differential equation for the current through the capacitor was then expressed and solved, giving the definition of the resonance ratio in terms of the reactances of the energy storage components, X_C and X_L , and the damping factor, β .
- 3) This current was integrated to give the voltage across the capacitor. The constant of integration is zero.
- 4) The differential equations for the currents in each of the phases was then expressed in terms of this voltage and solved. The total number of unknowns is $2N+1$, where N is the number of three phase inverters; there are two constants for every set of three phase currents, since they are balanced, and an additional 1 because the differential equation for the current through the capacitor is second order.
- 5) The unknowns are solved by ensuring that the current through the chosen phase is continuous and anti-symmetric and that the voltage across the capacitor has the same value at the end of the interval as it does at the start. Thus the current in one phase on the secondary side of the transformers is known for a whole cycle.
- 6) The current in one phase of the primary side can then be calculated from the relationships defined in steps 1 and 2 of section 8.2a.

c) Series Connected Transformer Primaries

In the equipment with the transformer primaries connected in series:

- 1) The relationships between the currents and voltages on the primary and secondary sides were used to express all of the currents on the secondary side of the transformers in terms of the currents in two of the secondary phases and to express two of the phase to neutral voltages on the secondary side in terms of the voltages on the secondary and primary sides.
- 2) Manipulating these expressions gave equations for the currents in the two specified phases in terms of the voltages on the primary side of the transformers and other known circuit parameters.
- 3) The current through the capacitor was expressed in terms of these currents and a second order differential equation was produced and solved to give the current through the capacitor and the definition of the resonance ratio.
- 4) This current was integrated to give the voltage across the capacitor.
- 5) From this voltage and one of the equations from point 2 a first order differential equation was produced and solved for one of the unknown currents and the other found from the definition of the capacitor current in terms of the two unknown currents from point 3.
- 6) The boundary conditions are that the voltage across the capacitor must be the same at the end of the interval as it is at the start and any two from the continuity of current equations used in the parallel connected case. Thus the current in one phase on the secondary side of the transformers is defined for a whole cycle.
- 7) The current in one phase of the primary can then be established using points 1 and 2 of section 8-2a.

§8.3 Calculation of Fourier Series

In calculating the Fourier series the integrals can be expressed in terms of either the phase of the system voltage, θ , or that of the inverter output voltage, ϕ . Expressing them in terms of the latter means that the solutions to the integrations do not depend upon θ_0 and it is apparent then that the θ_0 dependence of each harmonic in the system current is as $\sin\theta_0$ and $\cos\theta_0$. Using θ results in significantly more complicated integrals which have to be performed and means that the relationships between the terms in the series and θ_0 are opaque.

In both the parallel and series connected cases the harmonics can be plotted in terms of the reduced firing angle. This shows that the relationship between the magnitude of a particular harmonic and the reduced firing angle is an approximately linear one for all values of the resonance ratio. Therefore the normalised coefficient of the harmonic, t_n , can be approximately expressed in terms of the intercept, c_n , and the gradient, $-s_n$, of the slope of the plot of t_n against θ_{ob} .

Because of the form of the dependence on θ_0 the expressions for s_n and c_n have been calculated by evaluating the terms in the Fourier series at $\theta_0 = 0$ and at $\theta_0 = \pi/2$. Using this simplification means that s_n and c_n are defined in terms of the square root of the sum of the squares of the Fourier coefficients. The sign is then chosen so that c_n is positive and s_n is negative at very low values of the resonance ratio. The sign is reversed as necessary so that s_n and c_n vary smoothly.

§8.4 Definition of the Resonance Ratio

The resonance ratio k is the ratio of the natural frequency of the circuit to the system frequency. It is defined differently in the different circuits but is always of the form

$$k = \sqrt{\frac{\kappa X_C}{X_L} - \beta^2} \quad (8.1)$$

where

κ is the parameter which gives the effective value of the capacitance as seen from the a.c. side of the converter or the effective value of the inductance as seen from the d.c. side. It is a function of the pulse number of the circuit and the connection arrangement. The different values for the various circuits are tabulated in table 8.1.

Table 8.1. Values of κ .

<u>Circuit</u>	<u>κ</u>	<u>Approximate Value</u>
Single Phase	1	1
Three Phase	$\frac{2}{3}$	0.667
Parallel 12-Pulse	$\frac{4}{3}$	1.333
Series 12-Pulse	$\frac{2+\sqrt{3}}{3}$	1.244
Parallel 24-Pulse	$\frac{8}{3}$	2.667
Series 24-Pulse	$\frac{(\sqrt{2}+1)(\sqrt{3}+1)(\sqrt{3}+\sqrt{2})}{6\sqrt{2}}$	2.446

In the parallel connected cases

$$\kappa = 2N/3 \quad (8.2)$$

and in the series cases

$$\kappa = \frac{1}{6N \sin^2 \pi/6N} \quad (8.2a)$$

where

N is the number of three phase converters.

§8.5 Significance of the Resonance Ratio

The minima in the q_2 against m graphs for the different equipments occur at characteristic integer values of k : in the single phase circuit the minima occur at $k = 3, 5, 7, \dots$; in the three phase circuit they occur at $k = 6, 12, \dots$; in the twelve pulse circuit they occur at $k = 12, 24, \dots$ i.e. in all of the circuits, except the single phase one, the minima occur at integer multiples of the pulse number of the circuit.

For the three phase circuit a per phase equivalent circuit for the equipment, as seen from the a.c. system, was presented in section 5.11. Alternatively, an equivalent circuit can be produced as seen from the d.c. side of the converter. From the definition of the resonance ratio for the three phase circuit, this must consist of the energy reservoir capacitor in series with a resistance and inductance of $3/2$ times their values in the actual circuit, together with a source. The frequencies present in the output from the source must be such as to give harmonics of $n = 0, 6, 12, \dots$ in the voltage across the capacitor so that this voltage is the same as that in the actual circuit.

From this equivalent circuit, if the circuit is resonant at sixth harmonic, i.e. $k = 6$, the voltage across the capacitor will be dominated by this harmonic. Considering the full circuit, the voltage at the inverter terminals will be highly distorted and the system current will be dominated by harmonics; the performance of the equipment will be poor. However, if the system is resonant at, for example, fifth harmonic, then the voltage across the capacitor will have a substantial d.c. component and so the voltage at the a.c. terminals of the converter will have a substantial fundamental frequency component and the performance will be as desired. For higher pulse numbers this argument is still valid and so the performance of these circuits will be poor when the equipment is resonant at the pulse number.

In the single phase case the equivalent circuit, as seen from the d.c. side of the converter, consists of the energy reservoir capacitor in series with a source and an inductor and resistor of the same values as in the actual circuit. In this case, if the circuit is resonant at second harmonic, there will be a substantial amount of second harmonic in the voltage across the capacitor. At the a.c. terminals of the converter this second harmonic on the d.c. side will still produce a substantial amount of fundamental frequency component and so the performance of the circuit is not greatly affected.

The minima in the q_2 against m curve for the single phase circuit can be understood by considering the equivalent circuit produced in section 4.9. From this, if the circuit is resonant at third harmonic, the system current produced will be dominated by this third harmonic and the performance of the circuit will be poor.

§8·6 Optimisation of the Energy Storage Components

For all of the circuits considered there is a range of values of the resonance ratio above which the performance of the equipment is radically reduced and below which the energy storage components increase in size without any significant improvement in performance. This range of values therefore defines the size of the energy storage components.

The reduction in the size of the energy reservoir at higher pulse numbers can be illustrated by considering the knee points of the q_2 against m graphs. Table 8·2 shows the value of m at the knee point of these graphs and shows the per unit admittance of the capacitance assuming that the inductors are the leakage reactances of the transformers connecting the equipment to the system and that all of the transformers have a leakage reactance of 20% of their rating.

Table 8·2. The Admittance of the Energy Reservoir
at the Knee Point of the q_2 Against m Graphs.

<u>Circuit</u>	<u>m</u>	<u>YC / p.u.</u>
Single Phase	0·6	1·80
Three Phase	0·24	0·19
Parallel 12–Pulse	0·11	0·16
Series 12–Pulse	0·11	0·15
Parallel 24–Pulse	0·048	0·12
Series 24–Pulse	0·048	0·11

The optimum values of the pulse number and the resonance ratio are complicated functions of the costs of the losses, the capacitance, the inductances or leakage reactances, the transformers, the filters, the site costs, and the cost and ratings of the devices and the ability to connect them in series and/or in parallel.

For all but the single phase circuit the energy storage components are significantly reduced in comparison to those of a conventional SVC, improving the possibility of making the equipment portable, as discussed in section 1·5e.

The cost of the energy stores can be optimised by considering their relative cost in a compensator of rated voltage V and rated reactive power Q . This optimisation assumes parallel connected transformers, but the results would be similar for series connected ones. The rated current, I , is given by

$$I = \frac{Q}{\sqrt{3}V} \quad (8.3)$$

The cost of the capacitor is dependent on its admittance and voltage rating and in this case is taken as

$$C_C Y_C V^2 \quad (8.4)$$

where

C_C is the cost per unit reactive power of capacitance in £/VA.

The cost of an inductor is dependent on its reactance and current rating and in this case is taken as

$$C_L X_L I_L^2 \quad (8.5)$$

where

C_L is the cost per unit reactive power of inductance in £/VA

and I_L is the current through the inductor.

For a three phase compensator with N 6-pulse converters the current in each inductor is $1/N$ times the total current. The cost of all of the inductors is therefore

$$3 C_L N X_L (I/N)^2 \quad (8.6)$$

The total cost of the energy stores, C_T , is given by

$$C_T = C_C Y_C V^2 + 3 C_L X_L \frac{I^2}{N} \quad (8.7)$$

The relationship between Y_C and X_L in the parallel circuits is

$$k = \sqrt{\frac{\kappa}{Y_C X_L} - \beta^2} \quad (8.8)$$

In parallel connected equipment $\kappa = 2N/3$ and so substituting in (8.8), and replacing k by $1/m$, gives

$$\frac{1}{m^2} \approx \frac{2 N}{3 Y_C X_L} \quad (8.9)$$

Substituting for Y_C in the expression for the total cost of the energy stores, equation (8.7), and expressing in terms of the rated voltage and reactive power, gives

$$C_T = C_C V^2 \frac{2 N m^2}{3 X_L} + \frac{C_L X_L Q^2}{N V^2} \quad (8.10)$$

Setting the derivative of (8-10), with respect to X_L , to zero gives

$$C_C V^2 \frac{2 N m^2}{3 X_L^2} = \frac{C_L Q^2}{N V^2} \quad (8-11)$$

Hence the minimum total cost occurs when

$$X_L = \frac{V^2}{Q} m N \sqrt{\frac{2 C_C}{3 C_L}} \quad (8-12)$$

At this value of X_L the admittance of the capacitor is

$$Y_C = \frac{Q}{V^2} m \sqrt{\frac{2 C_L}{3 C_C}} \quad (8-13)$$

The minimum total cost is

$$C_T = Q m \sqrt{\frac{8 C_C C_L}{3}} \quad (8-14)$$

The reduced firing angle at rated reactive power, approximating $q_2 = 0.5$ and $q_1 = 0$, is

$$\theta_{ob} = m \sqrt{\frac{8 C_C}{3 C_L}} \quad (8-15)$$

The analysis is intended as a comparison between different possible circuits and so the reactive power and voltage rating of the equipments has been assumed to be the same. In this case then X_L , Y_C and Q can all be expressed as per unit quantities.

The base impedance, Z_b , is taken as

$$Z_b = \frac{V^2}{Q} \quad (8-16)$$

The per unit value of the capacitance is given by

$$Y_C \text{ p.u.} = m \sqrt{\frac{2 C_L}{3 C_C}} \quad (8-17)$$

For N sets of inductors each inductor has only to be rated for $(1/N)$ of the total reactive power and therefore the base impedance for each inductor is $(1/N)$ that given in equation (8-16). The per unit value of inductance is therefore

$$X_L \text{ p.u.} = m \sqrt{\frac{2 C_C}{3 C_L}} \quad (8-18)$$

Table 8-3 gives some exemplary figures taking C_C/C_L to be 3 and defining the total cost of the energy stores to be 1 in the six pulse circuit.

Table 8.3. Optimised Values of the Energy Stores.

Pulse No.	N	m	Y_C / p.u.	X_L / p.u.	θ_{ob} / rad	Cost
6	1	0.24	0.113	0.339	0.68	1.00
12	2	0.11	0.052	0.156	0.31	0.46
24	4	0.048	0.023	0.068	0.14	0.20

Although the costs have been simplified to include only the energy storage components necessary for the correct operation of the equipment, in particular the cost of the transformer has been neglected, it is expected that a fuller analysis would again bring out the feature that at higher pulse number the total amount of energy storage components can be reduced.

§8.7 Practical Results

From the six pulse 1kVAr model the following points are apparent:

- 1) The current waveforms are almost identical with the theoretical ones.
- 2) The effective resistance in the circuit includes a significant contribution from the volt drop of the devices. Because the volt drop is different for the MOSFETs and the diodes some asymmetry results in the current waveform.
- 3) The system is very sensitive to fluctuations in the mains voltage so some form of closed loop control would be necessary for a large system.

From the twenty-four pulse 4kVAr model:

- 1) Exact phase shifts on the transformers are needed to produce the expected harmonic neutralisation.

§8·8 Summary of Important Formulae

In the parallel connected circuits the relationship between the V_m and the system voltage, V , is

$$V = \frac{\sqrt{3} V_m}{\sqrt{2}} \quad (8.19)$$

In the series connected circuits the equivalent relationship is given by

$$V = \frac{\sqrt{3} V_m N}{\sqrt{2}} \quad (8.19a)$$

The approximate relationship between the reactive power from a parallel connected three phase compensator and the reduced firing angle is given by

$$Q \approx -\frac{3 N V_m^2}{2 X_L} [q_1 + q_2 \theta_{ob}] \quad (8.20)$$

In the case of the series connected compensator

$$Q \approx -\frac{3 V_m^2}{2 X_L} [q_1 + q_2 \theta_{ob}] \quad (8.20a)$$

For a correctly sized compensator $q_2 \approx 0.5$ and $q_1 \approx 0$ and so substituting these in both parts of (8.18), and also for the rated voltage, gives

$$\text{Parallel:} \quad Q \approx -\frac{N V^2}{2 X_L} \theta_{ob} \quad (8.21)$$

$$\text{Series:} \quad Q \approx -\frac{V^2}{2 N X_L} \theta_{ob} \quad (8.21a)$$

In both cases then this can be written

$$Q \approx -\frac{V^2}{2 X_E} \theta_{ob} \quad (8.22)$$

where

X_E is the reactance of N reactances in parallel in the circuit with the transformer primaries connected in parallel and of N reactances in series in the circuit with the transformer primaries in series.

The losses can be approximated to

$$P \approx \frac{\beta V^2}{2 X_E} \theta_{ob} \quad (8.23)$$

The formula for the coefficient of the harmonics for both the series and the parallel cases can be written as

$$I_{nc} = \frac{\sqrt{2} V}{\sqrt{3 X_E}} [c_n - s_n \theta_{ob}] \quad (8.24)$$

§8·9 Further Work

This thesis has established the steady state performance of the voltage source type of converter compensator.

The analyses of the different circuits show similarities between equipments of different pulse number; it may be possible to derive expressions for a general STATCON of pulse number $6N$ in both the series and the parallel cases which would reduce the total amount of algebra and illustrate the form of the results more directly.

Multiple parallel connected converters with series connection of the primaries of the phase-shifting transformers is believed to be the most financially attractive of the converters systems considered, although a full analysis of the PWM and the multi-level systems has not been carried out.

These circuits are worthy of further consideration. Neither of these circuits require phase-shifting transformers. This means that they can be connected directly to the tertiary winding of existing grid transformers, provided that they are at a suitable voltage rating. If these equipments are small enough, or can be constructed in a modular fashion, then the possibility of relocating them as the system demands change, as discussed in section 1·5, becomes realistic. This is much less likely to be possible with a system involving phase-shifting transformers.

In the PWM system the following points need to be addressed:

- 1) the size of the energy stores,
- 2) the losses,
- 3) the optimum number of harmonics to eliminate with this technique and whether any filters are needed,
- 4) the use of energy recovery snubber circuits to reduce the losses and
- 5) the overall size of the equipment.

In the case of the multi-level system:

- 1) the size of the energy stores,
- 2) the configuration of the devices,
- 3) the firing pattern,
- 4) the optimum number of harmonics to eliminate,
- 5) whether all of the capacitors should be of the same value,
- 6) the losses and
- 7) the overall size of the equipment.

Either of these equipments might be preferred to the type of converter compensator discussed in this thesis if the overall size of the equipment is sufficiently low to permit relocation, even if the losses are markedly higher and the initial cost higher.

This thesis has addressed only the steady state performance of the STATCON. The results from this steady state analysis are sufficiently encouraging to merit studying the transient and fault performance of the equipment:

- 1) The speed of response of the equipment to changes in the reactive power demand. It has been reported that the theoretical response of multi-pulse STATCONs is faster than that of conventional SVCs (Gyugyi et al., 1990). This property could be very useful under certain fault conditions. In particular, it has been used to damp power system oscillations (Mori et al., 1993) but may be useful in other situations.
- 2) The performance of the equipment under either internal or external fault has not been assessed. The internal fault to be considered is mis-firing of the thyristors. Further work on series and parallel connection of the GTO thyristors may be worthwhile. External faults to be considered include the sudden loss of voltage, in either one, two or all three phases, the presence of harmonics in the system voltage and a sudden change in system frequency.

The practical work described in the thesis has had various limitations. Areas which need improvement are

- 1) A suitable closed loop control scheme to prevent fluctuations in the reactive power output as a result of changes in the system voltage, although a number of these have already been proposed (Mori et al., 1993), (Schauder and Mehta, 1993).
- 2) The harmonic neutralisation in the 24-pulse equipment is not as good as had been expected because the transformer phase shifts are not exactly as required. It may be possible to alter the MOSFET firing angles to correct for this, although this would introduce asymmetry into the capacitor voltage.

References

Alexandrovitz, A., Yair, A. and Epstein, E.: "Analysis of a Static VAR Compensator with Optimal Energy Storage Element", IEEE Transactions on Industrial Electronics, Vol. 31, No. 1, pp28 – 33, February 1984.

Akagi, H., Kanazawa, Y. and Nabae, A.: "Instantaneous Reactive Power Compensators Comprising Switching Devices without Energy Storage Components", IEEE Transactions on Industry Applications, Vol. 20, No. 3, pp625 – 630, May/June 1984.

Ashbrook, A. and Hill, J. E. (a): "1kVAr Three Phase Voltage Sourced Inverter ASVC", Proceedings of the 28th Universities Power Engineering Conference, pp243 – 246, Stafford, England, September 1993.

Ashbrook, A. and Hill, J. E. (b): "The Design and Performance of a 1kVAr Voltage Sourced Inverter Type of Advanced Static VAR Compensator", Aston University Electric Power Group Internal Note, FE/MEE/PGN/20/93, Birmingham, England, 1993.

Bradley, M. E.: "Voltage and MVAR Control Modes for SVCs and MSCs", IEE Colloquium on "International Practices in Reactive Power Control", Digest No. 1993/079, London, England, April 1993.

Edwards, C. W., Mattern, K. E., Nannery, P. R. and Gubernick, J.: "Advanced Static VAR Generator Employing GTO Thyristors", IEEE Transactions on Power Delivery, Vol. 3, No. 4, pp1622 – 1627, October 1988.

Epstein, E., Yair, A. and Alexandrovitz, A.: "Three-Phase Static VAR Compensator with Reduced Energy Storage", etzArchiv, Bd. 8, H. 6, pp213 – 219, 1986.

Erinmez, I. A.: "Static VAR Compensators", Cigré Report from Working Group 38-01, Task Force No. 2 on SVC, Paris, France, 1986.

Gyugyi, L.: "Control of Shunt Compensation with Reference to New Design Concepts", IEE Proc., Part C, Vol. 128, No. 6, pp374 – 381, November 1981.

Gyugyi, L.: "Solid-State Control of Electric Power in A.C. Transmission Systems", International Symposium on Electric Energy Converters in Power Systems, Invited Paper No. 4, Capri, Italy, May 1989.

Gyugyi, L., Hingorani, N. G., Nannery, P. R. and Tai, N.: "Advanced Static VAR Compensator Using Gate Turn-Off Thyristors for Utility Applications", Cigré paper 23-203, 1990.

Heumann, V. K.: "Elektrotechnische Grundlagen der Zwangskommutierung – Neue Möglichkeiten der Stromrichtertechnik", E. und M., Jg. 84, H. 3, pp99 – 112, 1966.

Hill, J. E., Chileshe, C. M., Boardman, S. M. and Westrick, M. P.: "Experimental Model of a Harmonic Neutralised STATCON", Proceedings of the 29th Universities Power Engineering Conference, pp338 – 341, Galway, Ireland, September 1994.

Hill, J. E. and Norris, W. T.: "Development of an Equivalent Circuit for a Single Phase Advanced Static VAR Compensator", Aston University Electric Power Group Internal Note, FE/MEE/PGN/39/94, Birmingham, England, 1994.

Hindmarsh, J.: "Electrical Machines and Their Applications", 4th Edition, Pergamon Press Ltd., Oxford, England, 1984.

Hughes, E.: "Electrical Technology", 6th Edition, Longman Scientific & Technical, Harlow, England, 1987.

James, D. A. and Hill, J. E.: "Harmonic Reduction On Three Phase Statcons Using Pulse Width Modulation", Aston University Electric Power Group Internal Note, FE/MEE/PGN/38/94, Birmingham, England, 1994.

Jolley, L. B. W.: "Summation of Series", 2nd Revised Edition, Constable and Company, London, England, 1961.

Larsen, E., Miller, N., Nilsson, S. and Lindgren, S.: "Benefits of GTO-Based Compensation Systems for Electric Utility Applications", IEEE Transactions on Power Delivery, Vol. 7, No. 4, pp2056 – 2065, October 1992.

Lander, C. W.: "Power Electronics", 2nd Edition, McGraw-Hill Book Company Ltd., Maidenhead, England, 1987.

Liang, W., Qionglin, Z. and Rongtai, H.: "Analysis and Design of a 3 – Phase Negative VAR & Harmonic Current Compensator", IEEE International Conference on Industrial Electronics, Control and Instrumentation, pp741 – 746, Kobe, Japan, October 1991.

Le Du, A., Tontini, G. and Winfield, M.: "Which FACTS Equipment for Which Need? Identification of the Technology Developments to Meet the Needs of Electricité de France (EDF), Ente Nazionale per l'Energia Elettrica (ENEL) and National Grid Company (NGC)", Cigré paper 14/37/38-08, 1992.

McMurray, W.: "Feasibility of Gate-Turnoff Thyristors in a High-Voltage Direct-Current Transmission System", Electric Power Research Institute EL-5332, August 1987.

Miller, T. J. E.: "Reactive Power Control in Electric Systems", John Wiley and Sons, Inc., New York, USA, 1982.

Mohan N., Undeland, T. M. and Robbins, W. P.: "Power Electronics: Converters, Applications, and Design", John Wiley & Sons, Inc., New York, USA, 1989.

Moran, L. T., Ziogas, P. D. and Joos, G. (a): "Analysis and Design of a Three-Phase Current Source Solid-State Var Compensator", IEEE Transactions on Industry Applications, Vol. 25, No. 2, pp356 – 364, March/April 1989.

Moran, L. T., Ziogas, P. D. and Joos, G. (b): "Analysis and Design of a Three-Phase Synchronous Solid-State Var Compensator", IEEE Transactions on Industry Applications, Vol. 25, No. 4, pp598 – 608, July/August 1989.

Mori, S., Matsuno, K., Hasegawa, T., Ohnishi, S., Takeda, M., Seto, M., Murakami, S. and Ishiguro, F.: "Development of a Large Static VAR Generator Using Self-Commutated Inverters for Improving Power System Stability", IEEE Transactions on Power Systems, Vol. 8, No. 1, pp371 – 377, February 1993.

National Grid Company plc: "The Grid Code", Version 11, St. Albans, England, October 1994.

National Grid Company plc: "High Speed Response Variable Static Var Compensators", National Grid Technical Specification 2.11, Issue 1, Guildford, England, December 1992.

Norris, W. T. and Hill, J. E.: "Analysis of a Single Phase Advanced Static VAR Compensator with Capacitor Reservoir", Aston University Internal Power Group Note, FE/MEE/PGN/22/93, 2nd edition, Birmingham, England, 1993.

Pedersen, J. K. and Rasmussen, T.: "A Solid State VAR-Compensator with Floating Intermediate Circuit Voltage", Proceedings of the 29th Universities Power Engineering Conference, pp557 – 560, Galway, Ireland, September 1994.

Schauder, C. and Mehta, H.: "Vector Analysis and Control of Advanced Static VAR Compensators", IEE Proc., Part C, Vol. 140, No. 4, pp299 – 306, July 1993.

Shepherd, W. and Zand, P.: "Energy flow and power factor in nonsinusoidal circuits", Cambridge University Press, Cambridge, England, 1979.

Sumi, Y., Harumoto, Y., Hasegawa, T., Yano, M., Ikeda, K. and Matsuura, T.: "New Static VAR Control Using Force-Commutated Inverters", IEEE Transactions on Power Apparatus and Systems, Vol. 100, No. 9, pp4216 – 4224, September 1981.

Trainer, D. R. and Tennakoon, S. B.: "A Study of a Self Commutated Converter Based Reactive Power Compensator", Proceedings of the 25th Universities Power Engineering Conference, pp321 – 324, Aberdeen, Scotland, September 1990.

Trainer, D. R., Tennakoon, S. B. and Morrison, R. E.: "Analysis of GTO-based static VAR compensators", IEE Proceedings on Electric Power Applications, Vol. 141, No. 6, pp293 – 302, November 1994.

Van Wyk, J. D., Marshall, D. A. and Boshoff, S.: "Simulation and Experimental Study of a Reactively Loaded PWM Converter as a Fast Source of Reactive Power", IEEE Transactions on Industry Applications, Vol. 22, No. 6, pp1082 – 1089, November/December 1986.

Walker, L. H.: "Force-Commutated Reactive-Power Compensator", IEEE Transactions on Industry Applications, Vol. 22, No. 6, pp1091 – 1104, November/December 1986.

Weedy, B. M.: "Electric Power Systems", Third Edition Revised, John Wiley and Sons, Ltd., Chichester, England, 1987.

Williams, B. W.: "Power Electronics Devices, Drivers, Applications and Passive Components", 2nd edition, The MacMillan Press Ltd., Houndmills, England, 1992.

Appendix 1

Analysis of a Single Phase Voltage Sourced STATCON

a) Determination of the Current

Figure A1.1 shows the circuit.

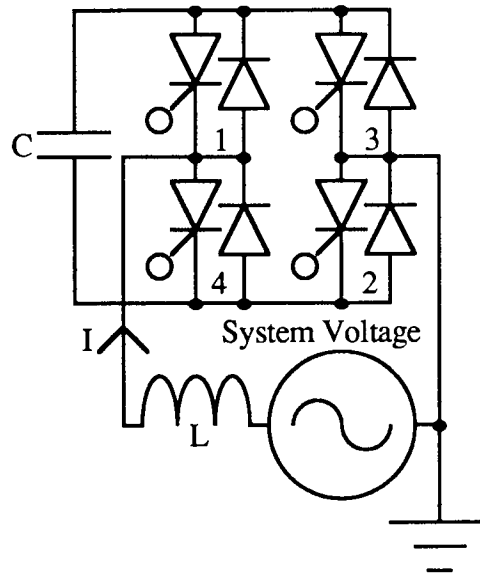


Figure A1.1. The Single Phase STATCON with Capacitor Energy Reservoir.

The supply voltage, V_S , is assumed to be sinusoidal, and substituting from (3.1), this can be expressed as

$$V_S = V_m \sin \theta = V_m \sin(\phi + \theta_0) \quad (\text{A1.1})$$

When thyristors 1 and 2 are turned on, assuming that the current through the capacitor is continuous, the circuit is as shown in figure A1.2. Following this current path in figure A1.1 it is apparent that the total resistance, R , is the resistance in the inductance plus twice the resistance of one of the devices. This assumes that the resistances of the diodes and of the controllable devices are equal and that they are linear. The volt drops of the devices have been neglected.

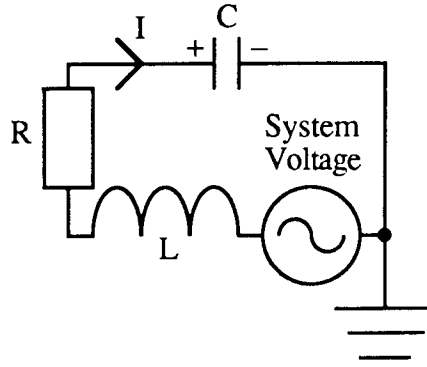


Figure A1.2. Single Phase Circuit with Devices 1 and 2 Turned On.

The equation describing the current during this interval, $0 \leq \phi \leq \pi$, is

$$\frac{d^2I}{d\phi^2} + \frac{R}{X_L} \frac{dI}{d\phi} + \frac{X_C}{X_L} I = \frac{V_m}{X_L} \cos(\phi + \theta_0) \quad (\text{A1.2})$$

The solution to (A1.2), assuming it is under-damped, i.e. $R < 2\sqrt{X_C X_L}$, is

$$I = \frac{V_m}{hX_L} \sin(\phi + \theta_0 + \gamma) + A_1 e^{-\beta\phi} \sin k\phi + A_2 e^{-\beta\phi} \cos k\phi \quad (\text{A1.3})$$

where

$$h = \sqrt{(\beta^2 + k^2 - 1)^2 + 4\beta^2} \quad (\text{A1.3a})$$

$$k = \sqrt{\frac{X_C}{X_L} - \beta^2} \quad (\text{A1.3b})$$

$$\beta = \frac{R}{2X_L} \quad (\text{A1.3c})$$

$$\sin\gamma = \frac{\beta^2 + k^2 - 1}{h}$$

and $\cos\gamma = \frac{2\beta}{h}$

hence $\tan\gamma = \frac{\beta^2 + k^2 - 1}{2\beta} \quad (\text{A1.3d})$

k is the ratio of the damped natural frequency of the circuit to the supply frequency and is referred to as the resonance ratio. To simplify any computations the angle γ is defined so that it is in the range $-\pi/2 < \gamma < \pi/2$.

The voltage across the capacitor, V_c , when thyristors 1 and 2 are turned on, from figure A1.2, is given by

$$V_c = X_C \int I d\phi \quad (\text{A1.4})$$

Substituting (A1.3) in (A1.4) and integrating gives

$$\frac{V_c}{X_C} = -\frac{V_m}{hX_L} \cos(\phi + \theta_0 + \gamma) - \frac{e^{-\beta\phi}}{(\beta^2 + k^2)} [(\beta A_1 - k A_2) \sin k\phi + (k A_1 + \beta A_2) \cos k\phi] \quad (\text{A1.5})$$

In general equations of the same sort as (A1.5) include a constant of integration. This one cannot because in a circuit with resistance it is impossible to generate, from an a.c. source, a voltage which does not decay.

During the next half-cycle thyristors 3 and 4 are turned on and thyristors 1 and 2 are turned off. The circuit during this interval is shown in figure A1.3.

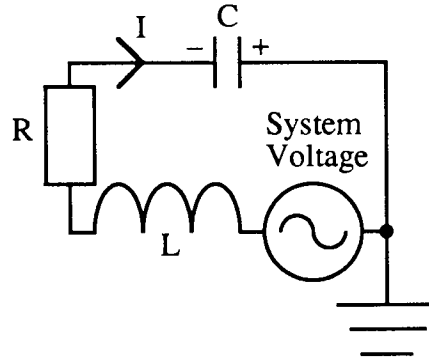


Figure A1.3. Single Phase Circuit with Devices 3 and 4 Turned On.

From figures A1.2 and A1.3 it is apparent that firing the opposite pair of devices reverses the connection of the capacitor into the circuit. Since there is no constant voltage across the capacitor it follows that, if the system voltage is as in (A1.1), the current must be half wave anti-symmetric. Since the action of the inverter reverses the current through the capacitor then this current, and the voltage across the capacitor, must be half wave symmetric. The boundary conditions can therefore be written as

$$I(\phi = \pi) = -I(\phi = 0) \quad (\text{A1.6})$$

$$V_c(\phi = \pi) = V_c(\phi = 0) \quad (\text{A1.6a})$$

Evaluating (A1.6) from (A1.3) gives

$$A_1 e^{-\beta\pi} \sin k\pi = -A_2 [1 + e^{-\beta\pi} \cos k\pi] \quad (\text{A1.7})$$

and evaluating (A1.6a) from (A1.5) gives

$$-\frac{2V_m}{hX_L} \cos(\theta_0 + \gamma) = \frac{1}{(\beta^2 + k^2)} \{ (kA_1 + \beta A_2) [1 - e^{-\beta\pi} \cos k\pi] - (\beta A_1 - kA_2) e^{-\beta\pi} \sin k\pi \} \quad (\text{A1.7a})$$

Manipulating (A1.7) and (A1.7a) gives, after simplifying,

$$A_1 = -\frac{2V_m (\beta^2 + k^2) (1 + e^{-\beta\pi} \cos k\pi) \cos(\theta_0 + \gamma)}{hX_L [k - 2\beta e^{-\beta\pi} \sin k\pi - k e^{-2\beta\pi}]} \quad (\text{A1.8})$$

and

$$A_2 = \frac{2V_m (\beta^2 + k^2) e^{-\beta\pi} \sin k\pi \cos(\theta_0 + \gamma)}{hX_L [k - 2\beta e^{-\beta\pi} \sin k\pi - k e^{-2\beta\pi}]} \quad (\text{A1.8a})$$

Substituting from equation (A1.8) and (A1.8a) in (A1.3) gives

$$I = \frac{V_m}{hX_L} \{ \sin(\phi + \theta_0 + \gamma) - \frac{2(\beta^2 + k^2) \cos(\theta_0 + \gamma) e^{-\beta\phi}}{[k - 2\beta e^{-\beta\pi} \sin k\pi - k e^{-2\beta\pi}]} [(1 + e^{-\beta\pi} \cos k\pi) \sin k\phi - e^{-\beta\pi} \sin k\pi \cos k\phi] \} \quad (A1.9)$$

b) Fourier Series

The current can be expressed, during the interval $0 \leq \phi \leq \pi$, from equation (A1.9), as

$$I = \frac{V_m}{hX_L} \{ \sin(\phi + \theta_0 + \gamma) - G e^{-\beta\phi} [(1 + e^{-\beta\pi} \cos k\pi) \sin k\phi - e^{-\beta\pi} \sin k\pi \cos k\phi] \} \quad (A1.10)$$

where

$$G = \frac{2(\beta^2 + k^2) \cos(\theta_0 + \gamma)}{[k - 2\beta e^{-\beta\pi} \sin k\pi - k e^{-2\beta\pi}]} \quad (A1.10a)$$

By performing the Fourier series the current can be expressed as

$$I = \sum_{n=1}^{\infty} a_n \cos n\phi + b_n \sin n\phi \quad (A1.11)$$

where

$$a_n = \frac{1}{\pi} \int_0^{2\pi} I(\phi) \cos n\phi \, d\phi \quad \text{and} \quad b_n = \frac{1}{\pi} \int_0^{2\pi} I(\phi) \sin n\phi \, d\phi \quad (A1.11a)$$

Considering the a_n term only, expanding, making a change of variables and then renaming, gives

$$\pi a_n = \int_0^{\pi} I(\phi) \cos n\phi \, d\phi - \int_0^{\pi} I(\phi) \cos n(\phi + \pi) \, d\phi \quad (A1.12)$$

Simplifying gives

$$\pi a_n = [1 - \cos n\pi] \int_0^{\pi} I(\phi) \cos n\phi \, d\phi \quad (A1.13)$$

Performing similar algebra for the b_n terms shows that the Fourier series only has components for the odd harmonics:

$$a_n = \frac{2}{\pi} \int_0^{\pi} I(\phi) \cos n\phi \, d\phi \quad \text{and} \quad b_n = \frac{2}{\pi} \int_0^{\pi} I(\phi) \sin n\phi \, d\phi \quad (A1.14)$$

Using these definitions of a_n and b_n , integrating, and simplifying gives, for odd n ,

$$I = \frac{V_m}{hX_L} \left\{ \sin(\phi + \theta_0 + \gamma) - \frac{2Gk}{\pi} [1 + 2e^{-\beta\pi} \cos k\pi + e^{-2\beta\pi}] \sum_{n=1}^{\infty} \frac{\sin(n\phi + \gamma_n)}{h_n} \right\} \quad (\text{A1.15})$$

where

$$h_n = \sqrt{(\beta^2 + k^2 - n^2)^2 + 4\beta^2 n^2} \quad (\text{A1.15a})$$

$$\sin \gamma_n = \frac{\beta^2 + k^2 - n^2}{h_n}$$

and $\cos \gamma_n = \frac{2\beta n}{h_n}$

hence $\tan \gamma_n = \frac{\beta^2 + k^2 - n^2}{2\beta n}$ (A1.15b)

Expanding equation (A1.15) in terms of θ gives

$$I = \frac{V_m}{hX_L} \left\{ [\sin \theta \cos \gamma + \cos \theta \sin \gamma] - \frac{2Gk}{\pi} [1 + 2e^{-\beta\pi} \cos k\pi + e^{-2\beta\pi}] \sum_{n=1}^{\infty} \frac{\sin(\gamma_n - n\theta) \cos n\theta + \cos(\gamma_n - n\theta) \sin n\theta}{h_n} \right\} \quad (\text{A1.16})$$

The fundamental component of the current, I_1 , can be separated into the contribution which is in phase with the system voltage and the contribution which is in quadrature:

$$I_1 = I_p \sin \theta + I_q \cos \theta \quad (\text{A1.17})$$

After substituting from (A1.10a) into (A1.16) these become

$$I_q = \frac{V_m}{hX_L} \sin \gamma - \frac{2V_m k}{\pi h^2 X_L} \frac{[1 + 2e^{-\beta\pi} \cos k\pi + e^{-2\beta\pi}]}{[k - 2\beta e^{-\beta\pi} \sin k\pi - k e^{-2\beta\pi}]} (\beta^2 + k^2) [2 \sin \gamma \cos \gamma - \sin 2\theta_0] \quad (\text{A1.18})$$

and

$$I_p = \frac{V_m}{hX_L} \cos \gamma - \frac{4V_m k}{\pi h^2 X_L} \frac{[1 + 2e^{-\beta\pi} \cos k\pi + e^{-2\beta\pi}]}{[k - 2\beta e^{-\beta\pi} \sin k\pi - k e^{-2\beta\pi}]} (\beta^2 + k^2) [\cos^2 \gamma - \sin^2 \theta_0] \quad (\text{A1.18a})$$

To show the dependence of the fundamental component of the current on the firing angle these can be expressed as

$$I_q = \frac{V_m}{X_L} \left(q_1 + q_2 \frac{\sin 2\theta_0}{2\beta} \right) \approx \frac{V_m}{X_L} [q_1 + q_2 \theta_{ob}] \quad (A1.19)$$

and
$$I_p = \frac{\beta V_m}{X_L} \left(p_1 + q_2 \frac{\sin^2 \theta_0}{\beta^2} \right) \approx \frac{\beta V_m}{X_L} [p_1 + q_2 \theta_{ob}^2] \quad (A1.19a)$$

where

$$\theta_{ob} = \frac{\theta_0}{\beta} \quad (A1.19b)$$

$$q_2 = \frac{4\beta k}{\pi h^2} \frac{1 + 2e^{-\beta\pi} \cos k\pi + e^{-2\beta\pi}}{k - 2\beta e^{-\beta\pi} \sin k\pi - k e^{-2\beta\pi}} (\beta^2 + k^2) \quad (A1.19c)$$

$$q_1 = \frac{\sin \gamma}{h} (1 - 2q_2) = \frac{\beta^2 + k^2 - 1}{h^2} (1 - 2q_2) \quad (A1.19d)$$

$$p_1 = \frac{\cos \gamma}{\beta h} (1 - 2q_2) = \frac{2}{h^2} (1 - 2q_2) \quad (A1.19e)$$

The approximation in equations (A1.19) and (A1.19a) is that θ_0 is small, as it must be for low losses, as discussed in chapter 3.

The magnitude of the harmonic component of the current of frequency $n\theta$, $|I_n|$, is given by, using (A1.19c) in equation (A.16),

$$|I_n| = \left| \frac{V_m}{X_L} \frac{hq_2}{\beta h_n} \cos(\theta_0 + \gamma) \right| \quad (\text{A1.20})$$

The coefficient of the harmonic of frequency $n\theta$, I_n , is therefore defined as $+|I_n|$ or $-|I_n|$ so that I_n is a smooth function, i.e. it is not reflected at $I_n = 0$. The sign of $|I_n|$ is chosen by comparing the situation with a large value for the capacitor to that with a battery: with a large capacitor the resonance ratio k is small and so $\sin\gamma$ is negative. From the work in chapter 3 an increase in the firing angle, for a large capacitor, gives an increase in the voltage across the capacitor and so the magnitude of any particular harmonic increases. Thus it is desirable that, for low k , the coefficient of the $\sin\theta_0$ term should be positive. I_n is therefore defined as

$$I_n = \frac{V_m}{X_L} \frac{hq_2}{\beta h_n} \cos(\theta_0 + \gamma) \quad (\text{A1.21})$$

To show the dependence of the normalised coefficient of the harmonic, t_n , on the firing angle I_n can be expressed as

$$I_n = \frac{V_m}{X_L} t_n = \frac{V_m}{X_L} \left(c_n \cos\theta_0 - s_n \frac{\sin\theta_0}{\beta} \right) \approx \frac{V_m}{X_L} [c_n - s_n \theta_{ob}] \quad (\text{A1.22})$$

where

$$c_n = \frac{h \cos\gamma}{\beta h_n} q_2 = \frac{2q_2}{h_n} \quad (\text{A1.22a})$$

$$s_n = \frac{h \sin\gamma}{h_n} q_2 = \frac{q_2}{h_n} (\beta^2 + k^2 - 1) \quad (\text{A1.22b})$$

Thus the coefficient of the harmonics can be seen to depend almost linearly on θ_{ob} for small θ_0 .

Appendix 2

Derivation of an Equivalent Circuit for the Single Phase Voltage Sourced STATCON

In section 4.9 it was argued that an equivalent circuit could be produced for the single phase STATCON which consisted of a square wave voltage source in series with an R L C circuit and the system voltage.

The Fourier series of the square wave source, V_{SQ} , is given by

$$V_{SQ} = \sum_{n=1}^{\infty} \frac{4V_{sq}}{n\pi} \sin n\phi \quad \text{for } n \text{ odd} \quad (\text{A2.1})$$

where

V_{sq} is the positive voltage of the square wave.

The system voltage is defined as

$$V_S = V_m \sin(\phi + \theta_0) \quad (\text{A2.2})$$

The impedance of the circuit to a frequency of $n\theta$ is

$$Z(n) = R + jnX_L - j \frac{X_C}{n} = \frac{h_n^2 X_L}{n[2\beta n + j(\beta^2 + k^2 - n^2)]} \quad (\text{A2.3})$$

where

$$h_n = \sqrt{(\beta^2 + k^2 - n^2)^2 + 4\beta^2 n^2} \quad (\text{A2.3a})$$

The current, I , is therefore

$$I = \frac{V_m}{hX_L} \sin(\phi + \theta_0 + \gamma) - \frac{4V_{sq}}{\pi X_L} \sum_{n=1}^{\infty} \frac{\sin(n\phi + \gamma_n)}{h_n} \quad (\text{A2.4})$$

where

$$\sin \gamma_n = \frac{\beta^2 + k^2 - n^2}{h_n} \quad (\text{A2.4a})$$

$$\text{and } \cos \gamma_n = \frac{2\beta n}{h_n} \quad (\text{A2.4b})$$

$$\text{hence } \tan \gamma_n = \frac{\beta^2 + k^2 - n^2}{2\beta n} \quad (\gamma_n \text{ is in the range } -\pi/2 < \gamma_n < \pi/2) \quad (\text{A2.4c})$$

The voltage across the capacitor in the equivalent circuit, V_{ec} , is given by

$$V_{ec} = j \frac{X_C}{n} I \quad (\text{A2.5})$$

Substituting for the current from (A2.4) and simplifying gives

$$\frac{V_{ec}}{X_C} = \frac{V_m}{hX_L} \cos(\phi + \theta_0 + \gamma) - \frac{4V_{sq}}{\pi X_L} \sum_{n=1}^{\infty} \frac{\cos(n\phi + \gamma_n)}{nh_n} \quad (A2.6)$$

From the derivation, section 4.9, $V_{ec} = 0$ at $\phi = 0$. Hence

$$V_{sq} = \frac{\pi V_m}{8\beta h J} \cos(\theta_0 + \gamma) \quad (A2.7)$$

where

$$J = \sum_{n=1}^{\infty} \frac{1}{h_n^2} \quad \text{for } n \text{ odd} \quad (A2.8)$$

V_{sq} could thus be evaluated numerically for any choice of β and k and the parameters q_1, q_2 etc. could then be evaluated. Alternatively it is possible to expand this equation and prove that this method gives the same result as that used in appendix 1:

$$J = \sum_{n=1}^{\infty} \frac{1}{(\beta^2 + k^2 - n^2)^2 + 4\beta^2 n^2} \quad \text{for odd } n \quad (A2.9)$$

Using partial fractions (A2.9) becomes

$$J = \frac{j}{4\beta k} \left(\sum_{n=1}^{\infty} \frac{1}{n^2 + (\beta + jk)^2} - \frac{1}{n^2 + (\beta - jk)^2} \right) \quad \text{for odd } n \quad (A2.10)$$

The sums of these series are known (Jolley, 1961, p22):

$$\sum_{n=1}^{\infty} \frac{1}{n^2 + x^2} = \frac{\pi}{2x} \left(\frac{e^{\pi x} + e^{-\pi x}}{e^{\pi x} - e^{-\pi x}} \right) - \frac{1}{2x^2} \quad \text{for all } n \quad (A2.11)$$

and

$$\sum_{n=1}^{\infty} \frac{(-1)^n}{n^2 + x^2} = \frac{2\pi}{2x} \left(\frac{1}{e^{\pi x} - e^{-\pi x}} \right) - \frac{1}{2x^2} \quad \text{for all } n \quad (A2.11a)$$

Subtracting (A2.11a) from (A2.11) gives

$$\sum_{n=1}^{\infty} \frac{1}{n^2 + x^2} = \frac{\pi}{4x} \left(\frac{e^{\pi x} + e^{-\pi x} - 2}{e^{\pi x} - e^{-\pi x}} \right) \quad \text{for odd } n \quad (A2.12)$$

Employing (A2.12) twice in (A2.10), expanding, then simplifying, gives

$$J = \frac{\pi}{8\beta k(\beta^2 + k^2)} \left(\frac{k - 2\beta e^{-\beta\pi} \operatorname{sinc} k\pi - k e^{-2\beta\pi}}{1 + 2e^{-\beta\pi} \operatorname{cosec} k\pi + e^{-2\beta\pi}} \right) \quad (A2.13)$$

Substituting equation (A2.13) in equation (A2.7) gives V_{sq} and substituting in (A2.4) gives the expression for the Fourier series of the current. Comparing that equation with the expression for the Fourier series derived in appendix 1, (A1.15), the expressions can be seen to be identical.

Appendix 3

Analysis of a Three Phase Voltage Sourced STATCON

a) Determination of the Current

Figure A3-1 shows the circuit.

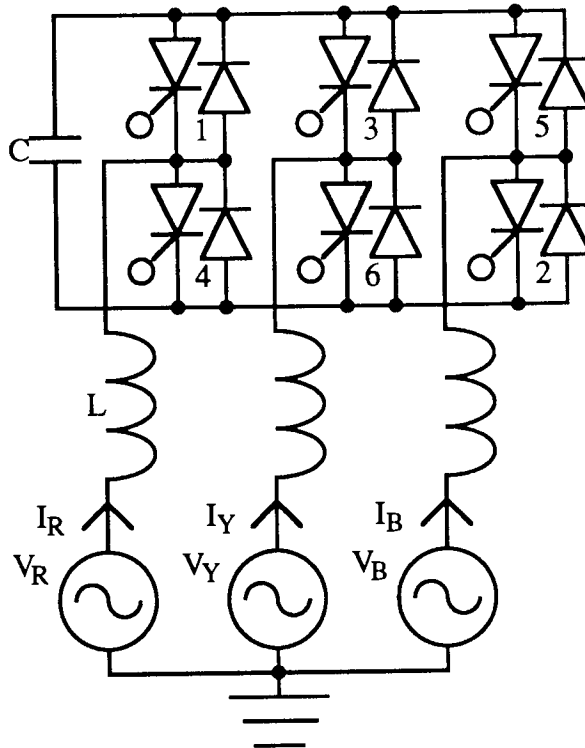


Figure A3-1. The Three Phase STATCON with Capacitor Energy Reservoir.

The supply voltage is assumed to be balanced:

$$V_R = V_m \sin(\phi + \theta_0) \quad V_Y = V_m \sin(\phi + \theta_0 - 2\pi/3) \quad V_B = V_m \sin(\phi + \theta_0 + 2\pi/3) \quad (\text{A3-1})$$

where

V_R , V_Y and V_B are the phase to neutral voltages in the red, yellow and blue phases respectively.

Expanding the sum of the three voltages in (A3-1) gives zero, hence

$$V_B = -(V_R + V_Y) \quad (\text{A3-2})$$

From figure A3-1 the sum of all three currents can be seen to be zero:

$$I_B = -(I_R + I_Y) \quad (\text{A3-3})$$

where

I_R , I_Y , and I_B are the currents in the red, yellow and blue phases.

There is a constant phase relationship between the currents in the three phases:

$$I_R(\phi) = I_Y(\phi+2\pi/3) = I_B(\phi-2\pi/3) \quad (\text{A3-4})$$

In addition, by a similar argument to that used in the single phase circuit, the current is half wave anti-symmetric:

$$I_R(\phi+\pi) = -I_R(\phi) \quad (\text{A3-5})$$

From equations (A3-4) and (A3-5) the current in the red phase for a whole cycle can be determined from the currents in the three phases during the first era. Table A3-1 expresses the current in the red phase using the currents in all three phases during the interval $0 \leq \phi \leq \pi/3$.

Table A3-1. Current Relationships in the Three Phase Equipment.

ϕ	I_R
$0 \leq \phi \leq \pi/3$	$I_R(\phi)$
$\pi/3 \leq \phi \leq 2\pi/3$	$-I_Y(\phi-\pi/3)$
$2\pi/3 \leq \phi \leq \pi$	$I_B(\phi-2\pi/3)$
$\pi \leq \phi$	$-I_R(\phi-\pi)$

During the interval $0 < \phi < \pi/3$ thyristors 1, 5 and 6 are turned on, from table 5-1. The circuit during this interval is shown in figure A3-2, where, from following the current path with these devices turned on in figure A3-1, R is the resistance in the inductance plus that of one of the devices. This differs slightly from the definition used in the single phase equipment.

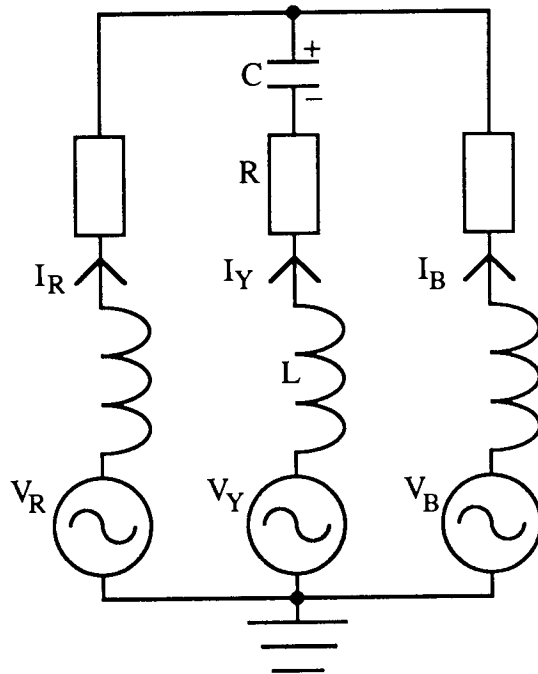


Figure A3.2. Three Phase Circuit with Devices 1, 5 and 6 Turned On.

From figure A3-2 the following equations can be deduced

$$V_R - V_+ = X_L \frac{dI_R}{d\phi} + R I_R \quad (\text{A3-6})$$

$$V_Y - V_+ = X_L \frac{dI_Y}{d\phi} + R I_Y - V_C \quad (\text{A3-6a})$$

$$V_B - V_+ = X_L \frac{dI_B}{d\phi} + R I_B \quad (\text{A3-6b})$$

where

V_+ is the voltage at the positive terminal of the capacitor.

During this interval, from figure A3-2,

$$V_C = -X_C \int I_Y d\phi \quad (\text{A3-7})$$

Summing all three parts of equation (A3-6) and using (A3-2) and (A3-3) gives, during this interval,

$$V_+ = \frac{V_C}{3} \quad (\text{A3-8})$$

Substituting from (A3-1), (A3-7) and (A3-8), in (A3-6) and (A3-6a), and differentiating the latter again, gives

$$\frac{d^2 I_Y}{d\phi^2} + 2\beta \frac{dI_Y}{d\phi} + \frac{2X_C}{3X_L} I_Y = \frac{V_m}{X_L} \cos(\phi + \theta_0 - 2\pi/3) \quad (\text{A3-9})$$

$$\frac{dI_R}{d\phi} + 2\beta I_R = \frac{V_m}{X_L} \sin(\phi + \theta_0) - \frac{V_C}{3X_L} \quad (\text{A3-9a})$$

The solution to equation (A3-9), assuming $R < \sqrt{8 X_C X_L / 3}$, is

$$I_Y = \frac{V_m}{hX_L} \sin(\phi + \theta_0 + \gamma - 2\pi/3) + A_1 e^{-\beta\phi} \sin k\phi + A_2 e^{-\beta\phi} \cos k\phi \quad (\text{A3-10})$$

where

$$k = \sqrt{\frac{2X_C}{3X_L} - \beta^2} \quad (\text{A3-10a})$$

Substituting for I_Y in equation (A3-7) and integrating gives

$$\frac{V_c}{X_C} = \frac{V_m}{hX_L} \cos(\phi + \theta_0 + \gamma - 2\pi/3) + \frac{e^{-\beta\phi}}{(\beta^2 + k^2)} [(\beta A_1 - k A_2) \sin k\phi + (k A_1 + \beta A_2) \cos k\phi] \quad (\text{A3-11})$$

Substituting for V_c in equation (A3-9a), integrating and simplifying gives

$$I_R = \frac{V_m}{hX_L} \sin(\phi + \theta_0 + \gamma) - \frac{\sqrt{3} V_m (\beta^2 + k^2)}{2hX_L (1 + 4\beta^2)} [\cos(\phi + \theta_0 + \gamma - 2\pi/3) - 2\beta \sin(\phi + \theta_0 + \gamma - 2\pi/3)] - \frac{A_1}{2} e^{-\beta\phi} \sin k\phi - \frac{A_2}{2} e^{-\beta\phi} \cos k\phi + A_3 e^{-2\beta\phi} \quad (\text{A3-12})$$

From table A3-1 and knowledge of the devices which are turned on and off during any interval, as given in table 5-1, the current through the capacitor can be shown to be the same during each interval, and so the voltage across the capacitor must be the same during each interval. The boundary condition on the capacitor voltage can therefore be written as

$$V_c(\phi = \pi/3) = V_c(\phi = 0) \quad (\text{A3-13})$$

The boundary conditions on the currents can be deduced from table A3-1:

$$I_R(\phi = \pi/3) = -I_Y(\phi = 0) \quad (\text{A3-13a})$$

$$I_Y(\phi = \pi/3) = -I_B(\phi = 0) \quad (\text{A3-13b})$$

The expressions for the steady state currents in the red and yellow phases involve a term which is the steady state current in a conventional, i.e. one with no switches, R L C circuit. This is the term in $(\phi + \theta_0 + \gamma)$ in the red phase and the term in $(\phi + \theta_0 + \gamma - 2\pi/3)$ in the yellow phase. A similar term to that in the red phase was produced in expression for the current in the single phase circuit, equation (A1-3). The expression for the current in the yellow phase expresses the current in the red phase during a different part of the cycle therefore these terms must be equal at the changes in circuit topology. They will therefore not appear in the solutions of the current boundary equations, as the term in the single phase equipment did not appear in the current boundary condition, (A1-7).

Evaluating (A3-13) from (A3-11) gives, after simplifying,

$$\frac{V_m}{hX_L} (\beta^2+k^2)\cos(\theta_0+\gamma) = (kA_1 + \beta A_2)[1 - e^{-\beta\pi/3}\cos k\pi/3] - (\beta A_1 - kA_2)e^{-\beta\pi/3}\sin k\pi/3 \quad (\text{A3-14})$$

Evaluating (A3-13a) from (A3-10) and (A3-12) gives

$$-\frac{\sqrt{3}V_m}{2hX_L} \frac{(\beta^2+k^2)}{(1+4\beta^2)} [\cos(\theta_0+\gamma-\pi/3) - 2\beta\sin(\theta_0+\gamma-\pi/3)] - \frac{A_1}{2} e^{-\beta\pi/3}\sin k\pi/3 - \frac{A_2}{2} e^{-\beta\pi/3}\cos k\pi/3 + A_3 e^{-2\beta\pi/3} = -A_2 \quad (\text{A3-14a})$$

Evaluating (A3-13b) from (A3-10) and (A3-12), using (A3-3), gives

$$-\frac{\sqrt{3}V_m}{2hX_L} \frac{(\beta^2+k^2)}{(1+4\beta^2)} [\cos(\theta_0+\gamma-2\pi/3) - 2\beta\sin(\theta_0+\gamma-2\pi/3)] + \frac{A_2}{2} + A_3 = A_1 e^{-\beta\pi/3}\sin k\pi/3 + A_2 e^{-\beta\pi/3}\cos k\pi/3 \quad (\text{A3-14b})$$

Manipulating and simplifying gives

$$A_1 = -\frac{V_m}{dhX_L} \frac{(\beta^2+k^2)}{(1+4\beta^2)} \{2[\beta(1-e^{-\beta\pi/3}\cos k\pi/3) + ke^{-\beta\pi/3}\sin k\pi/3]f + (1+4\beta^2)\cos(\theta_0+\gamma)[(2e^{2\beta\pi/3}-1) - (e^{\beta\pi/3} - 2e^{-\beta\pi/3})\cos k\pi/3]\} \quad (\text{A3-15})$$

$$A_2 = \frac{V_m}{dhX_L} \frac{(\beta^2+k^2)}{(1+4\beta^2)} \{2[k(1-e^{-\beta\pi/3}\cos k\pi/3) - \beta e^{-\beta\pi/3}\sin k\pi/3]f + (1+4\beta^2)\cos(\theta_0+\gamma)[(2e^{-\beta\pi/3} - e^{\beta\pi/3})\sin k\pi/3]\} \quad (\text{A3-15a})$$

$$A_3 = \frac{\sqrt{3}V_m}{2hX_L} \frac{(\beta^2+k^2)}{(1+4\beta^2)} [\cos(\theta_0+\gamma-2\pi/3) - 2\beta\sin(\theta_0+\gamma-2\pi/3)] - \frac{V_m}{2dhX_L} \frac{(\beta^2+k^2)}{(1+4\beta^2)} \{2[\beta e^{-\beta\pi/3}\sin k\pi/3 + k(1 - 3e^{-\beta\pi/3}\cos k\pi/3 - 2e^{-2\beta\pi/3})]f + (1+4\beta^2)\cos(\theta_0+\gamma)[3e^{\beta\pi/3}\sin k\pi/3]\} \quad (\text{A3-15b})$$

where

$$d = \beta(e^{\beta\pi/3}+e^{-\beta\pi/3})\sin k\pi/3 - 2k(e^{2\beta\pi/3}-e^{-2\beta\pi/3}) + 3k(e^{\beta\pi/3}-e^{-\beta\pi/3})\cos k\pi/3 \quad (\text{A3-15c})$$

and

$$f = \frac{\sqrt{3}}{2} \{[\cos(\theta_0+\gamma-2\pi/3) - 2\beta\sin(\theta_0+\gamma-2\pi/3)] - e^{-2\beta\pi/3}[\cos(\theta_0+\gamma-\pi/3) - 2\beta\sin(\theta_0+\gamma-\pi/3)]\} \quad (\text{A3-15d})$$

b) Fourier Series

Because the voltage across the capacitor depends only upon A_1 and A_2 , it is simpler to take the Fourier series of the voltage at the a.c. terminals of the inverter and then calculate the Fourier series of the current:

$$V_I = \sum_{n=1}^{\infty} d_n \cos n\phi + e_n \sin n\phi \quad (\text{A3-16})$$

Because the current and the system voltage are half wave anti-symmetric the voltage at the a.c. terminals of the inverter must also be half wave anti-symmetric. d_n and e_n are therefore zero when n is even.

$$d_n = \frac{2}{\pi} \int_0^{\pi} V_{ac}(\phi) \cos n\phi \, d\phi \quad \text{and} \quad e_n = \frac{2}{\pi} \int_0^{\pi} V_{ac}(\phi) \sin n\phi \, d\phi$$

The voltage at the a.c. terminals of the red phase of the inverter is one-third of the voltage across the capacitor during the first interval, i.e. for $0 < \phi < \pi/3$, two-thirds during the second and one-third during the third:

$$\frac{3\pi d_n}{2} = \int_0^{\pi/3} V_c(\phi) \cos n\phi \, d\phi + 2 \int_{\pi/3}^{2\pi/3} V_c(\phi - \pi/3) \cos n\phi \, d\phi + \int_{2\pi/3}^{\pi} V_c(\phi - 2\pi/3) \cos n\phi \, d\phi \quad (\text{A3-17})$$

with a similar expression for e_n , but with $\cos n\phi$ replaced by $\sin n\phi$.

Considering the term in d_n only, making suitable changes of variables, renaming and simplifying gives

$$\frac{3\pi d_n}{2} = 2[1 + \cos n\pi/3] \int_0^{\pi/3} V_c(\phi) \cos n(\phi + \pi/3) \, d\phi \quad (\text{A3-18})$$

From (A3-18) it is apparent that d_n is zero if n is an odd triple- n , i.e. 3, 9, 15..., harmonic. Performing similar algebra for e_n obtains the same result, hence, for $n = 6i \pm 1$, where $i = 0, 1, 2, \dots$

$$\frac{\pi d_n}{2} = \int_0^{\pi/3} V_c(\phi) \cos n(\phi + \pi/3) \, d\phi \quad (\text{A3-19})$$

$$\frac{\pi e_n}{2} = \int_0^{\pi/3} V_c(\phi) \sin n(\phi + \pi/3) \, d\phi \quad (\text{A3-19a})$$

Substituting for $V_c(\phi)$ from (A3-11), reducing by using (A3-10a), integrating, and simplifying, gives

$$\begin{aligned}
 d_1 = & \frac{3V_m}{2\pi h} (\beta^2+k^2) ((\sqrt{3}/2) - (\pi/3))\cos(\theta_0+\gamma) \\
 + & \frac{3(\beta A_1 - kA_2)X_L}{2\pi h} [k[\sin\gamma - \sqrt{3}\cos\gamma] + \\
 & e^{-\beta\pi/3} \{ [k\sin\gamma\cos\pi/3 + (\beta\sin\gamma + \cos\gamma)\sin\pi/3] + \\
 & \sqrt{3}[k\cos\gamma\cos\pi/3 - (\sin\gamma - \beta\cos\gamma)\sin\pi/3] \}] \\
 + & \frac{3(kA_1 + \beta A_2)X_L}{2\pi h} [[(\beta\sin\gamma + \cos\gamma) + \sqrt{3}(\sin\gamma - \beta\cos\gamma)] - \\
 & e^{-\beta\pi/3} \{ [k\sin\gamma\sin\pi/3 - (\beta\sin\gamma + \cos\gamma)\cos\pi/3] + \\
 & \sqrt{3}[k\cos\gamma\sin\pi/3 + (\sin\gamma - \beta\cos\gamma)\cos\pi/3] \}] \quad (A3-20)
 \end{aligned}$$

$$\begin{aligned}
 n > 1 \quad d_n = & \frac{3V_m}{2\pi h} \frac{(\beta^2+k^2)}{(n^2-1)} (2n\sin n\pi/3 - \sqrt{3})\cos(\theta_0+\gamma) \\
 + & \frac{3(\beta A_1 - kA_2)X_L}{2\pi h_n} [k[\sin\gamma_n - 2\sin n\pi/3 \cos\gamma_n] + \\
 & e^{-\beta\pi/3} \{ [k\sin\gamma_n\cos\pi/3 + (\beta\sin\gamma_n + n\cos\gamma_n)\sin\pi/3] + \\
 & 2\sin n\pi/3 [k\cos\gamma_n\cos\pi/3 - (n\sin\gamma_n - \beta\cos\gamma_n)\sin\pi/3] \}] \\
 + & \frac{3(kA_1 + \beta A_2)X_L}{2\pi h_n} [[(\beta\sin\gamma_n + n\cos\gamma_n) + 2\sin n\pi/3(n\sin\gamma_n - \beta\cos\gamma_n)] - \\
 & e^{-\beta\pi/3} \{ [k\sin\gamma_n\sin\pi/3 - (\beta\sin\gamma_n + n\cos\gamma_n)\cos\pi/3] + \\
 & 2\sin n\pi/3 [k\cos\gamma_n\sin\pi/3 + (n\sin\gamma_n - \beta\cos\gamma_n)\cos\pi/3] \}] \quad (A3-20a)
 \end{aligned}$$

$$\begin{aligned}
 e_1 = & \frac{3V_m}{2\pi h} (\beta^2+k^2) ((\sqrt{3}/2) + (\pi/3))\sin(\theta_0+\gamma) \\
 + & \frac{3(\beta A_1 - kA_2)X_L}{2\pi h} [k[\cos\gamma + \sqrt{3}\sin\gamma] + \\
 & e^{-\beta\pi/3} \{ [k\cos\gamma\cos\pi/3 + (\beta\cos\gamma - \sin\gamma)\sin\pi/3] - \\
 & \sqrt{3}[k\sin\gamma\cos\pi/3 + (\cos\gamma + \beta\sin\gamma)\sin\pi/3] \}] \\
 + & \frac{3(kA_1 + \beta A_2)X_L}{2\pi h} [[(\beta\cos\gamma - \sin\gamma) + \sqrt{3}(\cos\gamma + \beta\sin\gamma)] - \\
 & e^{-\beta\pi/3} \{ [k\cos\gamma\sin\pi/3 - (\beta\cos\gamma - \sin\gamma)\cos\pi/3] - \\
 & \sqrt{3}[k\sin\gamma\sin\pi/3 - (\cos\gamma + \beta\sin\gamma)\cos\pi/3] \}] \quad (A3-20b)
 \end{aligned}$$

$$\begin{aligned}
 n > 1 \quad e_n = & \frac{3V_m}{2\pi h} \frac{(\beta^2+k^2)}{(n^2-1)} (\sqrt{3}n - 2\sin n\pi/3)\sin(\theta_0+\gamma) \\
 + & \frac{3(\beta A_1 - kA_2)X_L}{2\pi h_n} [k[\cos\gamma_n + 2\sin n\pi/3 \sin\gamma_n] + \\
 & e^{-\beta\pi/3} \{ [k\cos\gamma_n\cos\pi/3 + (\beta\cos\gamma_n - n\sin\gamma_n)\sin\pi/3] - \\
 & 2\sin n\pi/3 [k\sin\gamma_n\cos\pi/3 + (n\cos\gamma_n + \beta\sin\gamma_n)\sin\pi/3] \}] \\
 + & \frac{3(kA_1 + \beta A_2)X_L}{2\pi h_n} [[(\beta\cos\gamma_n - n\sin\gamma_n) + 2\sin n\pi/3(n\cos\gamma_n + \beta\sin\gamma_n)] - \\
 & e^{-\beta\pi/3} \{ [k\cos\gamma_n\sin\pi/3 - (\beta\cos\gamma_n - n\sin\gamma_n)\cos\pi/3] - \\
 & 2\sin n\pi/3 [k\sin\gamma_n\sin\pi/3 - (n\cos\gamma_n + \beta\sin\gamma_n)\cos\pi/3] \}] \quad (A3-20c)
 \end{aligned}$$

The circuit model is shown in figure A3.3.

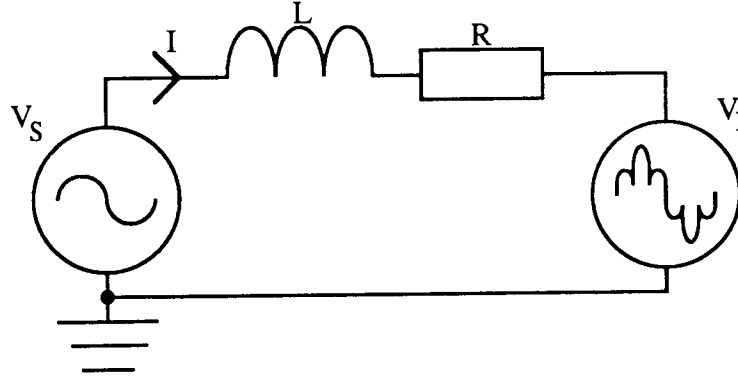


Figure A3.3. Per Phase Circuit Model for the Three Phase STATCON.

The Fourier series for the current in the red phase can be expressed as

$$I_R = \frac{V_m \sin(\phi + \theta_0) - \sum_{n=1}^{\infty} d_n \cos n\phi + e_n \sin n\phi}{R + j n X_L} \quad (\text{A3-21})$$

$$I_R = -\frac{V_m}{X_L(1+4\beta^2)} [\cos(\phi + \theta_0) - 2\beta \sin(\phi + \theta_0)] + \sum_{n=1}^{\infty} \frac{1}{X_L(n^2+4\beta^2)} [(ne_n - 2\beta d_n) \cos n\phi - (nd_n + 2\beta e_n) \sin n\phi] \quad (\text{A3-22})$$

Inspection of all parts of (A3-20) and the expressions for A_1 and A_2 , (A3-15) and (A3-15a), shows that the voltage at the a.c. terminals of the inverter, and therefore the current, always varies as either $\sin\theta_0$ or $\cos\theta_0$. d_n and e_n can therefore be split up into coefficients of $\cos\theta_0$ and of $\sin\theta_0$:

$$d_n = d_{nc} \cos\theta_0 + d_{ns} \sin\theta_0 \quad (\text{A3-23})$$

$$e_n = e_{nc} \cos\theta_0 + e_{ns} \sin\theta_0 \quad (\text{A3-23a})$$

Substituting for d_n and e_n in (A3-22), expanding, simplifying and expressing in terms of θ gives

$$I_q = \frac{1}{X_L(1+4\beta^2)} \{ [e_{1c} - 2\beta d_{1c} - V_m] + [d_{1s} + 2\beta e_{1s} - (e_{1c} - 2\beta d_{1c})] \sin^2\theta_0 + [d_{1c} + 2\beta e_{1c} + e_{1s} - 2\beta d_{1s}] \frac{\sin 2\theta_0}{2} \} \quad (\text{A3-24})$$

$$I_p = \frac{1}{X_L(1+4\beta^2)} \{ [2\beta V_m - (d_{1c} + 2\beta e_{1c})] + [d_{1c} + 2\beta e_{1c} + e_{1s} - 2\beta d_{1s}] \sin^2\theta_0 - [d_{1s} + 2\beta e_{1s} - (e_{1c} - 2\beta d_{1c})] \frac{\sin 2\theta_0}{2} \} \quad (\text{A3-24a})$$

By analogy with the single phase case the following definitions are used:

$$I_q = \frac{V_m}{X_L} \left(q_1 + q_2 \frac{\sin 2\theta_0}{2\beta} + q_3 \sin^2 \theta_0 \right) \quad (\text{A3.25})$$

$$I_p = \frac{\beta V_m}{X_L} \left(p_1 + q_2 \frac{\sin^2 \theta_0}{\beta^2} - q_3 \frac{\sin 2\theta_0}{2\beta} \right) \quad (\text{A3.25a})$$

Comparing both parts of (A3.24) with both parts of (A3.25) gives

$$q_1 = -\frac{1}{(1+4\beta^2)} + \frac{e_{1c} - 2\beta d_{1c}}{V_m(1+4\beta^2)} = -\frac{1}{(1+4\beta^2)} + \frac{e_1 - 2\beta d_1}{V_m(1+4\beta^2)} \Big|_{\theta_0=0} \quad (\text{A3.26})$$

$$p_1 = \frac{2}{(1+4\beta^2)} - \frac{d_{1c} + 2\beta e_{1c}}{\beta V_m(1+4\beta^2)} = \frac{2}{(1+4\beta^2)} - \frac{d_1 + 2\beta e_1}{\beta V_m(1+4\beta^2)} \Big|_{\theta_0=0} \quad (\text{A3.26a})$$

$$q_2 = \frac{\beta[d_{1c} + 2\beta e_{1c} + e_{1s} - 2\beta d_{1s}]}{V_m(1+4\beta^2)} = \frac{\beta(d_1 + 2\beta e_1)}{V_m(1+4\beta^2)} \Big|_{\theta_0=0} + \frac{\beta(e_1 - 2\beta d_1)}{V_m(1+4\beta^2)} \Big|_{\theta_0=\pi/2} \quad (\text{A3.26b})$$

$$q_3 = \frac{[d_{1s} + 2\beta e_{1s} - (e_{1c} - 2\beta d_{1c})]}{V_m(1+4\beta^2)} = \frac{d_1 + 2\beta e_1}{V_m(1+4\beta^2)} \Big|_{\theta_0=\pi/2} - \frac{e_1 - 2\beta d_1}{V_m(1+4\beta^2)} \Big|_{\theta_0=0} \quad (\text{A3.26c})$$

From section 2.3c and figure 2.6 it is apparent that, when using a battery as the energy reservoir, as θ_0 is varied from zero there is an increase in the active power that flows in the circuit, either provided by the system or by the battery. The same must also be true when using a capacitor as the energy reservoir; any departure in the firing angle from zero must cause an increase in the active power provided by the supply. It follows therefore that q_3 must be zero otherwise the minimum value for the losses would not occur at $\theta_0 = 0$. This was verified numerically using (A3.26c).

The form of the fundamental component of the current is therefore the same as that in the single phase equipment:

$$I_q = \frac{V_m}{X_L} \left(q_1 + q_2 \frac{\sin 2\theta_0}{2\beta} \right) \quad (\text{A3.27})$$

$$I_p = \frac{\beta V_m}{X_L} \left(p_1 + q_2 \frac{\sin^2 \theta_0}{\beta^2} \right) \quad (\text{A3.27a})$$

Considering the magnitude of the harmonics of (A3-22), after substituting from equations (A3-23) and (A3-23a), gives

$$|I_n| = \frac{1}{X_L} \sqrt{\frac{(d_{nc} \cos\theta_0 + d_{ns} \sin\theta_0)^2 + (e_{nc} \cos\theta_0 + e_{ns} \sin\theta_0)^2}{(n^2+4\beta^2)}} \quad (\text{A3-28})$$

as in the single phase case this can be expressed in terms of the normalised magnitude of the harmonic, $|t_n|$:

$$|I_n| = \frac{V_m}{X_L} |t_n| = \frac{V_m}{X_L} \sqrt{\frac{[d_{nc}^2 + e_{nc}^2] \cos^2\theta_0 + [d_{ns}^2 + e_{ns}^2] \sin^2\theta_0 + [d_{nc} d_{ns} + e_{nc} e_{ns}] \sin 2\theta_0}{V_m^2 (n^2+4\beta^2)}} \quad (\text{A3-29})$$

Figure A3.4 shows $|t_n|$ as a function of θ_{ob} for different values of the resonance ratio, for $n = 5$ and 7. In both cases $|t_n|$ appears to depend linearly on θ_{ob} .

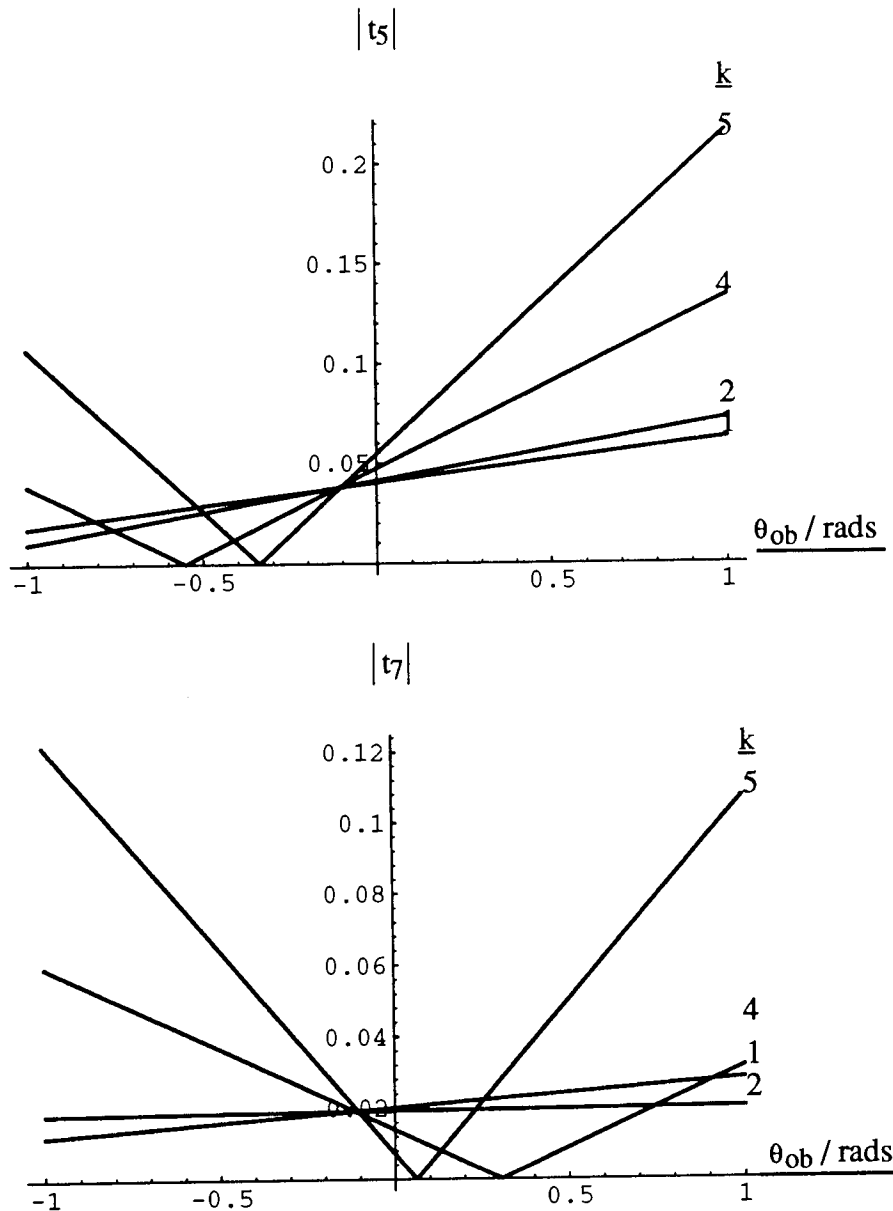


Figure A3.4. Graphs of the Magnitude of the Normalised Harmonic Component of the Current as a Function of the Reduced Firing Angle.

By analogy with the single phase equipment this can be expressed as

$$I_{nc} \approx \frac{V_m}{X_L} [c_n - s_n \theta_{ob}] \quad (A3.30)$$

Using the small θ_0 approximation in equation (A3.29) gives

$$|I_n| \approx \frac{V_m}{X_L} \sqrt{\frac{[d_{nc}^2 + e_{nc}^2] + \beta^2 [d_{ns}^2 + e_{ns}^2] \theta_{ob}^2 + 2\beta [d_{nc} d_{ns} + e_{nc} e_{ns}] \theta_{ob}}{(n^2 + 4\beta^2)}} \quad (A3.31)$$

Equating (A3-30) and the coefficient of the harmonics from (A3-31), assuming the curves in figure A3-4 are straight lines, gives

$$c_n = \frac{1}{V_m} \sqrt{\frac{d_n^2 + e_n^2}{(n^2 + 4\beta^2)}} \Big|_{\theta_0 = 0} \quad (\text{A3-32})$$

$$s_n = -\frac{\beta}{V_m} \sqrt{\frac{d_n^2 + e_n^2}{(n^2 + 4\beta^2)}} \Big|_{\theta_0 = \pi/2} \quad (\text{A3-32a})$$

where the signs have been chosen so that c_n is positive and s_n is negative for very low values of k . They are reversed as necessary so that c_n and s_n vary smoothly. Graphs are given in section 5-9, where it is also shown that c_n and s_n have very little dependence on β . The values of the magnitudes from the approximate graphs, figure 5-8, and those from the actual graph, figures A3-4, appear to be very similar.

Appendix 4

Derivation of an Equivalent Circuit for the Three Phase Voltage Sourced STATCON

The equivalent circuit is shown in figure A4.1.

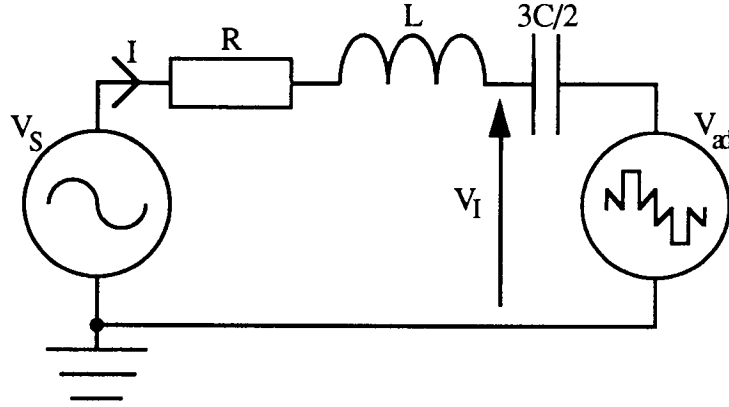


Figure A4.1. Per Phase Equivalent Circuit.

During the first interval the voltage at the a.c. terminals of the inverter is one-third of the voltage across the capacitor, two-thirds during the next interval and one-third again during the next era. It is half wave anti-symmetric. From equation (A3.11), after reducing using (A3.10a), the voltage at the a.c. terminals of the inverter, in the red phase, is given by

$$V_I = \frac{V_m(\beta^2+k^2)}{2h} \cos(\phi+\theta_0+\gamma-2\pi/3) \quad \text{for } 0 < \phi < \pi/3$$

$$+ \frac{X_L e^{-\beta\phi}}{2} \{(\beta A_1 - k A_2) \text{sinc} \phi + (k A_1 + \beta A_2) \text{cos} \phi\} \quad (\text{A4.1})$$

$$V_I = \frac{V_m(\beta^2+k^2)}{h} \cos(\phi+\theta_0+\gamma-\pi) \quad \text{for } \pi/3 < \phi < 2\pi/3$$

$$+ X_L e^{-\beta(\phi-\pi/3)} \{(\beta A_1 - k A_2) \text{sinc}(\phi-\pi/3) + (k A_1 + \beta A_2) \text{cos}(\phi-\pi/3)\} \quad (\text{A4.1a})$$

$$V_I = \frac{V_m(\beta^2+k^2)}{2h} \cos(\phi+\theta_0+\gamma-4\pi/3) \quad \text{for } 2\pi/3 < \phi < \pi$$

$$+ \frac{X_L e^{-\beta(\phi-2\pi/3)}}{2} \{(\beta A_1 - k A_2) \text{sinc}(\phi-2\pi/3) + (k A_1 + \beta A_2) \text{cos}(\phi-2\pi/3)\} \quad (\text{A4.1b})$$

The current in the red phase, from table A3-1 and equations (A3-10), (A3-12) and equation (A3-3), is given by

$$I_R = \frac{V_m}{hX_L} \sin(\phi + \theta_0 + \gamma) - \frac{\sqrt{3}V_m(k^2 + \beta^2)}{2hX_L(1 + 4\beta^2)} [\cos(\phi + \theta_0 + \gamma - 2\pi/3) - 2\beta \sin(\phi + \theta_0 + \gamma - 2\pi/3)] - \frac{A_1}{2} e^{-\beta\phi} \sin k\phi - \frac{A_2}{2} e^{-\beta\phi} \cos k\phi + A_3 e^{-2\beta\phi}$$

for $0 \leq \phi \leq \pi/3$ (A4.2)

$$I_R = \frac{V_m}{hX_L} \sin(\phi + \theta_0 + \gamma) - A_1 e^{-\beta(\phi - \pi/3)} \sin[k(\phi - \pi/3)] - A_2 e^{-\beta(\phi - \pi/3)} \cos[k(\phi - \pi/3)]$$

for $\pi/3 \leq \phi \leq 2\pi/3$ (A4.2a)

$$I_R = \frac{V_m}{hX_L} \sin(\phi + \theta_0 + \gamma) + \frac{\sqrt{3}V_m(k^2 + \beta^2)}{2hX_L(1 + 4\beta^2)} [\cos(\phi + \theta_0 + \gamma - 4\pi/3) - 2\beta \sin(\phi + \theta_0 + \gamma - 4\pi/3)] - \frac{A_1}{2} e^{-\beta(\phi - 2\pi/3)} \sin[k(\phi - 2\pi/3)] - \frac{A_2}{2} e^{-\beta(\phi - 2\pi/3)} \cos[k(\phi - 2\pi/3)] - A_3 e^{-2\beta(\phi - 2\pi/3)}$$

for $2\pi/3 \leq \phi \leq \pi$ (A4.2b)

The voltage across the capacitor in the equivalent circuit, V_{ec} , is given by, from figure A4-1,

$$V_{ec} = \frac{2X_C}{3} \int I d\phi \quad (A4.3)$$

Integrating all parts of (A4.2), and simplifying using the definition of k, gives

$$\begin{aligned}
 V_{ec} = & -\frac{V_m(\beta^2+k^2)}{h} \cos(\phi+\theta_0+\gamma) \\
 & + \frac{X_L e^{-\beta\phi}}{2} \{(\beta A_1 - k A_2) \sin k\phi + (k A_1 + \beta A_2) \cos k\phi\} \\
 & - \frac{\sqrt{3} V_m (\beta^2+k^2)^2}{2h (1+4\beta^2)} [\sin(\phi+\theta_0+\gamma-2\pi/3) + 2\beta \cos(\phi+\theta_0+\gamma-2\pi/3)] \\
 & - V_1 - \frac{X_L(\beta^2+k^2)}{2\beta} A_3 e^{-2\beta\phi} \quad \text{for } 0 \leq \phi \leq \pi/3 \quad (A4.4)
 \end{aligned}$$

$$\begin{aligned}
 V_{ec} = & -\frac{V_m(\beta^2+k^2)}{h} \cos(\phi+\theta_0+\gamma) \\
 & + X_L e^{-\beta(\phi-\pi/3)} \{(\beta A_1 - k A_2) \sin k(\phi-\pi/3) + (k A_1 + \beta A_2) \cos k(\phi-\pi/3)\} \\
 & - V_2 \quad \text{for } \pi/3 \leq \phi \leq 2\pi/3 \quad (A4.4a)
 \end{aligned}$$

$$\begin{aligned}
 V_{ec} = & -\frac{V_m(\beta^2+k^2)}{h} \cos(\phi+\theta_0+\gamma) \\
 & + \frac{X_L e^{-\beta(\phi-2\pi/3)}}{2} \{(\beta A_1 - k A_2) \sin k(\phi-2\pi/3) + (k A_1 + \beta A_2) \cos k(\phi-2\pi/3)\} \\
 & + \frac{\sqrt{3} V_m (\beta^2+k^2)^2}{2h (1+4\beta^2)} [\sin(\phi+\theta_0+\gamma-4\pi/3) + 2\beta \cos(\phi+\theta_0+\gamma-4\pi/3)] \\
 & - V_3 + \frac{X_L(\beta^2+k^2)}{2\beta} A_3 e^{-2\beta(\phi-2\pi/3)} \quad \text{for } 2\pi/3 \leq \phi \leq \pi \quad (A4.4b)
 \end{aligned}$$

where

$-V_1$, $-V_2$ and $-V_3$ are the constants of integration.

There cannot be any discontinuities in the voltage across the capacitor and it must be half wave anti-symmetric. Manipulating (A4.4), (A4.4a) and (A4.4b) gives

$$V_1 = \frac{\sqrt{3}V_m(\beta^2+k^2)^2}{2h(1+4\beta^2)} [\sin(\theta_0+\gamma+\pi/3) + 2\beta\cos(\theta_0+\gamma+\pi/3)] \quad (A4.5)$$

$$- \frac{(kA_1 + \beta A_2)X_L}{2} [1 - 2e^{-\beta\pi/3}\cos k\pi/3] + (\beta A_1 - kA_2)X_L e^{-\beta\pi/3}\sin k\pi/3$$

$$- \frac{(\beta^2+k^2)X_L}{2\beta} A_3$$

$$V_2 = \frac{\sqrt{3}V_m(\beta^2+k^2)^2}{2h(1+4\beta^2)} [\sin(\theta_0+\gamma) + 2\beta\cos(\theta_0+\gamma)] \quad (A4.5a)$$

$$+ \frac{(kA_1 + \beta A_2)X_L}{2} [1 + e^{-\beta\pi/3}\cos k\pi/3] + \frac{(\beta A_1 - kA_2)X_L}{2} e^{-\beta\pi/3}\sin k\pi/3$$

$$- \frac{(\beta^2+k^2)X_L}{2\beta} A_3 (1 - e^{-2\beta\pi/3})$$

$$V_3 = \frac{\sqrt{3}V_m(\beta^2+k^2)^2}{2h(1+4\beta^2)} [\sin(\theta_0+\gamma-\pi/3) + 2\beta\cos(\theta_0+\gamma-\pi/3)] \quad (A4.5b)$$

$$+ \frac{(kA_1 + \beta A_2)X_L}{2} [2 - e^{-\beta\pi/3}\cos k\pi/3] - \frac{(\beta A_1 - kA_2)X_L}{2} e^{-\beta\pi/3}\sin k\pi/3$$

$$+ \frac{(\beta^2+k^2)X_L}{2\beta} A_3 e^{-2\beta\pi/3}$$

From figure A4.1 V_{ad} is given by

$$V_{ad} = V_1 - V_{ec} \quad (A4.6)$$

Subtracting each part of (A4.4) from the corresponding part of (A4.1) gives

$$V_{ad} = \frac{\sqrt{3}V_m(\beta^2+k^2)}{2h} \sin(\phi+\theta_0+\gamma+\pi/3)$$

$$+ \frac{\sqrt{3}V_m(\beta^2+k^2)^2}{2h(1+4\beta^2)} [\sin(\phi+\theta_0+\gamma-2\pi/3) + 2\beta\cos(\phi+\theta_0+\gamma-2\pi/3)]$$

$$+ V_1 + \frac{A_3 X_L(\beta^2+k^2)}{2\beta} e^{-2\beta\phi}$$

for $0 < \phi < \pi/3$ (A4.7)

$$V_{ad} = V_2 \quad (A4.7a)$$

for $\pi/3 < \phi < 2\pi/3$

$$V_{ad} = -\frac{\sqrt{3}V_m(\beta^2+k^2)}{2h} \sin(\phi+\theta_0+\gamma-\pi/3)$$

$$- \frac{\sqrt{3}V_m(\beta^2+k^2)^2}{2h(1+4\beta^2)} [\sin(\phi+\theta_0+\gamma-4\pi/3) + 2\beta\cos(\phi+\theta_0+\gamma-4\pi/3)]$$

$$+ V_3 - \frac{A_3 X_L(\beta^2+k^2)}{2\beta} e^{-2\beta(\phi-2\pi/3)}$$

for $2\pi/3 < \phi < \pi$ (A4.7b)

Appendix 5

Analysis of a Twelve Pulse STATCON with Parallel Connected Transformer Primaries

a) Determination of the Current on the Transformer Secondary Side

The analysis of the circuit, from the point of view of the secondaries of the transformers, can be performed in the same way as that for the three phase circuit with the twelve pulse circuit being regarded as having a six phase unbalanced voltage source.

The circuit, as seen from the secondary side of the transformers, is shown in figure A5.1.

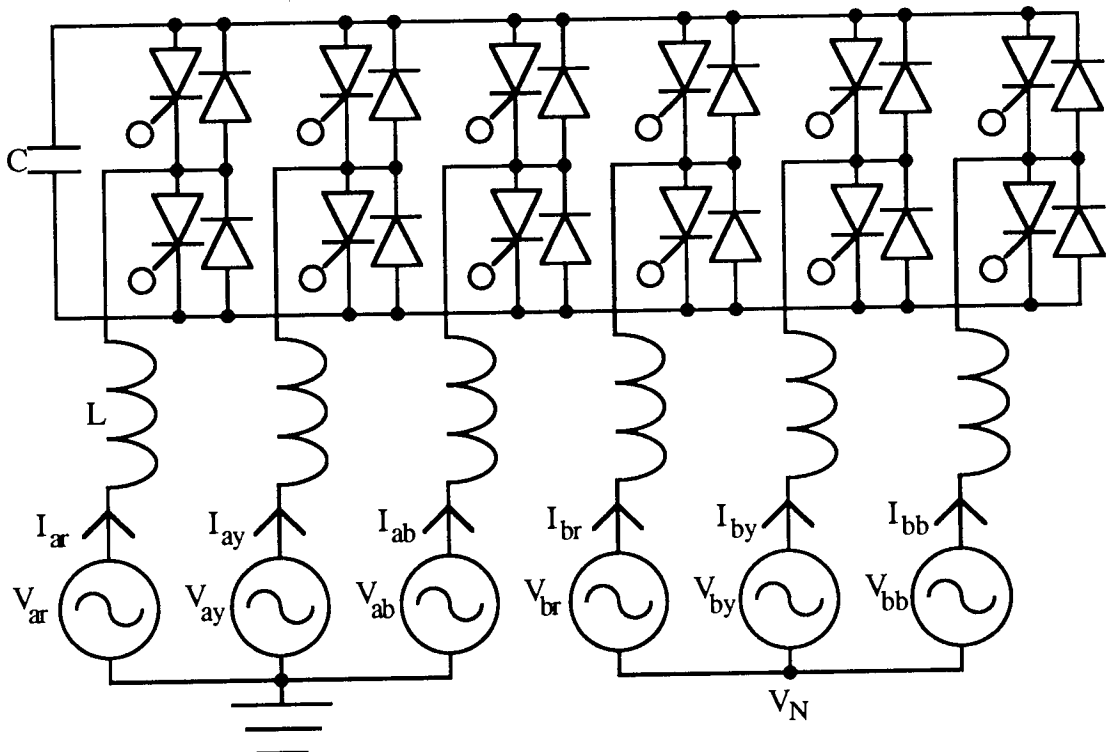


Figure A5.1. The Twelve Pulse STATCON with Capacitor Energy Reservoir.

The voltage sources, relative to their star points, with the star point of the secondary of the first transformer earthed, are defined as

$$\begin{aligned} V_{ar} &= V_m \sin(\phi + \theta_0 + \pi/12) & V_{br} &= V_{brn} - V_N = V_m \sin(\phi + \theta_0 - \pi/12) \\ V_{ay} &= V_m \sin(\phi + \theta_0 - 7\pi/12) & V_{by} &= V_{byn} - V_N = V_m \sin(\phi + \theta_0 - 3\pi/4) \\ V_{ab} &= V_m \sin(\phi + \theta_0 - 5\pi/4) & V_{bb} &= V_{bbn} - V_N = V_m \sin(\phi + \theta_0 - 17\pi/12) \end{aligned} \quad (A5.1)$$

where

V_N is the potential of the neutral (star) point of the secondary of the second transformer.

As in the three phase equipment, both the currents and the voltages out of each transformers sum to zero:

$$\begin{aligned} V_{ab} &= -(V_{ar} + V_{ay}) & V_{bb} &= -(V_{br} + V_{by}) \\ I_{ab} &= -(I_{ar} + I_{ay}) & I_{bb} &= -(I_{br} + I_{by}) \end{aligned} \quad (A5.2)$$

There is again a constant phase relationship between the currents in the six phases:

$$I_{ar}(\phi) = I_{ay}(\phi + 2\pi/3) = I_{ab}(\phi - 2\pi/3) = I_{br}(\phi + \pi/6) = I_{by}(\phi + 5\pi/6) = I_{bb}(\phi - \pi/2) \quad (A5.3)$$

From (A5.3) and the information that the current is half wave anti-symmetric the current in the red phase on the secondary side of the first transformer can be determined from the currents in all six phases during the first era:

Table A5.1. Current Relationships in the Twelve Pulse Equipment.

ϕ	$I_{ar}(\phi)$
$-\pi/12 \leq \phi \leq \pi/12$	$I_{ar}(\phi)$
$\pi/12 \leq \phi \leq \pi/4$	$-I_{by}(\phi - \pi/6)$
$\pi/4 \leq \phi \leq 5\pi/12$	$-I_{ay}(\phi - \pi/3)$
$5\pi/12 \leq \phi \leq 7\pi/12$	$I_{bb}(\phi - \pi/2)$
$7\pi/12 \leq \phi \leq 3\pi/4$	$I_{ab}(\phi - 2\pi/3)$
$3\pi/4 \leq \phi \leq 11\pi/12$	$-I_{br}(\phi - 5\pi/6)$
$11\pi/12 \leq \phi$	$-I_{ar}(\phi - \pi)$

During the interval $-\pi/12 < \phi < \pi/12$ the circuit is as shown in figure A5.2, from the data in table 6.1, where, as in the three phase work, the lumped parameter resistance, R , is the resistance in one device plus the resistance in the inductance.

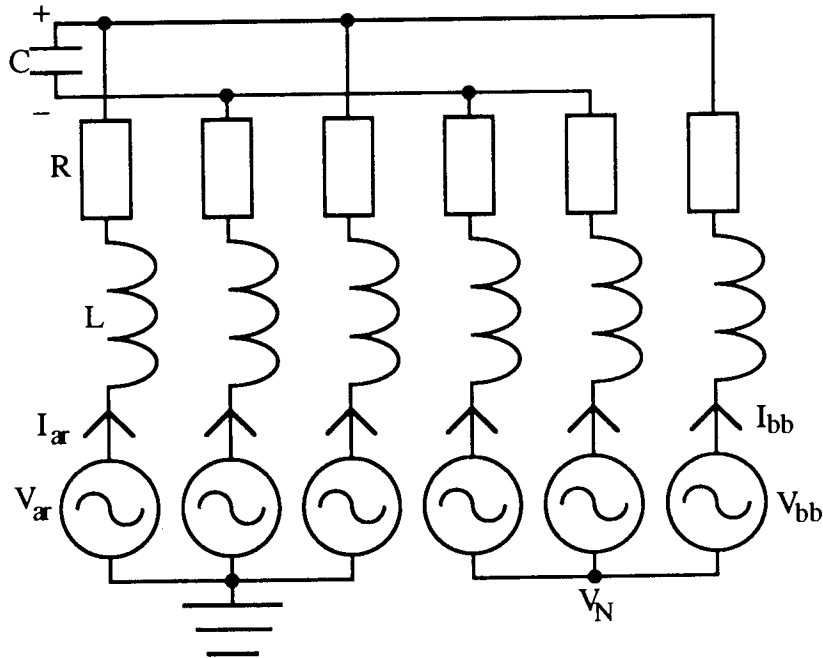


Figure A5.2. The Twelve Pulse STATCON During the Interval $-\pi/12 < \phi < \pi/12$.

From figure A5.2 the following equations can be deduced

$$\begin{aligned}
 V_{ar} - V_+ &= X_L \frac{dI_{ar}}{d\phi} + R I_{ar} & V_{br} + V_N - V_+ &= X_L \frac{dI_{br}}{d\phi} + R I_{br} - V_c \\
 V_{ay} - V_+ &= X_L \frac{dI_{ay}}{d\phi} + R I_{ay} - V_c & V_{by} + V_N - V_+ &= X_L \frac{dI_{by}}{d\phi} + R I_{by} - V_c \\
 V_{ab} - V_+ &= X_L \frac{dI_{ab}}{d\phi} + R I_{ab} & V_{bb} + V_N - V_+ &= X_L \frac{dI_{bb}}{d\phi} + R I_{bb}
 \end{aligned}
 \tag{A5.4}$$

The current through the capacitor, I_c , from - to + is given by

$$I_c = I_{ay} - I_{bb} \tag{A5.5}$$

and so, as in the three phase work,

$$V_c = -X_C \int I_c d\phi \tag{A5.6}$$

Summing the three equations on the left hand side of (A5.4) and using (A5.2) gives

$$V_+ = \frac{V_c}{3} \tag{A5.7}$$

Summing the three equations on the right hand side of (A5.4), and using (A5.7), gives, during this interval,

$$V_N = -\frac{V_c}{3} \tag{A5.8}$$

Since, at least during this interval, there is a potential difference between the two star points on the secondary side of the transformers it follows that these two points cannot be connected; the secondaries of both transformers cannot be earthed.

Substituting (A5.7) and (A5.8) in (A5.4) gives

$$\begin{aligned}
 V_{ar} &= X_L \frac{dI_{ar}}{d\phi} + R I_{ar} + \frac{V_c}{3} & V_{br} &= X_L \frac{dI_{br}}{d\phi} + R I_{br} - \frac{V_c}{3} \\
 V_{ay} &= X_L \frac{dI_{ay}}{d\phi} + R I_{ay} - \frac{2V_c}{3} & V_{by} &= X_L \frac{dI_{by}}{d\phi} + R I_{by} - \frac{V_c}{3} \\
 V_{ab} &= X_L \frac{dI_{ab}}{d\phi} + R I_{ab} + \frac{V_c}{3} & V_{bb} &= X_L \frac{dI_{bb}}{d\phi} + R I_{bb} + \frac{2V_c}{3}
 \end{aligned}
 \tag{A5.9}$$

Subtracting the last part of (A5.9) from the second part, and using (A5.5), gives

$$V_{ay} - V_{bb} = X_L \frac{dI_c}{d\phi} + R I_c - \frac{4V_c}{3} \tag{A5.10}$$

Substituting from (A5.1) and (A5.6), and differentiating again, gives, after simplifying,

$$\frac{d^2 I_c}{d\phi^2} + 2\beta \frac{dI_c}{d\phi} + \frac{4X_C}{3X_L} I_c = \frac{2V_m}{X_L} \cos\pi/12 \sin(\phi+\theta_0) \tag{A5.11}$$

Assuming $R < 2\sqrt{4X_C X_L/3}$ the solution to equation (A5.11) is

$$I_c = -\frac{2V_m}{hX_L} \cos\pi/12 \cos(\phi+\theta_0+\gamma) + A_1 e^{-\beta\phi} \sin k\phi + A_2 e^{-\beta\phi} \cos k\phi \tag{A5.12}$$

where

$$k = \sqrt{\frac{4X_C}{3X_L} - \beta^2} \tag{A5.12a}$$

Substituting (A5.12) in (A5.6) and integrating gives

$$\frac{V_c}{X_C} = \frac{2V_m}{hX_L} \cos\pi/12 \sin(\phi+\theta_0+\gamma) + \frac{e^{-\beta\phi}}{(\beta^2+k^2)} [(\beta A_1 - k A_2) \sin k\phi + (k A_1 + \beta A_2) \cos k\phi] \tag{A5.13}$$

Substituting in the relevant parts of (A5.9) from (A5.13), using (A5.12a), integrating, and simplifying, gives

$$I_{ay} = \frac{V_m}{hX_L} \sin(\phi+\theta_0+\gamma-7\pi/12) - \frac{V_m (\beta^2+k^2)}{hX_L (1+4\beta^2)} \cos\pi/12 [\cos(\phi+\theta_0+\gamma) - 2\beta\sin(\phi+\theta_0+\gamma)] \\ - \frac{V_m (\beta^2+k^2)}{hX_L (1+4\beta^2)} [\sin(\phi+\theta_0+\gamma-7\pi/12) + 2\beta\cos(\phi+\theta_0+\gamma-7\pi/12)] \\ + \frac{e^{-\beta\phi}}{2} [A_1\sin\phi + A_2\cos\phi] + A_3e^{-2\beta\phi} \quad (A5.14)$$

$$I_{ar} = \frac{V_m}{hX_L} \sin(\phi+\theta_0+\gamma+\pi/12) + \frac{V_m (\beta^2+k^2)}{hX_L (1+4\beta^2)} \frac{\cos\pi/12}{2} [\cos(\phi+\theta_0+\gamma) - 2\beta\sin(\phi+\theta_0+\gamma)] \\ - \frac{V_m (\beta^2+k^2)}{hX_L (1+4\beta^2)} [\sin(\phi+\theta_0+\gamma+\pi/12) + 2\beta\cos(\phi+\theta_0+\gamma+\pi/12)] \\ - \frac{e^{-\beta\phi}}{4} [A_1\sin\phi + A_2\cos\phi] + A_4e^{-2\beta\phi} \quad (A5.14a)$$

$$I_{br} = \frac{V_m}{hX_L} \sin(\phi+\theta_0+\gamma-\pi/12) - \frac{V_m (\beta^2+k^2)}{hX_L (1+4\beta^2)} \frac{\cos\pi/12}{2} [\cos(\phi+\theta_0+\gamma) - 2\beta\sin(\phi+\theta_0+\gamma)] \\ - \frac{V_m (\beta^2+k^2)}{hX_L (1+4\beta^2)} [\sin(\phi+\theta_0+\gamma-\pi/12) + 2\beta\cos(\phi+\theta_0+\gamma-\pi/12)] \\ + \frac{e^{-\beta\phi}}{4} [A_1\sin\phi + A_2\cos\phi] + A_5e^{-2\beta\phi} \quad (A5.14b)$$

Substituting (A5.14) and (A5.14a) in (A5.2) and simplifying gives

$$I_{ab} = \frac{V_m}{hX_L} \sin(\phi+\theta_0+\gamma-5\pi/4) + \frac{V_m (\beta^2+k^2)}{hX_L (1+4\beta^2)} \frac{\cos\pi/12}{2} [\cos(\phi+\theta_0+\gamma) - 2\beta\sin(\phi+\theta_0+\gamma)] \\ - \frac{V_m (\beta^2+k^2)}{hX_L (1+4\beta^2)} [\sin(\phi+\theta_0+\gamma-5\pi/4) + 2\beta\cos(\phi+\theta_0+\gamma-5\pi/4)] \\ - \frac{e^{-\beta\phi}}{4} [A_1\sin\phi + A_2\cos\phi] - (A_3+A_4)e^{-2\beta\phi} \quad (A5.14c)$$

Using (A5.2) in (A5.5) and substituting (A5.14) and (A5.14b) gives

$$I_{by} = \frac{V_m}{hX_L} \sin(\phi+\theta_0+\gamma-3\pi/4) - \frac{V_m (\beta^2+k^2)}{hX_L (1+4\beta^2)} \frac{\cos\pi/12}{2} [\cos(\phi+\theta_0+\gamma) - 2\beta\sin(\phi+\theta_0+\gamma)] \\ - \frac{V_m (\beta^2+k^2)}{hX_L (1+4\beta^2)} [\sin(\phi+\theta_0+\gamma-3\pi/4) + 2\beta\cos(\phi+\theta_0+\gamma-3\pi/4)] \\ + \frac{e^{-\beta\phi}}{4} [A_1\sin\phi + A_2\cos\phi] - (A_3+A_5)e^{-2\beta\phi} \quad (A5.14d)$$

Substituting (A5.14b) and (A5.14d) in (A5.2) and simplifying gives

$$I_{bb} = \frac{V_m}{hX_L} \sin(\phi+\theta_0+\gamma-17\pi/12) + \frac{V_m (\beta^2+k^2)}{hX_L (1+4\beta^2)} \cos\pi/12 [\cos(\phi+\theta_0+\gamma) - 2\beta\sin(\phi+\theta_0+\gamma)] \\ - \frac{V_m (\beta^2+k^2)}{hX_L (1+4\beta^2)} [\sin(\phi+\theta_0+\gamma-17\pi/12) + 2\beta\cos(\phi+\theta_0+\gamma-17\pi/12)] \\ - \frac{e^{-\beta\phi}}{2} [A_1\sin\phi + A_2\cos\phi] + A_3e^{-2\beta\phi} \quad (A5.14e)$$

As in the three phase circuit the current through the capacitor is the same in each interval and so the voltage boundary condition is

$$V_c(\phi = \pi/12) = V_c(\phi = -\pi/12) \quad (\text{A5.15})$$

The boundary conditions on the current can be deduced from table A5.1:

$$I_{ar}(\phi = \pi/12) = -I_{by}(\phi = -\pi/12) \quad (\text{A5.15a})$$

$$I_{by}(\phi = \pi/12) = I_{ay}(\phi = -\pi/12) \quad (\text{A5.15b})$$

$$I_{ay}(\phi = \pi/12) = -I_{bb}(\phi = -\pi/12) \quad (\text{A5.15c})$$

$$I_{bb}(\phi = \pi/12) = I_{ab}(\phi = -\pi/12) \quad (\text{A5.15d})$$

Evaluating (A5.15) and simplifying gives

$$\begin{aligned} & \frac{V_m}{hX_L} (\beta^2+k^2)\cos(\theta_0+\gamma) = \\ & A_1[k(e^{\beta\pi/12}-e^{-\beta\pi/12})\cosk\pi/12 - \beta(e^{\beta\pi/12}+e^{-\beta\pi/12})\sinks\pi/12] + \\ & A_2[\beta(e^{\beta\pi/12}-e^{-\beta\pi/12})\cosk\pi/12 + k(e^{\beta\pi/12}+e^{-\beta\pi/12})\sinks\pi/12] \end{aligned} \quad (\text{A5.16})$$

Evaluating (A5.15a) gives

$$\begin{aligned} & \frac{V_m (\beta^2+k^2)}{hX_L (1+4\beta^2)} [\sin(\theta_0+\gamma) + 2\beta \cos(\theta_0+\gamma)] = -A_1(e^{\beta\pi/12}+e^{-\beta\pi/12})\sinks\pi/12 \\ & + A_2(e^{\beta\pi/12}-e^{-\beta\pi/12})\cosk\pi/12 - 4(A_3+A_5)e^{\beta\pi/6} + 4A_4e^{-\beta\pi/6} \end{aligned} \quad (\text{A5.16a})$$

Evaluating (A5.15b) gives

$$\begin{aligned} & \frac{2V_m (\beta^2+k^2)}{hX_L (1+4\beta^2)} \\ & \{ [\sin(\theta_0+\gamma) + 2\beta \cos(\theta_0+\gamma)] + \cos\pi/12[\cos(\theta_0+\gamma+\pi/12) - 2\beta\sin(\theta_0+\gamma+\pi/12)] \} = \\ & - A_1(2e^{\beta\pi/12}+e^{-\beta\pi/12})\sinks\pi/12 + A_2(2e^{\beta\pi/12}-e^{-\beta\pi/12})\cosk\pi/12 \\ & + 4A_3(e^{\beta\pi/6}+e^{-\beta\pi/6}) + 4A_5e^{-\beta\pi/6} \end{aligned} \quad (\text{A5.16b})$$

Evaluating (A5.15c) gives

$$\begin{aligned} & \frac{V_m (\beta^2+k^2)}{hX_L (1+4\beta^2)} [\sin(\theta_0+\gamma) + 2\beta \cos(\theta_0+\gamma)] = -A_1(e^{\beta\pi/12}+e^{-\beta\pi/12})\sinks\pi/12 \\ & + A_2(e^{\beta\pi/12}-e^{-\beta\pi/12})\cosk\pi/12 - 2A_3(e^{\beta\pi/6}+e^{-\beta\pi/6}) \end{aligned} \quad (\text{A5.16c})$$

Evaluating (A5.15d) gives

$$\begin{aligned} & \frac{2V_m (\beta^2+k^2)}{hX_L (1+4\beta^2)} \\ & \{ [\sin(\theta_0+\gamma) + 2\beta \cos(\theta_0+\gamma)] - \cos\pi/12[\cos(\theta_0+\gamma-\pi/12) - 2\beta\sin(\theta_0+\gamma-\pi/12)] \} = \\ & - A_1(e^{\beta\pi/12}+2e^{-\beta\pi/12})\sinks\pi/12 + A_2(e^{\beta\pi/12}-2e^{-\beta\pi/12})\cosk\pi/12 \\ & + 4A_3(e^{\beta\pi/6}+e^{-\beta\pi/6}) + 4A_4e^{\beta\pi/6} \end{aligned} \quad (\text{A5.16d})$$

For this many unknowns substitution, as used in the three phase case, is complicated. It is simpler to use matrix manipulation:

$$[V] = [F] \cdot [A] \quad (A5.17)$$

where

$[V]$ = the voltage column matrix, i.e. the left hand sides of equations (A5.16) to (A5.16d),

$[A]$ = the column matrix of unknown constants, i.e. A_1 to A_5 ,

and $[F]$ = the matrix of the coefficients of A_1 to A_5 , i.e. the right hand sides of equations (A5.16) to (A5.16d).

$$[V] = \frac{V_m}{hX_L} (\beta^2+k^2)\cos(\theta_0+\gamma),$$

$$\frac{V_m (\beta^2+k^2)}{hX_L (1+4\beta^2)} [\sin(\theta_0+\gamma) + 2\beta \cos(\theta_0+\gamma)],$$

$$\frac{2V_m (\beta^2+k^2)}{hX_L (1+4\beta^2)}$$

$$\{[\sin(\theta_0+\gamma) + 2\beta \cos(\theta_0+\gamma)] + \cos\pi/12[\cos(\theta_0+\gamma+\pi/12) - 2\beta\sin(\theta_0+\gamma+\pi/12)]\},$$

$$\frac{V_m (\beta^2+k^2)}{hX_L (1+4\beta^2)} [\sin(\theta_0+\gamma) + 2\beta \cos(\theta_0+\gamma)],$$

$$\frac{2V_m (\beta^2+k^2)}{hX_L (1+4\beta^2)}$$

$$\{[\sin(\theta_0+\gamma) + 2\beta \cos(\theta_0+\gamma)] - \cos\pi/12[\cos(\theta_0+\gamma-\pi/12) - 2\beta\sin(\theta_0+\gamma-\pi/12)]\}$$

$$(A5.17a)$$

$$[F] = \{ \{ [k(e^{\beta\pi/12}-e^{-\beta\pi/12})\cos k\pi/12 - \beta(e^{\beta\pi/12}+e^{-\beta\pi/12})\sin k\pi/12],$$

$$[\beta(e^{\beta\pi/12}-e^{-\beta\pi/12})\cos k\pi/12 + k(e^{\beta\pi/12}+e^{-\beta\pi/12})\sin k\pi/12], 0, 0, 0 \},$$

$$\{ [-(e^{\beta\pi/12}+e^{-\beta\pi/12})\sin k\pi/12], [(e^{\beta\pi/12}-e^{-\beta\pi/12})\cos k\pi/12],$$

$$-4 e^{\beta\pi/6}, 4 e^{-\beta\pi/6}, -4 e^{-\beta\pi/6} \},$$

$$\{ [-(2e^{\beta\pi/12}+e^{-\beta\pi/12})\sin k\pi/12], [(2e^{\beta\pi/12}-e^{-\beta\pi/12})\cos k\pi/12],$$

$$4 (e^{\beta\pi/6}+e^{-\beta\pi/6}), 0, 4 e^{-\beta\pi/6} \},$$

$$\{ [-(e^{\beta\pi/12}+e^{-\beta\pi/12})\sin k\pi/12], [(e^{\beta\pi/12}-e^{-\beta\pi/12})\cos k\pi/12],$$

$$-2(e^{\beta\pi/6}+e^{-\beta\pi/6}), 0, 0 \},$$

$$\{ [-(e^{\beta\pi/12}+2e^{-\beta\pi/12})\sin k\pi/12], [(e^{\beta\pi/12}-2e^{-\beta\pi/12})\cos k\pi/12],$$

$$4 (e^{\beta\pi/6}+e^{-\beta\pi/6}), 4 e^{\beta\pi/6}, 0 \} \}$$

$$(A5.17b)$$

Inverting (A5.17) gives

$$[A] = [F]^{-1} \cdot [V] \quad (A5.18)$$

Thus A_1 to A_5 can be evaluated for any set of values of θ_0 , k , and β . From equations (A5-14) to (A5-14e), the currents in all of the phases on the secondary side of the transformers are known, and from table A5-1 the current in one of these phases for a whole cycle is known.

b) Determination of the Current on the Transformer Primary Side

For the red phase of the first transformer, i.e. the one leading on the supply voltage, assuming an effective transformer ratio of 1 to 1, the voltage is

$$V_{ar} = V_m \sin(\phi + \theta_0 + \pi/12) \tag{A5-19}$$

This voltage is made up of a combination of some of the red phase less some of the yellow phase:

$$\sin(\phi + \theta_0 + \pi/12) = N_1 \sin(\phi + \theta_0) - N_2 \sin(\phi + \theta_0 - 2\pi/3) \tag{A5-20}$$

where

N_1 and N_2 are the turns ratios, relative to the number of turns on each of the primary windings, as shown in figure A5-3.

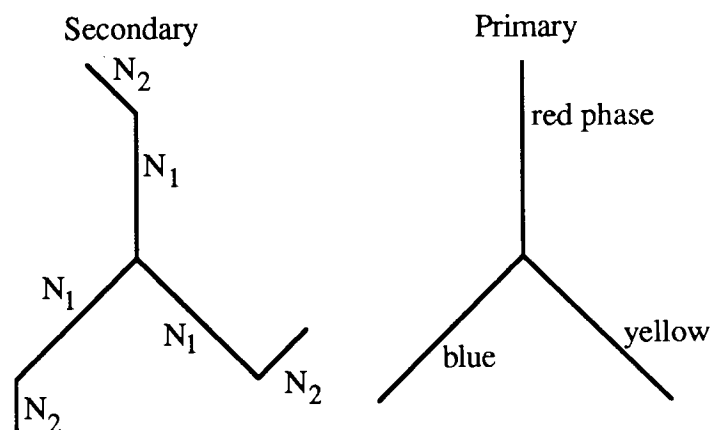


Figure A5-3. Turns Ratios for the First Transformer.

Equating the coefficients of $\cos(\phi + \theta_0)$ and $\sin(\phi + \theta_0)$ in equation (A5-20) gives

$$N_2 = \frac{\sin \pi/12}{\sin 2\pi/3} = \frac{\sqrt{3} - 1}{\sqrt{6}} \tag{A5-21}$$

$$N_1 = \cos \pi/12 + \frac{\sin \pi/12}{\tan 2\pi/3} = \frac{\sin 3\pi/4}{\sin 2\pi/3} = \sqrt{\frac{2}{3}} \tag{A5-21a}$$

The phase shift of transformer 2 is in the opposite sense to that of transformer 1, i.e. the red phase of transformer 2 is lagging on the red phase of the supply voltage by 15° . This gives the same turns ratios for the second transformer as for the first, but the N_2 turn is coupled to the other phase of the primary; for the red phase of the secondary of the first transformer the N_2 contribution comes from the yellow phase winding of the

primary but for the red phase of the secondary of the second transformer the N_2 contribution comes from the blue phase winding of the primary.

The other secondary phases are cyclic permutations of the formulae defining the voltages on the secondary red phases:

$$\begin{aligned} V_{ar} &= N_1 V_R - N_2 V_Y & V_{ay} &= N_1 V_Y - N_2 V_B & V_{ab} &= N_1 V_B - N_2 V_R \\ V_{br} &= N_1 V_R - N_2 V_B & V_{by} &= N_1 V_Y - N_2 V_R & V_{bb} &= N_1 V_B - N_2 V_Y \end{aligned} \quad (\text{A5.22})$$

The current in one phase of the primary of the first transformer is a function of the currents in the secondary of the first transformer to which that phase of the primary is coupled. The current in one phase of the voltage source is the sum of the currents in each of the phases in the two primaries. The turns ratios relating the currents are the inverses of those relating the voltages:

$$\begin{aligned} I_R &= N_1 (I_{ar} + I_{br}) - N_2 (I_{ab} + I_{by}) \\ I_Y &= N_1 (I_{ay} + I_{by}) - N_2 (I_{ar} + I_{bb}) \\ I_B &= N_1 (I_{ab} + I_{bb}) - N_2 (I_{ay} + I_{br}) \end{aligned} \quad (\text{A5.23})$$

c) Fourier Series

As in the three phase case the Fourier series of the voltage at the a.c. terminals of the inverter is calculated first and then the Fourier series of the current is calculated.

The voltage at the a.c. terminals of the inverter during the first two eras, each of one-sixth of a cycle duration, is one-third of the voltage across the capacitor, it is two-thirds during both of the next two eras, and one-third again during the third set of two eras, as shown in figure 6.4. Thus, as in the three phase case, the voltage at the a.c. terminals of the inverter has harmonics for $n = 6i \pm 1$, for $i = 0, 1, 2, \dots$

The Fourier series of the voltage at the inverter terminals of the red phase of inverter 1 can therefore defined as

$$V_I = \sum_{n=1}^{\infty} d_n \cos n(\phi + \pi/12) + e_n \sin n(\phi + \pi/12) \quad (\text{A5.24})$$

$$\text{for } n = 6i \pm 1, \text{ for } i = 0, 1, 2, \dots$$

where

$$d_n = \frac{2}{\pi} \int_{-\pi/12}^{11\pi/12} V_I(\phi) \cos n(\phi + \pi/12) d\phi \quad \text{and} \quad e_n = \frac{2}{\pi} \int_{-\pi/12}^{11\pi/12} V_I(\phi) \sin n(\phi + \pi/12) d\phi$$

Considering the d_n terms only this can be split up into six intervals, for each half cycle, of duration $\pi/6$:

$$\begin{aligned} \frac{3\pi d_n}{2} = & \int_{-\pi/12}^{\pi/12} V_c(\phi) \cos n(\phi + \pi/12) d\phi + \int_{\pi/12}^{\pi/4} V_c(\phi - \pi/6) \cos n(\phi + \pi/12) d\phi + \\ & 2 \int_{\pi/4}^{5\pi/12} V_c(\phi - \pi/3) \cos n(\phi + \pi/12) d\phi + 2 \int_{7\pi/12}^{\pi/2} V_c(\phi - \pi/2) \cos n(\phi + \pi/12) d\phi + \\ & \int_{3\pi/4}^{7\pi/12} V_c(\phi - 2\pi/3) \cos n(\phi + \pi/12) d\phi + \int_{11\pi/12}^{3\pi/4} V_c(\phi - 5\pi/6) \cos n(\phi + \pi/12) d\phi \end{aligned} \quad (A5-25)$$

with

e_n of the same form but with cos replaced by sin.

Making a change of variables in each of the integrals, renaming and simplifying gives

$$\frac{3\pi d_n}{4} = - [\sin n\pi/12 + \sin n\pi/4 + 2\sin 5n\pi/12] \int_{-\pi/12}^{\pi/12} V_c(\phi) \sin n\phi d\phi \quad (A5-26)$$

$$\frac{3\pi e_n}{4} = [\sin n\pi/12 + \sin n\pi/4 + 2\sin 5n\pi/12] \int_{-\pi/12}^{\pi/12} V_c(\phi) \cos n\phi d\phi \quad (A5-26a)$$

Substituting for $V_c(\phi)$, from (A5-13), using (A5-12a), integrating and simplifying gives

$$\begin{aligned}
 d_1 = & -\frac{3}{2} \frac{(\sqrt{3}+1)}{\sqrt{2}} \left\{ \frac{2V_m}{\pi h} (\beta^2+k^2) \cos\pi/12 \cos(\theta_0+\gamma) \left(\frac{\pi}{12} - \frac{1}{4} \right) \right. \\
 & + \frac{(\beta A_1 - k A_2) X_L}{\pi h^2} \left[k \cos k\pi/12 [(e^{\beta\pi/12} - e^{-\beta\pi/12}) 2\beta \cos\pi/12 - \right. \\
 & \quad (e^{\beta\pi/12} + e^{-\beta\pi/12})(\beta^2+k^2-1)\sin\pi/12] - \\
 & \quad \sin k\pi/12 [(e^{\beta\pi/12} + e^{-\beta\pi/12})(\beta^2-k^2+1)\cos\pi/12] + \\
 & \quad \left. \beta \sin k\pi/12 [(e^{\beta\pi/12} - e^{-\beta\pi/12})(\beta^2+k^2+1)\sin\pi/12] \right] \\
 & + \frac{(k A_1 + \beta A_2) X_L}{\pi h^2} \left[k \sin k\pi/12 [(e^{\beta\pi/12} + e^{-\beta\pi/12}) 2\beta \cos\pi/12 - \right. \\
 & \quad (e^{\beta\pi/12} - e^{-\beta\pi/12})(\beta^2+k^2-1)\sin\pi/12] + \\
 & \quad \cos k\pi/12 [(e^{\beta\pi/12} - e^{-\beta\pi/12})(\beta^2-k^2+1)\cos\pi/12] - \\
 & \quad \left. \beta \cos k\pi/12 [(e^{\beta\pi/12} - e^{-\beta\pi/12})(\beta^2+k^2+1)\sin\pi/12] \right] \left. \right\} \quad (A5-27)
 \end{aligned}$$

$$\begin{aligned}
 n > 1 \quad d_n = & -[\sin n\pi/12 + \sin n\pi/4 + 2\sin 5n\pi/12] \left\{ \right. \\
 & \frac{2V_m}{\pi h} (\beta^2+k^2) \frac{\cos\pi/12}{\sqrt{2(n^2-1)}} \cos(\theta_0+\gamma) [(1-\sqrt{3})n \cos n\pi/12 + (1+\sqrt{3})\sin n\pi/12] \\
 & + \frac{(\beta A_1 - k A_2) X_L}{\pi h_n^2} \left[k \cos k\pi/12 [(e^{\beta\pi/12} - e^{-\beta\pi/12}) 2\beta n \cos n\pi/12 - \right. \\
 & \quad (e^{\beta\pi/12} + e^{-\beta\pi/12})(\beta^2+k^2-n^2)\sin n\pi/12] - \\
 & \quad n \sin k\pi/12 [(e^{\beta\pi/12} + e^{-\beta\pi/12})(\beta^2-k^2+n^2)\cos n\pi/12] + \\
 & \quad \left. \beta \sin k\pi/12 [(e^{\beta\pi/12} - e^{-\beta\pi/12})(\beta^2+k^2+n^2)\sin n\pi/12] \right] \\
 & + \frac{(k A_1 + \beta A_2) X_L}{\pi h_n^2} \left[k \sin k\pi/12 [(e^{\beta\pi/12} + e^{-\beta\pi/12}) 2\beta n \cos n\pi/12 - \right. \\
 & \quad (e^{\beta\pi/12} - e^{-\beta\pi/12})(\beta^2+k^2-n^2)\sin n\pi/12] + \\
 & \quad n \cos k\pi/12 [(e^{\beta\pi/12} - e^{-\beta\pi/12})(\beta^2-k^2+n^2)\cos n\pi/12] - \\
 & \quad \left. \beta \cos k\pi/12 [(e^{\beta\pi/12} - e^{-\beta\pi/12})(\beta^2+k^2+n^2)\sin n\pi/12] \right] \left. \right\} \quad (A5-27a)
 \end{aligned}$$

$$\begin{aligned}
e_1 = & \frac{3}{2} \frac{(\sqrt{3} + 1)}{\sqrt{2}} \left\{ \frac{2V_m}{\pi h} (\beta^2 + k^2) \cos\pi/12 \sin(\theta_0 + \gamma) \left(\frac{\pi}{12} + \frac{1}{4} \right) \right. \\
& + \frac{(\beta A_1 - k A_2) X_L}{\pi h^2} \left[k \cos k\pi/12 [(e^{\beta\pi/12} - e^{-\beta\pi/12})(\beta^2 + k^2 - 1) \cos\pi/12 + \right. \\
& \quad (e^{\beta\pi/12} + e^{-\beta\pi/12}) 2\beta \sin\pi/12] - \\
& \quad \beta \sin k\pi/12 [(e^{\beta\pi/12} + e^{-\beta\pi/12})(\beta^2 + k^2 + 1) \cos\pi/12] - \\
& \quad \left. \left. \sin k\pi/12 [(e^{\beta\pi/12} - e^{-\beta\pi/12})(\beta^2 - k^2 + 1) \sin\pi/12] \right] \right\} \\
& + \frac{(k A_1 + \beta A_2) X_L}{\pi h^2} \left[k \sin k\pi/12 [(e^{\beta\pi/12} + e^{-\beta\pi/12})(\beta^2 + k^2 - 1) \cos\pi/12 + \right. \\
& \quad (e^{\beta\pi/12} - e^{-\beta\pi/12}) 2\beta \sin\pi/12] + \\
& \quad \beta \cos k\pi/12 [(e^{\beta\pi/12} - e^{-\beta\pi/12})(\beta^2 + k^2 + 1) \cos\pi/12] + \\
& \quad \left. \left. \cos k\pi/12 [(e^{\beta\pi/12} - e^{-\beta\pi/12})(\beta^2 - k^2 + 1) \sin\pi/12] \right] \right\} \quad (A5.27b)
\end{aligned}$$

$$\begin{aligned}
n > 1 \quad e_n = & \left[\sin n\pi/12 + \sin n\pi/4 + 2\sin 5n\pi/12 \right] \left\{ \right. \\
& \frac{2V_m}{\pi h} (\beta^2 + k^2) \frac{\cos\pi/12}{\sqrt{2(n^2 - 1)}} \sin(\theta_0 + \gamma) [(1 - \sqrt{3}) \cos n\pi/12 + (1 + \sqrt{3}) n \sin n\pi/12] \\
& + \frac{(\beta A_1 - k A_2) X_L}{\pi h_n^2} \left[k \cos k\pi/12 [(e^{\beta\pi/12} - e^{-\beta\pi/12})(\beta^2 + k^2 - n^2) \cos n\pi/12 + \right. \\
& \quad (e^{\beta\pi/12} + e^{-\beta\pi/12}) 2\beta n \sin n\pi/12] - \\
& \quad \beta \sin k\pi/12 [(e^{\beta\pi/12} + e^{-\beta\pi/12})(\beta^2 + k^2 + n^2) \cos n\pi/12] - \\
& \quad \left. \left. n \sin k\pi/12 [(e^{\beta\pi/12} - e^{-\beta\pi/12})(\beta^2 - k^2 + n^2) \sin n\pi/12] \right] \right\} \\
& + \frac{(k A_1 + \beta A_2) X_L}{\pi h_n^2} \left[k \sin k\pi/12 [(e^{\beta\pi/12} + e^{-\beta\pi/12})(\beta^2 + k^2 - n^2) \cos n\pi/12 + \right. \\
& \quad (e^{\beta\pi/12} - e^{-\beta\pi/12}) 2\beta n \sin n\pi/12] + \\
& \quad \beta \cos k\pi/12 [(e^{\beta\pi/12} - e^{-\beta\pi/12})(\beta^2 + k^2 + n^2) \cos n\pi/12] + \\
& \quad \left. \left. n \cos k\pi/12 [(e^{\beta\pi/12} - e^{-\beta\pi/12})(\beta^2 - k^2 + n^2) \sin n\pi/12] \right] \right\} \quad (A5.27c)
\end{aligned}$$

(A5.27) to (A5.27c) could also have been written out in terms of the angle γ , as were the equivalent expressions in the three phase case, (A3.20) to (A3.20c).

The Fourier series of the current on the secondary side of the transformers is given by, using the method employed in the six pulse case,

$$\begin{aligned}
I_{ar} = & - \frac{V_m}{X_L(1+4\beta^2)} [\cos(\phi + \theta_0 + \pi/12) - 2\beta \sin(\phi + \theta_0 + \pi/12)] \quad (A5.28) \\
& + \sum_{n=1}^{\infty} \frac{1}{X_L(n^2+4\beta^2)} [(ne_n - 2\beta d_n) \cos n(\phi + \pi/12) - (nd_n + 2\beta e_n) \sin n(\phi + \pi/12)]
\end{aligned}$$

The expressions for the currents in the other phases, on the secondary side of the transformers, are of the same form as equation (A5.28) but with $(\phi + \pi/12)$ replaced by the angle of the applied voltage source, from equation (A5.1).

The current in the red phase of the supply, I_R , is given by applying equation (A5-23) to (A5-28) and the similar contributions from the other phases. For the fundamental component, after simplifying using (A5-21) and (A5-21a),

$$I_{R1} = \frac{2}{X_L(1+4\beta^2)} \{-V_m[\cos(\phi+\theta_0) - 2\beta\sin(\phi+\theta_0)] + (e_1 - 2\beta d_1)\cos\phi - (d_1 + 2\beta e_1)\sin\phi\} \quad (A5-29)$$

and for the harmonics:

$$I_{Rn} = \frac{2}{X_L(n^2+4\beta^2)} [N_1\cos n\pi/12 + N_2\cos n\pi/4] \{(ne_n - 2\beta d_n)\cos n\phi - (nd_n + 2\beta e_n)\sin n\phi\} \quad (A5-30)$$

The form of the expression for the fundamental, (A5-29), is the same as that in the three phase equipment, from (A3-22), but because of the parallel connection of the transformer primaries (A5-29) is twice as big. As in the three phase equipment d_n and e_n can be separated into terms in $\sin\theta_0$ and $\cos\theta_0$ only so the derivations of the expressions for p_1 , q_1 and q_2 are identical, equations (A3-26) to (A3-26b) respectively. The contributions to the fundamental component of the current are therefore given by

$$I_q = \frac{2V_m}{X_L} \left(q_1 + q_2 \frac{\sin 2\theta_0}{2\beta} \right) \quad (A5-31)$$

$$I_p = \frac{2\beta V_m}{X_L} \left(p_1 + q_2 \frac{\sin^2 \theta_0}{\beta^2} \right) \quad (A5-31a)$$

For the harmonics $|N_1\cos n\pi/12 + N_2\cos n\pi/4| = 1$ for $n = 12i \pm 1$ and 0 for $n = 5, 7, 17, 19, \dots$, therefore

$$|I_n| = \frac{2}{X_L} \sqrt{\frac{d_n^2 + e_n^2}{(n^2+4\beta^2)}} = \frac{2V_m}{X_L} |t_n| \quad (A5-32)$$

The exact form of t_n is the same as that given in the three phase case, (A3-29). Plotting the exact solution shows that the harmonics again appear to vary linearly with the reduced firing angle and so the approximate form for t_n , from equation (A3-30), is also valid, as are the equations for c_n and s_n , (A3-32) and (A3-32a).

The parallel connection of the transformer primaries gives

$$I_{nc} \approx \frac{2V_m}{X_L} [c_n - s_n \theta_{ob}] \quad (A5-33)$$

Appendix 6

Analysis of a Twelve Pulse STATCON with Series Connected Transformer Primaries

a) Determination of the Current on the Transformer Secondary Side

When the primaries of the transformers are connected in series the voltage on the secondaries is no longer defined directly from the system voltage and the turns ratios but also depends upon the current.

The devices are fired in the same order as in the parallel connected case, as in table 6-1, and so all parts of equation (A5-9) are valid but V_{ar} to V_{bb} are not now known at the outset of the analysis.

Because of the series connection of the transformer primaries the current in each of the primary windings must be the same. Figure A6-1 shows the transformer configuration.

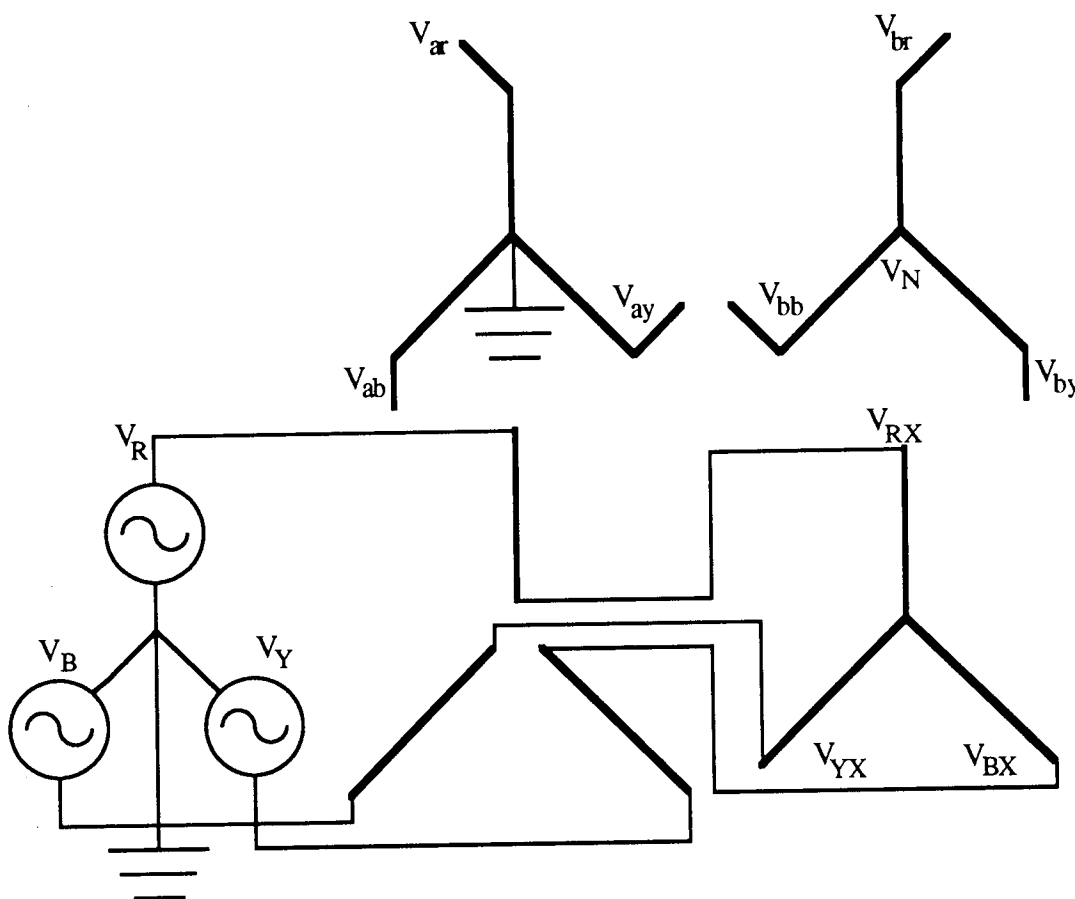


Figure A6-1. Twelve Pulse Series Connected Transformer Arrangement.

The relationships between the voltages are

$$\begin{aligned} V_{ar} &= N_1(V_R - V_{RX}) - N_2(V_Y - V_{YX}) & V_{br} &= N_1 V_{RX} - N_2 V_{BX} \\ V_{ay} &= N_1(V_Y - V_{YX}) - N_2(V_B - V_{BX}) & V_{by} &= N_1 V_{YX} - N_2 V_{RX} \\ V_{ab} &= N_1(V_B - V_{BX}) - N_2(V_R - V_{RX}) & V_{bb} &= N_1 V_{BX} - N_2 V_{YX} \end{aligned} \quad (\text{A6.1})$$

The transformer turns ratios, N_1 and N_2 , are equal to those in the parallel case, equations (A5.21) and (A5.21a).

The relationships between the currents are

$$\begin{aligned} I_R &= N_1 I_{ar} - N_2 I_{ab} = N_1 I_{br} - N_2 I_{by} \\ I_Y &= N_1 I_{ay} - N_2 I_{ar} = N_1 I_{by} - N_2 I_{bb} \\ I_B &= N_1 I_{ab} - N_2 I_{ay} = N_1 I_{bb} - N_2 I_{br} \end{aligned} \quad (\text{A6.2})$$

As in the parallel case the sum of the currents in each set of three phases, and the sum of the supply voltages, is zero:

$$\begin{aligned} I_{ab} &= -(I_{ar} + I_{ay}) & I_{bb} &= -(I_{br} + I_{by}) \\ I_B &= -(I_R + I_Y) & V_B &= -(V_R + V_Y) \end{aligned} \quad (\text{A6.3})$$

Because the sets of three voltages on the secondary side of the transformers, and that at the connection between the two primaries, are functions of the current, the sum of each set of three voltages is not as apparent as those given in (A6.3) are, but it can be deduced by considering general Fourier series expressions for three voltages separated by $2\pi/3$ rads:

$$V_{RX} + V_{YX} + V_{BX} = \sum_{n=1}^{\infty} |V_n| [\sin n(\phi + \psi_n) + \sin[n(\phi - 2\pi/3) + \psi_n] + \sin[n(\phi + 2\pi/3) + \psi_n]] \quad (\text{A6.4})$$

Expanding gives

$$V_{RX} + V_{YX} + V_{BX} = [1 + 2\cos 2n\pi/3] \sum_{n=1}^{\infty} |V_n| \sin(n\phi + \psi_n) \quad (\text{A6.5})$$

Evaluating for different values of n gives

$$V_{RX} + V_{YX} + V_{BX} = 3 \sum_{n=1}^{\infty} |V_n| \sin(n\phi + \psi_n) \quad \text{for } n = 0, 3, 6, 9, \dots \quad (\text{A6.6})$$

else

$$V_{RX} + V_{YX} + V_{BX} = 0 \quad (\text{A6.7})$$

In the six pulse circuit harmonics are not generated for triple-n harmonics so, in the twelve pulse system,

$$\begin{aligned} V_{ab} &= -(V_{ar} + V_{ay}) & V_{bb} &= -(V_{br} + V_{by}) \\ V_{BX} &= -(V_{RX} + V_{YX}) \end{aligned} \quad (A6.8)$$

There are six unknown currents on the secondary side of the transformers. Using the fact that each set of three currents sum to zero gives two equations so the number of unknown currents is four. The first two equations of (A6.2) express the relationships between the currents so the number of unknown currents can be reduced to two. The third equation in (A6.2) is not independent; it is a function of the first two equations of (A6.2) and equation (A6.3).

The currents in the two red phases were taken as the unknowns, and simplifying by using the values of N_1 and N_2 , gives

$$I_{ay} = \sqrt{3} I_{br} - 2 I_{ar} \quad (A6.9)$$

$$I_{ab} = -\sqrt{3} I_{br} + I_{ar} \quad (A6.9a)$$

$$I_{by} = I_{br} - \sqrt{3} I_{ar} \quad (A6.9b)$$

$$I_{bb} = -2 I_{br} + \sqrt{3} I_{ar} \quad (A6.9c)$$

Similarly substituting from (A6.8) and (A6.3) in (A6.1) and simplifying gives

$$V_{ay} = -2 V_{ar} - \sqrt{3} V_{br} + \sqrt{3} N_1 V_R - \sqrt{3} N_2 V_B \quad (A6.10)$$

$$V_{ab} = V_{ar} + \sqrt{3} V_{br} - \sqrt{3} N_1 V_R + \sqrt{3} N_2 V_B \quad (A6.10a)$$

$$V_{by} = \sqrt{3} V_{ar} + V_{br} - \sqrt{3} N_1 V_R + \sqrt{3} N_2 V_Y \quad (A6.10b)$$

$$V_{bb} = -\sqrt{3} V_{ar} - 2 V_{br} + \sqrt{3} N_1 V_R - \sqrt{3} N_2 V_Y \quad (A6.10c)$$

The current through the capacitor depends upon the currents in the same phases as in the parallel case:

$$I_c = I_{ay} - I_{bb} \quad (A6.11)$$

Substituting from (A6.9) and (A6.9c) in (A6.11) gives

$$I_c = (2 + \sqrt{3})(I_{br} - I_{ar}) \quad (A6.12)$$

Substituting from the relevant parts of (A6-9) and (A6-10) in (A5-9) gives

$$V_{ar} = X_L \frac{dI_{ar}}{d\phi} + R I_{ar} + \frac{V_c}{3} \quad (\text{A6-13})$$

$$V_{br} = X_L \frac{dI_{br}}{d\phi} + R I_{br} - \frac{V_c}{3} \quad (\text{A6-13a})$$

$$-2 V_{ar} - \sqrt{3} V_{br} + \sqrt{3} N_1 V_R - \sqrt{3} N_2 V_B = X_L \frac{d(\sqrt{3} I_{br} - 2 I_{ar})}{d\phi} + R (\sqrt{3} I_{br} - 2 I_{ar}) - \frac{2V_c}{3} \quad (\text{A6-13b})$$

$$\sqrt{3} V_{ar} + V_{br} - \sqrt{3} N_1 V_R + \sqrt{3} N_2 V_Y = X_L \frac{d(I_{br} - \sqrt{3} I_{ar})}{d\phi} + R (I_{br} - \sqrt{3} I_{ar}) - \frac{V_c}{3} \quad (\text{A6-13c})$$

Simplifying (A6-13b) + 2(A6-13) + $\sqrt{3}$ (A6-13a) gives

$$\frac{dI_{br}}{d\phi} + 2\beta I_{br} - \frac{V_c}{6X_L} = \frac{1}{2X_L} [N_1 V_R - N_2 V_B] \quad (\text{A6-14})$$

and (A6-8c) - $\sqrt{3}$ (A6-8) - (A6-8a)

$$\frac{dI_{ar}}{d\phi} + 2\beta I_{ar} + \frac{V_c}{6X_L} = \frac{1}{2X_L} [N_1 V_R - N_2 V_Y] \quad (\text{A6-14a})$$

The voltage source is defined as twice that in the parallel connected case:

$$V_R = 2V_m \sin(\phi + \theta_0) \quad V_Y = 2V_m \sin(\phi + \theta_0 - 2\pi/3) \quad V_B = 2V_m \sin(\phi + \theta_0 + 2\pi/3) \quad (\text{A6-15})$$

Taking (A6-14) - (A6-14a), substituting from (A6-12) and (A6-15), simplifying then differentiating gives

$$\frac{d^2 I_c}{d\phi^2} + 2\beta \frac{dI_c}{d\phi} + \frac{2+\sqrt{3}}{3} \frac{X_C}{X_L} I_c = \frac{2V_m}{X_L} \cos\pi/12 \sin(\phi + \theta_0) \quad (\text{A6-16})$$

This equation is similar to the equivalent one in the parallel case, (A5-11), in particular the forcing function is the same. The coefficient of the I_c term is different. The solution is therefore of the same form as that in the parallel case, (A5-12), assuming $R < 2\sqrt{(2+\sqrt{3})X_C X_L}/3$, but with k defined differently:

$$I_c = -\frac{2V_m}{hX_L} \cos\pi/12 \cos(\phi + \theta_0 + \gamma) + A_1 e^{-\beta\phi} \sin k\phi + A_2 e^{-\beta\phi} \cos k\phi \quad (\text{A6-17})$$

where

$$k = \sqrt{\frac{2+\sqrt{3}}{3} \frac{X_C}{X_L} - \beta^2} \quad (\text{A6-17a})$$

Since the expression for the current through the capacitor is the same as that in the parallel case the ratio of the voltage across the capacitor to the impedance of the capacitor is also of the same form:

$$\frac{V_c}{X_C} = \frac{2V_m}{hX_L} \cos\pi/12 \sin(\phi+\theta_0+\gamma) + \frac{e^{-\beta\phi}}{(\beta^2+k^2)} [(\beta A_1 - kA_2)\text{sink}\phi + (kA_1 + \beta A_2)\text{cosk}\phi] \quad (\text{A6}\cdot 18)$$

Substituting from (A6-18) in equation (A6-14a), using (A6-17a), solving and simplifying gives

$$I_{ar} = \frac{V_m}{hX_L} \sin(\phi+\theta_0+\gamma+\pi/12) - \frac{V_m}{hX_L} \cos\pi/12 \frac{(\beta^2+k^2)}{(1+4\beta^2)} [\sin(\phi+\theta_0+\gamma) + 2\beta\cos(\phi+\theta_0+\gamma)] \\ - \frac{A_1}{2(2+\sqrt{3})} e^{-\beta\phi}\text{sink}\phi - \frac{A_2}{2(2+\sqrt{3})} e^{-\beta\phi}\text{cosk}\phi + A_3 e^{-2\beta\phi} \quad (\text{A6}\cdot 19)$$

Substituting (A6-19) and (A6-17) in (A6-12) and simplifying gives

$$I_{br} = \frac{V_m}{hX_L} \sin(\phi+\theta_0+\gamma-\pi/12) - \frac{V_m}{hX_L} \cos\pi/12 \frac{(\beta^2+k^2)}{(1+4\beta^2)} [\sin(\phi+\theta_0+\gamma) + 2\beta\cos(\phi+\theta_0+\gamma)] \\ + \frac{A_1}{2(2+\sqrt{3})} e^{-\beta\phi}\text{sink}\phi + \frac{A_2}{2(2+\sqrt{3})} e^{-\beta\phi}\text{cosk}\phi + A_3 e^{-2\beta\phi} \quad (\text{A6}\cdot 20)$$

The boundary conditions are three of those used in the parallel case:

$$V_c(\phi = \pi/12) = V_c(\phi = -\pi/12) \quad (\text{A6}\cdot 21)$$

$$I_{ar}(\phi = \pi/12) = -I_{by}(\phi = -\pi/12) \quad (\text{A6}\cdot 21a)$$

$$I_{by}(\phi = \pi/12) = I_{ay}(\phi = -\pi/12) \quad (\text{A6}\cdot 21b)$$

Because the expression for the V_c/X_C is the same in both the series and parallel cases, evaluating (A6-21) gives the same equation as in the parallel case, (A5-16):

$$\frac{V_m}{hX_L} (\beta^2+k^2)\cos(\theta_0+\gamma) = \\ A_1[k(e^{\beta\pi/12}-e^{-\beta\pi/12})\text{cosk}\pi/12 - \beta(e^{\beta\pi/12}+e^{-\beta\pi/12})\text{sink}\pi/12] + \\ A_2[\beta(e^{\beta\pi/12}-e^{-\beta\pi/12})\text{cosk}\pi/12 + k(e^{\beta\pi/12}+e^{-\beta\pi/12})\text{sink}\pi/12] \quad (\text{A6}\cdot 22)$$

Evaluating (A6-21a), using (A6-9a), gives, after simplifying,

$$-\frac{V_m}{2hX_L} \frac{(\beta^2+k^2)}{(1+4\beta^2)} [\cos(\theta_0+\gamma-\pi/6) - 2\beta\sin(\theta_0+\gamma-\pi/6)] = \\ \frac{A_1 \text{sink}\pi/12}{2(2+\sqrt{3})} [e^{-\beta\pi/12} + (\sqrt{3}+1)e^{\beta\pi/12}] + \frac{A_2 \text{cosk}\pi/12}{2(2+\sqrt{3})} [e^{-\beta\pi/12} - (\sqrt{3}+1)e^{\beta\pi/12}] \\ + A_3 [-e^{-\beta\pi/6} + (\sqrt{3}-1)e^{\beta\pi/6}] \quad (\text{A6}\cdot 22a)$$

Evaluating (A6.21b) and simplifying gives

$$\begin{aligned}
& -\frac{V_m}{2hX_L} \frac{(\beta^2+k^2)}{(1+4\beta^2)} [\sin(\theta_0+\gamma+\pi/6) + 2\beta\cos(\theta_0+\gamma+\pi/6)] = \\
& \frac{A_1 \operatorname{sinc}\pi/12}{2(2+\sqrt{3})} [(\sqrt{3}+1)e^{-\beta\pi/12} + (\sqrt{3}+2)e^{\beta\pi/12}] \\
& + \frac{A_2 \operatorname{cosk}\pi/12}{2(2+\sqrt{3})} [(\sqrt{3}+1)e^{-\beta\pi/12} - (\sqrt{3}+2)e^{\beta\pi/12}] \\
& + A_3 [-(\sqrt{3}-1)e^{-\beta\pi/6} + (2-\sqrt{3})e^{\beta\pi/6}] \tag{A6.22b}
\end{aligned}$$

As in the parallel case matrix manipulation can be used to compute A_1 , A_2 and A_3 . The current in the voltage source is the same as that in the primary of the transformers, equation (A6.3). Applying (A6.4), (A6.9) and (A6.9a) to (A6.3) gives

$$I_R = (N_1 - N_2)I_{ar} + \sqrt{3} N_2 I_{br} \tag{A6.23}$$

b) Fourier Series

Because the voltages on the secondary sides of the transformers are not known, although they could be calculated, it is simpler to calculate the Fourier series of the current, rather than calculating that of the inverter voltage and then deducing that of the current. The current on the secondary side of the transformers for the whole of a cycle can be deduced from equations (A6.9), (A6.9a), (A6.19) and (A6.20) and from Table A5.1:

$$\begin{aligned}
I_{ar} = & \frac{V_m}{hX_L} \sin(\phi+\theta_0+\gamma+\pi/12) - \frac{e^{-\beta\phi}}{2(2+\sqrt{3})} [A_1 \operatorname{sinc}\phi + A_2 \operatorname{cosk}\phi] \\
& - \frac{V_m}{hX_L} \frac{(\beta^2+k^2)}{(1+4\beta^2)} \cos\pi/12 [\sin(\phi+\theta_0+\gamma) + 2\beta\cos(\phi+\theta_0+\gamma)] + A_3 e^{-2\beta\phi} \\
& \text{for } -\pi/12 \leq \phi \leq \pi/12 \tag{A6.24}
\end{aligned}$$

$$\begin{aligned}
I_{ar} = & \frac{V_m}{hX_L} \sin(\phi+\theta_0+\gamma+\pi/12) - \frac{(\sqrt{3}+1)e^{-\beta(\phi-\pi/6)}}{2(2+\sqrt{3})} [A_1 \operatorname{sinc}(\phi-\pi/6) + A_2 \operatorname{cosk}(\phi-\pi/6)] \\
& - (\sqrt{3}-1) \frac{V_m}{hX_L} \frac{(\beta^2+k^2)}{(1+4\beta^2)} \cos\pi/12 [\sin(\phi+\theta_0+\gamma-\pi/6) + 2\beta\cos(\phi+\theta_0+\gamma-\pi/6)] \\
& + (\sqrt{3}-1)A_3 e^{-2\beta(\phi-\pi/6)} \quad \text{for } \pi/12 \leq \phi \leq \pi/4 \tag{A6.24a}
\end{aligned}$$

$$\begin{aligned}
I_{ar} = & \frac{V_m}{hX_L} \sin(\phi+\theta_0+\gamma+\pi/12) - \frac{e^{-\beta(\phi-\pi/3)}}{2} [A_1 \operatorname{sinc}(\phi-\pi/3) + A_2 \operatorname{cosk}(\phi-\pi/3)] \\
& - (2-\sqrt{3}) \frac{V_m}{hX_L} \frac{(\beta^2+k^2)}{(1+4\beta^2)} \cos\pi/12 [\sin(\phi+\theta_0+\gamma-\pi/3) + 2\beta\cos(\phi+\theta_0+\gamma-\pi/3)] \\
& + (2-\sqrt{3})A_3 e^{-2\beta(\phi-\pi/3)} \quad \text{for } \pi/4 \leq \phi \leq 5\pi/12 \tag{A6.24b}
\end{aligned}$$

$$\begin{aligned}
I_{ar} = & \frac{V_m}{hX_L} \sin(\phi+\theta_0+\gamma+\pi/12) - \frac{e^{-\beta(\phi-\pi/2)}}{2} [A_1 \operatorname{sinc}(\phi-\pi/2) + A_2 \operatorname{cosk}(\phi-\pi/2)] \\
& + (2-\sqrt{3}) \frac{V_m}{hX_L} \frac{(\beta^2+k^2)}{(1+4\beta^2)} \cos\pi/12 [\sin(\phi+\theta_0+\gamma-\pi/2) + 2\beta\cos(\phi+\theta_0+\gamma-\pi/2)] \\
& - (2-\sqrt{3})A_3 e^{-2\beta(\phi-\pi/2)} \quad \text{for } 5\pi/12 \leq \phi \leq 7\pi/12 \tag{A6.24c}
\end{aligned}$$

$$\begin{aligned}
I_{ar} = & \frac{V_m}{hX_L} \sin(\phi+\theta_0+\gamma+\pi/12) - \frac{(\sqrt{3}+1)e^{-\beta(\phi-2\pi/3)}}{2(2+\sqrt{3})} [A_1 \text{sinc}(\phi-2\pi/3) + A_2 \text{cosk}(\phi-2\pi/3)] \\
& + (\sqrt{3}-1) \frac{V_m (\beta^2+k^2)}{hX_L (1+4\beta^2)} \cos\pi/12 [\sin(\phi+\theta_0+\gamma-2\pi/3) + 2\beta \cos(\phi+\theta_0+\gamma-2\pi/3)] \\
& - (\sqrt{3}-1) A_3 e^{-2\beta(\phi-2\pi/3)} \quad \text{for } 7\pi/12 \leq \phi \leq 3\pi/4 \quad (\text{A6.24d})
\end{aligned}$$

$$\begin{aligned}
I_{ar} = & \frac{V_m}{hX_L} \sin(\phi+\theta_0+\gamma+\pi/12) - \frac{e^{-\beta(\phi-5\pi/6)}}{2(2+\sqrt{3})} [A_1 \text{sinc}(\phi-5\pi/6) + A_2 \text{cosk}(\phi-5\pi/6)] \\
& + \frac{V_m (\beta^2+k^2)}{hX_L (1+4\beta^2)} \cos\pi/12 [\sin(\phi+\theta_0+\gamma-3\pi/4) + 2\beta \cos(\phi+\theta_0+\gamma-3\pi/4)] \\
& - A_3 e^{-2\beta(\phi-5\pi/6)} \quad \text{for } 3\pi/4 \leq \phi \leq 11\pi/12 \quad (\text{A6.24e})
\end{aligned}$$

$$I_{ar} = -I_{ar}(\phi - \pi) \quad \text{for } 11\pi/12 \leq \phi \quad (\text{A6.24f})$$

The Fourier series for the current in this phase can be defined as

$$I_{ar} = \sum_{n=1}^{\infty} a_n \cos n(\phi+\pi/12) + b_n \sin n(\phi+\pi/12) \quad (\text{A6.25})$$

where

$$a_n = \frac{2}{\pi} \int_{-\pi/12}^{11\pi/12} I_{ar}(\phi) \cos n(\phi+\pi/12) d\phi \quad \text{and} \quad b_n = \frac{2}{\pi} \int_{-\pi/12}^{11\pi/12} I_{ar}(\phi) \sin n(\phi+\pi/12) d\phi$$

The Fourier series of the current in the other phases is given by the same values for a_n and b_n but are of different phase.

The Fourier series of each part can now be taken:

$$1) \frac{V_m (\beta^2 + k^2)}{hX_L (1 + 4\beta^2)} \cos \pi/12$$

$$\begin{aligned} -\pi/12 < \phi < \pi/12 & - [\sin(\phi + \theta_0 + \gamma) + 2\beta \cos(\phi + \theta_0 + \gamma)] \\ \pi/12 < \phi < \pi/4 & - (\sqrt{3}-1) [\sin(\phi + \theta_0 + \gamma - \pi/6) + 2\beta \cos(\phi + \theta_0 + \gamma - \pi/6)] \\ \pi/4 < \phi < 5\pi/12 & - (2-\sqrt{3}) [\sin(\phi + \theta_0 + \gamma - \pi/3) + 2\beta \cos(\phi + \theta_0 + \gamma - \pi/3)] \\ 5\pi/12 < \phi < 7\pi/12 & (2-\sqrt{3}) [\sin(\phi + \theta_0 + \gamma - \pi/2) + 2\beta \cos(\phi + \theta_0 + \gamma - \pi/2)] \\ 7\pi/12 < \phi < 3\pi/4 & (\sqrt{3}-1) [\sin(\phi + \theta_0 + \gamma - 2\pi/3) + 2\beta \cos(\phi + \theta_0 + \gamma - 2\pi/3)] \\ 3\pi/4 < \phi < 11\pi/12 & [\sin(\phi + \theta_0 + \gamma - 5\pi/6) + 2\beta \cos(\phi + \theta_0 + \gamma - 5\pi/6)] \end{aligned}$$

$$a_1 = -\frac{6\sqrt{2}(\sqrt{3}-1)}{\pi} \left(\frac{\pi}{12} + \frac{1}{4} \right) [\sin(\theta_0 + \gamma) + 2\beta \cos(\theta_0 + \gamma)] \quad (A6.26)$$

$$b_1 = -\frac{6\sqrt{2}(\sqrt{3}-1)}{\pi} \left(\frac{\pi}{12} - \frac{1}{4} \right) [\cos(\theta_0 + \gamma) - 2\beta \sin(\theta_0 + \gamma)] \quad (A6.26a)$$

$$n > 1 \quad a_n = -\frac{2\sqrt{2}}{\pi(n^2-1)} [\cos n\pi/12 + (\sqrt{3}-1)\cos n\pi/4 + (2-\sqrt{3})\cos 5n\pi/12] \quad (A6.26b)$$

$$n > 1 \quad b_n = -\frac{2\sqrt{2}}{\pi(n^2-1)} [\cos n\pi/12 + (\sqrt{3}-1)\cos n\pi/4 + (2-\sqrt{3})\cos 5n\pi/12] \quad (A6.26c)$$

$$[(1+\sqrt{3})\sin n\pi/12 - (\sqrt{3}-1)\cos n\pi/12][\sin(\theta_0 + \gamma) + 2\beta \cos(\theta_0 + \gamma)]$$

$$[(1+\sqrt{3})\sin n\pi/12 - (\sqrt{3}-1)\cos n\pi/12][\cos(\theta_0 + \gamma) - 2\beta \sin(\theta_0 + \gamma)]$$

2) A_3

$$\begin{aligned} -\pi/12 < \phi < \pi/12 & e^{-2\beta\phi} \\ \pi/12 < \phi < \pi/4 & (\sqrt{3}-1) e^{-2\beta(\phi-\pi/6)} \\ \pi/4 < \phi < 5\pi/12 & (2-\sqrt{3}) e^{-2\beta(\phi-\pi/3)} \\ 5\pi/12 < \phi < 7\pi/12 & -(2-\sqrt{3}) e^{-2\beta(\phi-\pi/2)} \\ 7\pi/12 < \phi < 3\pi/4 & -(\sqrt{3}-1) e^{-2\beta(\phi-2\pi/3)} \\ 3\pi/4 < \phi < 11\pi/12 & -e^{-2\beta(\phi-5\pi/6)} \end{aligned}$$

The following equations are valid for all n, including n = 1.

$$a_n = \frac{4}{\pi(n^2+4\beta^2)} [\cos n\pi/12 + (\sqrt{3}-1)\cos n\pi/4 + (2-\sqrt{3})\cos 5n\pi/12] \quad (A6.27)$$

$$\{ (e^{\beta\pi/6} + e^{-\beta\pi/6})\sin n\pi/12 + (e^{\beta\pi/6} - e^{-\beta\pi/6})2\beta \cos n\pi/12 \}$$

$$b_n = \frac{4}{\pi(n^2+4\beta^2)} [\cos n\pi/12 + (\sqrt{3}-1)\cos n\pi/4 + (2-\sqrt{3})\cos 5n\pi/12] \quad (A6.27a)$$

$$\{ (e^{\beta\pi/6} - e^{-\beta\pi/6})\cos n\pi/12 - (e^{\beta\pi/6} + e^{-\beta\pi/6})2\beta \sin n\pi/12 \}$$

$$3) \frac{A_1}{2(2+\sqrt{3})}$$

$$\begin{aligned} -\pi/12 < \phi < \pi/12 & - e^{-\beta\phi} \text{sink}\phi \\ \pi/12 < \phi < \pi/4 & - (\sqrt{3}+1) e^{-\beta(\phi-\pi/6)} \text{sink}(\phi-\pi/6) \\ \pi/4 < \phi < 5\pi/12 & - (\sqrt{3}+2) e^{-\beta(\phi-\pi/3)} \text{sink}(\phi-\pi/3) \\ 5\pi/12 < \phi < 7\pi/12 & - (\sqrt{3}+2) e^{-\beta(\phi-\pi/2)} \text{sink}(\phi-\pi/2) \\ 7\pi/12 < \phi < 3\pi/4 & - (\sqrt{3}+2) e^{-\beta(\phi-2\pi/3)} \text{sink}(\phi-2\pi/3) \\ 3\pi/4 < \phi < 11\pi/12 & - e^{-\beta(\phi-5\pi/6)} \text{sink}(\phi-5\pi/6) \end{aligned}$$

$$\begin{aligned} a_n = \frac{4}{\pi h_n^2} & [\text{sinn}\pi/12 + (\sqrt{3}+1)\text{sinn}\pi/4 + (\sqrt{3}+2)\text{sin}5\pi/12] \\ & \{ k \cos k\pi/12 [(e^{\beta\pi/12} - e^{-\beta\pi/12})(2\beta n) \cos n\pi/12 - \\ & (e^{\beta\pi/12} + e^{-\beta\pi/12})(\beta^2 + k^2 - n^2) \text{sinn}\pi/12] - \\ & n \text{sink}\pi/12 [(e^{\beta\pi/12} + e^{-\beta\pi/12})(\beta^2 - k^2 + n^2) \cos n\pi/12 + \\ & \beta \text{sink}\pi/12 [(e^{\beta\pi/12} - e^{-\beta\pi/12})(\beta^2 + k^2 + n^2) \text{sinn}\pi/12]] \} \quad (\text{A6-28}) \end{aligned}$$

$$\begin{aligned} b_n = -\frac{4}{\pi h_n^2} & [\text{sinn}\pi/12 + (\sqrt{3}+1)\text{sinn}\pi/4 + (\sqrt{3}+2)\text{sin}5\pi/12] \\ & \{ k \cos k\pi/12 [(e^{\beta\pi/12} - e^{-\beta\pi/12})(\beta^2 + k^2 - n^2) \cos n\pi/12 + \\ & (e^{\beta\pi/12} + e^{-\beta\pi/12})(2\beta n) \text{sinn}\pi/12] - \\ & \beta \text{sink}\pi/12 [(e^{\beta\pi/12} + e^{-\beta\pi/12})(\beta^2 + k^2 + n^2) \cos n\pi/12 - \\ & n \text{sink}\pi/12 [(e^{\beta\pi/12} - e^{-\beta\pi/12})(\beta^2 - k^2 + n^2) \text{sinn}\pi/12]] \} \quad (\text{A6-28a}) \end{aligned}$$

$$4) \frac{A_2}{2(2+\sqrt{3})}$$

$$\begin{aligned} -\pi/12 < \phi < \pi/12 & - e^{-\beta\phi} \text{cosk}\phi \\ \pi/12 < \phi < \pi/4 & - (\sqrt{3}+1) e^{-\beta(\phi-\pi/6)} \text{cosk}(\phi-\pi/6) \\ \pi/4 < \phi < 5\pi/12 & - (\sqrt{3}+2) e^{-\beta(\phi-\pi/3)} \text{cosk}(\phi-\pi/3) \\ 5\pi/12 < \phi < 7\pi/12 & - (\sqrt{3}+2) e^{-\beta(\phi-\pi/2)} \text{cosk}(\phi-\pi/2) \\ 7\pi/12 < \phi < 3\pi/4 & - (\sqrt{3}+2) e^{-\beta(\phi-2\pi/3)} \text{cosk}(\phi-2\pi/3) \\ 3\pi/4 < \phi < 11\pi/12 & - e^{-\beta(\phi-5\pi/6)} \text{cosk}(\phi-5\pi/6) \end{aligned}$$

$$\begin{aligned} a_n = \frac{4}{\pi h_n^2} & [\text{sinn}\pi/12 + (\sqrt{3}+1)\text{sinn}\pi/4 + (\sqrt{3}+2)\text{sin}5\pi/12] \\ & \{ \text{ksink}\pi/12[(e^{\beta\pi/12}+e^{-\beta\pi/12})(2\beta n)\text{cosn}\pi/12 - \\ & (e^{\beta\pi/12}-e^{-\beta\pi/12})(\beta^2+k^2-n^2)\text{sinn}\pi/12] + \\ & n\text{cosk}\pi/12[(e^{\beta\pi/12}-e^{-\beta\pi/12})(\beta^2-k^2+n^2)\text{cosn}\pi/12 - \\ & \beta\text{cosk}\pi/12[(e^{\beta\pi/12}+e^{-\beta\pi/12})(\beta^2+k^2+n^2)\text{sinn}\pi/12]] \} \quad (\text{A6}\cdot 29) \end{aligned}$$

$$\begin{aligned} b_n = -\frac{4}{\pi h_n^2} & [\text{sinn}\pi/12 + (\sqrt{3}+1)\text{sinn}\pi/4 + (\sqrt{3}+2)\text{sin}5\pi/12] \\ & \{ \text{ksink}\pi/12[(e^{\beta\pi/12}+e^{-\beta\pi/12})(\beta^2+k^2-n^2)\text{cosn}\pi/12 + \\ & (e^{\beta\pi/12}-e^{-\beta\pi/12})(2\beta n)\text{sinn}\pi/12] + \\ & \beta\text{cosk}\pi/12[(e^{\beta\pi/12}+e^{-\beta\pi/12})(\beta^2+k^2+n^2)\text{cosn}\pi/12 + \\ & n\text{cosk}\pi/12[(e^{\beta\pi/12}+e^{-\beta\pi/12})(\beta^2-k^2+n^2)\text{sinn}\pi/12]] \} \quad (\text{A6}\cdot 29\text{a}) \end{aligned}$$

All parts of equations (A6·26) to (A6·29), together with the term describing the current which would be produced in a conventional R, L, $3C/(2+\sqrt{3})$ circuit, gives the Fourier series of the current on the secondary side of the transformers.

The Fourier series on the primary side can be deduced from these equations, with similar contributions from the Fourier series of I_{br} , and equation (A6·23).

For $n = 1$ this simplifies to

$$I_{R1} = \frac{V_m}{hX_L} \sin(\phi + \theta_0 + \gamma) + a_1 \cos\phi + b_1 \sin\phi \quad (\text{A6-30})$$

where

a_1 and b_1 are the sum of all of the above a_1 and b_1 terms respectively, from equations (A6-26) to (A6-29).

The dependence on θ_0 of a_n and b_n is as either $\cos\theta_0$ and $\sin\theta_0$:

$$a_n = a_{nc} \cos\theta_0 + a_{ns} \sin\theta_0 \quad (\text{A6-31})$$

$$b_n = b_{nc} \cos\theta_0 + b_{ns} \sin\theta_0 \quad (\text{A6-31a})$$

Substituting in (A6-30) and replacing ϕ with $\theta - \theta_0$, simplifying and separating gives

$$I_q = \frac{V_m}{hX_L} \sin\gamma + a_{1c} + (a_{1s} - b_{1c}) \frac{\sin 2\theta_0}{2} - (a_{1c} + b_{1s}) \sin^2\theta_0 \quad (\text{A6-32})$$

$$I_p = \frac{V_m}{hX_L} \cos\gamma + b_{1c} + (a_{1s} + b_{1c}) \sin^2\theta_0 + (a_{1c} + b_{1s}) \frac{\sin 2\theta_0}{2} \quad (\text{A6-32a})$$

By analogy with earlier work

$$q_1 = \frac{\sin\gamma}{h} + \frac{X_L}{V_m} a_1 \Big|_{\theta_0=0} = 0 \quad (\text{A6-33})$$

$$p_1 = \frac{\cos\gamma}{\beta h} + \frac{X_L}{\beta V_m} b_1 \Big|_{\theta_0=0} = 0 \quad (\text{A6-33a})$$

$$q_2 = \frac{\beta X_L}{V_m} (a_1 \Big|_{\theta_0=\pi/2} - b_1 \Big|_{\theta_0=0}) \quad (\text{A6-33b})$$

$$q_3 = -\frac{X_L}{V_m} (a_1 \Big|_{\theta_0=0} - b_1 \Big|_{\theta_0=\pi/2}) \quad (\text{A6-33c})$$

The argument that q_3 must be zero, from appendix 3, is also true in this case. Again this was verified numerically. The contributions to the fundamental component of the current are therefore given by

$$I_q = \frac{V_m}{X_L} \left(q_1 + q_2 \frac{\sin 2\theta_0}{2\beta} \right) \quad (\text{A6-34})$$

$$I_p = \frac{\beta V_m}{X_L} \left(p_1 + q_2 \frac{\sin^2\theta_0}{\beta^2} \right) \quad (\text{A6-34a})$$

For the harmonics, after simplifying,

$$|I_n| = \sqrt{a_n^2 + b_n^2} \quad (\text{A6-35})$$

Expanding and substituting from (A6-31) and (A6-31a) gives, after simplifying,

$$|I_n| = \sqrt{[a_{nc}^2 + b_{nc}^2] \cos^2 \theta_0 + [a_{ns}^2 + b_{ns}^2] \sin^2 \theta_0 + [a_{nc} a_{ns} + b_{nc} b_{ns}] \sin 2\theta_0} \quad (\text{A6-36})$$

By analogy with the earlier work, this is written as,

$$|I_n| = \frac{V_m}{X_L} |t_n| \quad (\text{A6-37})$$

Plotting (A6-36), indicates an approximately linear relationship between t_n and θ_{ob} , hence

$$I_{nc} \approx \frac{V_m}{X_L} [c_n - s_n \theta_{ob}] \quad (\text{A6-38})$$

Using the small θ_0 approximation in (A6-36), and comparing with (A6-38), gives

$$c_n = \frac{X_L}{V_m} \sqrt{a_n^2 + b_n^2} \quad | \quad \theta_0 = 0 \quad (\text{A6-39})$$

$$s_n = -\frac{\beta X_L}{V_m} \sqrt{a_n^2 + b_n^2} \quad | \quad \theta_0 = \pi/2 \quad (\text{A6-39a})$$

Appendix 7

Analysis of a Twenty-Four Pulse STATCON with Parallel Connected Transformer Primaries

a) Determination of the Current on the Transformer Secondary Side

The analysis of the circuit on the secondary side of the transformers can be performed in a similar way to that of the parallel connected twelve pulse circuit. The voltages at the secondaries of the transformers are regarded as being a twelve phase unbalanced source. The relationship between the currents in the first interval and the current in one of the phases during all of the intervals is given in table A7.1.

Table A7.1. Current Relationships in the Twenty-Four Pulse Equipment.

ϕ	$I_{ar}(\phi)$
$-\pi/8 \leq \phi \leq -\pi/24$	$I_{ar}(\phi)$
$-\pi/24 \leq \phi \leq \pi/24$	$-I_{dy}(\phi - \pi/12)$
$\pi/24 \leq \phi \leq \pi/8$	$-I_{cy}(\phi - \pi/6)$
$\pi/8 \leq \phi \leq 5\pi/24$	$-I_{by}(\phi - \pi/4)$
$5\pi/24 \leq \phi \leq 7\pi/24$	$-I_{ay}(\phi - \pi/3)$
$7\pi/24 \leq \phi \leq 9\pi/24$	$I_{db}(\phi - 5\pi/12)$
$9\pi/24 \leq \phi \leq 11\pi/24$	$I_{cb}(\phi - \pi/2)$
$11\pi/24 \leq \phi \leq 13\pi/24$	$I_{bb}(\phi - 7\pi/12)$
$13\pi/24 \leq \phi \leq 15\pi/24$	$I_{ab}(\phi - 2\pi/3)$
$15\pi/24 \leq \phi \leq 17\pi/24$	$-I_{dr}(\phi - 3\pi/4)$
$17\pi/24 \leq \phi \leq 19\pi/24$	$-I_{cr}(\phi - 5\pi/6)$
$19\pi/24 \leq \phi \leq 21\pi/24$	$-I_{br}(\phi - 11\pi/12)$
$21\pi/24 \leq \phi$	$-I_{ar}(\phi - \pi)$

The circuit during the first era is shown in figure A7.1.

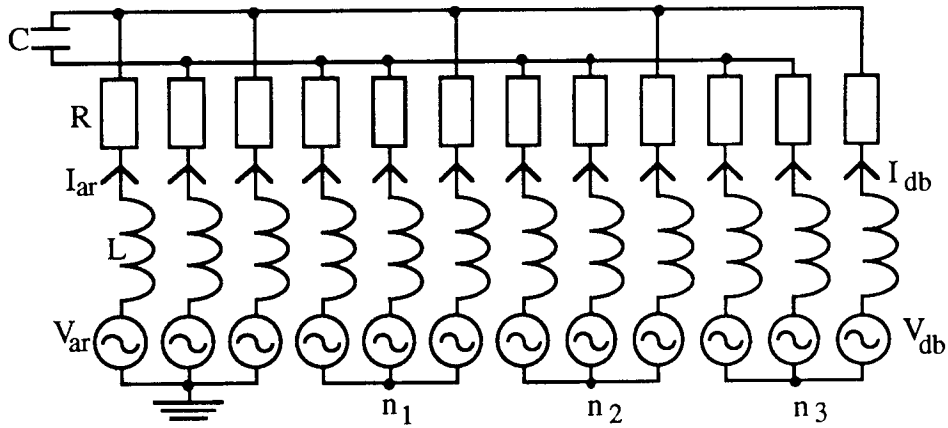


Figure A7.1. Twenty-Four Pulse STATCON During the Interval $-\pi/8 < \phi < -\pi/24$.

The voltage sources, relative to their star points, with the star point of the secondary of the first transformer earthed, are defined as

$$V_{ar} = V_m \sin(\phi + \theta_0 + \pi/8)$$

$$V_{ay} = V_m \sin(\phi + \theta_0 - 13\pi/24)$$

$$V_{ab} = V_m \sin(\phi + \theta_0 - 29\pi/24)$$

$$V_{br} = V_{brn} - V_{n1} = V_m \sin(\phi + \theta_0 + \pi/24)$$

$$V_{by} = V_{byn} - V_{n1} = V_m \sin(\phi + \theta_0 - 5\pi/8)$$

$$V_{bb} = V_{bbn} - V_{n1} = V_m \sin(\phi + \theta_0 - 31\pi/24)$$

$$V_{cr} = V_{crn} - V_{n2} = V_m \sin(\phi + \theta_0 - \pi/24)$$

$$V_{cy} = V_{cyn} - V_{n2} = V_m \sin(\phi + \theta_0 - 17\pi/24)$$

$$V_{cb} = V_{cbn} - V_{n2} = V_m \sin(\phi + \theta_0 - 11\pi/8)$$

$$V_{dr} = V_{drn} - V_{n3} = V_m \sin(\phi + \theta_0 - \pi/8)$$

$$V_{dy} = V_{dyn} - V_{n3} = V_m \sin(\phi + \theta_0 - 19\pi/24)$$

$$V_{db} = V_{dbn} - V_{n3} = V_m \sin(\phi + \theta_0 - 35\pi/24) \quad (A7.1)$$

Again the sums of the voltages and the currents out of each transformer are zero:

$$V_{ab} = -(V_{ar} + V_{ay}) \text{ etc.}$$

$$I_{ab} = -(I_{ar} + I_{ay}) \text{ etc.} \quad (A7.2)$$

The current through the capacitor, from - to +, is given by

$$I_c = I_{ay} - (I_{bb} + I_{cb} + I_{db}) \quad (A7.3)$$

From figure A7.1 the following equations can be deduced

$$\begin{aligned}
 V_{ar} - V_+ &= X_L \frac{dI_{ar}}{d\phi} + R I_{ar} \\
 V_{ay} - V_+ &= X_L \frac{dI_{ay}}{d\phi} + R I_{ay} - V_c \\
 V_{ab} - V_+ &= X_L \frac{dI_{ab}}{d\phi} + R I_{ab} \\
 V_{br} + V_{n1} - V_+ &= X_L \frac{dI_{br}}{d\phi} + R I_{br} - V_c \\
 V_{by} + V_{n1} - V_+ &= X_L \frac{dI_{by}}{d\phi} + R I_{by} - V_c \\
 V_{bb} + V_{n1} - V_+ &= X_L \frac{dI_{bb}}{d\phi} + R I_{bb} \\
 V_{cr} + V_{n2} - V_+ &= X_L \frac{dI_{cr}}{d\phi} + R I_{cr} - V_c \\
 V_{cy} + V_{n2} - V_+ &= X_L \frac{dI_{cy}}{d\phi} + R I_{cy} - V_c \\
 V_{cb} + V_{n2} - V_+ &= X_L \frac{dI_{cb}}{d\phi} + R I_{cb} \\
 V_{dr} + V_{n3} - V_+ &= X_L \frac{dI_{dr}}{d\phi} + R I_{dr} - V_c \\
 V_{dy} + V_{n3} - V_+ &= X_L \frac{dI_{dy}}{d\phi} + R I_{dy} - V_c \\
 V_{db} + V_{n3} - V_+ &= X_L \frac{dI_{db}}{d\phi} + R I_{db}
 \end{aligned} \tag{A7.4}$$

where, as in earlier work,

$$V_c = -X_C \int I_c d\phi \tag{A7.4a}$$

Summing the first three equations of (A7.4) gives

$$V_+ = \frac{V_c}{3} \tag{A7.5}$$

and summing the second, third and fourth sets of three equations gives, during this interval,

$$V_{n1} = V_{n2} = V_{n3} = -\frac{V_c}{3} \tag{A7.6}$$

Although the potentials of these three star points are the same during this era, they cannot be connected because they will not be the same during different eras; during this interval the devices which are turned on are the same in each inverter, in different eras different devices will be turned on giving different voltages at the star points.

Substituting for V_+ , V_{n1} , V_{n2} and V_{n3} into (A7.4), using (A7.3), substituting from (A7.1), differentiating again, and simplifying gives

$$\frac{d^2 I_c}{d\phi^2} + 2\beta \frac{dI_c}{d\phi} + \frac{8X_C}{3X_L} I_c = \frac{V_m}{2X_L} \frac{1}{\sin\pi/24} \sin(\phi+\theta_0+\pi/12) \quad (\text{A7.7})$$

Integrating (A7.7), assuming $R < 2\sqrt{8X_C X_L/3}$, gives

$$I_c = -\frac{V_m}{2hX_L} \frac{1}{\sin\pi/24} \cos(\phi+\theta_0+\gamma+\pi/12) + A_1 e^{-\beta\phi} \sin k\phi + A_2 e^{-\beta\phi} \cos k\phi \quad (\text{A7.8})$$

where

$$k = \sqrt{\frac{8X_C}{3X_L} - \beta^2} \quad (\text{A7.8a})$$

Substituting (A7.8) in (A7.4a) and integrating gives, after simplifying,

$$\begin{aligned} \frac{V_c}{X_C} &= \frac{V_m}{2hX_L} \frac{1}{\sin\pi/24} \sin(\phi+\theta_0+\gamma+\pi/12) \\ &+ \frac{e^{-\beta\phi}}{(\beta^2+k^2)} [(\beta A_1 - k A_2) \sin k\phi + (k A_1 + \beta A_2) \cos k\phi] \end{aligned} \quad (\text{A7.9})$$

Substituting for V_c , from (A7.9), in the relevant parts of (A7.4), using (A7.5), (A7.6) and (A7.8a) gives, after integrating and simplifying,

$$\begin{aligned} I_{ar} &= \frac{V_m}{hX_L} \sin(\phi+\theta_0+\gamma+\pi/8) - \frac{e^{-\beta\phi}}{8} [A_1 \sin k\phi + A_2 \cos k\phi] + A_3 e^{-2\beta\phi} \\ &+ \frac{V_m}{16hX_L} \frac{(\beta^2+k^2)}{(1+4\beta^2)} \frac{1}{\sin\pi/24} [\cos(\phi+\theta_0+\gamma+\pi/12) - 2\beta \sin(\phi+\theta_0+\gamma+\pi/12)] \\ &- \frac{V_m}{hX_L} \frac{(\beta^2+k^2)}{(1+4\beta^2)} [\sin(\phi+\theta_0+\gamma+\pi/8) + 2\beta \cos(\phi+\theta_0+\gamma+\pi/8)] \end{aligned} \quad (\text{A7.10})$$

$$\begin{aligned} I_{br} &= \frac{V_m}{hX_L} \sin(\phi+\theta_0+\gamma+\pi/24) + \frac{e^{-\beta\phi}}{8} [A_1 \sin k\phi + A_2 \cos k\phi] + A_4 e^{-2\beta\phi} \\ &- \frac{V_m}{16hX_L} \frac{(\beta^2+k^2)}{(1+4\beta^2)} \frac{1}{\sin\pi/24} [\cos(\phi+\theta_0+\gamma+\pi/12) - 2\beta \sin(\phi+\theta_0+\gamma+\pi/12)] \\ &- \frac{V_m}{hX_L} \frac{(\beta^2+k^2)}{(1+4\beta^2)} [\sin(\phi+\theta_0+\gamma+\pi/24) + 2\beta \cos(\phi+\theta_0+\gamma+\pi/24)] \end{aligned} \quad (\text{A7.10a})$$

$$\begin{aligned} I_{by} &= \frac{V_m}{hX_L} \sin(\phi+\theta_0+\gamma-5\pi/8) + \frac{e^{-\beta\phi}}{8} [A_1 \sin k\phi + A_2 \cos k\phi] + A_5 e^{-2\beta\phi} \\ &- \frac{V_m}{16hX_L} \frac{(\beta^2+k^2)}{(1+4\beta^2)} \frac{1}{\sin\pi/24} [\cos(\phi+\theta_0+\gamma+\pi/12) - 2\beta \sin(\phi+\theta_0+\gamma+\pi/12)] \\ &- \frac{V_m}{hX_L} \frac{(\beta^2+k^2)}{(1+4\beta^2)} [\sin(\phi+\theta_0+\gamma-5\pi/8) + 2\beta \cos(\phi+\theta_0+\gamma-5\pi/8)] \end{aligned} \quad (\text{A7.10b})$$

$$\begin{aligned}
I_{cr} = & \frac{V_m}{hX_L} \sin(\phi+\theta_0+\gamma-\pi/24) + \frac{e^{-\beta\phi}}{8} [A_1 \sin k\phi + A_2 \cos k\phi] + A_6 e^{-2\beta\phi} \\
& - \frac{V_m}{16hX_L} \frac{(\beta^2+k^2)}{(1+4\beta^2)} \frac{1}{\sin\pi/24} [\cos(\phi+\theta_0+\gamma+\pi/12) - 2\beta \sin(\phi+\theta_0+\gamma+\pi/12)] \\
& - \frac{V_m}{hX_L} \frac{(\beta^2+k^2)}{(1+4\beta^2)} [\sin(\phi+\theta_0+\gamma-\pi/24) + 2\beta \cos(\phi+\theta_0+\gamma-\pi/24)] \quad (A7.10c)
\end{aligned}$$

$$\begin{aligned}
I_{cy} = & \frac{V_m}{hX_L} \sin(\phi+\theta_0+\gamma-17\pi/24) + \frac{e^{-\beta\phi}}{8} [A_1 \sin k\phi + A_2 \cos k\phi] + A_7 e^{-2\beta\phi} \\
& - \frac{V_m}{16hX_L} \frac{(\beta^2+k^2)}{(1+4\beta^2)} \frac{1}{\sin\pi/24} [\cos(\phi+\theta_0+\gamma+\pi/12) - 2\beta \sin(\phi+\theta_0+\gamma+\pi/12)] \\
& - \frac{V_m}{hX_L} \frac{(\beta^2+k^2)}{(1+4\beta^2)} [\sin(\phi+\theta_0+\gamma-17\pi/24) + 2\beta \cos(\phi+\theta_0+\gamma-17\pi/24)] \quad (A7.10d)
\end{aligned}$$

$$\begin{aligned}
I_{dr} = & \frac{V_m}{hX_L} \sin(\phi+\theta_0+\gamma-\pi/8) + \frac{e^{-\beta\phi}}{8} [A_1 \sin k\phi + A_2 \cos k\phi] + A_8 e^{-2\beta\phi} \\
& - \frac{V_m}{16hX_L} \frac{(\beta^2+k^2)}{(1+4\beta^2)} \frac{1}{\sin\pi/24} [\cos(\phi+\theta_0+\gamma+\pi/12) - 2\beta \sin(\phi+\theta_0+\gamma+\pi/12)] \\
& - \frac{V_m}{hX_L} \frac{(\beta^2+k^2)}{(1+4\beta^2)} [\sin(\phi+\theta_0+\gamma-\pi/8) + 2\beta \cos(\phi+\theta_0+\gamma-\pi/8)] \quad (A7.10e)
\end{aligned}$$

$$\begin{aligned}
I_{dy} = & \frac{V_m}{hX_L} \sin(\phi+\theta_0+\gamma-19\pi/24) + \frac{e^{-\beta\phi}}{8} [A_1 \sin k\phi + A_2 \cos k\phi] + A_9 e^{-2\beta\phi} \\
& - \frac{V_m}{16hX_L} \frac{(\beta^2+k^2)}{(1+4\beta^2)} \frac{1}{\sin\pi/24} [\cos(\phi+\theta_0+\gamma+\pi/12) - 2\beta \sin(\phi+\theta_0+\gamma+\pi/12)] \\
& - \frac{V_m}{hX_L} \frac{(\beta^2+k^2)}{(1+4\beta^2)} [\sin(\phi+\theta_0+\gamma-19\pi/24) + 2\beta \cos(\phi+\theta_0+\gamma-19\pi/24)] \quad (A7.10f)
\end{aligned}$$

Substituting (A7.10a) and (A7.10b) in the appropriate part of (A7.2) and simplifying gives

$$\begin{aligned}
I_{bb} = & \frac{V_m}{hX_L} \sin(\phi+\theta_0+\gamma-31\pi/24) - \frac{e^{-\beta\phi}}{4} [A_1 \sin k\phi + A_2 \cos k\phi] - (A_4+A_5)e^{-2\beta\phi} \\
& + \frac{V_m}{16hX_L} \frac{(\beta^2+k^2)}{(1+4\beta^2)} \frac{1}{\sin\pi/24} [\cos(\phi+\theta_0+\gamma+\pi/12) - 2\beta \sin(\phi+\theta_0+\gamma+\pi/12)] \\
& - \frac{V_m}{hX_L} \frac{(\beta^2+k^2)}{(1+4\beta^2)} [\sin(\phi+\theta_0+\gamma-31\pi/24) + 2\beta \cos(\phi+\theta_0+\gamma-31\pi/24)] \quad (A7.10g)
\end{aligned}$$

and performing the same operations using (A7.10c) and (A7.10d) gives

$$\begin{aligned}
I_{cb} = & \frac{V_m}{hX_L} \sin(\phi+\theta_0+\gamma-11\pi/8) - \frac{e^{-\beta\phi}}{4} [A_1 \sin k\phi + A_2 \cos k\phi] - (A_6+A_7)e^{-2\beta\phi} \\
& + \frac{V_m}{8hX_L} \frac{(\beta^2+k^2)}{(1+4\beta^2)} \frac{1}{\sin\pi/24} [\cos(\phi+\theta_0+\gamma+\pi/12) - 2\beta \sin(\phi+\theta_0+\gamma+\pi/12)] \\
& - \frac{V_m}{hX_L} \frac{(\beta^2+k^2)}{(1+4\beta^2)} [\sin(\phi+\theta_0+\gamma-11\pi/8) + 2\beta \cos(\phi+\theta_0+\gamma-11\pi/8)] \quad (A7.10h)
\end{aligned}$$

and for I_{db} :

$$\begin{aligned}
 I_{db} = & \frac{V_m}{hX_L} \sin(\phi+\theta_0+\gamma-35\pi/24) - \frac{e^{-\beta\phi}}{4} [A_1 \sin k\phi + A_2 \cos k\phi] - (A_8+A_9)e^{-2\beta\phi} \\
 & + \frac{V_m}{8hX_L} \frac{(\beta^2+k^2)}{(1+4\beta^2)} \frac{1}{\sin\pi/24} [\cos(\phi+\theta_0+\gamma+\pi/12) - 2\beta \sin(\phi+\theta_0+\gamma+\pi/12)] \\
 & - \frac{V_m}{hX_L} \frac{(\beta^2+k^2)}{(1+4\beta^2)} [\sin(\phi+\theta_0+\gamma-35\pi/24) + 2\beta \cos(\phi+\theta_0+\gamma-35\pi/24)] \quad (A7-10i)
 \end{aligned}$$

Substituting (A7-10g), (A7-10h), (A7-10i) and (A7-8) in (A7-3) gives, after simplifying,

$$\begin{aligned}
 I_{ay} = & \frac{V_m}{hX_L} \sin(\phi+\theta_0+\gamma-13\pi/24) + \frac{e^{-\beta\phi}}{4} [A_1 \sin k\phi + A_2 \cos k\phi] \\
 & - (A_4 + A_5 + A_6 + A_7 + A_8 + A_9)e^{-2\beta\phi} \\
 & - \frac{V_m}{8hX_L} \frac{(\beta^2+k^2)}{(1+4\beta^2)} \frac{1}{\sin\pi/24} [\cos(\phi+\theta_0+\gamma+\pi/12) - 2\beta \sin(\phi+\theta_0+\gamma+\pi/12)] \\
 & - \frac{V_m}{hX_L} \frac{(\beta^2+k^2)}{(1+4\beta^2)} [\sin(\phi+\theta_0+\gamma-13\pi/24) + 2\beta \cos(\phi+\theta_0+\gamma-13\pi/24)] \quad (A7-10j)
 \end{aligned}$$

Substituting (A7-10j) and (A7-10) in (A7-2) gives

$$\begin{aligned}
 I_{ab} = & \frac{V_m}{hX_L} \sin(\phi+\theta_0+\gamma-29\pi/24) - \frac{e^{-\beta\phi}}{8} [A_1 \sin k\phi + A_2 \cos k\phi] \\
 & + (-A_3 + A_4 + A_5 + A_6 + A_7 + A_8 + A_9)e^{-2\beta\phi} \\
 & + \frac{V_m}{16hX_L} \frac{(\beta^2+k^2)}{(1+4\beta^2)} \frac{1}{\sin\pi/24} [\cos(\phi+\theta_0+\gamma+\pi/12) - 2\beta \sin(\phi+\theta_0+\gamma+\pi/12)] \\
 & - \frac{V_m}{hX_L} \frac{(\beta^2+k^2)}{(1+4\beta^2)} [\sin(\phi+\theta_0+\gamma-29\pi/24) + 2\beta \cos(\phi+\theta_0+\gamma-29\pi/24)] \quad (A7-10k)
 \end{aligned}$$

The boundary conditions are

$$V_c(\phi = -\pi/24) = V_c(\phi = -\pi/8) \quad (A7-11)$$

$$I_{ar}(\phi = -\pi/24) = -I_{dy}(\phi = -\pi/8) \quad (A7-11a)$$

$$I_{dy}(\phi = -\pi/24) = I_{cy}(\phi = -\pi/8) \quad (A7-11b)$$

$$I_{cy}(\phi = -\pi/24) = I_{by}(\phi = -\pi/8) \quad (A7-11c)$$

$$I_{by}(\phi = -\pi/24) = I_{ay}(\phi = -\pi/8) \quad (A7-11d)$$

$$I_{ay}(\phi = -\pi/24) = -I_{db}(\phi = -\pi/8) \quad (A7-11e)$$

$$I_{db}(\phi = -\pi/24) = I_{cb}(\phi = -\pi/8) \quad (A7-11f)$$

$$I_{cb}(\phi = -\pi/24) = I_{bb}(\phi = -\pi/8) \quad (A7-11g)$$

$$I_{bb}(\phi = -\pi/24) = I_{ab}(\phi = -\pi/8) \quad (A7-11h)$$

Using (A7-9), or the appropriate parts of (A7-10), and simplifying gives

$$\begin{aligned}
 & \frac{V_m}{hX_L} (\beta^2+k^2) \cos(\theta_0+\gamma) = \\
 & e^{\beta\pi/24} \{ A_1 [\beta(\sin k\pi/24 - e^{\beta\pi/12} \sin k\pi/8) - k(\cos k\pi/24 - e^{\beta\pi/12} \cos k\pi/8)] - \\
 & A_2 [\beta(\cos k\pi/24 - e^{\beta\pi/12} \cos k\pi/8) + k(\sin k\pi/24 - e^{\beta\pi/12} \sin k\pi/8)] \} \quad (A7-12)
 \end{aligned}$$

$$\frac{V_m (\beta^2+k^2)}{hX_L (1+4\beta^2)} [\sin(\theta_0+\gamma) + 2\beta\cos(\theta_0+\gamma)] = e^{\beta\pi/24} \{ A_1[\sin\pi/24 - e^{\beta\pi/12}\sin\pi/8] - A_2[\cos\pi/24 - e^{\beta\pi/12}\cos\pi/8] \} + 8A_3e^{\beta\pi/12} + 8A_9e^{\beta\pi/4} \quad (A7\cdot12a)$$

$$\frac{V_m (\beta^2+k^2)}{hX_L (1+4\beta^2)} [\sin(\theta_0+\gamma) + 2\beta\cos(\theta_0+\gamma)] = e^{\beta\pi/24} \{ A_1[\sin\pi/24 - e^{\beta\pi/12}\sin\pi/8] - A_2[\cos\pi/24 - e^{\beta\pi/12}\cos\pi/8] \} - 8A_9e^{\beta\pi/12} + 8A_7e^{\beta\pi/4} \quad (A7\cdot12b)$$

$$\frac{V_m (\beta^2+k^2)}{hX_L (1+4\beta^2)} [\sin(\theta_0+\gamma) + 2\beta\cos(\theta_0+\gamma)] = e^{\beta\pi/24} \{ A_1[\sin\pi/24 - e^{\beta\pi/12}\sin\pi/8] - A_2[\cos\pi/24 - e^{\beta\pi/12}\cos\pi/8] \} - 8A_7e^{\beta\pi/12} + 8A_5e^{\beta\pi/4} \quad (A7\cdot12c)$$

$$\frac{V_m (\beta^2+k^2)}{hX_L (1+4\beta^2)} [\sin(\theta_0+\gamma) + 2\beta\cos(\theta_0+\gamma)] + \frac{2\sqrt{2}}{(\sqrt{3}-1)} \frac{V_m (\beta^2+k^2)}{hX_L (1+4\beta^2)} \cos\pi/24 [\cos(\theta_0+\gamma-\pi/24) - 2\beta\sin(\theta_0+\gamma-\pi/24)] = e^{\beta\pi/24} \{ A_1[\sin\pi/24 - e^{\beta\pi/12}\sin\pi/8] - A_2[\cos\pi/24 - e^{\beta\pi/12}\cos\pi/8] \} - 8A_5e^{\beta\pi/12} - 8(A_4 + A_5 + A_6 + A_7 + A_8 + A_9)e^{\beta\pi/4} \quad (A7\cdot12d)$$

$$\frac{V_m (\beta^2+k^2)}{hX_L (1+4\beta^2)} [\sin(\theta_0+\gamma) + 2\beta\cos(\theta_0+\gamma)] = e^{\beta\pi/24} \{ A_1[\sin\pi/24 - e^{\beta\pi/12}\sin\pi/8] - A_2[\cos\pi/24 - e^{\beta\pi/12}\cos\pi/8] \} + 4(A_4 + A_5 + A_6 + A_7 + A_8 + A_9)e^{\beta\pi/12} + 4(A_8 + A_9)e^{\beta\pi/4} \quad (A7\cdot12e)$$

$$\frac{V_m (\beta^2+k^2)}{hX_L (1+4\beta^2)} [\sin(\theta_0+\gamma) + 2\beta\cos(\theta_0+\gamma)] = e^{\beta\pi/24} \{ A_1[\sin\pi/24 - e^{\beta\pi/12}\sin\pi/8] - A_2[\cos\pi/24 - e^{\beta\pi/12}\cos\pi/8] \} - 4(A_8 + A_9)e^{\beta\pi/12} + 4(A_6 + A_7)e^{\beta\pi/4} \quad (A7\cdot12f)$$

$$\frac{V_m (\beta^2+k^2)}{hX_L (1+4\beta^2)} [\sin(\theta_0+\gamma) + 2\beta\cos(\theta_0+\gamma)] = e^{\beta\pi/24} \{ A_1[\sin\pi/24 - e^{\beta\pi/12}\sin\pi/8] - A_2[\cos\pi/24 - e^{\beta\pi/12}\cos\pi/8] \} - 4(A_6 + A_7)e^{\beta\pi/12} + 4(A_4 + A_5)e^{\beta\pi/4} \quad (A7\cdot12g)$$

$$\begin{aligned} & \frac{V_m (\beta^2+k^2)}{hX_L (1+4\beta^2)} [\sin(\theta_0+\gamma) + 2\beta\cos(\theta_0+\gamma)] \\ & - \frac{2\sqrt{2}}{(\sqrt{3}-1)} \frac{V_m (\beta^2+k^2)}{hX_L (1+4\beta^2)} \cos\pi/24 [\cos(\theta_0+\gamma+\pi/24) - 2\beta\sin(\theta_0+\gamma+\pi/24)] = \\ & e^{\beta\pi/24} \{ A_1 [2\sin\pi/24 - e^{\beta\pi/12}\sin\pi/8] - A_2 [2\cos\pi/24 - e^{\beta\pi/12}\cos\pi/8] \} \\ & - 8(A_4 + A_5)e^{\beta\pi/12} - 8(-A_3 + A_4 + A_5 + A_6 + A_7 + A_8 + A_9)e^{\beta\pi/4} \quad (A7.12h) \end{aligned}$$

Again matrix manipulation can be used to compute A_1 to A_9 .

b) Determination of the Current on the Transformer Primary Side

The transformer phase shifts are 15° apart and are symmetrically disposed about zero, i.e. at -22.5° , -7.5° , 7.5° , and 22.5° . The turns ratios are defined in figure A7.2.

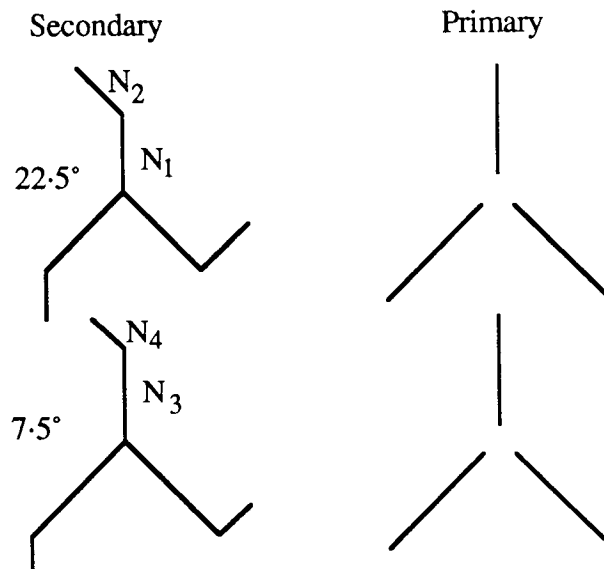


Figure A7.2. Turns Ratios for the Advanced Phase Shifting Transformers.

As in Appendix 5 the values of the turns ratios can be calculated by equating the coefficients of the $\sin\theta$ and $\cos\theta$ terms:

$$\begin{aligned} V_{ar} &= N_1 V_R - N_2 V_Y & V_{br} &= N_3 V_R - N_4 V_Y \\ V_{cr} &= N_3 V_R - N_4 V_B & V_{dr} &= N_1 V_R - N_2 V_B \end{aligned} \quad (A7.13)$$

$$N_1 = \cos\pi/8 + \frac{\sin\pi/8}{\tan 2\pi/3} = \frac{\sin 5\pi/24}{\sin 2\pi/3} \quad (A7.14)$$

$$N_2 = \frac{\sin\pi/8}{\sin 2\pi/3} = \frac{\sin\pi/8}{\sin 2\pi/3} \quad (A7.14a)$$

$$N_3 = \cos\pi/24 + \frac{\sin\pi/24}{\tan 2\pi/3} = \frac{\sin 7\pi/24}{\sin 2\pi/3} \quad (A7.14b)$$

$$N_4 = \frac{\sin\pi/24}{\sin 2\pi/3} = \frac{\sin\pi/24}{\sin 2\pi/3} \quad (A7.14c)$$

The current on the primary side is given by

$$I_R = N_1(I_{ar} + I_{dr}) - N_2(I_{ab} + I_{dy}) + N_3(I_{br} + I_{cr}) - N_4(I_{bb} + I_{cy}) \quad (A7-15)$$

c) Fourier Series of the System Current

As in the twelve pulse parallel connected circuit the Fourier series of the voltage at the a.c. terminals of the inverter is calculated first and then that of the system current.

The integrals for the Fourier series are given by

$$\begin{aligned} \frac{3\pi d_n}{2} = & \int_{-\pi/24}^{\pi/24} V_c(\phi) \cos n(\phi+\pi/8) d\phi + \int_{-\pi/8}^{\pi/8} V_c(\phi-\pi/12) \cos n(\phi+\pi/8) d\phi \\ & + \int_{\pi/24}^{\pi/8} V_c(\phi-\pi/6) \cos n(\phi+\pi/8) d\phi + \int_{\pi/8}^{5\pi/24} V_c(\phi-\pi/4) \cos n(\phi+\pi/8) d\phi \\ & + 2 \int_{5\pi/24}^{7\pi/24} V_c(\phi-\pi/3) \cos n(\phi+\pi/8) d\phi + 2 \int_{7\pi/24}^{3\pi/8} V_c(\phi-5\pi/12) \cos n(\phi+\pi/8) d\phi \\ & + 2 \int_{11\pi/24}^{3\pi/8} V_c(\phi-\pi/2) \cos n(\phi+\pi/8) d\phi + 2 \int_{13\pi/24}^{11\pi/24} V_c(\phi-7\pi/12) \cos n(\phi+\pi/8) d\phi \\ & + \int_{13\pi/24}^{5\pi/8} V_c(\phi-2\pi/3) \cos n(\phi+\pi/8) d\phi + \int_{5\pi/8}^{17\pi/24} V_c(\phi-3\pi/4) \cos n(\phi+\pi/8) d\phi \\ & + \int_{17\pi/24}^{19\pi/24} V_c(\phi-5\pi/6) \cos n(\phi+\pi/8) d\phi + \int_{19\pi/24}^{7\pi/8} V_c(\phi-11\pi/12) \cos n(\phi+\pi/8) d\phi \end{aligned} \quad (A7-16)$$

with the equation for e_n being the same except for sin replacing cos.

Making suitable changes of variables and simplifying gives

$$\begin{aligned} \frac{3\pi d_n}{2} &= - [2\cos n\pi/24 + \cos 7n\pi/24 + \cos 9n\pi/24] \\ &\quad -\pi/24 \\ &\quad \int_{-\pi/8} V_c(\phi) \cos n\phi \, d\phi \\ - [2\sin n\pi/8 + 2\sin 5n\pi/24 + 3\sin 7n\pi/24 + 3\sin 9n\pi/24 + 4\sin 11n\pi/24] \\ &\quad -\pi/24 \\ &\quad \int_{-\pi/8} V_c(\phi) \sin n\phi \, d\phi \end{aligned} \quad (A7.17)$$

and

$$\begin{aligned} \frac{3\pi e_n}{2} &= - [2\cos n\pi/24 + \cos 7n\pi/24 + \cos 9n\pi/24] \\ &\quad -\pi/24 \\ &\quad \int_{-\pi/8} V_c(\phi) \sin n\phi \, d\phi \\ + [2\sin n\pi/8 + 2\sin 5n\pi/24 + 3\sin 7n\pi/24 + 3\sin 9n\pi/24 + 4\sin 11n\pi/24] \\ &\quad -\pi/24 \\ &\quad \int_{-\pi/8} V_c(\phi) \cos n\phi \, d\phi \end{aligned} \quad (A7.17a)$$

Substituting for $V_c(\phi)$ from (A7.9), reducing using (A7.8a), integrating and simplifying gives

$$\begin{aligned}
 d_1 = & -\frac{2[2\cos\pi/24 + \cos 7\pi/24 + \cos 9\pi/24]}{3\pi} \left\{ \right. \\
 & \left[\frac{3\sqrt{2}}{4(\sqrt{3}-1)} \frac{V_m}{h} (\beta^2+k^2) \cos\pi/24 \right. \\
 & \left. \left(\cos(\theta_0+\gamma-5\pi/12) \left(\frac{\pi}{24} - \frac{\sqrt{54-9\sqrt{2}}}{48} \right) - \sin(\theta_0+\gamma-5\pi/12) \left(\frac{1-\sqrt{3}}{8\sqrt{2}} \right) \right) \right] \\
 & + \frac{3(\beta A_1 - k A_2) X_L e^{\beta\pi/24}}{8h^2} \\
 & \left[k (\beta^2+k^2-1) (-\cos k\pi/24 \cos\pi/24 + e^{\beta\pi/12} \cos k\pi/8 \cos\pi/8) + \right. \\
 & \beta (\beta^2+k^2+1) (\sin k\pi/24 \cos\pi/24 - e^{\beta\pi/12} \sin k\pi/8 \cos\pi/8) + \\
 & 2\beta k (-\cos k\pi/24 \sin\pi/24 + e^{\beta\pi/12} \cos k\pi/8 \sin\pi/8) + \\
 & \left. (\beta^2-k^2+1) (\sin k\pi/24 \sin\pi/24 - e^{\beta\pi/12} \sin k\pi/8 \sin\pi/8) \right] \\
 & + \frac{3(k A_1 + \beta A_2) X_L e^{\beta\pi/24}}{8h^2} \\
 & \left. \left[\beta (\beta^2+k^2+1) (-\cos k\pi/24 \cos\pi/24 + e^{\beta\pi/12} \cos k\pi/8 \cos\pi/8) + \right. \right. \\
 & k (\beta^2+k^2-1) (-\sin k\pi/24 \cos\pi/24 + e^{\beta\pi/12} \sin k\pi/8 \cos\pi/8) + \\
 & 2\beta k (-\sin k\pi/24 \sin\pi/24 + e^{\beta\pi/12} \sin k\pi/8 \sin\pi/8) + \\
 & \left. \left. (\beta^2-k^2+1) (-\cos k\pi/24 \sin\pi/24 + e^{\beta\pi/12} \cos k\pi/8 \sin\pi/8) \right] \right\} \\
 & -\frac{2[2\sin\pi/8 + 2\sin 5\pi/24 + 3\sin 7\pi/24 + 3\sin 9\pi/24 + 4\sin 11\pi/24]}{3\pi} \left\{ \right. \\
 & \left[\frac{3\sqrt{2}}{4(\sqrt{3}-1)} \frac{V_m}{h} (\beta^2+k^2) \cos\pi/24 \right. \\
 & \left. \left(\cos(\theta_0+\gamma-5\pi/12) \left(\frac{1-\sqrt{3}}{8\sqrt{2}} \right) - \sin(\theta_0+\gamma-5\pi/12) \left(\frac{\pi}{24} + \frac{\sqrt{54-9\sqrt{2}}}{48} \right) \right) \right] \\
 & + \frac{3(\beta A_1 - k A_2) X_L e^{\beta\pi/24}}{8h^2} \\
 & \left[2\beta k (-\cos k\pi/24 \cos\pi/24 + e^{\beta\pi/12} \cos k\pi/8 \cos\pi/8) + \right. \\
 & (\beta^2-k^2+1) (\sin k\pi/24 \cos\pi/24 - e^{\beta\pi/12} \sin k\pi/8 \cos\pi/8) + \\
 & k (\beta^2+k^2-1) (\cos k\pi/24 \sin\pi/24 - e^{\beta\pi/12} \cos k\pi/8 \sin\pi/8) + \\
 & \left. \beta (\beta^2+k^2+1) (-\sin k\pi/24 \sin\pi/24 + e^{\beta\pi/12} \sin k\pi/8 \sin\pi/8) \right] \\
 & + \frac{3(k A_1 + \beta A_2) X_L e^{\beta\pi/24}}{8h^2} \\
 & \left[(\beta^2-k^2+1) (-\cos k\pi/24 \cos\pi/24 + e^{\beta\pi/12} \cos k\pi/8 \cos\pi/8) + \right. \\
 & 2\beta k (-\sin k\pi/24 \cos\pi/24 + e^{\beta\pi/12} \sin k\pi/8 \cos\pi/8) + \\
 & \beta (\beta^2+k^2+1) (\cos k\pi/24 \sin\pi/24 - e^{\beta\pi/12} \cos k\pi/8 \sin\pi/8) + \\
 & \left. \left. k (\beta^2+k^2-1) (\sin k\pi/24 \sin\pi/24 - e^{\beta\pi/12} \sin k\pi/8 \sin\pi/8) \right] \right\} \quad (A7.18)
 \end{aligned}$$

$$\begin{aligned}
d_n = & - \frac{2[2\cos n\pi/24 + \cos 7n\pi/24 + \cos 9n\pi/24]}{3\pi} \left\{ \right. \\
& \left[\frac{3\sqrt{2}}{4(\sqrt{3}-1)} \frac{V_m (\beta^2+k^2)}{h (n^2-1)} \cos \pi/24 \right. \\
& \left. \left. \left\{ \cos(\theta_0+\gamma-5\pi/12) \right. \right. \right. \\
& \left. \left. \left. [\cos n\pi/24 \sin \pi/24 - \cos n\pi/8 \sin \pi/8 - n \sin n\pi/24 \cos \pi/24 + n \sin n\pi/8 \cos \pi/8] \right. \right. \right. \\
& \left. \left. \left. - \sin(\theta_0+\gamma-5\pi/12) \right. \right. \right. \\
& \left. \left. \left. [\cos n\pi/24 \cos \pi/24 - \cos n\pi/8 \cos \pi/8 + n \sin n\pi/24 \sin \pi/24 - n \sin n\pi/8 \sin \pi/8] \right\} \right] \\
& + \frac{3(\beta A_1 - k A_2) X_L e^{\beta\pi/24}}{8h_n^2} \\
& \left[k (\beta^2+k^2-n^2) (-\cos k\pi/24 \cos n\pi/24 + e^{\beta\pi/12} \cos k\pi/8 \cos n\pi/8) + \right. \\
& \beta (\beta^2+k^2+n^2) (\sin k\pi/24 \cos n\pi/24 - e^{\beta\pi/12} \sin k\pi/8 \cos n\pi/8) + \\
& 2\beta nk (-\cos k\pi/24 \sin n\pi/24 + e^{\beta\pi/12} \cos k\pi/8 \sin n\pi/8) + \\
& \left. n (\beta^2-k^2+n^2) (\sin k\pi/24 \sin n\pi/24 - e^{\beta\pi/12} \sin k\pi/8 \sin n\pi/8) \right] \\
& + \frac{3(k A_1 + \beta A_2) X_L e^{\beta\pi/24}}{8h_n^2} \\
& \left[\beta (\beta^2+k^2+n^2) (-\cos k\pi/24 \cos n\pi/24 + e^{\beta\pi/12} \cos k\pi/8 \cos n\pi/8) + \right. \\
& k (\beta^2+k^2-n^2) (-\sin k\pi/24 \cos n\pi/24 + e^{\beta\pi/12} \sin k\pi/8 \cos n\pi/8) + \\
& 2\beta nk (-\sin k\pi/24 \sin n\pi/24 + e^{\beta\pi/12} \sin k\pi/8 \sin n\pi/8) + \\
& \left. n (\beta^2-k^2+n^2) (-\cos k\pi/24 \sin n\pi/24 + e^{\beta\pi/12} \cos k\pi/8 \sin n\pi/8) \right] \left. \right\} \\
& - \frac{2[2\sin n\pi/8 + 2\sin 5n\pi/24 + 3\sin 7n\pi/24 + 3\sin 9n\pi/24 + 4 \sin 11n\pi/24]}{3\pi} \left\{ \right. \\
& \left[\frac{3\sqrt{2}}{4(\sqrt{3}-1)} \frac{V_m (\beta^2+k^2)}{h (n^2-1)} \cos \pi/24 \right. \\
& \left. \left. \left\{ \cos(\theta_0+\gamma-5\pi/12) \right. \right. \right. \\
& \left. \left. \left. [-\sin n\pi/24 \sin \pi/24 + \sin n\pi/8 \sin \pi/8 - n \cos n\pi/24 \cos \pi/24 + n \cos n\pi/8 \cos \pi/8] \right. \right. \right. \\
& \left. \left. \left. - \sin(\theta_0+\gamma-5\pi/12) \right. \right. \right. \\
& \left. \left. \left. [-\sin n\pi/24 \cos \pi/24 + \sin n\pi/8 \cos \pi/8 + n \cos n\pi/24 \sin \pi/24 - n \cos n\pi/8 \sin \pi/8] \right\} \right] \\
& + \frac{3(\beta A_1 - k A_2) X_L e^{\beta\pi/24}}{8h_n^2} \\
& \left[2\beta nk (-\cos k\pi/24 \cos n\pi/24 + e^{\beta\pi/12} \cos k\pi/8 \cos n\pi/8) + \right. \\
& n (\beta^2-k^2+n^2) (\sin k\pi/24 \cos n\pi/24 - e^{\beta\pi/12} \sin k\pi/8 \cos n\pi/8) + \\
& k (\beta^2+k^2-n^2) (\cos k\pi/24 \sin n\pi/24 - e^{\beta\pi/12} \cos k\pi/8 \sin n\pi/8) + \\
& \left. \beta (\beta^2+k^2+n^2) (-\sin k\pi/24 \sin n\pi/24 + e^{\beta\pi/12} \sin k\pi/8 \sin n\pi/8) \right] \\
& + \frac{3(k A_1 + \beta A_2) X_L e^{\beta\pi/24}}{8h_n^2} \\
& \left[n (\beta^2-k^2+n^2) (-\cos k\pi/24 \cos n\pi/24 + e^{\beta\pi/12} \cos k\pi/8 \cos n\pi/8) + \right. \\
& 2\beta nk (-\sin k\pi/24 \cos n\pi/24 + e^{\beta\pi/12} \sin k\pi/8 \cos n\pi/8) + \\
& \beta (\beta^2+k^2+n^2) (\cos k\pi/24 \sin n\pi/24 - e^{\beta\pi/12} \cos k\pi/8 \sin n\pi/8) + \\
& \left. k (\beta^2+k^2-n^2) (\sin k\pi/24 \sin n\pi/24 - e^{\beta\pi/12} \sin k\pi/8 \sin n\pi/8) \right] \left. \right\} \quad (A7-18a)
\end{aligned}$$

$$\begin{aligned}
e_1 = & - \frac{2[2\cos\pi/24 + \cos 7\pi/24 + \cos 9\pi/24]}{3\pi} \left\{ \right. \\
& \left[\frac{3\sqrt{2}}{4(\sqrt{3}-1)} \frac{V_m}{h} (\beta^2+k^2) \cos\pi/24 \right. \\
& \left. \left(\cos(\theta_0+\gamma-5\pi/12) \left(\frac{1-\sqrt{3}}{8\sqrt{2}} \right) - \sin(\theta_0+\gamma-5\pi/12) \left(\frac{\pi}{24} - \frac{\sqrt{54-9\sqrt{2}}}{48} \right) \right) \right] \\
& + \frac{3(\beta A_1 - k A_2) X_L e^{\beta\pi/24}}{8h^2} \\
& \left[2\beta k (-\cos k\pi/24 \cos\pi/24 + e^{\beta\pi/12} \cos k\pi/8 \cos\pi/8) + \right. \\
& (\beta^2-k^2+1) (\sin k\pi/24 \cos\pi/24 - e^{\beta\pi/12} \sin k\pi/8 \cos\pi/8) + \\
& k (\beta^2+k^2-1) (\cos k\pi/24 \sin\pi/24 - e^{\beta\pi/12} \cos k\pi/8 \sin\pi/8) + \\
& \left. \beta (\beta^2+k^2+1) (-\sin k\pi/24 \sin\pi/24 + e^{\beta\pi/12} \sin k\pi/8 \sin\pi/8) \right] \\
& + \frac{3(k A_1 + \beta A_2) X_L e^{\beta\pi/24}}{8h^2} \\
& \left. \left[(\beta^2-k^2+1) (-\cos k\pi/24 \cos\pi/24 + e^{\beta\pi/12} \cos k\pi/8 \cos\pi/8) + \right. \right. \\
& 2\beta k (-\sin k\pi/24 \cos\pi/24 + e^{\beta\pi/12} \sin k\pi/8 \cos\pi/8) + \\
& \left. \beta (\beta^2+k^2+1) (\cos k\pi/24 \sin\pi/24 - e^{\beta\pi/12} \cos k\pi/8 \sin\pi/8) + \right. \\
& \left. \left. k (\beta^2+k^2-1) (\sin k\pi/24 \sin\pi/24 - e^{\beta\pi/12} \sin k\pi/8 \sin\pi/8) \right] \right\} \\
& + \frac{2[2\sin\pi/8 + 2\sin 5\pi/24 + 3\sin 7\pi/24 + 3\sin 9\pi/24 + 4\sin 11\pi/24]}{3\pi} \left\{ \right. \\
& \left[\frac{3\sqrt{2}}{4(\sqrt{3}-1)} \frac{V_m}{h} (\beta^2+k^2) \cos\pi/24 \right. \\
& \left. \left(\cos(\theta_0+\gamma-5\pi/12) \left(\frac{\pi}{24} - \frac{\sqrt{54-9\sqrt{2}}}{48} \right) - \sin(\theta_0+\gamma-5\pi/12) \left(\frac{1-\sqrt{3}}{8\sqrt{2}} \right) \right) \right] \\
& + \frac{3(\beta A_1 - k A_2) X_L e^{\beta\pi/24}}{8h^2} \\
& \left[k (\beta^2+k^2-1) (-\cos k\pi/24 \cos\pi/24 + e^{\beta\pi/12} \cos k\pi/8 \cos\pi/8) + \right. \\
& \beta (\beta^2+k^2+1) (\sin k\pi/24 \cos\pi/24 - e^{\beta\pi/12} \sin k\pi/8 \cos\pi/8) + \\
& 2\beta k (-\cos k\pi/24 \sin\pi/24 + e^{\beta\pi/12} \cos k\pi/8 \sin\pi/8) + \\
& \left. (\beta^2-k^2+1) (\sin k\pi/24 \sin\pi/24 - e^{\beta\pi/12} \sin k\pi/8 \sin\pi/8) \right] \\
& + \frac{3(k A_1 + \beta A_2) X_L e^{\beta\pi/24}}{8h^2} \\
& \left[\beta (\beta^2+k^2+1) (-\cos k\pi/24 \cos\pi/24 + e^{\beta\pi/12} \cos k\pi/8 \cos\pi/8) + \right. \\
& k (\beta^2+k^2-1) (-\sin k\pi/24 \cos\pi/24 + e^{\beta\pi/12} \sin k\pi/8 \cos\pi/8) + \\
& 2\beta k (-\sin k\pi/24 \sin\pi/24 + e^{\beta\pi/12} \sin k\pi/8 \sin\pi/8) + \\
& \left. \left. (\beta^2-k^2+1) (-\cos k\pi/24 \sin\pi/24 + e^{\beta\pi/12} \cos k\pi/8 \sin\pi/8) \right] \right\} \quad (A7.18b)
\end{aligned}$$

$$\begin{aligned}
e_n = & -\frac{2[2\cos n\pi/24 + \cos 7n\pi/24 + \cos 9n\pi/24]}{3\pi} \left\{ \right. \\
& \left[\frac{3\sqrt{2}}{4(\sqrt{3}-1)} \frac{V_m (\beta^2+k^2)}{h (n^2-1)} \cos \pi/24 \right. \\
& \left. \left. \left\{ \cos(\theta_0+\gamma-5\pi/12) \right. \right. \right. \\
& \left. \left. \left. [-\sin n\pi/24 \sin \pi/24 + \sin n\pi/8 \sin \pi/8 - n \cos n\pi/24 \cos \pi/24 + n \cos n\pi/8 \cos \pi/8] - \right. \right. \right. \\
& \left. \left. \left. -\sin(\theta_0+\gamma-5\pi/12) \right. \right. \right. \\
& \left. \left. \left. [-\sin n\pi/24 \cos \pi/24 + \sin n\pi/8 \cos \pi/8 + n \cos n\pi/24 \sin \pi/24 - n \cos n\pi/8 \sin \pi/8] \right\} \right] \\
& + \frac{3(\beta A_1 - k A_2) X_L e^{\beta\pi/24}}{8h_n^2} \\
& \left[2\beta nk (-\cos k\pi/24 \cos n\pi/24 + e^{\beta\pi/12} \cos k\pi/8 \cos n\pi/8) + \right. \\
& n(\beta^2 - k^2 + n^2) (\sin k\pi/24 \cos n\pi/24 - e^{\beta\pi/12} \sin k\pi/8 \cos n\pi/8) + \\
& k(\beta^2 + k^2 - n^2) (\cos k\pi/24 \sin n\pi/24 - e^{\beta\pi/12} \cos k\pi/8 \sin n\pi/8) + \\
& \left. \beta(\beta^2 + k^2 + n^2) (-\sin k\pi/24 \sin n\pi/24 + e^{\beta\pi/12} \sin k\pi/8 \sin n\pi/8) \right] \\
& + \frac{3(k A_1 + \beta A_2) X_L e^{\beta\pi/24}}{8h_n^2} \\
& \left[n(\beta^2 - k^2 + 1) (-\cos k\pi/24 \cos n\pi/24 + e^{\beta\pi/12} \cos k\pi/8 \cos n\pi/8) + \right. \\
& 2\beta nk (-\sin k\pi/24 \cos n\pi/24 + e^{\beta\pi/12} \sin k\pi/8 \cos n\pi/8) + \\
& \beta(\beta^2 + k^2 + 1) (\cos k\pi/24 \sin n\pi/24 - e^{\beta\pi/12} \cos k\pi/8 \sin n\pi/8) + \\
& \left. k(\beta^2 + k^2 - 1) (\sin k\pi/24 \sin n\pi/24 - e^{\beta\pi/12} \sin k\pi/8 \sin n\pi/8) \right] \left. \right\} \\
& + \frac{2[2\sin n\pi/8 + 2\sin 5n\pi/24 + 3\sin 7n\pi/24 + 3\sin 9n\pi/24 + 4\sin 11n\pi/24]}{3\pi} \left\{ \right. \\
& \left[\frac{3\sqrt{2}}{4(\sqrt{3}-1)} \frac{V_m (\beta^2+k^2)}{h (n^2-1)} \cos \pi/24 \right. \\
& \left. \left. \left\{ \cos(\theta_0+\gamma-5\pi/12) \right. \right. \right. \\
& \left. \left. \left. [\cos n\pi/24 \sin \pi/24 - \cos n\pi/8 \sin \pi/8 - n \sin n\pi/24 \sin \pi/24 + n \sin n\pi/8 \cos \pi/8] \right. \right. \right. \\
& \left. \left. \left. -\sin(\theta_0+\gamma-5\pi/12) \right. \right. \right. \\
& \left. \left. \left. [\cos n\pi/24 \cos \pi/24 - \cos n\pi/8 \cos \pi/8 + n \sin n\pi/24 \sin \pi/24 - n \sin n\pi/8 \sin \pi/8] \right\} \right] \\
& + \frac{3(\beta A_1 - k A_2) X_L e^{\beta\pi/24}}{8h_n^2} \\
& \left[k(\beta^2 + k^2 - n^2) (-\cos k\pi/24 \cos n\pi/24 + e^{\beta\pi/12} \cos k\pi/8 \cos n\pi/8) + \right. \\
& \beta(\beta^2 + k^2 + n^2) (\sin k\pi/24 \cos n\pi/24 - e^{\beta\pi/12} \sin k\pi/8 \cos n\pi/8) + \\
& 2\beta nk (-\cos k\pi/24 \sin n\pi/24 + e^{\beta\pi/12} \cos k\pi/8 \sin n\pi/8) + \\
& \left. n(\beta^2 - k^2 + n^2) (\sin k\pi/24 \sin n\pi/24 - e^{\beta\pi/12} \sin k\pi/8 \sin n\pi/8) \right] \\
& + \frac{3(k A_1 + \beta A_2) X_L e^{\beta\pi/24}}{8h_n^2} \\
& \left[\beta(\beta^2 + k^2 + n^2) (-\cos k\pi/24 \cos n\pi/24 + e^{\beta\pi/12} \cos k\pi/8 \cos n\pi/8) + \right. \\
& k(\beta^2 + k^2 - n^2) (-\sin k\pi/24 \cos n\pi/24 + e^{\beta\pi/12} \sin k\pi/8 \cos n\pi/8) + \\
& 2\beta nk (-\sin k\pi/24 \sin n\pi/24 + e^{\beta\pi/12} \sin k\pi/8 \sin n\pi/8) + \\
& \left. n(\beta^2 - k^2 + n^2) (-\cos k\pi/24 \sin n\pi/24 + e^{\beta\pi/12} \cos k\pi/8 \sin n\pi/8) \right] \left. \right\} \quad (A7.18c)
\end{aligned}$$

The Fourier series on the secondary side of the transformers, for the red phase of the first transformer, is given by

$$I_{ar} = -\frac{V_m}{X_L(1+4\beta^2)} [\cos(\phi+\theta_0+\pi/8) - 2\beta\sin(\phi+\theta_0+\pi/8)] \quad (A7-19)$$

$$+ \sum_{n=1}^{\infty} \frac{1}{X_L(n^2+4\beta^2)} [(ne_n - 2\beta d_n)\cos n(\phi+\pi/8) - (nd_n + 2\beta e_n)\sin n(\phi+\pi/8)]$$

The Fourier series of the current on the primary side is calculated by employing equation (A7-19), and similar equations for the other phases, in equation (A7-15). After simplifying this gives

$$I_{R1} = \frac{4}{X_L(1+4\beta^2)} \quad (A7-20)$$

$$\{-V_m[\cos(\phi+\theta_0) - 2\beta\sin(\phi+\theta_0)] + e_1[\cos\phi - 2\beta\sin\phi] - d_1[\sin\phi + 2\beta\cos\phi]\}$$

and for the harmonics, after simplifying,

$$|I_n| = \frac{4}{X_L} \sqrt{\frac{d_n^2 + e_n^2}{(n^2+4\beta^2)}} \quad (A7-21)$$

The equations to determine the parameters for the fundamental component are the same as those for the three phase case, equations (A3-26) to (A3-26b), hence

$$I_q = \frac{4V_m}{X_L} \left(q_1 + q_2 \frac{\sin 2\theta_0}{2\beta} \right) \quad (A7-22)$$

$$I_p = \frac{4\beta V_m}{X_L} \left(p_1 + q_2 \frac{\sin^2 \theta_0}{\beta^2} \right) \quad (A7-22a)$$

For the harmonics the equation for the exact value of t_n is as in the three phase case, equation (A3-29). Plotting this as a function of θ_{ob} shows that $|I_n|$ is linear. The equations for c_n and s_n are therefore as those in the three phase case, equations (A3-32) and (A3-32a), respectively. In this case, because of the parallel connection of the transformer primaries,

$$I_{nc} \approx \frac{4V_m}{X_L} [c_n - s_n \theta_{ob}] \quad (A7-23)$$

Appendix 8

Analysis of a Twenty-Four Pulse STATCON with Series Connected Transformer Primaries

a) Determination of the Current on the Transformer Secondary Side

The transformer arrangement is shown in figure A8-1.

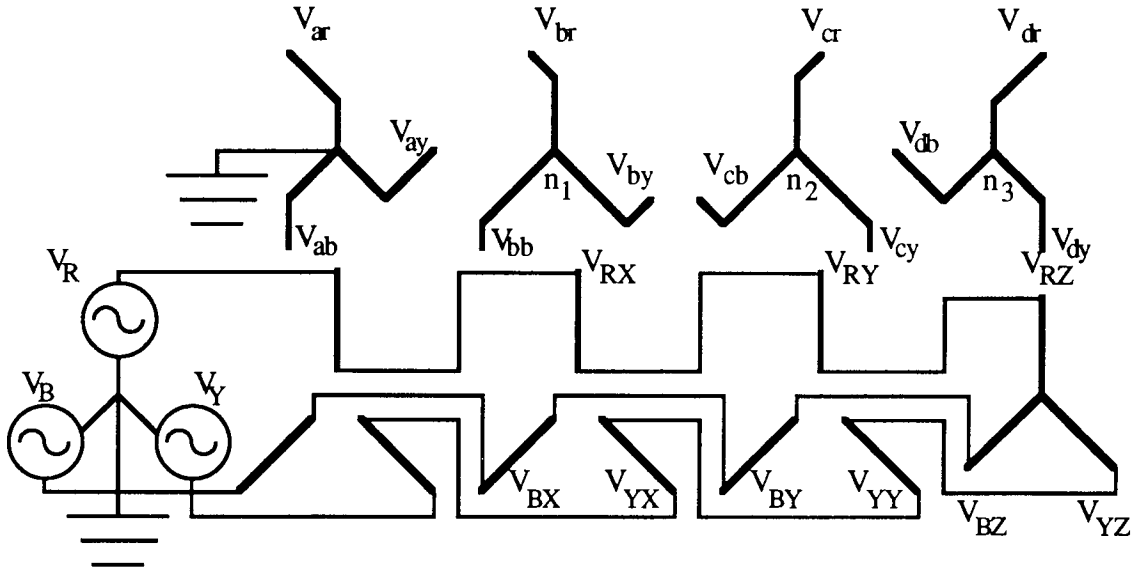


Figure A8-1. Twenty-Four Pulse Series Connected Transformer Arrangement.

The relationships between the voltages are

$$\begin{aligned}
 V_{ar} &= N_1(V_R - V_{RX}) - N_2(V_Y - V_{YX}) \\
 V_{br} &= N_3(V_{RX} - V_{RY}) - N_4(V_{YX} - V_{YY}) \\
 V_{cr} &= N_3(V_{RY} - V_{RZ}) - N_4(V_{BY} - V_{BZ}) \\
 V_{dr} &= N_1 V_{RZ} - N_2 V_{BZ}
 \end{aligned} \tag{A8-1}$$

The values for the transformer turns ratios are given in equations (A7-14) to (A7-14c).

The relationships between the currents are

$$I_R = N_1 I_{ar} - N_2 I_{ab} = N_3 I_{br} - N_4 I_{bb} = N_3 I_{cr} - N_4 I_{cy} = N_1 I_{dr} - N_2 I_{dy} \tag{A8-2}$$

Following the same argument used in appendix 6, the sum of each of the sets of three voltages and currents out of each transformer is zero:

$$\begin{aligned}
 I_B &= -(I_R + I_Y) & I_{ab} &= -(I_{ar} + I_{ay}) \\
 V_B &= -(V_R + V_Y) & V_{ab} &= -(V_{ar} + V_{ay}) \\
 V_{BX} &= -(V_{RX} + V_{RY}) & & \text{etc.}
 \end{aligned} \tag{A8-3}$$

Using the same method as that outlined in appendix 6 these relationships, (A8.1), (A8.2) and (A8.3), can be used to reduce the number of unknown currents and voltages.

The expressions reduce to

$$I_{ay} = -(2+\sqrt{3}) I_{ar} + \frac{\sqrt{3}(\sqrt{3}+1)}{\sqrt{2}} I_{br} \quad (\text{A8.4})$$

$$I_{by} = -\frac{\sqrt{3}(\sqrt{3}+1)}{\sqrt{2}} I_{ar} + (\sqrt{3}+1) I_{br} \quad (\text{A8.4a})$$

$$I_{cr} = -I_{ar} + \frac{(\sqrt{3}+1)}{\sqrt{2}} I_{br} \quad (\text{A8.4b})$$

$$I_{cy} = -(\sqrt{3}+1) I_{ar} + \frac{(\sqrt{3}+1)}{\sqrt{2}} I_{br} \quad (\text{A8.4c})$$

$$I_{dr} = -\frac{(\sqrt{3}+1)}{\sqrt{2}} I_{ar} + (\sqrt{3}+1) I_{br} \quad (\text{A8.4d})$$

$$I_{dy} = -\frac{(\sqrt{3}+1)}{\sqrt{2}} I_{ar} + I_{br} \quad (\text{A8.4e})$$

$$V_{ay} = -\frac{\sqrt{3}(\sqrt{3}+1)}{\sqrt{2}} \quad (\text{A8.4f})$$

$$\left(\frac{\sqrt{2}(2+\sqrt{3})}{\sqrt{3}(\sqrt{3}+1)} V_{ar} + V_{br} + \frac{\sqrt{2}}{\sqrt{3}} V_{cr} - \frac{\sqrt{2}}{\sqrt{3}(\sqrt{3}+1)} V_{cy} + \frac{1}{\sqrt{3}} V_{dr} - \frac{1}{\sqrt{3}} V_{dy} - N_3 V_R + N_4 V_Y \right)$$

$$V_{by} = -\frac{\sqrt{3}(\sqrt{3}+1)}{\sqrt{2}} \quad (\text{A8.4g})$$

$$\left(-V_{ar} - \frac{\sqrt{2}}{\sqrt{3}} V_{br} - \frac{1}{\sqrt{3}} V_{cr} + \frac{1}{\sqrt{3}} V_{cy} - \frac{\sqrt{2}}{\sqrt{3}(\sqrt{3}+1)} V_{dr} + \frac{\sqrt{2}}{\sqrt{3}} V_{dy} + N_1 V_R - N_2 V_Y \right)$$

The current through the capacitor has the same dependence on the currents on the secondary sides of the transformers as in the parallel case so substituting from the relevant parts of (A8.4) and (A8.3) gives

$$I_c = \frac{(\sqrt{2}+1)(\sqrt{3}+1)(\sqrt{3}+\sqrt{2})}{\sqrt{2}} (I_{br} - I_{ar}) \quad (\text{A8.5})$$

Substituting from the different parts of (A8-4) into the relevant parts of (A7-4), using (A7-5) and (A7-6), and simplifying gives

$$V_{ar} = X_L \frac{dI_{ar}}{d\phi} + R I_{ar} + \frac{V_c}{3} \quad (\text{A8-6})$$

$$\begin{aligned} & \left(\frac{\sqrt{2}(2+\sqrt{3})}{\sqrt{3}(\sqrt{3}+1)} V_{ar} + V_{br} + \frac{\sqrt{2}}{\sqrt{3}} V_{cr} - \frac{\sqrt{2}}{\sqrt{3}(\sqrt{3}+1)} V_{cy} + \frac{1}{\sqrt{3}} V_{dr} - \frac{1}{\sqrt{3}} V_{dy} - N_3 V_R + N_4 V_Y \right) \\ & = X_L \frac{d}{d\phi} \left(\frac{\sqrt{2}(2+\sqrt{3})}{\sqrt{3}(\sqrt{3}+1)} I_{ar} - I_{br} \right) + R \left(\frac{\sqrt{2}(2+\sqrt{3})}{\sqrt{3}(\sqrt{3}+1)} I_{ar} - I_{br} \right) + \frac{2\sqrt{2} V_c}{3\sqrt{3}(\sqrt{3}+1)} \end{aligned} \quad (\text{A8-6a})$$

$$V_{br} = X_L \frac{dI_{br}}{d\phi} + R I_{br} - \frac{V_c}{3} \quad (\text{A8-6b})$$

$$\begin{aligned} & \left(-V_{ar} - \frac{\sqrt{2}}{\sqrt{3}} V_{br} - \frac{1}{\sqrt{3}} V_{cr} + \frac{1}{\sqrt{3}} V_{cy} - \frac{\sqrt{2}}{\sqrt{3}(\sqrt{3}+1)} V_{dr} + \frac{\sqrt{2}}{\sqrt{3}} V_{dy} + N_1 V_R - N_2 V_Y \right) \\ & = X_L \frac{d}{d\phi} \left(I_{ar} - \frac{\sqrt{2}}{\sqrt{3}} I_{br} \right) + R \left(I_{ar} - \frac{\sqrt{2}}{\sqrt{3}} I_{br} \right) + \frac{\sqrt{2} V_c}{3\sqrt{3}(\sqrt{3}+1)} \end{aligned} \quad (\text{A8-6c})$$

$$V_{cr} = X_L \frac{d}{d\phi} \left(-I_{ar} + \frac{(\sqrt{3}+1)}{\sqrt{2}} I_{br} \right) + R \left(-I_{ar} + \frac{(\sqrt{3}+1)}{\sqrt{2}} I_{br} \right) - \frac{V_c}{3} \quad (\text{A8-6d})$$

$$V_{cy} = X_L \frac{d}{d\phi} \left(-(\sqrt{3}+1) I_{ar} + \frac{(\sqrt{3}+1)}{\sqrt{2}} I_{br} \right) + R \left(-(\sqrt{3}+1) I_{ar} + \frac{(\sqrt{3}+1)}{\sqrt{2}} I_{br} \right) - \frac{V_c}{3} \quad (\text{A8-6e})$$

$$V_{dr} = X_L \frac{d}{d\phi} \left(-\frac{(\sqrt{3}+1)}{\sqrt{2}} I_{ar} + (\sqrt{3}+1) I_{br} \right) + R \left(-\frac{(\sqrt{3}+1)}{\sqrt{2}} I_{ar} + (\sqrt{3}+1) I_{br} \right) - \frac{V_c}{3} \quad (\text{A8-6f})$$

$$V_{dy} = X_L \frac{d}{d\phi} \left(-\frac{(\sqrt{3}+1)}{\sqrt{2}} I_{ar} + I_{br} \right) + \left(-\frac{(\sqrt{3}+1)}{\sqrt{2}} I_{ar} + I_{br} \right) - \frac{V_c}{3} \quad (\text{A8-6g})$$

Simplifying

$$\begin{aligned}
 & (A8.6a) - \frac{\sqrt{2}(2+\sqrt{3})}{\sqrt{3}(\sqrt{3}+1)} (A8.6) - (A8.6b) - \frac{\sqrt{2}}{\sqrt{3}} (A8.6d) \\
 & + \frac{\sqrt{2}}{\sqrt{3}(\sqrt{3}+1)} (A8.6e) - \frac{1}{\sqrt{3}} (A8.6f) + \frac{1}{\sqrt{3}} (A8.6g) \quad \text{gives} \\
 & \frac{dI_{br}}{d\phi} + 2\beta I_{br} - \frac{V_c}{12X_L} = \frac{N_3 V_R - N_4 V_Y}{4X_L} \quad (A8.7)
 \end{aligned}$$

and simplifying

$$\begin{aligned}
 & (A8.6c) + (A8.6) + \frac{\sqrt{2}}{\sqrt{3}} (A8.6b) + \frac{1}{\sqrt{3}} (A8.6d) \\
 & - \frac{1}{\sqrt{3}} (A8.6e) + \frac{\sqrt{2}}{\sqrt{3}(\sqrt{3}+1)} (A8.6f) - \frac{\sqrt{2}}{\sqrt{3}} (A8.6g) \quad \text{gives} \\
 & \frac{dI_{ar}}{d\phi} + 2\beta I_{ar} + \frac{V_c}{12X_L} = \frac{N_1 V_R - N_2 V_Y}{4X_L} \quad (A8.7a)
 \end{aligned}$$

In this case the voltage source is defined as four times that in the parallel connected case:

$$V_R = 4V_m \sin(\phi + \theta_0) \quad V_Y = 4V_m \sin(\phi + \theta_0 - 2\pi/3) \quad V_B = 4V_m \sin(\phi + \theta_0 + 2\pi/3) \quad (A8.8)$$

Taking (A8.7) – (A8.7a), substituting from (A8.8) and (A8.5), differentiating again and simplifying using the definitions of the turns ratios, equations (A7.14) to (A7.14c), gives

$$\frac{d^2 I_c}{d\phi^2} + 2\beta \frac{dI_c}{d\phi} + \frac{(\sqrt{2}+1)(\sqrt{3}+1)(\sqrt{3}+\sqrt{2})}{6\sqrt{2}} I_c = \frac{V_m}{2X_L} \frac{1}{\sin\pi/24} \sin(\phi + \theta_0 + \pi/12) \quad (A8.9)$$

This equation has the same form as the equivalent equation in the parallel case, (A7.7), except for the coefficient of the I_c term. The solution is therefore of the same form as that in the parallel case, assuming $R < 2 \sqrt{\frac{(\sqrt{2}+1)(\sqrt{3}+1)(\sqrt{3}+\sqrt{2}) X_C X_L}{6\sqrt{2}}}$:

$$I_c = -\frac{V_m}{2hX_L} \frac{1}{\sin\pi/24} \cos(\phi + \theta_0 + \gamma + \pi/12) + A_1 e^{-\beta\phi} \sin k\phi + A_2 e^{-\beta\phi} \cos k\phi \quad (A8.10)$$

where

$$k = \sqrt{\frac{(\sqrt{2}+1)(\sqrt{3}+1)(\sqrt{3}+\sqrt{2}) X_C X_L}{6\sqrt{2}} - \beta^2} \quad (A8.10a)$$

The voltage across the capacitor divided by the impedance of the capacitor is also of the same form as that in the parallel case, (A7.9):

$$\begin{aligned}
 \frac{V_c}{X_C} &= \frac{V_m}{2hX_L} \frac{1}{\sin\pi/24} \sin(\phi + \theta_0 + \gamma + \pi/12) \\
 &+ \frac{e^{-\beta\phi}}{(\beta^2 + k^2)} [(\beta A_1 - k A_2) \sin k\phi + (k A_1 + \beta A_2) \cos k\phi] \quad (A8.11)
 \end{aligned}$$

Substituting from (A8.11) in (A8.7a) and integrating, gives, after simplifying

$$\begin{aligned} I_{ar} &= \frac{V_m}{hX_L} \sin(\phi + \theta_0 + \gamma + \pi/8) \\ &- \frac{V_m (\beta^2 + k^2)}{hX_L (1 + 4\beta^2)} \cos\pi/24 [\sin(\phi + \theta_0 + \gamma + \pi/12) + 2\beta \cos(\phi + \theta_0 + \gamma + \pi/12)] \\ &- \frac{e^{-\beta\phi}}{\sqrt{2}(\sqrt{2}+1)(\sqrt{3}+1)(\sqrt{3}+\sqrt{2})} (A_1 \sin k\phi + A_2 \cos k\phi) + A_3 e^{-2\beta\phi} \end{aligned} \quad (A8.12)$$

Substituting (A8.12) and (A8.10) in (A8.5) and simplifying gives

$$\begin{aligned} I_{br} &= \frac{V_m}{hX_L} \sin(\phi + \theta_0 + \gamma + \pi/24) \\ &- \frac{V_m (\beta^2 + k^2)}{hX_L (1 + 4\beta^2)} \cos\pi/24 [\sin(\phi + \theta_0 + \gamma + \pi/12) + 2\beta \cos(\phi + \theta_0 + \gamma + \pi/12)] \\ &+ \frac{e^{-\beta\phi}}{\sqrt{2}(\sqrt{2}+1)(\sqrt{3}+1)(\sqrt{3}+\sqrt{2})} (A_1 \sin k\phi + A_2 \cos k\phi) + A_3 e^{-2\beta\phi} \end{aligned} \quad (A8.13)$$

The boundary conditions are three of those used in the parallel case:

$$V_c(\phi = -\pi/24) = V_c(\phi = -\pi/8) \quad (A8.14)$$

$$I_{ar}(\phi = -\pi/24) = -I_{dy}(\phi = -\pi/8) \quad (A8.14a)$$

$$I_{dy}(\phi = -\pi/24) = I_{cy}(\phi = -\pi/8) \quad (A8.14b)$$

As in the twelve pulse circuits, the voltage boundary condition is the same in both the parallel, (A7.12), and series connections:

$$\begin{aligned} &\frac{V_m}{hX_L} (\beta^2 + k^2) \cos(\theta_0 + \gamma) = \\ &e^{\beta\pi/24} \{ A_1 [\beta(\sin k\pi/24 - e^{\beta\pi/12} \sin k\pi/8) - k(\cos k\pi/24 - e^{\beta\pi/12} \cos k\pi/8)] - \\ &A_2 [\beta(\cos k\pi/24 - e^{\beta\pi/12} \cos k\pi/8) + k(\sin k\pi/24 - e^{\beta\pi/12} \sin k\pi/8)] \} \end{aligned} \quad (A8.15)$$

Evaluating (A8.14a) gives

$$\begin{aligned} &\frac{V_m (\beta^2 + k^2)}{hX_L (1 + 4\beta^2)} \sin\pi/12 [\sin(\theta_0 + \gamma + 5\pi/12) + 2\beta \cos(\theta_0 + \gamma + 5\pi/12)] = \\ &\frac{e^{\beta\pi/24}}{2(\sqrt{2}+1)(\sqrt{3}+1)(\sqrt{3}+\sqrt{2})} \\ &\{ \sqrt{2} [A_1 \sin k\pi/24 - A_2 \cos k\pi/24] - (\sqrt{3}+1+\sqrt{2}) e^{\beta\pi/12} [A_1 \sin k\pi/8 - A_2 \cos k\pi/8] \} \\ &- \frac{A_3 e^{\beta\pi/12}}{\sqrt{2}} [(\sqrt{3}+1-\sqrt{2}) e^{\beta\pi/6} - \sqrt{2}] \end{aligned} \quad (A8.15a)$$

Evaluating (A8.14b) gives

$$\frac{V_m (\beta^2 + k^2)}{hX_L (1 + 4\beta^2)} \sin\pi/12 [\sin(\theta_0 + \gamma + \pi/3) + 2\beta\cos(\theta_0 + \gamma + \pi/3)] =$$

$$\frac{e^{\beta\pi/24}}{2(\sqrt{2}+1)(\sqrt{3}+1)(\sqrt{3}+\sqrt{2})}$$

$$\{(\sqrt{3}+1+\sqrt{2})[A_1\sin k\pi/24 - A_2\cos k\pi/24] -$$

$$(\sqrt{3}+1)(\sqrt{2}+1)e^{\beta\pi/12}[A_1\sin k\pi/8 - A_2\cos k\pi/8]\}$$

$$- \frac{A_3 e^{\beta\pi/12}}{\sqrt{2}} [(\sqrt{2}-1)(\sqrt{3}+1)e^{\beta\pi/6} - (\sqrt{3}+1-\sqrt{2})] \quad (A8.15b)$$

The current on the primary side of the transformers is given by (A8.2), substituting from the relevant parts of (A8.3) and (A8.4), gives

$$I_R = [N_1 - (\sqrt{3}+1)N_2] I_{ar} + \frac{\sqrt{3}(\sqrt{3}+1)N_2}{\sqrt{2}} I_{br} \quad (A8.16)$$

b) Fourier Series

As in the twelve pulse case with series connected primaries the current is established directly, separating each term. The current during each of the intervals can be established from table A7.1 and equations (A8.3), (A8.4) to (A8.4e), (A8.12) and (A8.13).

The Fourier series can be defined as

$$I_{ar} = \sum_{n=1}^{\infty} a_n \cos n(\phi + \pi/8) + b_n \sin n(\phi + \pi/8) \quad (A8.17)$$

where

$$a_n = \frac{2}{\pi} \int_{-\pi/8}^{21\pi/24} I_{ar}(\phi) \cos n(\phi + \pi/8) d\phi \quad \text{and} \quad b_n = \frac{2}{\pi} \int_{-\pi/8}^{21\pi/24} I_{ar}(\phi) \sin n(\phi + \pi/8) d\phi$$

$$\begin{aligned}
1) \frac{V_m (\beta^2+k^2)}{hX_L (1+4\beta^2)} \cos\pi/24 & \\
-\pi/8 < \phi < -\pi/24 & - [\sin(\phi+\theta_0+\gamma+\pi/12) + 2\beta\cos(\phi+\theta_0+\gamma+\pi/12)] \\
-\pi/24 < \phi < \pi/24 & - \frac{\sqrt{3+1}-\sqrt{2}}{\sqrt{2}} [\sin(\phi+\theta_0+\gamma) + 2\beta\cos(\phi+\theta_0+\gamma)] \\
\pi/24 < \phi < \pi/8 & - \frac{(\sqrt{2}-1)(\sqrt{3+1})}{\sqrt{2}} [\sin(\phi+\theta_0+\gamma-\pi/12) + 2\beta\cos(\phi+\theta_0+\gamma-\pi/12)] \\
\pi/8 < \phi < 5\pi/24 & - \frac{(\sqrt{3}-\sqrt{2})(\sqrt{3+1})}{\sqrt{2}} [\sin(\phi+\theta_0+\gamma-\pi/6) + 2\beta\cos(\phi+\theta_0+\gamma-\pi/6)] \\
5\pi/24 < \phi < 7\pi/24 & \frac{\sqrt{3}(\sqrt{3+1}) - \sqrt{2}(2+\sqrt{3})}{\sqrt{2}} [\sin(\phi+\theta_0+\gamma-\pi/4) + 2\beta\cos(\phi+\theta_0+\gamma-\pi/4)] \\
7\pi/24 < \phi < 9\pi/24 & - [\sqrt{2}(\sqrt{3+1}) - (2+\sqrt{3})] [\sin(\phi+\theta_0+\gamma-\pi/3) + 2\beta\cos(\phi+\theta_0+\gamma-\pi/3)] \\
9\pi/24 < \phi < 11\pi/24 & \frac{[\sqrt{2}(\sqrt{3+1}) - (2+\sqrt{3})]}{\sqrt{2}} [\sin(\phi+\theta_0+\gamma-5\pi/12) + 2\beta\cos(\phi+\theta_0+\gamma-5\pi/12)] \\
11\pi/24 < \phi < 13\pi/24 & - \frac{\sqrt{3}(\sqrt{3+1}) - \sqrt{2}(2+\sqrt{3})}{\sqrt{2}} [\sin(\phi+\theta_0+\gamma-\pi/2) + 2\beta\cos(\phi+\theta_0+\gamma-\pi/2)] \\
13\pi/24 < \phi < 15\pi/24 & \frac{(\sqrt{3}-\sqrt{2})(\sqrt{3+1})}{\sqrt{2}} [\sin(\phi+\theta_0+\gamma-7\pi/12) + 2\beta\cos(\phi+\theta_0+\gamma-7\pi/12)] \\
15\pi/24 < \phi < 17\pi/24 & \frac{(\sqrt{2}-1)(\sqrt{3+1})}{\sqrt{2}} [\sin(\phi+\theta_0+\gamma-2\pi/3) + 2\beta\cos(\phi+\theta_0+\gamma-2\pi/3)] \\
17\pi/24 < \phi < 19\pi/24 & \frac{\sqrt{3+1}-\sqrt{2}}{\sqrt{2}} [\sin(\phi+\theta_0+\gamma-3\pi/4) + 2\beta\cos(\phi+\theta_0+\gamma-3\pi/4)] \\
19\pi/24 < \phi < 21\pi/24 & [\sin(\phi+\theta_0+\gamma-5\pi/6) + 2\beta\cos(\phi+\theta_0+\gamma-5\pi/6)]
\end{aligned}$$

Performing suitable changes of variables leads to the following definitions:

$$\begin{aligned}
\cos na = - \{ & \cos n\pi/8 + \frac{\sqrt{3+1}-\sqrt{2}}{\sqrt{2}} \cos 5n\pi/24 + \frac{(\sqrt{2}-1)(\sqrt{3+1})}{\sqrt{2}} \cos 7n\pi/24 + \\
& \frac{(\sqrt{3}-\sqrt{2})(\sqrt{3+1})}{\sqrt{2}} \cos 9n\pi/24 - \frac{[\sqrt{3}(\sqrt{3+1}) - \sqrt{2}(2+\sqrt{3})]}{\sqrt{2}} \cos 11n\pi/24 + \\
& \frac{[\sqrt{2}(\sqrt{3+1}) - (2+\sqrt{3})]}{\sqrt{2}} \cos 13n\pi/24 - [\sqrt{2}(\sqrt{3+1}) - (2+\sqrt{3})] \cos 15n\pi/24 + \\
& \frac{[\sqrt{3}(\sqrt{3+1}) - \sqrt{2}(2+\sqrt{3})]}{\sqrt{2}} \cos 17n\pi/24 - \frac{(\sqrt{3}-\sqrt{2})(\sqrt{3+1})}{\sqrt{2}} \cos 19n\pi/24 - \\
& \frac{(\sqrt{2}-1)(\sqrt{3+1})}{\sqrt{2}} \cos 21n\pi/24 - \frac{\sqrt{3+1}-\sqrt{2}}{\sqrt{2}} \cos 23n\pi/24 - \cos 25n\pi/24 \} \quad (A8.18)
\end{aligned}$$

and

$$\begin{aligned}
\sin na = - \{ & \sin n\pi/8 + \frac{\sqrt{3+1}-\sqrt{2}}{\sqrt{2}} \sin 5n\pi/24 + \frac{(\sqrt{2}-1)(\sqrt{3+1})}{\sqrt{2}} \sin 7n\pi/24 + \\
& \frac{(\sqrt{3}-\sqrt{2})(\sqrt{3+1})}{\sqrt{2}} \sin 9n\pi/24 - \frac{[\sqrt{3}(\sqrt{3+1}) - \sqrt{2}(2+\sqrt{3})]}{\sqrt{2}} \sin 11n\pi/24 + \\
& \frac{[\sqrt{2}(\sqrt{3+1}) - (2+\sqrt{3})]}{\sqrt{2}} \sin 13n\pi/24 - [\sqrt{2}(\sqrt{3+1}) - (2+\sqrt{3})] \sin 15n\pi/24 + \\
& \frac{[\sqrt{3}(\sqrt{3+1}) - \sqrt{2}(2+\sqrt{3})]}{\sqrt{2}} \sin 17n\pi/24 - \frac{(\sqrt{3}-\sqrt{2})(\sqrt{3+1})}{\sqrt{2}} \sin 19n\pi/24 - \\
& \frac{(\sqrt{2}-1)(\sqrt{3+1})}{\sqrt{2}} \sin 21n\pi/24 - \frac{\sqrt{3+1}-\sqrt{2}}{\sqrt{2}} \sin 23n\pi/24 - \sin 25n\pi/24 \} \quad (A8.18a)
\end{aligned}$$

with

$$\cos 1a = \cos na \text{ when } n = 1$$

and

$$\sin 1a = \sin na \text{ when } n = 1$$

$$a_1 = \frac{2}{\pi} [\sin(\theta_0 + \gamma + \pi/12) + 2\beta \cos(\theta_0 + \gamma + \pi/12)] \left\{ \cos 1a \frac{9\sqrt{2} - \sqrt{54} + 2\pi}{48} - \sin 1a \frac{1 - \sqrt{3}}{8\sqrt{2}} \right\} + \frac{2}{\pi} [\cos(\theta_0 + \gamma + \pi/12) - 2\beta \sin(\theta_0 + \gamma + \pi/12)] \left\{ \cos 1a \frac{1 - \sqrt{3}}{8\sqrt{2}} - \sin 1a \frac{\sqrt{54} - 9\sqrt{2} + 2\pi}{48} \right\} \quad (\text{A8-19})$$

$$b_1 = \frac{2}{\pi} [\sin(\theta_0 + \gamma + \pi/12) + 2\beta \cos(\theta_0 + \gamma + \pi/12)] \left\{ \cos 1a \frac{1 - \sqrt{3}}{8\sqrt{2}} + \sin 1a \frac{9\sqrt{2} - \sqrt{54} + 2\pi}{48} \right\} + \frac{2}{\pi} [\cos(\theta_0 + \gamma + \pi/12) - 2\beta \sin(\theta_0 + \gamma + \pi/12)] \left\{ \cos 1a \frac{\sqrt{54} - 9\sqrt{2} + 2\pi}{48} + \sin 1a \frac{1 - \sqrt{3}}{8\sqrt{2}} \right\} \quad (\text{A8-19a})$$

$n > 1$

$$a_n = \frac{2}{\pi} \frac{[\sin(\theta_0 + \gamma + \pi/12) + 2\beta \cos(\theta_0 + \gamma + \pi/12)]}{(n^2 - 1)} \{ \cos n a [\cos n \pi / 24 \sin \pi / 24 - \cos n \pi / 8 \sin \pi / 8 - n \sin n \pi / 24 \cos \pi / 24 + n \sin n \pi / 8 \cos \pi / 8] + \sin n a [\sin n \pi / 24 \sin \pi / 24 - \sin n \pi / 8 \sin \pi / 8 + n \cos n \pi / 24 \cos \pi / 24 - n \cos n \pi / 8 \cos \pi / 8] \} + \frac{2}{\pi} \frac{[\cos(\theta_0 + \gamma + \pi/12) - 2\beta \sin(\theta_0 + \gamma + \pi/12)]}{(n^2 - 1)} \{ \cos n a [\cos n \pi / 24 \cos \pi / 24 - \cos n \pi / 8 \cos \pi / 8 + n \sin n \pi / 24 \sin \pi / 24 - n \sin n \pi / 8 \sin \pi / 8] + \sin n a [\sin n \pi / 24 \cos \pi / 24 - \sin n \pi / 8 \cos \pi / 8 - n \cos n \pi / 24 \sin \pi / 24 + n \cos n \pi / 8 \sin \pi / 8] \} \quad (\text{A8-19b})$$

$$b_n = \frac{2}{\pi} \frac{[\sin(\theta_0 + \gamma + \pi/12) + 2\beta \cos(\theta_0 + \gamma + \pi/12)]}{(n^2 - 1)} \{ -\cos n a [\sin n \pi / 24 \sin \pi / 24 - \sin n \pi / 8 \sin \pi / 8 + n \cos n \pi / 24 \cos \pi / 24 - n \cos n \pi / 8 \cos \pi / 8] + \sin n a [\cos n \pi / 24 \sin \pi / 24 - \cos n \pi / 8 \sin \pi / 8 - n \sin n \pi / 24 \cos \pi / 24 + n \sin n \pi / 8 \cos \pi / 8] \} + \frac{2}{\pi} \frac{[\cos(\theta_0 + \gamma + \pi/12) - 2\beta \sin(\theta_0 + \gamma + \pi/12)]}{(n^2 - 1)} \{ -\cos n a [\sin n \pi / 24 \cos \pi / 24 - \sin n \pi / 8 \cos \pi / 8 - n \cos n \pi / 24 \sin \pi / 24 + n \cos n \pi / 8 \sin \pi / 8] + \sin n a [\cos n \pi / 24 \cos \pi / 24 - \cos n \pi / 8 \cos \pi / 8 + n \sin n \pi / 24 \sin \pi / 24 - n \sin n \pi / 8 \sin \pi / 8] \} \quad (\text{A8-19c})$$

2) A_3

$$\begin{aligned}
 -\pi/8 < \phi < -\pi/24 & e^{-2\beta\phi} \\
 -\pi/24 < \phi < \pi/24 & \frac{\sqrt{3+1}-\sqrt{2}}{\sqrt{2}} e^{-2\beta(\phi-\pi/12)} \\
 \pi/24 < \phi < \pi/8 & \frac{(\sqrt{2}-1)(\sqrt{3+1})}{\sqrt{2}} e^{-2\beta(\phi-\pi/6)} \\
 \pi/8 < \phi < 5\pi/24 & \frac{(\sqrt{3}-\sqrt{2})(\sqrt{3+1})}{\sqrt{2}} e^{-2\beta(\phi-\pi/4)} \\
 5\pi/24 < \phi < 7\pi/24 & -\frac{\sqrt{3}(\sqrt{3+1})-\sqrt{2}(2+\sqrt{3})}{\sqrt{2}} e^{-2\beta(\phi-\pi/3)} \\
 7\pi/24 < \phi < 9\pi/24 & [\sqrt{2}(\sqrt{3+1})-(2+\sqrt{3})] e^{-2\beta(\phi-5\pi/12)} \\
 9\pi/24 < \phi < 11\pi/24 & -[\sqrt{2}(\sqrt{3+1})-(2+\sqrt{3})] e^{-2\beta(\phi-\pi/2)} \\
 11\pi/24 < \phi < 13\pi/24 & \frac{\sqrt{3}(\sqrt{3+1})-\sqrt{2}(2+\sqrt{3})}{\sqrt{2}} e^{-2\beta(\phi-7\pi/12)} \\
 13\pi/24 < \phi < 15\pi/24 & -\frac{(\sqrt{3}-\sqrt{2})(\sqrt{3+1})}{\sqrt{2}} e^{-2\beta(\phi-2\pi/3)} \\
 15\pi/24 < \phi < 17\pi/24 & -\frac{(\sqrt{2}-1)(\sqrt{3+1})}{\sqrt{2}} e^{-2\beta(\phi-3\pi/4)} \\
 17\pi/24 < \phi < 19\pi/24 & -\frac{\sqrt{3+1}-\sqrt{2}}{\sqrt{2}} e^{-2\beta(\phi-5\pi/6)} \\
 19\pi/24 < \phi < 21\pi/24 & -e^{-2\beta(\phi-11\pi/12)}
 \end{aligned}$$

The following equations are valid for all n .

$$a_n = \frac{2}{\pi} \frac{e^{\beta\pi/12}}{(n^2+4\beta^2)}$$

$$\{\cos na[n(\sin n\pi/24 - e^{\beta\pi/6}\sin n\pi/8) + 2\beta(\cos n\pi/24 - e^{\beta\pi/6}\cos n\pi/8)] - \sin na[n\cos n\pi/24 - e^{\beta\pi/6}\cos n\pi/8] - 2\beta(\sin n\pi/24 - e^{\beta\pi/6}\sin n\pi/8)\} \quad (\text{A8.20})$$

$$b_n = \frac{2}{\pi} \frac{e^{\beta\pi/12}}{(n^2+4\beta^2)}$$

$$\{\cos na[n(\cos n\pi/24 - e^{\beta\pi/6}\cos n\pi/8) - 2\beta(\sin n\pi/24 - e^{\beta\pi/6}\sin n\pi/8)] + \sin na[n\sin n\pi/24 - e^{\beta\pi/6}\sin n\pi/8) + 2\beta(\cos n\pi/24 - e^{\beta\pi/6}\cos n\pi/8)]\} \quad (\text{A8.20a})$$

$$\begin{array}{ll}
3) \frac{A_1}{\sqrt{2}(\sqrt{2+1})(\sqrt{3+1})(\sqrt{3+\sqrt{2}})} & \\
-\pi/8 < \phi < -\pi/24 & - e^{-\beta\phi} \text{sinc}\phi \\
-\pi/24 < \phi < \pi/24 & - \frac{\sqrt{3+1}+\sqrt{2}}{\sqrt{2}} e^{-\beta(\phi-\pi/12)} \text{sinc}(\phi-\pi/12) \\
\pi/24 < \phi < \pi/8 & - \frac{(\sqrt{2+1})(\sqrt{3+1})}{\sqrt{2}} e^{-\beta(\phi-\pi/6)} \text{sinc}(\phi-\pi/6) \\
\pi/8 < \phi < 5\pi/24 & - \frac{(\sqrt{3+\sqrt{2}})(\sqrt{3+1})}{\sqrt{2}} e^{-\beta(\phi-\pi/4)} \text{sinc}(\phi-\pi/4) \\
5\pi/24 < \phi < 7\pi/24 & - \frac{\sqrt{3}(\sqrt{3+1}) + \sqrt{2}(2+\sqrt{3})}{\sqrt{2}} e^{-\beta(\phi-\pi/3)} \text{sinc}(\phi-\pi/3) \\
7\pi/24 < \phi < 9\pi/24 & - [\sqrt{2}(\sqrt{3+1}) + (2+\sqrt{3})] e^{-\beta(\phi-5\pi/12)} \text{sinc}(\phi-5\pi/12) \\
9\pi/24 < \phi < 11\pi/24 & - [\sqrt{2}(\sqrt{3+1}) + (2+\sqrt{3})] e^{-\beta(\phi-\pi/2)} \text{sinc}(\phi-\pi/2) \\
11\pi/24 < \phi < 13\pi/24 & - \frac{\sqrt{3}(\sqrt{3+1}) + \sqrt{2}(2+\sqrt{3})}{\sqrt{2}} e^{-\beta(\phi-7\pi/12)} \text{sinc}(\phi-7\pi/12) \\
13\pi/24 < \phi < 15\pi/24 & - \frac{(\sqrt{3+\sqrt{2}})(\sqrt{3+1})}{\sqrt{2}} e^{-\beta(\phi-2\pi/3)} \text{sinc}(\phi-2\pi/3) \\
15\pi/24 < \phi < 17\pi/24 & - \frac{(\sqrt{2+1})(\sqrt{3+1})}{\sqrt{2}} e^{-\beta(\phi-3\pi/4)} \text{sinc}(\phi-3\pi/4) \\
17\pi/24 < \phi < 19\pi/24 & - \frac{\sqrt{3+1}+\sqrt{2}}{\sqrt{2}} e^{-\beta(\phi-5\pi/6)} \text{sinc}(\phi-5\pi/6) \\
19\pi/24 < \phi < 21\pi/24 & - e^{-\beta(\phi-11\pi/12)} \text{sinc}(\phi-11\pi/12)
\end{array}$$

Making the same change of variables as in section b1, equations (A8·18) and (A8·18a), the following definitions become transparent:

$$\begin{aligned}
\cos nb = & \left\{ \cos n\pi/8 + \frac{\sqrt{3+1}+\sqrt{2}}{\sqrt{2}} \cos 5n\pi/24 + \frac{(\sqrt{2+1})(\sqrt{3+1})}{\sqrt{2}} \cos 7n\pi/24 + \right. \\
& \frac{(\sqrt{3+\sqrt{2}})(\sqrt{3+1})}{\sqrt{2}} \cos 9n\pi/24 + \frac{[\sqrt{3}(\sqrt{3+1}) + \sqrt{2}(2+\sqrt{3})]}{\sqrt{2}} \cos 11n\pi/24 + \\
& \frac{[\sqrt{2}(\sqrt{3+1}) + (2+\sqrt{3})]}{\sqrt{2}} \cos 13n\pi/24 + \frac{[\sqrt{2}(\sqrt{3+1}) + (2+\sqrt{3})]}{\sqrt{2}} \cos 15n\pi/24 + \\
& \frac{[\sqrt{3}(\sqrt{3+1}) + \sqrt{2}(2+\sqrt{3})]}{\sqrt{2}} \cos 17n\pi/24 + \frac{(\sqrt{3+\sqrt{2}})(\sqrt{3+1})}{\sqrt{2}} \cos 19n\pi/24 + \\
& \left. \frac{(\sqrt{2+1})(\sqrt{3+1})}{\sqrt{2}} \cos 21n\pi/24 + \frac{\sqrt{3+1}+\sqrt{2}}{\sqrt{2}} \cos 23n\pi/24 + \cos 25n\pi/24 \right\} \quad (\text{A8·21})
\end{aligned}$$

and

$$\begin{aligned}
\sin nb = & \left\{ \sin n\pi/8 + \frac{\sqrt{3+1}+\sqrt{2}}{\sqrt{2}} \sin 5n\pi/24 + \frac{(\sqrt{2+1})(\sqrt{3+1})}{\sqrt{2}} \sin 7n\pi/24 + \right. \\
& \frac{(\sqrt{3+\sqrt{2}})(\sqrt{3+1})}{\sqrt{2}} \sin 9n\pi/24 + \frac{[\sqrt{3}(\sqrt{3+1}) + \sqrt{2}(2+\sqrt{3})]}{\sqrt{2}} \sin 11n\pi/24 + \\
& \frac{[\sqrt{2}(\sqrt{3+1}) + (2+\sqrt{3})]}{\sqrt{2}} \sin 13n\pi/24 + \frac{[\sqrt{2}(\sqrt{3+1}) + (2+\sqrt{3})]}{\sqrt{2}} \sin 15n\pi/24 + \\
& \frac{[\sqrt{3}(\sqrt{3+1}) + \sqrt{2}(2+\sqrt{3})]}{\sqrt{2}} \sin 17n\pi/24 + \frac{(\sqrt{3+\sqrt{2}})(\sqrt{3+1})}{\sqrt{2}} \sin 19n\pi/24 + \\
& \left. \frac{(\sqrt{2+1})(\sqrt{3+1})}{\sqrt{2}} \sin 21n\pi/24 + \frac{\sqrt{3+1}+\sqrt{2}}{\sqrt{2}} \sin 23n\pi/24 + \sin 25n\pi/24 \right\} \quad (\text{A8·21a})
\end{aligned}$$

$$\begin{aligned}
a_n = & -\frac{2}{\pi} \frac{e^{\beta\pi/24}}{h_n^2} \left\{ \cos nb \right. \\
& \left[k (\beta^2+k^2-n^2) (-\cos k\pi/24 \cos n\pi/24 + e^{\beta\pi/12} \cos k\pi/8 \cos n\pi/8) + \right. \\
& \beta (\beta^2+k^2+n^2) (\sin k\pi/24 \cos n\pi/24 - e^{\beta\pi/12} \sin k\pi/8 \cos n\pi/8) + \\
& 2\beta nk (-\cos k\pi/24 \sin n\pi/24 + e^{\beta\pi/12} \cos k\pi/8 \sin n\pi/8) + \\
& \left. n (\beta^2-k^2+n^2) (\sin k\pi/24 \sin n\pi/24 - e^{\beta\pi/12} \sin k\pi/8 \sin n\pi/8) \right] - \\
& \quad \sin nb \\
& \left[2\beta nk (-\cos k\pi/24 \cos n\pi/24 + e^{\beta\pi/12} \cos k\pi/8 \cos n\pi/8) + \right. \\
& n (\beta^2-k^2+n^2) (\sin k\pi/24 \cos n\pi/24 - e^{\beta\pi/12} \sin k\pi/8 \cos n\pi/8) + \\
& k (\beta^2+k^2-n^2) (\cos k\pi/24 \sin n\pi/24 - e^{\beta\pi/12} \cos k\pi/8 \sin n\pi/8) + \\
& \left. \beta (\beta^2+k^2+n^2) (-\sin k\pi/24 \sin n\pi/24 + e^{\beta\pi/12} \sin k\pi/8 \sin n\pi/8) \right] \left. \right\} \quad (A8-22)
\end{aligned}$$

$$\begin{aligned}
b_n = & -\frac{2}{\pi} \frac{e^{\beta\pi/24}}{h_n^2} \left\{ \cos nb \right. \\
& \left[2\beta nk (-\cos k\pi/24 \cos n\pi/24 + e^{\beta\pi/12} \cos k\pi/8 \cos n\pi/8) + \right. \\
& n (\beta^2-k^2+n^2) (\sin k\pi/24 \cos n\pi/24 - e^{\beta\pi/12} \sin k\pi/8 \cos n\pi/8) + \\
& k (\beta^2+k^2-n^2) (\cos k\pi/24 \sin n\pi/24 - e^{\beta\pi/12} \cos k\pi/8 \sin n\pi/8) + \\
& \left. \beta (\beta^2+k^2+n^2) (-\sin k\pi/24 \sin n\pi/24 + e^{\beta\pi/12} \sin k\pi/8 \sin n\pi/8) \right] + \\
& \quad \sin nb \\
& \left[k (\beta^2+k^2-n^2) (-\cos k\pi/24 \cos n\pi/24 + e^{\beta\pi/12} \cos k\pi/8 \cos n\pi/8) + \right. \\
& \beta (\beta^2+k^2+n^2) (\sin k\pi/24 \cos n\pi/24 - e^{\beta\pi/12} \sin k\pi/8 \cos n\pi/8) + \\
& 2\beta nk (-\cos k\pi/24 \sin n\pi/24 + e^{\beta\pi/12} \cos k\pi/8 \sin n\pi/8) + \\
& \left. n (\beta^2-k^2+n^2) (\sin k\pi/24 \sin n\pi/24 - e^{\beta\pi/12} \sin k\pi/8 \sin n\pi/8) \right] \left. \right\} \quad (A8-22a)
\end{aligned}$$

$$\begin{aligned}
& 4) \frac{A_2}{\sqrt{2}(\sqrt{2+1})(\sqrt{3+1})(\sqrt{3+\sqrt{2}})} \\
& -\pi/8 < \phi < -\pi/24 \quad - e^{-\beta\phi} \operatorname{cosh} \phi \\
& -\pi/24 < \phi < \pi/24 \quad - \frac{\sqrt{3+1}+\sqrt{2}}{\sqrt{2}} e^{-\beta(\phi-\pi/12)} \operatorname{cosh}(\phi-\pi/12) \\
& \pi/24 < \phi < \pi/8 \quad - \frac{(\sqrt{2+1})(\sqrt{3+1})}{\sqrt{2}} e^{-\beta(\phi-\pi/6)} \operatorname{cosh}(\phi-\pi/6) \\
& \pi/8 < \phi < 5\pi/24 \quad - \frac{(\sqrt{3+\sqrt{2}})(\sqrt{3+1})}{\sqrt{2}} e^{-\beta(\phi-\pi/4)} \operatorname{cosh}(\phi-\pi/4) \\
& 5\pi/24 < \phi < 7\pi/24 \quad - \frac{\sqrt{3}(\sqrt{3+1}) + \sqrt{2}(2+\sqrt{3})}{\sqrt{2}} e^{-\beta(\phi-\pi/3)} \operatorname{cosh}(\phi-\pi/3) \\
& 7\pi/24 < \phi < 9\pi/24 \quad - [\sqrt{2}(\sqrt{3+1}) + (2+\sqrt{3})] e^{-\beta(\phi-5\pi/12)} \operatorname{cosh}(\phi-5\pi/12) \\
& 9\pi/24 < \phi < 11\pi/24 \quad - [\sqrt{2}(\sqrt{3+1}) + (2+\sqrt{3})] e^{-\beta(\phi-\pi/2)} \operatorname{cosh}(\phi-\pi/2) \\
& 11\pi/24 < \phi < 13\pi/24 \quad - \frac{\sqrt{3}(\sqrt{3+1}) + \sqrt{2}(2+\sqrt{3})}{\sqrt{2}} e^{-\beta(\phi-7\pi/12)} \operatorname{cosh}(\phi-7\pi/12) \\
& 13\pi/24 < \phi < 15\pi/24 \quad - \frac{(\sqrt{3+\sqrt{2}})(\sqrt{3+1})}{\sqrt{2}} e^{-\beta(\phi-2\pi/3)} \operatorname{cosh}(\phi-2\pi/3) \\
& 15\pi/24 < \phi < 17\pi/24 \quad - \frac{(\sqrt{2+1})(\sqrt{3+1})}{\sqrt{2}} e^{-\beta(\phi-3\pi/4)} \operatorname{cosh}(\phi-3\pi/4) \\
& 17\pi/24 < \phi < 19\pi/24 \quad - \frac{\sqrt{3+1}+\sqrt{2}}{\sqrt{2}} e^{-\beta(\phi-5\pi/6)} \operatorname{cosh}(\phi-5\pi/6) \\
& 19\pi/24 < \phi < 21\pi/24 \quad - e^{-\beta(\phi-11\pi/12)} \operatorname{cosh}(\phi-11\pi/12)
\end{aligned}$$

$$\begin{aligned}
a_n = & -\frac{2}{\pi} \frac{e^{\beta\pi/24}}{h_n^2} \left\{ \cos nb \right. \\
& \left[\beta (\beta^2+k^2+n^2) (-\cos k\pi/24 \cos n\pi/24 + e^{\beta\pi/12} \cos k\pi/8 \cos n\pi/8) + \right. \\
& k (\beta^2+k^2-n^2) (-\sin k\pi/24 \cos n\pi/24 + e^{\beta\pi/12} \sin k\pi/8 \cos n\pi/8) + \\
& 2\beta nk (-\sin k\pi/24 \sin n\pi/24 + e^{\beta\pi/12} \sin k\pi/8 \sin n\pi/8) + \\
& \left. n (\beta^2-k^2+n^2) (-\cos k\pi/24 \sin n\pi/24 + e^{\beta\pi/12} \cos k\pi/8 \sin n\pi/8) \right] - \\
& \quad \sin nb \\
& \left[n (\beta^2-k^2+n^2) (-\cos k\pi/24 \cos n\pi/24 + e^{\beta\pi/12} \cos k\pi/8 \cos n\pi/8) + \right. \\
& 2\beta nk (-\sin k\pi/24 \cos n\pi/24 + e^{\beta\pi/12} \sin k\pi/8 \cos n\pi/8) + \\
& \beta (\beta^2+k^2+n^2) (\cos k\pi/24 \sin n\pi/24 - e^{\beta\pi/12} \cos k\pi/8 \sin n\pi/8) + \\
& \left. k (\beta^2+k^2-n^2) (\sin k\pi/24 \sin n\pi/24 - e^{\beta\pi/12} \sin k\pi/8 \sin n\pi/8) \right] \left. \right\} \quad (A8-23)
\end{aligned}$$

$$\begin{aligned}
b_n = & -\frac{2}{\pi} \frac{e^{\beta\pi/24}}{h_n^2} \left\{ \cos nb \right. \\
& \left[n (\beta^2-k^2+n^2) (-\cos k\pi/24 \cos n\pi/24 + e^{\beta\pi/12} \cos k\pi/8 \cos n\pi/8) + \right. \\
& 2\beta nk (-\sin k\pi/24 \cos n\pi/24 + e^{\beta\pi/12} \sin k\pi/8 \cos n\pi/8) + \\
& \beta (\beta^2+k^2+n^2) (\cos k\pi/24 \sin n\pi/24 - e^{\beta\pi/12} \cos k\pi/8 \sin n\pi/8) + \\
& \left. k (\beta^2+k^2-n^2) (\sin k\pi/24 \sin n\pi/24 - e^{\beta\pi/12} \sin k\pi/8 \sin n\pi/8) \right] + \\
& \quad \sin nb \\
& \left[\beta (\beta^2+k^2+n^2) (-\cos k\pi/24 \cos n\pi/24 + e^{\beta\pi/12} \cos k\pi/8 \cos n\pi/8) + \right. \\
& k (\beta^2+k^2-n^2) (-\sin k\pi/24 \cos n\pi/24 + e^{\beta\pi/12} \sin k\pi/8 \cos n\pi/8) + \\
& 2\beta nk (-\sin k\pi/24 \sin n\pi/24 + e^{\beta\pi/12} \sin k\pi/8 \sin n\pi/8) + \\
& \left. n (\beta^2-k^2+n^2) (-\cos k\pi/24 \sin n\pi/24 + e^{\beta\pi/12} \cos k\pi/8 \sin n\pi/8) \right] \left. \right\} \quad (A8-23a)
\end{aligned}$$

The Fourier series on the primary side of the transformers can be calculated from (A8.16) and (A8.17) with similar contributions from the other phases.

For the fundamental frequency component this reduces to, as in the twelve pulse equipment,

$$I_{R1} = \frac{V_m}{hX_L} \sin(\phi + \theta_0 + \gamma) + a_1 \cos\phi + b_1 \sin\phi \quad (\text{A8.24})$$

Since this is equivalent to that in the twelve pulse analysis, (A6.30), the derivations of p_1 , q_1 and q_2 are identical. The expressions for the contributions to the fundamental frequency component of the current are therefore given by

$$I_q = \frac{V_m}{X_L} \left(q_1 + q_2 \frac{\sin 2\theta_0}{2\beta} \right) \quad (\text{A8.25})$$

$$I_p = \frac{\beta V_m}{X_L} \left(p_1 + q_2 \frac{\sin^2 \theta_0}{\beta^2} \right) \quad (\text{A8.25a})$$

For the harmonics, after simplifying, the expression is reduced to

$$|I_n| = \sqrt{a_n^2 + b_n^2} \quad (\text{A8.26})$$

Again this is equivalent to that in the twelve pulse case, equation (A6.35), and so the definition for the exact value of t_n is the same. Plotting this, there again appears to be a linear relationship between t_n and θ_{ob} :

$$I_{nc} \approx \frac{V_m}{X_L} [c_n - s_n \theta_{ob}] \quad (\text{A8.27})$$

with the definitions of c_n and s_n as those in the twelve pulse case, equations (A6.39) and (A6.39a) respectively.

Appendix 9

Details of the Experimental Work

This appendix shows the experimental arrangement of the circuits for the practical work discussed in chapters 5 and 7. A block diagram for the control scheme is given in section 5.13 with full details given elsewhere (Ashbrook & Hill, 1993b).

Figure A9.1 shows the circuit for the 6-pulse model. Philips N-channel MOSFETs (type BUK437 – 500B) were used, with a continuous rating of 500V and 10A. The MOSFET modules included an internal anti-parallel diode. A diode, resistor and capacitor snubber circuit was connected across each MOSFET module. The resistance value was 47Ω and the capacitor was $0.22\mu\text{F}$.

When the model is first turned on the energy reservoir capacitor is charged from the mains through the diodes in the circuit. To reduce the inrush current into the capacitor a $1\text{k}\Omega$ resistor was included in each phase during the start-up period. After two seconds a second contactor was closed and the first opened and normal operation begins. The two contactors and timer are visible on the left of the photograph of the equipment, figure A9.2.

A $20\mu\text{F}$ capacitor was used as the energy reservoir and the inductors were each 40mH.

Current and voltage waveforms were stored as computer files using the LabView[†] data acquisition software and plotted for comparison with the theoretical and simulated results.

[†]LabView is a trademark of the National Instruments Corporation.

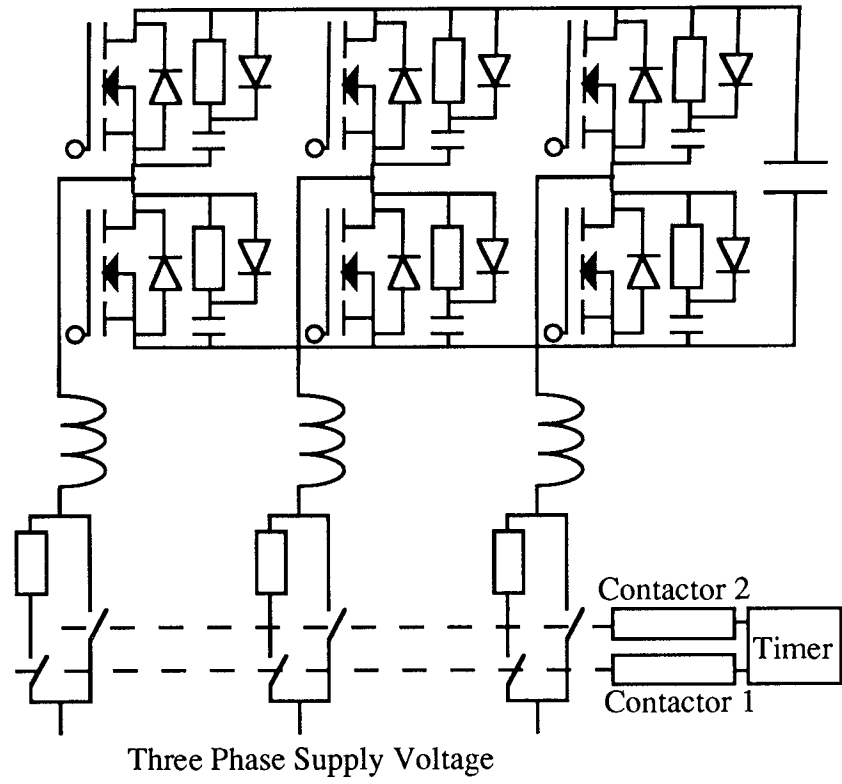


Figure A9.1. Circuit Diagram for the 6-Pulse Practical Equipment.

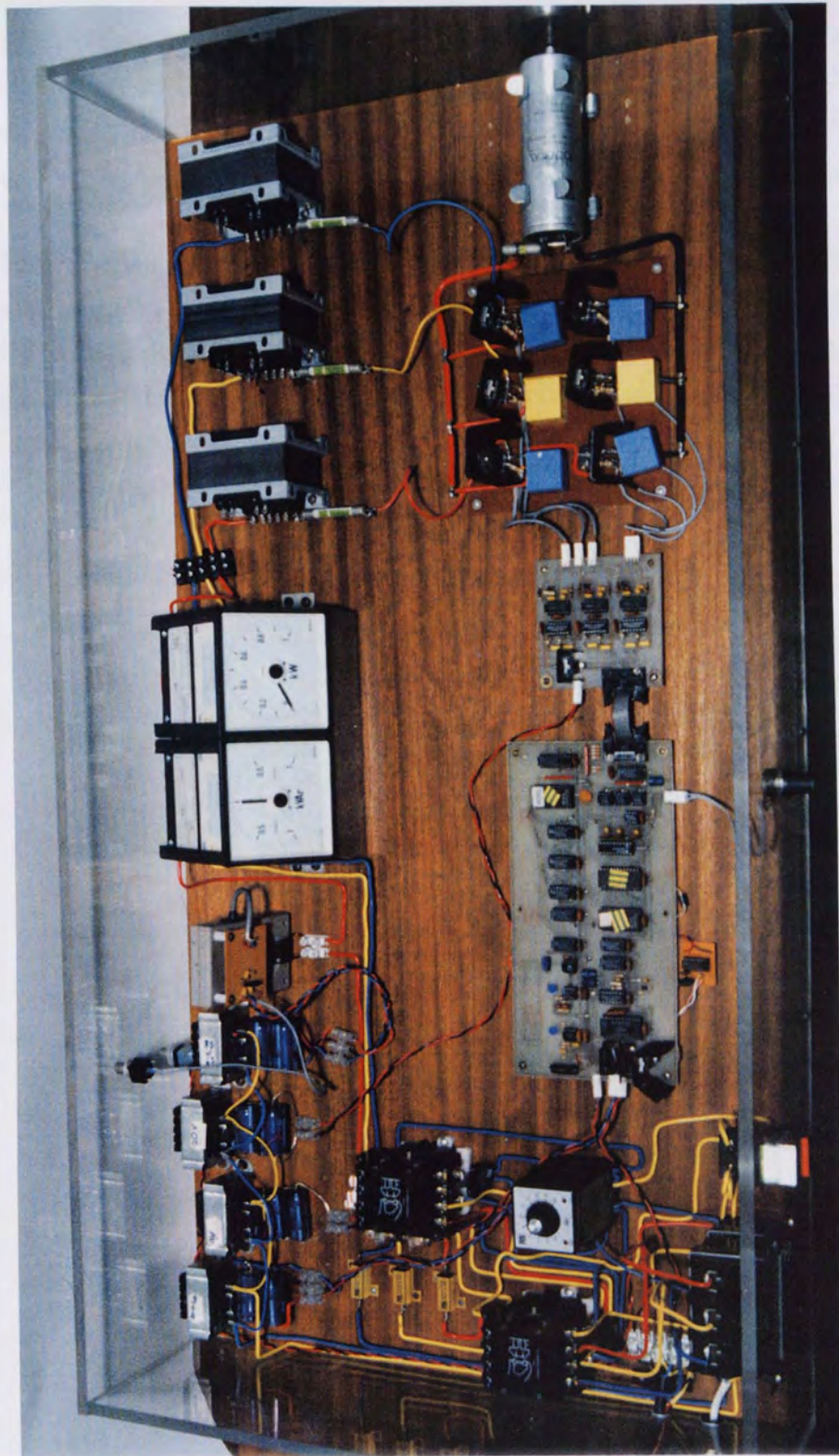


Figure A9-2. Photograph of the 6-Pulse Practical Equipment.

The 24-Pulse equipment used the same device and snubber circuits as in the 6-pulse model. The "soft-start" arrangement used with the 6-pulse equipment was not adopted because the circuit was always powered through a variac and so was always started at reduced voltage. The phase-shifting transformers, in the configuration shown in figure 7.3, are visible at the bottom of the photograph, figure A9.3. The d.c. power supplies which are visible in the photograph of the 6-pulse model are housed inside the metal box on the left of the photograph of the 24-pulse model to increase the noise immunity.

The equipment shown in the photograph was built and tested by other members of the research group (Hill, Chileshe, Boardman and Westrick, 1994); my contributions were only in discussions on the power aspects of the project and not on the control circuitry shown which was the work of the other members of the group listed above, to whom I am grateful.

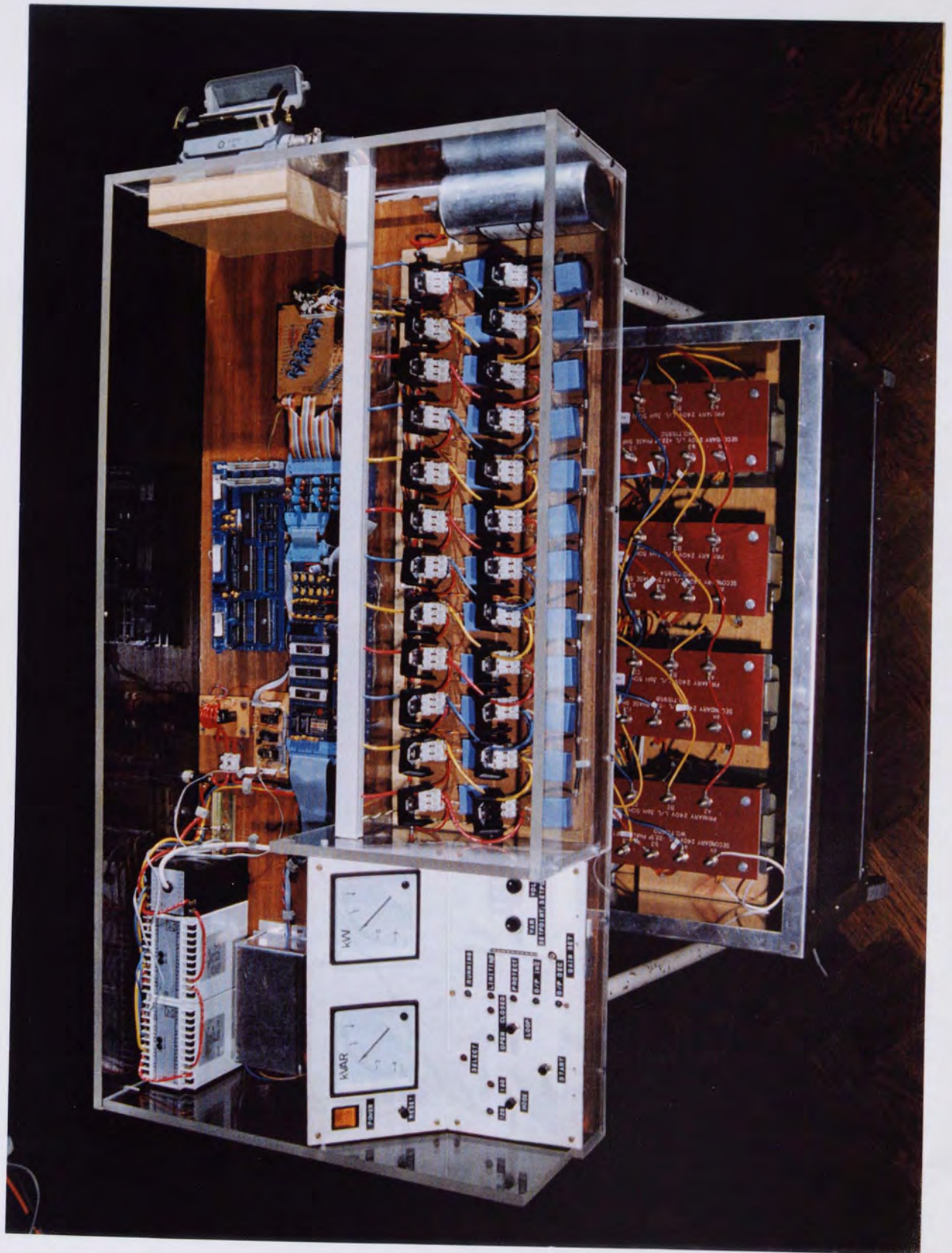


Figure A9.3. Photograph of the 24-Pulse Practical Equipment.